UNIVERSIDADE BEIRA INTERIOR

New Steroidal Arylidene Derivatives Potentially Useful in the Treatment of Prostatic Diseases

Vanessa Sofia Figueiredo de Brito

Tese para obtenção do Grau de Doutor em
Química
(3º ciclo de estudos)

Orientador: Prof. Doutor Paulo Jorge da Silva Almeida
Orientador: Prof. Doutor Samuel Martins Silvestre
Coorientador: Prof. Doutor Gilberto Lourenço Alves

Júri
Prof. Doutor Joaquim Mateus Paulo Serra
Prof. Doutor Rui Ferreira Alves Moreira
Prof. Doutora Maria Emília da Silva Pereira de Sousa
Prof. Doutor Samuel Martins Silvestre
Prof. Doutor Renato Emanuel Félix Boto
Prof. Doutora Maria Manuel da Cruz Silva
Prof. Doutora Maria Eugénia Gallardo Alba
Prof. Doutora Mariana Ruivo Matias
Doutor Nuno Ricardo Esteves Ferreira

Covilhã, 4 de julho de 2023

Declaração de Integridade

Eu, Vanessa Sofia Figueiredo de Brito, que abaixo assino, estudante com o número de inscrição D1950 do 3º Ciclo em Química da Faculdade de Ciências, declaro ter desenvolvido o presente trabalho e elaborado o presente texto em total consonância com o **Código de Integridade da Universidade da Beira Interior**.

Mais concretamente afirmo não ter incorrido em qualquer das variedades de Fraude Académica, e que aqui declaro conhecer, e que em particular atendi à exigida referenciação de frases, extratos, imagens e outras formas de trabalho intelectual, e assim assumo na íntegra as responsabilidades da autoria.

Universidade da Beira Interior, Covilhã

Assinado por: **Vanessa Sofia Figueiredo de Brito**
Num. de Identificação: 13850837
Data: 2023.07.13 21:29:12+01'00'

CHAVE MÓVEL

The experimental work presented in this thesis was performed under the scientific supervision of Professor Paulo Jorge da Silva Almeida, Professor Samuel Martins Silvestre, and Professor Gilberto Alves at the Health Sciences Research Centre, headquartered at the Faculty of Health Sciences, University of Beira Interior, and at the Faculty of Sciences, also at the University of Beira Interior.

O trabalho experimental apresentado na presente tese foi realizado sob a orientação científica do Professor Doutor Paulo Jorge da Silva Almeida, do Professor Doutor Samuel Martins Silvestre e do Professor Doutor Gilberto Lourenço Alves, no Centro de Investigação em Ciências da Saúde, situado nas instalações da Faculdade de Ciências da Saúde da Universidade da Beira Interior, e também na Faculdade de Ciências da mesma instituição.

The work developed under the scope of this thesis was mainly supported by *Fundação para a Ciência e a Tecnologia* (FCT), Portugal (SFRH/BD/131059/2017 and COVID/BD/151921/2021), FEDER funds through the POCI - COMPETE 2020 - Operational Programme Competitiveness and Internationalization in Axis I - Strengthening research, technological development and innovation (Project No. 007491). Moreover, support from National Funds by the FCT (Project UID/ Multi/ 00709) and from C4-Cloud Computing Competences Center Project (CENTRO-01-0145-FEDER-000019) were granted. Initially, this work was also supported by the grant BID/ ICI-FC/ *Santander Universidades*-UBI/ 2016.

"Drug development is about many things, but first of all about responsibility."

–Dr. Johanna Holldack, CEO, Founder at Kupando GmbH

Agradecimentos

"A·GRA·DE·CER |ê|
verbo transitivo
1. Dar agradecimentos por; retribuir com agradecimentos.
verbo intransitivo
2. Exprimir agradecimentos."

In Dicionário Priberam da Língua Portuguesa,
2008-2021, https://dicionario.priberam.org/agradecer
[consultado em 26-09-2022].

Agradecer é algo com significado muito mais lato do que aquele que encontramos no dicionário. Pelo menos no que diz respeito ao que vou aqui escrever. Não quero apenas retribuir ou exprimir agradecimentos, quero mostrar todo o carinho, gratidão e enorme estima por aqueles que estiveram sempre presentes nesta desafiante, longa e inquietante jornada. Sem dúvida alguma que não seria possível percorrer esta mesma jornada sozinha ou com as pessoas erradas ao meu lado. Portanto, no meio do trabalho, tive alguma sorte.

Em primeiro lugar, quero agradecer ao meu orientador Professor Doutor Samuel Silvestre. Além de toda a sua competência como profissional que é irrepreensível e fascinante, quero enaltecer sobretudo o amigo que foi (e é), o "psicólogo" que muitas vezes foi e a boa pessoa que sempre revelou ser. É muito raro encontrar alguém com tanta humildade, paciência, simplicidade e bondade (e tão inteligente). Quero agradecer todo o apoio, ajuda, ensinamentos partilhados e disponibilidade. Sei que muitas vezes foi difícil conseguir tempo para todas as tarefas, mas nunca me deixou desamparada. Tenho em si um exemplo. Foi um gosto trabalhar com o Professor. Um sincero e sentido obrigado.

Ao Professor Doutor Paulo Almeida, também orientador, que sempre se disponibilizou para me ajudar sem nunca hesitar, de forma célere e eficiente, o meu profundo agradecimento. Sempre muito perspicaz, contribuiu significativamente para o sucesso da execução deste projeto doutoral. Agradeço todo o conhecimento científico, apoio e oportunidades dadas. Espero um dia, alcançar metade do seu sucesso. É a prova que a

ambição é essencial para conquistar o que mais desejamos, e vou ter isso sempre em mente no meu futuro. Muito obrigada por tudo.

Quero agradecer também ao Professor Doutor Gilberto Alves, meu coorientador, pelos conhecimentos científicos que partilhou, pelo apoio e pela atenção prestada. Infelizmente, desta vez já não poderá ser meu arguente como aconteceu na defesa da dissertação de Mestrado. No entanto, e felizmente, será um orgulho tê-lo do "nosso lado" desta vez. Muito obrigada por ter aceitado este desafio sem hesitar. Sem dúvida que sem o seu contributo, este trabalho não teria o mesmo valor.

À Professora Doutora Adriana Santos, agradeço pela sua completa disponibilidade, prontidão e enorme apoio nas suas áreas de especialidade (biologia celular, bioestatística…). Sem dúvida que a partilha do seu conhecimento científico foi essencial na execução do meu projeto. Foi um gosto enorme aprender com alguém tão entusiasta, com enorme espírito crítico e gosto pela ciência. Um enorme obrigada!

Agradeço também a todos os meus colegas de laboratório que me acolheram inicialmente e que me ensinaram muito: Mariana Matias, Catarina Canário, Filipa Ramilo Gomes, Elisabete Alves e Sandrina Maçãs. A vossa paciência, disponibilidade e partilha de conhecimento foram cruciais para puder tornar-me independente e autónoma. Obrigada pela generosidade! Um grande obrigado aos restantes colegas de laboratório que foram passando no meu percurso, bem como aos funcionários do CICS e da Universidade da Beira Interior, que além de boa companhia, sempre ajudaram quando necessário: Octávio Ferreira, Pedro Soeiro, João Serrano, Eurico Lima, Marco Almeida, Joana Figueiredo, Marta Esteves, Catarina Almeida, Sofia Duarte, Margarida Carrilho, Cristina Gil, Joaquim Correia, Ricardo Relvas, Rui Costa e tantos outros.

À minha amiga e colega de laboratório Sara Meirinho um especial agradecimento pela ajuda que prestou nesta última etapa, cedendo muito e demasiado do seu tempo para me ensinar tudo o que podia. Além dos conhecimentos científicos, agradeço a tua amizade e apoio incondicional.

Quero agradecer à Sara Cristina, de quem muito me orgulho, e mais não é necessário dizer. Não imaginas a falta que me fizeste nestes últimos anos.

O meu enorme obrigada aos meus amigos (*aka* "meujamigos") que terei sempre na minha memória e coração. Sempre me apoiaram, animaram e aconselharam (e

aturaram, com tudo o que isso implica…), e com quem partilhei os melhores e os piores momentos durante este percurso. Marta Pereira, Jorge Ferreira, Ângela Gonçalves, Milene Gonçalves, Josué Carvalho, Patrícia Quintela, Fábio Rodrigues, Célia Lopes, André Furtado, Cátia Pratas e Raquel Costa, um bem-haja cheio de carinho.

À minha família biológica e à minha família por afinidade que permitiram que a conclusão desta etapa fosse possível. Obrigada aos meus avós, mãe e irmão por acreditarem em mim e fazerem-me chegar à Covilhã para concretizar o meu sonho. À Dona Fernanda, ao Sr. José, ao João Luís e à Francisca (e restantes de quem gosto muito). É uma sorte ter pessoas tão generosas ao meu lado. Para vocês já nem tenho palavras.

Ao João. Ao João mil vezes.
Tudo o que poderia escrever não seria nada comparado com o que fizeste por mim.

Obrigada, obrigada, obrigada!

Resumo Alargado

A glândula prostática humana é um órgão pertencente ao sistema reprodutor masculino, e na idade adulta, assemelha-se, tanto no tamanho como na forma, a uma castanha. A próstata é um órgão sensível a androgénios e, como tal necessita de androgénios e recetores de androgénios (RA) específicos para o normal desenvolvimento, crescimento e função. Esta glândula pode ser afetada principalmente por três condições: prostatite, hiperplasia benigna da próstata (HBP) e cancro prostático (CP). Globalmente, as duas últimas condições referidas afetam uma percentagem muito elevada de homens com idade superior a 65 anos, sendo uma das causas mais relevantes de morbilidade e mortalidade. Deste modo, a importância da terapia farmacológica na gestão destas doenças é, de facto, inquestionável.

Atualmente, a relevância das hormonas esteroides na fisiopatologia da HBP e do CP é conhecida e bem suportada pelas evidências científicas. Neste contexto, sabe-se que o aumento anormal da atividade da enzima 5α-redutase (5AR) resulta na produção de uma quantidade excessiva de 5α-dihidrotestosterona (DHT), produto da conversão irreversível da testosterona por esta enzima, e que esse aumento de DHT nos tecidos periféricos tem vido a ser associado à patogénese de ambas as doenças. Consequentemente, o papel da DHT nestes cenários de doença tem contribuído para o interesse na descoberta de inibidores da 5AR, dado que é uma estratégia importante e aplicada frequentemente no tratamento da HBP. Considerando as necessidades médicas não satisfeitas neste âmbito, é reconhecido que os inibidores da 5AR utilizados na prática clínica, como a finasterida, exibem baixa potência e diversos efeitos adversos que reduzem significativamente a qualidade de vida dos utentes. No que diz respeito ao tratamento do CP, o uso destes fármacos é bastante controverso, pois apesar da finasterida parecer levar à redução da sua incidência, foi reportado pelo "*Prostate Cancer Prevention Trial (PCPT)"* um aumento na incidência do CP maligno em comparação com o placebo. No entanto, teoricamente é uma estratégia válida e lógica a explorar. Neste âmbito, os arilidenoesteroides constituem uma classe importante de esteroides modificados cuja atividade antiproliferativa relevante e a sua potencial capacidade de inibir a enzima 5AR tem vindo a ser reportada em diversos estudos.

Neste contexto surge o principal objetivo deste trabalho, a preparação de novos arilidenos derivados de esteroides potencialmente úteis nas doenças prostáticas, apresentando capacidade inibitória da 5AR e/ou propriedades antiproliferativas em células tumorais. Globalmente, esta tese visa a descoberta de compostos "*hit*" para

posterior desenvolvimento no contexto da HBP e CP. Para alcançar este objetivo, diversas estratégicas de síntese química foram exploradas e obteve-se com sucesso novos arilidenos derivados de esteroides. Após síntese e respetiva caracterização estrutural, as atividades antitumorais e inibitórias da 5AR destes novos derivados foram avaliadas. Além da avaliação biológica *in vitro*, executaram-se simulações de "*docking"* molecular para verificar a afinidade dos novos compostos para importantes alvos de moléculas esteroides, nomeadamente na 5AR tipo 2, no recetor de estrogénios α (REα), no RA, na 17α-hidroxilase/17,20 liase de esteroides (CYP17A1) e na aromatase. É importante referir que esta tese também contempla a realização de estudos de avaliação biológica *in vitro*/*in silico,* como estudos compreensivos de relação estrutura-atividade tridimensional (3D-REA), de arilidenos derivados de 4-azaesteroides (**VB 4a**-**g** e **VB 7a**-**g**) previamente sintetizados no contexto da dissertação de Mestrado. Este estudo de 3D-REA considerou o efeito na atividade proliferativa em células tumorais da próstata dependentes (LNCaP) e não dependentes de androgénios (PC-3), e de facto, foram gerados modelos robustos que elucidaram a relação entre a atividade e a estrutura dos compostos testados, tendo-se observado que os grupos volumosos (arilidenos) e os átomos eletronegativos são importantes para a atividade antiproliferativa *in vitro*. Estes resultados foram incluídos na presente tese dado que se enquadravam no tema da mesma.

Relativamente ao projeto doutoral, após diversas tentativas falhadas para sintetizar novos 3-, 4- e 6-azaesteroides com heterociclos fundidos/ligados ao anel D, uma nova via sintética foi estudada e aplicada, tendo sido preparadas com sucesso três séries distintas séries de novos arilidenoesteroides oxidados a partir do esteroide desidroepiandrosterona. As estruturas químicas e o alto grau de pureza dos novos derivados de 16*E*-arilideno-5α,6α-epoxy-epiandrosterona, 16*E*-arilideno-3β,5α,6β-trihidroxi-androsten-17-ona, e 16*E*-arilideno-androst-4-ene-3,6,17-triona foram corroboradas pela determinação do ponto de fusão, espetroscopia de infravermelho, ressonância magnética nuclear e espetroscopia de massa de alta resolução. Seguidamente, com o intuito de determinar a potencial atividade antitumoral de todos os análogos sintetizados, a proliferação celular foi avaliada em diversas linhas humanas tumorais e não-tumorais através do ensaio colorimétrico de brometo de 3-(4,5-dimetiltiazol-2-il)-2,5-difeniltetrazólio (MTT). Os efeitos dos compostos preparados na viabilidade celular foram estudados em células de cancro da próstata dependentes de androgénios (LNCaP), cancro da próstata não-dependentes de androgénios (PC-3), células do cancro da mama expressando REα (MCF-7), células epiteliais normais da próstata (PNT1A), e ainda em fibroblastos humanos normais da derme (NHDF). Além

deste ensaio de viabilidade celular, foram realizados estudos preliminares do mecanismo de ação dos derivados mais promissores nas linhas celulares MCF-7, LNCaP, e PC-3, através do uso de técnicas como a imunocitoquímica, a microscopia de fluorescência e a avaliação da atividade das caspases. Por último, a potencial atividade inibitória da enzima 5AR de todos os derivados, incluindo os arilideno-4-azaesteroides sintetizados durante a execução do projeto de Mestrado, foi determinada através da quantificação de testosterona presente em microssomas de fígado de murganhos por cromatografia líquida de alta eficiência acoplado a um detetor de díodos (HPLC-DAD). Neste contexto, antes de aplicado, o método foi previamente adaptado, otimizado, parcialmente desenvolvido e validado de acordo com as normas estabelecidas pela Agência Europeia do Medicamento (EMA) e pela "*Food and Drug Administration*" (FDA). Adicionalmente, considerando os resultados obtidos, as principais interações entre os compostos mais ativos e a 5AR tipo 2 foram analisadas na tentativa de compreender a REA e de aferir quais as interações essenciais à atividade inibitória.

Vários destes novos arilidenos derivados de esteroides exibiram um interessante efeito de inibição do crescimento de células tumorais, e de uma forma geral revelaram ser menos citotóxicos em células não tumorais, apresentando valores de IC_{50} mais elevados. A redução mais relevante da proliferação celular foi observada após tratamento com os compostos **VB 9e** em células MCF-7 (IC_{50}= 3,47 μM), **VB 10e** em PC-3 (IC_{50}= 6,96 μM) e **VB 11c** em células LNCaP (IC_{50}= 6,48 μM). É igualmente importante referir que os valores de IC_{50} determinados para estes compostos é muito semelhante ao controlo positivo, 5-fluorouracilo (5-FU), um fármaco amplamente usado no tratamento de diversos tumores. Estudos biológicos complementares mostraram que os derivados esteroides **VB 9e** e **VB 11c** pareciam desencadear apoptose em células MCF-7 e LNCaP, respetivamente. O esteroide **VB 9e** causou alterações significativas na marcação com Ki67 (↓) e iodeto de propídio (↑) e causou modificações na morfologia nuclear e análise de distribuição celular em MCF-7. Por outro lado, o composto **VB 11c** causou as mesmas alterações morfológicas e na distribuição celular, e também pareceu levar ao aumento da atividade das caspases-3/7 em LNCaP.

Estudos de "*docking*" molecular mostraram que estes novos derivados apresentam potencialmente uma forte afinidade para as macromoléculas 5AR tipo 2 e CYP17A1, e fraca afinidade para os REα e RA. Relativamente à aromatase, foi verificada uma maior afinidade para as trionas derivadas de esteroides (**VB 11a**-**f**). Para terminar, os principais resultados relativos ao estudo do efeito dos derivados de arilidenoesteroides na atividade da 5AR revelaram que o composto **VB 11c** pareceu ser o inibidor mais potente (IC_{50}=

6,12 nM). Além deste estudo *in vitro,* a análise do interactoma através de ferramentas computacionais foi efetuada e observou-se que o esteroide **VB 11c** apresentou um número significativo de interações em comum com a finasterida, a referência utilizada, comparando com os restantes compostos testados. Curiosamente, neste caso, verificou-se a existência de uma correlação entre dados *in silico* e os dados experimentais.

Em conjunto, os resultados mostraram que o esteroide **VB 11c** parece ser a molécula mais promissora a ser considerada como composto "*hit*", apresentando seletividade para células tumorais da próstata, desencadeando potencialmente o mecanismo de morte celular por apoptose em LNCaP, e sendo a molécula mais potente na inibição *in vitro* da enzima 5AR.

Em conclusão, o trabalho de investigação aqui apresentado constitui um contributo importante para o conhecimento acerca de arilidenos derivados de esteroides como agentes com propriedades antiproliferativas e inibitórias da 5AR. Desta forma, foram aqui abertos novos caminhos para o desenvolvimento de novos inibidores baseados em moléculas esteroides com eventual interesse na HBP e no CP.

Palavras-chave

Arilidenos derivados de esteroides; cancro prostático; hiperplasia benigna da próstata; atividade antiproliferativa; *docking* molecular; inibição da 5α-redutase.

Abstract

The prostate is a male-specific hormone-responsive gland with a crucial role in the male reproductive system and requires androgenic hormones and an androgen receptor (AR) for proper growth and development. Generally, this gland is mainly affected by three pathologies, namely prostatitis, benign prostatic hyperplasia (BPH), and malignant prostate cancer (PCa). These disorders constitute a source of significant morbidity and mortality for men worldwide. Thus, pharmacological therapy's relevance in managing these prostatic disorders is unquestionable.

Currently, it is well established that the importance of steroidal hormones in the pathophysiology of BPH and PCa. In this context, it is known that the abnormally high 5α-reductase (5AR) activity in humans results in excessively high 5α-dihydrotestosterone (DHT) levels in peripheral tissues, which have been mainly implicated in the pathogenesis of BPH and PCa. Therefore, the role of DHT had contributed to the interest in finding 5AR inhibitors (5ARIs), comprising an important and commonly applied strategy principally in the treatment of BPH. Considering the unmet medical need, it is recognized that the 5ARIs clinically used, such as finasteride, exhibit low potency and several adverse side effects that significantly reduce the quality of life of patients. Furthermore, the effect of these drugs in the PCa treatment is controversial, although it seems a valid and logical approach to explore. In this context, arylidenosteroids, a class of modified steroids, have been reported with important antiproliferative activity and also with potential 5AR inhibitory activity.

In the present work, the preparation of novel steroidal arylidene derivatives potentially useful in prostatic diseases, displaying inhibitory capacity against 5AR and/or antiproliferative properties against tumoral cells was intended. Essentially, this thesis aimed the discover of hit compounds for further development in the context of BPH and PCa. To achieve this goal, different synthetic strategies were exploited and new series of steroidal arylidene derivatives were obtained, and their antitumoral and 5AR inhibitory activities were evaluated. Moreover, molecular docking simulations against important targets of steroidal molecules, 5AR type 2, estrogen receptor α (ERα), AR, steroid 17α-hydroxylase/17,20 lyase (CYP17A1), and aromatase, were performed to understand the possible affinity and interactions. This thesis also contemplates the conclusion of the biological evaluation of arylidene-4-azasteroids (**VB 4a-g** and **VB 7a-g**) synthesized at the Master's project and a comprehensive three-dimensional quantitative structure-activity relationship (3D-QSAR study considering the antiproliferative activity in

prostate cells, since this work fits into the context of this thesis. In relation to this last part, robust 3D-QSAR models generated to elucidate the relation of the proliferation of LNCaP (androgen-dependent) and PC-3 (non-androgen dependent) cells and the structure of tested compounds showed the importance of the presence of bulky groups and electronegative atoms.

Concerning the doctoral project, after several failed attempts to prepare new 3-,4- and 6-azasteroids modified at D-ring with fused/attached heterocycles, a new synthetic strategy was studied and applied and three distinct series of novel arylidene oxidized steroids were successfully obtained from dehydroepiandrosterone. The chemical structures and high purity of the new 16*E*-arylidene-5α,6α-epoxyepiandrosterone, 16*E*-arylidene-3β,5α,6β-trihydroxyandrosten-17-one, and 16*E*-arylidene-androst-4-ene-3,6,17-trione derivatives were corroborated by melting point determination, infrared spectroscopy, nuclear magnetic resonance spectroscopy, and high-resolution mass spectroscopy. Then, to determine their antitumoral potential, the activity of all synthesized analogs over the viability of tumoral cells was evaluated against several human tumoral and non-tumoral cell lines were assessed by (4,5-dimethylthiazol-2-yl)-2,5-diphenyltetrazolium bromide (MTT) assay. The effect of compounds on cell proliferation was evaluated against prostate cancer androgen-dependent cells (LNCaP), prostate cancer non-androgen dependent cells (PC-3), breast cancer cell line (MCF-7), normal prostate epithelium cells (PNT1A), and normal human dermal fibroblasts (NHDF). Furthermore, preliminary studies of the mechanism of action of the most promising derivatives were performed in MCF-7, LNCaP, and PC-3 cell lines using techniques, such as immunocytochemistry, fluorescence microscopy, and caspase activity assessment. Lastly, the potential 5AR inhibitory activity of all compounds, including the arylidene-4-azasteroids synthesized during the Master's project, were determined through testosterone quantification in mice liver microsomes by high-performance liquid chromatography coupled to a diode array detector (HPLC-DAD). This method was previously adapted, partially developed and validated, also in the context of the present project. Moreover, from the results of this assay, the main interactions of the best compounds against 5AR type 2 was also evaluated in the attempt of understanding the structure-activity relationship.

Several of these new steroidal derivatives exhibited an interesting growth-inhibition effect on human tumoral cells, and generally, these tested compounds revealed to be less cytotoxic to non-tumoral cells producing higher IC_{50} values. The most relevant reduction of cell proliferation was observed with compounds **VB 9e** in MCF-7 cells (IC_{50}= 3.47

μM), **VB 10e** in PC-3 cells (IC_{50}= 6.96 μM), and **VB 11c** in LNCaP cells (IC_{50}= 6.48 μM). Moreover, the determined IC_{50} values of these compounds are very similar to the positive control, 5-fluouracil (5-FU). Additional biological studies showed that steroidal derivatives **VB 9e** and **VB 11c** seemed to trigger apoptosis in MCF-7 and LNCaP cells, respectively. **VB 9e** caused significant alterations in Ki67 (↓) and propidium iodide (↑) staining and modifications in nuclear morphology and cell distribution analysis in MCF-7 cells. On the other hand, **VB 11c** caused the same morphological and cell distribution alterations, and also seemed to increase the activity of caspase-3/7 in the LNCaP cell line.

Molecular docking studies showed that these new derivatives presented stronger affinity to 5AR type 2 and CYP17A1, and poor affinity to ERα and AR. Relative to aromatase, it was verified higher affinity for steroidal 4-ene-3,6,17-triones. To finish, the effect of the steroidal arylidene derivatives on 5AR activity and the main results revealed that compound **VB 11c** seemed to be the most potent inhibitor (IC_{50}= 6.12 nM). In addition, the *in silico* interactome study was performed and it was observed that this steroid displayed a higher number of interactions in common with finasteride, the reference, compared with other tested compounds. Interestingly, in this case, there is a correlation between *in silico* and experimental data.

Taken together, the results showed that steroid **VB 11c** seemed to be the most promising molecule to be considered as a hit compound, presenting selectivity to tumoral prostate cells, potentially triggering the apoptotic cell death mechanism in the LNCaP cell line, and being the most potent against 5AR.

In conclusion, the research work constitutes an important contribution to the knowledge concerning steroidal arylidene derivatives as agents with antiproliferative and 5AR inhibitory properties. Therefore, new paths were opened, showing the possibility of successfully developing potential new inhibitors based on steroid molecules for further development in the context of BPH and PCa.

Keywords

Steroidal arylidene derivatives; prostate cancer; benign prostatic hyperplasia; antiproliferative activity; molecular docking; 5α-reductase inhibition.

Table of Contents

Resumo Alargado xv
Abstract xix
List of Figures xxix
List of Tables xxxix
List of Abbreviations xliii
List of Publications and Communications xlvii
Chapter I
1. General Introduction 1
1.1. Overview on principal prostatic diseases and main therapeutical approaches 1
1.1.1. The prostate gland 1
1.1.2. Benign prostatic hyperplasia 2
1.1.2.1. Pathophysiology 2
1.1.2.2. The role of androgens in the disease development 3
1.1.2.3. Therapeutic approaches 6
1.1.3. Prostatic cancer 16
1.1.3.1. Pathophysiology 17
1.1.3.2. Steroidal requirements in prostate cancer 20
1.1.3.3. Therapeutic approaches 23
1.2. Arylidenosteroids as bioactive molecules 39
1.2.1. Synthetic approaches to prepare arylidenosteroids 41
1.2.2. Bioactivity of 2- and 16*E*-arylideneandrostane derivatives 44
1.2.3. Bioactivity of 21*E*-arylidenepregnane derivatives 49
1.2.4. Bioactivity of 16*E*-arylidenoestrone and 16*E*-arylidenoestradiol derivatives 51
1.2.5. Relevance of steroidal arylidene derivatives as synthetic intermediates of bioactive compounds 53
1.3. Drug discovery and development process 63
1.3.1. Drug discovery 64
1.3.2. Preclinical and clinical trials 69
1.3.3. Approval and post-market monitoring 72

1.3.4. Other approaches and concepts in drug discovery and development 73
1.4. Objectives of this thesis 78
Chapter II.
2. Development of new azasteroids with potential interest in prostatic diseases 81
2.1. Studies on 4-aza-arylidene derivatives as cell growth inhibitors 81
2.1.1. Introduction 81
2.1.2. Results and discussion 83
2.1.2.1. *In vitro* biological studies 83
2.1.2.1.1. Screening of cell proliferation effects 83
2.1.2.1.2. Characterization of the cytotoxic effect 85
2.1.2.2. *In silico* studies 89
2.1.2.2.1. Molecular docking studies 89
2.1.2.2.2. 3D-QSAR analysis 90
2.1.3. Experimental section 94
2.1.3.1. General remarks 94
2.1.3.2. Biological studies 94
2.1.3.2.1. Cell culture 94
2.1.3.2.2. MTT cell proliferation assay 95
2.1.3.2.3. Fluorescence microscopy 95
2.1.3.2.4. Cell nuclear morphology and distribution analysis using ImageJ 96
2.1.3.2.5. Caspase-9 activity assay 96
2.1.3.2.6. Statistical analysis 96
2.1.3.3. *In silico* studies 97
2.1.3.3.1. Molecular docking 97
2.1.3.3.1.1. Preparation of protein and ligands 97
2.1.3.3.1.2. Grid map parameters 97
2.1.3.3.1.3. Method validation and molecular docking simulations 97
2.1.3.3.2. 3D-QSAR modeling 98
2.1.3.3.2.1. Biological data and molecular structures compilation 98

2.1.3.3.2.2. Molecular alignment and calculation of field descriptors and PLS regression 98

Chapter III.

3. Novel 16*E*-arylidene-5α,6α-epoxyepiandrosterone derivatives: synthesis, *in vitro* biological evaluation and *in silico* studies 99

3.1. Introduction 99

3.2. Results and discussion 100

3.2.1. Chemical synthesis 100

3.2.2. Biological evaluation 103

3.2.2.1. Antiproliferative activity 103

3.2.2.2. Characterization of effects on cell proliferation 106

3.2.3. Molecular docking studies 109

3.3. Experimental section 111

3.3.1. General remarks 111

3.3.2. Chemical synthesis 112

3.3.3. Biological evaluation 118

3.3.3.1. Cell culture 118

3.3.3.2. Preparation of compounds solutions 118

3.3.3.3. MTT cell proliferation assay 118

3.3.3.4. Immunocytochemistry assay 119

3.3.3.5. Propidium iodide incorporation 120

3.3.3.6. Analysis of cell nuclear morphology and distribution using ImageJ 120

3.3.3.7. Statistical analysis 120

3.3.4. Molecular docking 121

3.3.4.1. Preparation of macromolecules and ligands 121

3.3.4.2. Grid map parameters 121

3.3.4.3. Method validation and molecular docking simulations 121

Chapter IV.

4. Synthesis, antiproliferative activity and *in silico* studies of new series of steroidal 3β,5α,6β-triols and 4-ene-3,6,17-triones 123

4.1. Introduction 123

4.2. Results and discussion 125

4.2.1. Chemical synthesis 125
4.2.2. Biological evaluation 127
4.2.2.1. Antiproliferative activity 127
4.2.2.2. Characterization of effects on cell proliferation 130
4.2.3. Molecular docking studies 135
4.3. Experimental section 136
4.3.1. General remarks 136
4.3.2. Chemical synthesis 136
4.3.3. Biological evaluation 140
4.3.3.1. Cell culture 140
4.3.3.2. Preparation of compounds solutions 140
4.3.3.3. MTT cell proliferation assay 140
4.3.3.4. Fluorescence microscopy 140
4.3.3.5. Analysis of cell nuclear morphology and distribution using ImageJ 141
4.3.3.6. Caspase-3/7 activity assay 141
4.3.3.7. Statistical analysis 141
4.3.4. Molecular docking 141
4.3.4.1. Preparation of macromolecules and ligands 141
4.3.4.2. Grid map parameters 142
4.3.4.3. Method validation and molecular docking simulations 142

Chapter V.

5. **Screening of 5α-reductase *in vitro* inhibitory activity of steroidal arylidene derivatives** 143
5.1. Introduction 143
5.2. Results and discussion 145
5.2.1. Optimization studies and method validation 145
5.2.2. Studies on inhibitory 5α-reductase activity of steroidal arylidene derivatives 149
5.2.3. *In silico* analysis of interactions of the most potent derivatives with 5α-reductase enzyme 152
5.3. Experimental section 156
5.3.1. Reagents and solvents 156
5.3.2. Animals 156
5.3.3. Preparation of mice liver microsomes 157

5.3.4. Measurement of *in vitro* 5α-reductase activity using HPLC-DAD 157
5.3.4.1. Apparatus 157
5.3.4.2. Method adaptation, optimization, and validation 157
5.3.4.2.1. Partial method development 157
5.3.4.2.2. Method validation 158
5.3.4.3. *In vitro* 5α-reductase activity assay 159
5.3.4.4. Quantification of testosterone using HPLC-DAD 160
5.3.5. Statistical analysis 161
5.3.6. Molecular docking interaction studies 161
Chapter VI.
6. General Discussion 163
Chapter VII.
7. Conclusions and Future Perspectives 177
Chapter VIII.
8. References 181
Appendices
Appendix 1 225
Appendix 2 229
Appendix 3 231
A.3. Attempts to synthesize new 3-, 4- and 6-azasteroids 231
A.3.1. Introduction 231
A.3.2. Results and discussion 232
A.3.2.1. Approaches to synthesize 3- and 6-azasteroids 232
A.3.2.2. Approaches to prepare new 4-azasteroids 235
A.3.3. Experimental section 244
A.3.3.1. General remarks 244
A.3.3.2. Chemical synthesis: procedures of the attempts 245
Appendix 4 253
Appendix 5 255
Appendix 6 257
Appendix 7 259

List of Figures

Figure 1	Zones and regions of the prostate. *Adapted from Reeves et al. (2016) and De Marzo e. al. (2007).*	1
Figure 2	Androgen and androgen receptor (AR) signaling in the prostate cells. After testicular synthesis, testosterone is transported to target tissues and converted into 5α-dihydrotestosterone (DHT) by 5α-reductase (5AR). DHT binds to the ligand-binding pocket and promotes the dissociation of heat-shock proteins (Hsp) from the AR. Then, the AR translocates into the nucleus, dimerizes, and binds in the promoter region to the AR target genes, such as prostate-specific antigen (PSA) and transmembrane protease serine 2 (TMPRSS2).[38,41] Created with BioRender.com.	4
Figure 3	Simplified pathway of androgens biosynthesis and metabolism. *Adapted from Singh et al. (2005).* Created with BioRender.com.	6
Figure 4	Current therapeutic approaches to treat and manage benign prostatic hyperplasia (BPH) symptomatology. Created with BioRender.com.	7
Figure 5	Current drugs approved by Food and Drug Administration (FDA) and European Medicines Agency (EMA) for benign prostatic hyperplasia (BPH) treatment. Created with ChemDraw and BioRender.com.	8
Figure 6	Molecular structure of fedovapagon, a vasopressin V2 receptor agonist developed to treat nocturia. Created with ChemDraw.	16
Figure 7	Incidence and mortality of most common type of cancer in each country among men in 2020. The cancer type with the most incidence in developed countries is prostate cancer (PCa) – **green** – (America, Europe, Africa, and Oceania), being the second deathliest behind lung cancer. *Adapted from Sung et al. (2020*).	17
Figure 8	Gleason grading system currently applied. It was modified and implemented by the International Society of Urological Pathology, in 2015. Gleason patterns (1 to 5) correspond to different patterns of growth for prostatic adenocarcinomas. The Gleason score results from the sum of the two most common Gleason grades. *Retrieved from Shah and Zhou (2016).*	19
Figure 9	The standard model of the development and progression of prostatic cancer (PCa) based on genetic and epigenetic	20

	events. Overexpression of genes is shown with the arrow (↑), downregulation of expression with the arrow (↓) and, the deletion or inactivation of the tumor-suppressor genes is shown as (loss). *Adapted from Vasioukhin (2004) and Knudsen et. al (2010).*	
Figure 10	Treatment options for prostatic cancer (PCa). Created with BioRender.com.	24
Figure 11	The hypothalamic-pituitary-gonadal axis and targets for hormonal therapy agents in prostatic cancer (PCa). ACTH= Adrenocorticotropic hormone, GnRH-R = GnRH receptor, LH-R = Luteinizing hormone receptor, PR = Progesterone receptor, T = Testosterone. *Adapted from Nelson et al. (2020).*	25
Figure 12	Drugs approved for clinical use in the chemotherapy of metastatic castration-resistant prostatic cancer (CRPC). Created with ChemDraw.	33
Figure 13	Poly (ADP-ribose) polymerase (PARP) inhibitors approved for clinical use in metastatic castration-resistant prostatic cancer (CRPC) treatment. Created with ChemDraw.	35
Figure 14	Chemical structure and numbering of the basic steroid skeleton (gonane), and classification of steroids based on the number of carbons in the molecule. Created with ChemDraw.	39
Figure 15	16E- and 21*E*-Arylidenosteroids prepared by Claisen-Schmidt condensation. Created with ChemDraw.	42
Figure 16	Synthesis of 16*E*-arylidenosteroids from **1** and dehydroepiandrosterone (DHEA), using KF/Al_2SO_3 or KF/Al_2O_3 as catalysts in EtOH, under reflux. Created with ChemDraw.	43
Figure 17	Synthesis of 21*E*-arylidenepregnenolone acetate derivatives catalyzed by I_2-Al_2O_3 under microwave (MW) irradiation. Created with ChemDraw.	43
Figure 18	An alternative route to prepare 16*E*-arylidenoestrane derivatives by the employment of Mizoroki–Heck reaction. Created with ChemDraw.	44
Figure 19	Synthetic routes for preparation of steroidal arylpyrazolines from 16*E*- and 21*E*-arylidenosteroids. Created with ChemDraw.	54
Figure 20	Different pathways to synthesize steroidal arylpyrimidines and pyridines from 16*E*- and 21*E*-arylidenosteroids. Created with ChemDraw.	56

Figure 21	Synthesis of steroidal spiro-oxindoles and spiro-pyrrolidines from 16*E*-arylidenosteroids. Created with ChemDraw.	57
Figure 22	Overview of drug discovery and development process: drug discovery, preclinical and clinical trials. *Adapted from Gallego et al. (2021).*	64
Figure 23	Scheme of quantitative structure-activity relationship (QSAR)-based virtual screening (VS) approach in hit discovery. *Adapted from Neves et al. (2018).*	68
Figure 24	Map of interactions of human polypharmacology showing the relationship between proteins in the chemical space. Two proteins are interacting in chemical space (edge) if both bind one or more compounds within a defined difference in binding energy threshold. The number of proteins in this network is 486 (nodes), with 3,636 polypharmacology interactions (edges). *Adapted from Paolini et al. (2006) and Hopkins et al.* (2008).	74
Figure 25	Role of collaboration between academia and pharma/biotech industries in drug discovery and development. *Adapted from Flier et al. (2019).*	77
Figure 26	Flowchart of specific objectives of the present doctoral project (3D-QSAR= Three-dimensional quantitative structure-activity relationship, 5AR= 5α-reductase).	80
Figure 27	5α-Reductase inhibitors (5ARIs) approved for clinical use in the treatment of benign prostatic hyperplasia (BPH). Created with ChemDraw.	81
Figure 28	Preparation of novel 4-azasteroids from testosterone (**A**) and progesterone (**B**), and respective R group. Reactional conditions: **a**) PCC, DCM, r.t., 3 h; **b**) $NaIO_4$, $KMnO_4$, Na_2CO_3, *i*-PrOH, reflux, 3 h; **c**) ammonium acetate, GAA, reflux, 4 h; **d**) KOH, aldehyde, EtOH, r.t., 12-24 h. (PCC = Pyridinium chlorochromate, DCM = dichloromethane, GAA = Glacial acetic acid). Created with ChemDraw and BioRender.com.	83
Figure 29	Screening MTT screening results. Relative cell proliferation of PC-3 cells exposed to the compounds previously synthesized, substrates, DHT, finasteride, and 5-FU for 72 h at a concentration of 30 μM. The cell proliferation was determined by the MTT assay, spectrophotometrically quantifying formazan at 570 nm. Data are expressed as a percentage of cell proliferation in comparison with the negative control and are indicated as mean±SD and are representative of at least two independent experiments. *$p< 0.05$ vs the control	84

	(the Student *t*-test). (DHT= 5α-Dihydrotestosterone, 5-FU= 5-Fluorouracil).	
Figure 30	PI/Hoechst 33342 staining results. T47-D cells were incubated for 24, 48, and 72 h with 5-FU and **VB 7g** at 20 μM. Untreated cells are considered the control of the experiment. Cells were visualized in an Optical microscope Olympus CKX41 coupled to a digital camera (Olympus SP-500UZ) and in an Axio Imager A1 microscope (fluorescence). The resulting images were treated in ImageJ software. (PI= Propidium iodide, 5-FU= 5-Fluorouracil).	86
Figure 31	Ratio of PI/Hoechst 33342 staining results. T47-D cells were incubated during 24, 48, and 72 h with 5-FU and **VB 7g** at 20 μM. Untreated cells are considered the control of the experiment. Cells were visualized in an Axio Imager A1 microscope and the resulting images were treated in ImageJ. Data are indicated as mean±S*D* and are representative at least two independent experiments. **p*< 0.05 compared to control. (PI= Propidium iodide, 5-FU= 5-Fluorouracil).	87
Figure 32	(**A**) T47-D nuclear area of cells untreated (control) and cells treated with 5-fluorouracil (5-FU) and **VB 7g** at 20 μM, incubated 24, 48, and 72 h; (**B**) Nearest neighbor analysis of T47-D cells with the same conditions referred previously. Data are indicated as mean±S*D* and are representative at least two independent experiments. **p*< 0.05 compared to control.	87
Figure 33	T47-D cells stained with Hoechst 33342, after treatment with **VB 7g** during 72 h. Pycnotic cells with circular morphology are indicative of apoptosis.	88
Figure 34	T47-D caspase-9 activity results. Cells were treated for 48 h with doxorubicin (DOX) at 10 μM, as the positive control, and **VB 7g** at 10 and 20 μM, and the results are relative to untreated cells (control). The activity of caspase–9 was evaluated using a Caspase-Glo kit from Promega. Data are indicated as mean±SD and are representative at least two independent experiments. **p*< 0.05 compared to control.	88
Figure 35	Predicted *vs*. determined values of relative cell proliferation of LNCaP (**A**) and PC-3 (**B**) cells for training set (**blue**) and test set compounds (**red**).	92
Figure 36	PLS coefficient contour maps of the 3D-QSAR model with all superposed compounds (LNCaP). **(A)** Steric effects. **Green** (0.0015): bulky groups are prohibited, **yellow** (−0.003): bulky groups are favored. **(B)**	93

	Electrostatic potential. **Blue** (0.001): groups with positive partial charges are favored, **red** (−0.001): groups with negative partial charges are favored. (Favored = favors a decrease in cell proliferation). (PLS= Partial least squares, 3D-QSAR= Three-dimensional quantitative structure-activity relationship).	
Figure 37	PLS coefficient contour maps of the 3D-QSAR model with all superposed compounds (PC-3). **(A)** Steric effects. **Green** (0.0015): bulky groups are prohibited, **yellow** (−0.003): bulky groups are favored. **(B)** Electrostatic potential. **Blue** (0.001): groups with positive partial charges are favored, **red** (−0.001): groups with negative partial charges are favored. (Favored = favors a decrease in cell proliferation). (PLS= Partial least squares, 3D-QSAR= Three-dimensional quantitative structure-activity relationship).	94
Figure 38	Synthetic route to prepare novel 16*E*-arylidene-5α,6α-epoxyepiandrosterone derivatives (**VB 9a-m**). Reagents and conditions: **a**) aldehyde, aq. sol. KOH 50 %, EtOH, r.t., 2-24 h; **b**) MMPP, DCM/water, 5 °C, 24-30 h. (MMPP= Magnesium monoperoxyphthalate, DCM= dichloromethane). Created with ChemDraw.	101
Figure 39	Results of preliminary studies of cell viability at two concentrations, 10 and 50 μM in NHDF, PNT1A, LNCaP, PC-3 and MCF-7 cell lines. The effect of all the synthesized final products, during 72 h, was evaluated and 5-fluorouracil (5-FU) was used as positive control. Data are indicated as mean±SD and are representative at least two independent experiments. *$p<$ 0.05 in relation to a negative control (Student's *t*-test).	104
Figure 40	Results of Ki67 (**A**) and PI (**B**) staining in MCF-7 cells after treatment with 5-FU, as positive control, and **VB 9e** at concentrations 1 and 10 μM, during 48 h. Data are indicated as means±SEM and are representative at least two independent experiments. *$p<$ 0.05, ****$p<$ 0.0001 in relation to the negative control (ordinary one-way ANOVA test). (PI= Propidium iodide, 5-FU= 5-Fluorouracil).	107
Figure 41	Representative photomicrographs of MCF-7 cell line after (**A**) Hoechst-33342/Ki67 and (**B**) Hoechst-33342/PI staining. Cells were treated with 5-FU, as positive control, and **VB 9e** at 1 and 10 μM, during 48 h. (PI= Propidium iodide, 5-FU= 5-Fluorouracil).	108
Figure 42	(**A**) MCF-7 nuclear area of cells untreated (control) and cells treated with 5-fluorouracil (5-FU) and **VB 9e** at 1 and 10 μM, incubated during 48 h; (**B**) Nearest neighbor	109

	analysis of MCF-7 cells in the same conditions referred previously. Data are indicated as mean±SD and are representative at least two independent experiments. **p*< 0.05, ***p*< 0.01, ****p*< 0.001, *****p*< 0.0001 compared to control (unpaired two tailed Student's *t*-test).	
Figure 43	Representative examples of oxidized pregnenolone derivatives with relevant antiproliferative activity against PC-3 cells and/or with important 5α-reductase (5AR) inhibitory activity. ***(A)*** ***21***-benzoyloxypregna-4,16-diene-3,6,20-trione, (***B***) 21(*p*-fluoro)benzoyloxypregna-4,16-diene-3,6,20-trione and (**B**) 21(*p*-fluoro)benzoyloxy-5α-hydroxypregn-16-en-3,6,20-trione derivatives and respective percentage (%) of inhibition of PC-3 cell proliferation at 50 μM and/or IC_{50} values against 5AR type 1 and 2. Created with ChemDraw.	124
Figure 44	Synthetic pathway to obtain new steroidal 3β,5α,6β-triols (**VB 10a-f**) and 4-ene-3,6,17-triones (**VB 11a-f**). Reagents and conditions: **a)** MMPP, DCM/water, 5 °C, 24-30 h; **b)** $HClO_4$, acetone/water, r.t., 5 h; **c)** PCC, DMC, r.t., N_2, 24 h. (PCC = Pyridinium chlorochromate, DCM = Dichloromethane). Created with ChemDraw.	126
Figure 45	Results of preliminary studies of cell viability at two concentrations, 10 and 50 μM in NHDF, PNT1A, LNCaP, PC-3 and MCF-7 cell lines. The effect of all the synthesized final products, during 72 h, was evaluated and 5-fluorouracil (5-FU) was used as positive control. Data are indicated as mean±SD and are representative at least two independent experiments. **p*< 0.05 in relation to a negative control (Student's *t*-test).	128
Figure 46	Microphotographs taken after incubation of LNCaP cells with 5-fluorouracil (5-FU) and **VB 11c** at 20 μM (24, 48, and 72 h). Untreated cells are considered the control of the experiment. Cells were visualized in an Optical microscope Olympus CKX41 coupled to a digital camera (Olympus SP-500UZ) (zoom 100 ×).	131
Figure 47	Microphotographs taken after incubation of PC-3 cells with 5-fluorouracil (5-FU) and **VB 10e** at 20 μM (24, 48, and 72 h). Untreated cells are considered the control of the experiment. Cells were visualized in an Optical microscope Olympus CKX41 coupled to a digital camera (Olympus SP-500UZ) (zoom 100 ×).	132
Figure 48	(**A**) LNCaP nuclear area of cells untreated (control) and cells treated with 5-fluorouracil (5-FU) and **VB 11c** at 20 μM, incubated during 24, 48, and 72 h; (**B**) Nearest	133

	neighbor analysis of LNCaP cells in the same conditions referred previously. Data are indicated as mean±S*D* and are representative at least two independent experiments. **p*< 0.05, ***p*< 0.01, ****p*< 0.001, *****p*< 0.0001 compared to control (unpaired two tailed Student's *t*-test).	
Figure 49	(**A**) PC-3 nuclear area of cells untreated (control) and cells treated with 5-fluorouracil (5-FU) and **VB 10e** at 20 μM, incubated during 24, 48 and 72 h; (**B**) Nearest neighbor analysis of PC-3 cells in the same conditions referred previously. Data are indicated as mean±SD and are representative at least two independent experiments. **p*< 0.05, ***p*< 0.01, ****p*< 0.001, *****p*< 0.0001 compared to control (unpaired two tailed Student's *t*-test).	133
Figure 50	Assessment of apoptosis: Caspase-Glo® 3/7 assay results after 72 h of treatment with **VB 11c** at concentrations 10 and 20 μM, in LNCaP cells. Data are shown as mean percentage of caspase 3/7 activity referred to the untreated control (100 %)±SD. DOX and 5-FU were used as positive control. *****p*< 0.001 (Student's *t*-test), N = 2, *n* = 4. (DOX= Doxorubicin, 5-FU= 5-Fluorouracil).	134
Figure 51	Indirect method to access 5α-reductase (5AR) activity by the measurement of the substrate, testosterone. When occurs enzymatic activity inhibition, concentration of remaining testosterone, [T], is higher than concentration at normal activity of 5AR. (NADPH= Nicotinamide adenine dinucleotide phosphate, DHT= 5α-Dihydrotestosterone). Created with ChemDraw and BioRender.com.	145
Figure 52	Chromatogram of overlapping of testosterone peaks at different wavelengths (210, 240, 245, 250, and 260 nm).	146
Figure 53	Molecular structure of testosterone and the selected internal standard (IS), perampanel (PER). Created with ChemDraw.	147
Figure 54	Representative chromatogram obtained by HPLC-DAD (λ = 245 nm) and identification of peaks (testosterone, compound to be quantified, and perampanel (PER), the internal standard, IS).	147
Figure 55	5α-Reductase (5AR) inhibition screening results. Compounds that showed % inhibition > 85 % in the 10 μM screening were selected for a last screening at a lower concentration (1 μM). Steroids with inhibitory activity > 80 % were chosen for the determination of IC_{50} values.	150

	Finasteride was used as reference (positive control). Data shown are representative of at least two independent experiments and two replicates (N ≧ 2, *n*= 2). Statistical analysis was performed using Student's *t*-test, **p*< 0.05; ***p*< 0.01; ****p*< 0.001; *****p*< 0.0001. (NC = Negative control). **Blue**: 4-aza-androstenes; **red**: 4-azapregnenes; **green**: epoxyepiandrosterone derivatives; **light gray**: steroidal 3β,5α,6β-triols; **dark grey**: steroidal 3,6,17-triones	
Figure 56	Predicted 5α-reductase (5AR) interactions with finasteride. **Light green** = van der Waals interactions; **Green =** conventional hydrogen bond; **Pink =** alkyl/π-alkyl interactions. Created with BIOVIA Discovery Studio.	152
Figure 57	2D analysis of predicted 5α-reductase (5AR) interactions with *in vitro* most potent compounds **VB 7b**, **VB 9f**, **VB 9h**, **VB 9j**, and **VB 11c** (and finasteride). Created with BIOVIA Discovery Studio.	155
Figure 58	Overview on the synthetic pathway to obtain new series of steroidal arylidene derivatives, including 16*E*-arylidene-5α,6α-epoxyepiandrosterone derivatives, and steroidal 3β,5α,6β-triols and 4-ene-3,6,17-triones. Reactional conditions: **a)** aldehyde, aq. sol. KOH 50 %, EtOH, r.t., 2-24 h (η= 71-98 %); **b)** MMPP, DCM/water, 5 °C, 24-30 h (η= 33-87 %); **c)** $HClO_4$, acetone/water, r.t., 5 h (η= 82-95 %); **d)** PCC, DCM, N_2, r.t., 24 h (η= 20-70 %). (MMPP = Magnesium monoperoxyphthalate, DCM = Dichloromethane, PCC = Pyridinium chlorochromate). Created with ChemDraw.	166
Figure 59	Structure-activity relationship (SAR) analysis of 16*E*-arylidene-dehydroepiandrosterone derivatives in relation to antiproliferative activity. Created with ChemDraw and BioRender.com.	170
Figure 60	Heatmap of binding energies of the new series of 16*E*-arylidene-dehydroepiandrosterone derivatives against important targets of steroids **Red** is indicative of poor affinity, while **green** is indicative of strong affinity. (5AR= 5α-Reductase, ERα= Estrogen receptor α, AR= Androgen receptor, CYP17A1= Steroid 17α-hydroxylase/17,20 lyase).	172
Figure 61	Structure-activity relationship (SAR) analysis of steroid **VB 11c** for antiproliferative and 5α-reductase (5AR) inhibitory activities. Created with ChemDraw and BioRender.com.	175
Appendices		
Figure Ap 1	Attempt to prepare 3-azasteroids from testosterone. Reactional conditions: **a)** $NH_2OH.HCl$, pyridine, 6 h,	232

	reflux; **b)** $SOCl_2$/dioxane, toluene, 15 °C. Created with ChemDraw.	
Figure Ap 2	Attempts to synthesize 6-azasteroids from pregnenolone acetate using two different approaches. Reactional conditions: **a)** ACN/H_2O, NHPI/$NaClO_2$, 6 h, 50 °C; **b)** Na_2CO_3, $NaIO_4$/$KMnO_4$, *i*-PrOH, reflux; **c) 1**. *m*-CPBA, 6 h, r.t., **2.** Jones reagent/acetone/DCM, 3 h, 50 °C; **d)** CH_3COONH_4, GAA, reflux. (DHEA= Dehydroepiandrosterone, ACN= Acetonitrile, DMSO= dimethyl sulfoxide, GAA= Glacial acetic acid). Created with ChemDraw.	235
Figure Ap 3	Attempt to synthesize the arylpyrimidine **A7** from a 4-azasteroid derivative (**VB 4a**) previously prepared. Reactional conditions: **a)** 3-AT, *t*-BuOK, *t*-BuOH, reflux. (3-AT= 3-Amino-1,3,4-triazole). Created with ChemDraw.	236
Figure Ap 4	Attempt of obtain a new arylpyrazoline from a 21*E*-arylidene-4-azasteroidal derivative (**A8**) already synthesized (**VB 7b**). Reactional conditions: **a)** $NH_2NH_2.H_2O$, GAA, reflux. (GAA= Glacial acetic acid). Created with ChemDraw.	237
Figure Ap 5	Preparation of a steroidal arylpyrazoline from pregnenolone. Reactional conditions: **a)** benzaldehyde, aq. sol. KOH 50 %, EtOH, 24 h, r.t.; **b) 1.** $NH_2NH_2.H_2O$, GAA, 5 h, reflux; **2.** acetic anhydride, pyridine, 8 h, r.t.. (GGA= Glacial acetic acid). Created with ChemDraw.	238
Figure Ap 6	Pathway to prepare steroidal arylpyrazolines from DHEA. Reactional conditions: **a)** benzaldehyde, aq. sol. KOH 50 %, EtOH, 24 h, r.t.; **b)** $NH_2NH_2.H_2O$, GAA, 3 h, reflux; **c)** acetic anhydride, DMAP, THF, 5 h, r.t.. (DHEA= Dehydroepiandrosterone, GAA= Glacial acetic acid, DMAP= 4-Dimethylaminopyridine, THF= Tetrahydrofuran) Created with ChemDraw.	239
Figure Ap 7	Synthesis of D-ring fused arylpyrazoline-4-aza-androstene derivative from a 16*E*-aryl-4-azasteroid (**VB 4b**) already synthesized. Reactional conditions: **a)** $NH_2NH_2{\cdot}H_2O$, GAA, 3 h, reflux. (GAA= Glacial acetic acid). Created with ChemDraw.	240
Figure Ap 8	Attempt of synthesis of steroidal arylpyrimidines attached to the D-ring from a 21*E*-arylideneandrostene derivative (**A9**). Reactional conditions: **a)** 3-AT, *t*-BuOK, *t*-BuOH, reflux (3-AT= 3-Amino-1,3,4-triazole). Created with ChemDraw.	241
Figure Ap 9	Synthetic pathway to prepare steroidal arylpyridones from testosterone. Reactional conditions: **a)** PCC, DCM, 3 h, r.t.; **b**) benzaldehyde, aq. sol. KOH 50 %, EtOH, 2 days, r.t.; **c)** ethyl cyanoacetate, ammonium acetate, EtOH, 24 h, reflux. (PCC= Pyridinium chlorochromate, DCM= Dichloromethane). Created with ChemDraw.	242

Figure Ap 10	Attempts of preparation of new steroidal fused/attached D-ring arylpyridones from different 4-azasteroids previously synthesized. Reactional conditions: **a)** ethyl cyanoacetate, ammonium acetate, EtOH, 1-6 days, reflux. Created with ChemDraw.	243
Figure Ap 11	Attempt to prepare steroidal derivatives with a heterocycle fused to the D-ring from dehydroepiandrosterone (DHEA) and from the 4-aza-androstene **VB 3**. Reactional conditions: **a)** $CuBr_2$ (II), MeOH, 20 h, reflux; **b)** thiourea, NEt_3, EtOH, 2 days, reflux. Created with ChemDraw.	244
Figure Ap 12	Representative photograph shots of MCF-7 cells after 48 h of treatment with 5-fluorouracil (5-FU) and steroid **VB 9e** at 1 and 10 μM, and respective negative control (optical microscope coupled with a digital camera, zoom: 100 ×).	255
Figure Ap 13	Overlap of chromatograms of all tested mobile phase constitutions [water/acetonitrile (ACN): 50/50, 45/55, 40/60, and 30/70].	257
Figure Ap 14	Internal standard (IS) selection – overlap of chromatograms of potential IS (in **black**) and testosterone (in **pink**). (**A**) Stiripentol, (**B**) perampanel, (**C**) tolbutamide, (**D**) ketoconazole, and (**E**) hydrocortisone.	257
Figure Ap 15	Auxiliar figure of molecular structures of starting materials and synthesized steroids **VB 4a-g** and **VB 7a-g**. Created with ChemDraw.	259
Figure Ap 16	Auxiliar figure of molecular structures of steroidal epoxides **VB 9a-m**, triols **VB 10a-f**, and triones **VB 11a-f**. Created with ChemDraw.	260
Figure Ap 17	Auxiliar figure of molecular structures of important reference compounds in the context of the present thesis. Created with ChemDraw.	261

List of Tables

Table 1	Relevant drug candidates that may exert beneficial outcomes in the treatment of symptoms associated with the benign prostatic hyperplasia (BPH), mechanism of action, and respective references.	13
Table 2	Principal ongoing clinical trials with respect to drug therapy of benign prostatic hyperplasia (BPH).	16
Table 3	Approved drugs for clinical use in prostate cancer (PCa) treatment targeting androgen signaling, and respective mechanism of action. Molecular structures were created with ChemDraw.	29
Table 4	Principal ongoing clinical trials for novel agents in prostatic cancer (PCa) treatment.	36
Table 5	Examples of relevant compounds that may exert beneficial outcomes in the treatment of prostatic cancer (PCa), biological data, and respective references. Molecular structures created with ChemDraw.	37
Table 6	Representative examples of bioactive 2- and 16*E*-arylideneandrostane derivatives. Positive controls, when shown, are identified by the (+) symbol. Molecular structures created with ChemDraw.	47
Table 7	Examples of the most active 21*E*-arylidenepregnene derivatives. Positive controls, when shown, are identified by the (+) symbol. Molecular structures created with ChemDraw.	50
Table 8	The most representative examples of active 16*E*-arylidenoestrone and -estradiol derivatives. Positive controls, when shown, are identified by the (+) symbol. Molecular structures created with ChemDraw.	52
Table 9	The most representative active heterocyclic steroidal derivatives obtained from arylidenosteroids. Positive controls, when shown, are identified by the (+) symbol. Molecular structures created with ChemDraw.	59
Table 10	Estimated IC_{50} values for various compounds in PC-3 cell line.	84
Table 11	Predicted binding energies of previously prepared 4-azasteroids (**VB 4a-g** and **VB 7a-g**) calculated from molecular docking against 5α-reductase (5AR) type 2. The binding energy of ligand, finasteride (in yellow), present in the X-ray crystal structure was calculated by re-docking.	90
Table 12	Biological data/input for three-dimensional quantitative structure-activity relationship (3D-QSAR) study: relative cell	91

	proliferation (%) of LNCaP and PC-3 cells incubated with compounds synthesized, precursors, 5α-dihydrotestosterone (DHT), and finasteride, during 72 h of exposition in a concentration of 30 μM.	
Table 13	Statistical parameters of final three-dimensional quantitative structure-activity relationship (3D-QSAR) models for percentage of cell (LNCaP and PC-3) proliferation and respective logarithms methods of input data.	92
Table 14	Corresponding Ar-CHO groups, intermediates (**VB 8a-m**) and final products (**VB 9a-m**) with respective global yields. Molecular structures created with ChemDraw.	102
Table 15	Estimated IC_{50} values (μM) for final compounds and 5-fluorouracil (5-FU) in non-tumoral cells: NHDF and PNT1A, and in tumoral cells: LNCaP, PC-3, and MCF-7.	105
Table 16	Molecular docking results, including redocking energy values, obtained by vina executable. Lowest affinity energies are indicated in $Kcal.mol^{-1}$. All new compounds were tested with the most significant steroidal targets.	111
Table 17	Corresponding Ar-CHO groups, steroidal 3β,5α,6β-triols (**VB 10a-f**) and final products 4-ene-3,6,17-triones (**VB 11a-f**) with respective yields. Molecular structures created with ChemDraw.	127
Table 18	Estimated IC_{50} values (μM) of **VB 10a-f**, **VB 11a-f** and 5-fluorouracil (5-FU) in non-tumoral cells: NHDF, PNT1A and in tumoral cells: LNCaP, PC-3, and MCF-7.	130
Table 19	Molecular docking results, including redocking energy values, obtained by vina executable. Lowest affinity energies are indicated in $Kcal.mol^{-1}$. Novel compounds were tested against the most significant steroidal targets.	136
Table 20	Optimization of mobile phase results. Retention time of testosterone (in min).	145
Table 21	Selection of internal standard (IS). Tested compounds and respective retention times (in min) under previously selected running conditions [water/acetonitrile (ACN) 60:40, 40 ˚C].	146
Table 22	Calibration curve parameters of testosterone in mice liver microsomes (n= 3).	149
Table 23	Precision, accuracy, and recovery results. Intra- and interday precision (% CV) and accuracy (% bias) values obtained for testosterone in mice liver microsomes at the lower limit of quantification (QC_{LLOQ}) and at the low (QC_1), medium (QC_2), and high (QC_3) concentration levels representative of the calibration ranges. Percentage of recovery for QC_1, QC_2, and QC_3 are also shown.	149

Table 24	Determined IC_{50} values (nM) of the most potent compounds in the preliminary assays: **VB 7b**, **VB 9f**, **VB 9h**, **VB 9j** and **VB 11c**. Finasteride was used as reference (positive control). Molecular structures created with ChemDraw.	151
Table 25	5α-Reductase (5AR) inhibitory activity of the most potent compounds (IC_{50}), respective affinity binding energies obtained via vina executable, and common interactions with finasteride, used as reference, against 5AR.	156
Table 26	Arylidene steroidal derivatives most potent against each tumoral cell line (LNCaP, PC-3, and MCF-7), respective structure and IC_{50} value (μM). Determined IC_{50} values of 5-fluorouracil (5-FU), the positive control (+), are shown as reference. Molecular structures created with ChemDraw.	169
Appendices		
Table Ap 1	*In vitro* antiproliferative activities of the tested compounds: testosterone, progesterone, 5α-dihydrotestosterone (DHT), **VB 1-3**, **VB 4a-g**, **VB 5**, **VB 6**, **VB 7a-g**, finasteride, and 5-fluorouracil (5-FU) against PC-3 cell line, after 72 h of exposure. MTT screening results at 30 μM (data presented as average % of negative control±SD and are representative of at least two independent experiments).	225
Table Ap 2	Estimated IC_{50} values for most active 4-azaandrostene (**VB 4a-g**) and 4-azapregnene (**VB 7a-g**) derivatives against NHDF, LNCaP, PC-3, and T47-D cells.	226
Table Ap 3	Predicted binding energies of previously prepared 4-azasteroids (**VB 4a-g** and **VB 7a-g**) calculated from molecular docking against important targets of steroidal molecules. Binding energies of ligands (in yellow) present in the X-ray crystal structures were calculated by re-docking.	227
Table Ap 4	Re-docking results using vina executable of protein-ligand complexes, protein data bank (PDB) accession codes, and resolution.	229
Table Ap 5	*In vitro* antiproliferative activities of the tested compounds: **VB 9a-m**, **VB 10a-f**, **VB 11a-f**, and 5-fluorouracil (5-FU) against non-tumoral cell lines (PNT1A and NHDF), after 72 h of exposure. MTT screening results at 10 and 50 μM (data presented as average % of negative control±SD and are representative of at least two independent experiments).	253
Table Ap 6	*In vitro* antiproliferative activities of the tested compounds: **VB 9a-m**, **VB 10a-f**, **VB 11a-f**, and 5-fluorouracil (5-FU) against tumoral cell lines (LNCaP, PC-3, and MCF-7), after 72 h of exposure. MTT screening results at 10 and 50 μM (data presented as average % of negative control±SD and are representative of at least two independent experiments).	254

List of Abbreviations

[T]	Concentration of testosterone
$[T]_{0\ mim}$	Concentration of testosterone at the initial time
$[T]_{30\ mim}$	Concentration of testosterone at the end of the assay (30 min)
17β-HSD	17β-Hydroxysteroid dehydrogenase
2ME	2-Methoxyestradiol
3D-QSAR	Three-dimensional quantitative structure-activity relationship
3D-REA	Relação estrutura-atividade tridimensional
4-AT	4-Androstene-3,6,17-trione
5AR (PT/ENG)	5α-Redutase/ 5α-reductase
5ARIs	5α-Reductase inhibitors
5BR	5β-Reductase
5-FU (PT/ENG)	5-Fluorouracilo/ 5-Fluorouracil
6-OHT	6β-Hydroxytestosterone
A	
ab	10,000 units/mL penicillin G, 100 mg/mL streptomycin and 25 µg/mL amphotericin B
ACN	Acetonitrile
ACTH	Adrenocorticotropic hormone
ADME	Absorption, distribution, metabolism, and excretion
ADT	Androgen deprivation therapy
AIs	Aromatase inhibitors
A_{IS}	Area of the internal standard peak
AKT	Protein kinase B
AMP	Ampicillin
AR	Androgen receptor
A_T	Area of the testosterone peak
ATR	Attenuated total reflectance
AUA	American Urological Association
B	
BFR	Bone formation rate
bias	Deviation from nominal concentration
BPH	Benign prostatic hyperplasia
BUW	Block unscaled weighting
C	
CAB	Combined androgen blockade
CDK	Cyclin-dependent kinase
CEL	Celecoxib
Cis	Cisplatin
CMC	Chemistry, manufacturing, and control
CP	Cancro prostático
CRPC	Castration-resistant prostate cancer
CV	Coefficient of variation
CYP17A1 (PT/ENG)	17α-hidroxilase/17,20 liase de esteroides/ steroid 17α-hydroxylase/17,20 lyase
d	Doublet

D	
DCM	Dichloromethane
dd	Double doublet
DES	Diethylstilbestrol
DEX	Dexamethasone
DHEA	Dehydroepiandrosterone
DHT (PT/ENG)	5α-Dihidrotestosterona/ 5α-dihydrotestosterone
DMAP	4-Dimethylaminopyridine
DMEM	Dulbecco's Modified Eagle Medium
DMSO	Dimethyl sulfoxide
DMSO-d_6	Hexa-deuterated dimethyl sulfoxide
DNA	Deoxyribonucleic acid
DOX	Doxorubicin
E	
EAU	European Association of Urology
EGF	Epidermal growth factor
EMA	European Medicines Agency
EMT	Epithelial-mesenchymal transition
EN	English
ER	Estrogen receptor
ERα	Estrogen receptor α
F	
FBS	Fetal bovine serum
FDA	Food and Drug Administration
FFD	Fractional factorial design
G	
GLPs	Good laboratory practices
GnRH	Gonadotropin-releasing hormone
GnRH-R	Gonadotropin-releasing hormone receptor
GR	Glucocorticoid receptor
GC-MS/MS	Gas chromatography tandem mass spectrometry
H	
HBP	Hiperplasia benigna da próstata
HMG-CoA	3-Hydroxy-3-methylglutaryl-coenzyme A
HoLEP	Holmium laser enucleation of the prostate
HPLC-DAD (PT/ ENG)	Cromatografia líquida de alta eficiência acoplado a um detetor de díodos/ High-performance liquid chromatography with diode array detection
HRSM	High-resolution mass spectrometry
Hsp	Heat-shock proteins
HTS	High throughput screening
HUVEC	Human umbilical vein endothelial cells
Hz	Hertz
I	
I.P.	Intraperitoneal
IC_{50}	Half maximal inhibitory concentration
IND	Investigational New Drug
IPSS	International Prostate Symptom Score
IR	Infrared

IS	Internal standard
ISR	Incurred sample reanalysis
L	
LC_{50}	Median lethal concentration
LCC	Lewis lung carcinoma
LC-MS/MS	Liquid chromatography tandem mass spectrometry
LH	Luteinizing hormone
LH-R	Luteinizing hormone receptor
LHRH	Luteinizing hormone-releasing hormone
LLE	Liquid-liquid extraction
LLOQ	Low limit of quantification
LMO	Leave-many-out
LOO	Leave-one-out
LPS	Lipopolysaccharide
LUTS	Lower urinary tract symptoms
M	
m	Multiplet
m.p.	Melting point
MIFs	Molecular interactions fields
MMAE	Monomethyl auristatin E
MMPP	Magnesium monoperoxyphthalate
MRAs	Muscarinic receptor antagonists
MTD	Maximum tolerated dose
MTT (PT/ENG)	Brometo de 3-(4,5-dimetiltiazol-2-il)-2,5-difeniltetrazólio/ 3-(4,5-dimethylthiazol-2-yl)-2,5-diphenyltetrazolium bromide
MW	Molecular weight
MW	Microwave
N	
NA	Nuclear area
NADPH	Nicotinamide adenine dinucleotide phosphate
NC	Negative control
NCI	National Cancer Institute
NCI-60	National Cancer Institute-60 Human Tumor Cell Lines Screen
NDA	New Drug Application
NMR	Nuclear Magnetic Resonance
NND	Nearest neighbor analysis
O	
ORX	Orchiectomized
OVX	Ovariectomized
P	
PAE	Prostatic artery embolization
PARP	Poly (ADP-ribose) polymerase
PBS	Phosphate buffered saline
PCa	Prostate cancer
PCC	Pyridinium chlorochromate
PD	Pharmacodynamic
PDB	Protein Data Bank
PDE5	Phosphodiesterase type 5
PDE5Is	Phosphodiesterase type 5 inhibitors

PER	Perampanel
PI	Propidium iodide
PK	Pharmacokinetics
PLS	Partial least square
ppm	Parts per million
PR	Progesterone receptor
PSA	Prostate-specific antigen
PSMA	Prostate-specific membrane antigen
PT	Portuguese
PUL	Prostatic urethral lift
PVP	Photoselective vaporization of the prostate
Q	
q	Quartet
QC	Quality control
QSAR	Quantitative structure-activity relationship
R	
RA	Recetor de androgénios
RANK	Receptor activator of nuclear factor–κB
REα	Recetor de estrogénios α
RMSD	Root-mean-square deviation
RPMI	Roswell Park Memorial Institute
r.t.	Room temperature
S	
s	Singlet
S.C.	Subcutaneous
SAR	Structure-activity relationship
SD	Standard deviation
SMCs	Smooth muscle cells
SNPs	Single nucleotide polymorphisms
sp	10,000 units/mL penicillin G and 100 mg/mL of streptomycin
SRD	Smart region definition
SV	Seminal vesicles
T	
t	Triplet
T	Testosterone
THF	Tetrahydrofuran
ThuLEP	Thulium laser enucleation of the prostate
TMPRSS2	Transmembrane protease serine 2
TUIP	Transurethral incision of the prostate
TUMT	Transurethral microwave therapy
TUNA	Transurethral needle ablation
TURP	Transurethral resection of the prostate
TUVP	Transurethral vaporization of the prostate
U	
UGE	Urogenital sinus epithelium
UGM	Urogenital sinus mesenchyme
ULOQ	Upper limit of quantification
USA	United States of America

List of Publications and Communications

Publications and communications related with this thesis

a. Publications

1. Brito, V., Marques, M., Esteves, M., Serra-Almeida, C., Alves, G., Almeida, P., Bernardino, L. & Silvestre, S. M. Synthesis, In Vitro Biological Evaluation of Antiproliferative and Neuroprotective Effects and In Silico Studies of Novel 16*E*-Arylidene-5α,6α-epoxyepiandrosterone Derivatives. *Biomedicines* **11**(3), 812 (2023). **https://doi.org/10.3390/biomedicines11030812**
2. Brito, V., Santos, A. O., Alves, G., Almeida, P. & Silvestre, S. M. Novel 4-Azapregnene Derivatives as Potential Anticancer Agents: Synthesis, Antiproliferative Activity and Molecular Docking Studies. *Molecules* **27**, 1–18 (2022). **https://doi.org/10.3390/molecules27186126**
3. Brito, V., Alves, G., Almeida, P. & Silvestre, S. M. Oxidized Steroids as 5α-Reductase Inhibitors with Potential Interest in Prostatic Diseases: a Review. in *Advances in Health and Diseases* (ed. Duncan, L. T.) 1–35 (Nova Science Publishers, 2022). **https://novapublishers.com/shop/advances-in-health-and-disease-volume-57/**
4. Brito, V., Alves, G., Almeida, P. & Silvestre, S. Highlights on Steroidal Arylidene Derivatives as a Source of Pharmacologically Active Compounds: a Review. *Molecules* **26**, 1–21 (2021). **https://doi.org/10.3390/molecules26072032**
5. Brito, V., Santos, A. O., Almeida, P. & Silvestre, S. Novel 4-Azaandrostenes as Prostate Cancer Cell Growth Inhibitors: Synthesis, Antiproliferative Effects and Molecular Docking Studies. *Comptes Rendus Chim*. **22**, 73–83 (2018). **https://doi.org/10.1016/j.crci.2018.07.011**

b. Communications

1. Brito, V., Santos, A. O., Alves, G., Almeida, P. & Silvestre, S. (**2022**). Síntese, estudos de *Docking* Molecular e Avaliação Biológica de Novos 4-Azapregnenos como Potenciais Agentes Anticancerígenos. 23th and 24th September, Covilhã. *VIII Ciclo de Conferências da Faculdade de Ciências* (Poster).
2. Brito, V., Meirinho, S., Alves, G., Almeida, P. & Silvestre, S. (**2022**). Novel Steroidal Arylidene Derivatives as Potential 5α-Reductase Inhibitors: Evaluation of Enzymatic Activity in Mouse Liver Microsomes by HPLC-DAD. 20th to 22nd April, TRYP Lisboa – Caparica Mar Hotel, Lisbon. *14th National Organic Chemistry Meeting & 7th National Medicinal Chemistry Meeting* (Poster).

3. Brito, V., Meirinho, S., Alves, G., Almeida, P. & Silvestre, S. (**2021**). Screening of 5α-reductase Inhibitory Activity of New Steroidal Arylidene Derivatives using HPLC-DAD. 30th September and 1st October, CICS-UBI Health Sciences Research Centre of University of Beira Interior, Covilhã. *XVI Annual CICS-UBI Symposium* (Poster).
4. Brito, V., Meirinho, S., Alves, G., Almeida, P. & Silvestre, S. (**2021**). Novos Arilidenos Esteroides como Potenciais Inibidores da 5α-redutase: Avaliação da Atividade Enzimática em Microssomas de Fígado de Murganho por HPLC-DAD. 24th and 25th September, Covilhã. *VII Ciclo de Conferências da Faculdade de Ciências* (Poster).
5. Brito, V., Santos, A. O., Alves, G., Almeida, P. & Silvestre, S. (**2020**). Synthesis, Molecular Docking Studies and Biological Evaluation of New 4-Azapregnene Derivatives as Potential Anticancer Agents. 1st and 2nd October, CICS-UBI Health Sciences Research Centre of University of Beira Interior, Covilhã. *XV Annual CICS-UBI Symposium* (Poster).
6. Brito, V., Marques, M., Almeida, C., Esteves, M., Alves, G., Almeida, P., Bernardino, L. & Silvestre, S. (**2019**). Synthesis and Biological Evaluation of New 16*E*-arylidene-5α,6α-epoxydehydroepiandrosterone derivatives. 14th to 16th November, CICS-UBI Health Sciences Research Centre of University of Beira Interior, Covilhã. *III International Congress in Health Sciences Research towards innovation and entrepreneurship: Trends in Aging and Cancer* (Poster).
7. Brito, V., Alves, G., Almeida, P. & Silvestre, S. (**2019**). Novel 16*E*-Arylidene-5α,6α-epoxydehydroepiandrosterone Derivatives as Potential Anticancer Agents: Synthesis and Biological Evaluation. 4th and 5th July, CICS-UBI Health Sciences Research Centre of University of Beira Interior, Covilhã. *XIV Annual CICS-UBI Symposium* (Oral Communication).
8. Brito, V., Alves, G., Almeida, P. & Silvestre, S. (**2018**). Novel 16*E*-Arylidene-5α,6α-epoxydehydroepiandrosterone Derivatives: Synthesis and Cytotoxicity Evaluation. 21st to 23rd November, Faculty of Sciences of University of Porto, Porto. *XXIV Encontro Luso-Galego de Química (*Poster).
9. Brito, V., Serrano, J., Almeida, P. & Silvestre, S. (**2018**). 4-Azasteroid Derivatives as Inhibitors of Prostate Cells Proliferation: Study of Three-dimensional Quantitative Structure-activity Relationship (3D-QSAR). 21st to 23rd November, Faculty of Sciences of University of Porto, Porto. *XXIV Encontro Luso-Galego de Química* (Poster).

10. Brito, V., Alves, G., Almeida, P. & Silvestre, S. (**2018**). Synthesis and Cytotoxic Studies of New 16*E*-Arylidene-5α,6α-epoxydehydroepiandrosterone Derivatives. 5th and 6th July, CICS-UBI Health Sciences Research Centre of University of Beira Interior, Covilhã. *XIII Annual CICS-UBI Symposium* (Poster).
11. Brito, V., Serrano, J., Almeida, P. & Silvestre, S. (**2017**). 3D-QSAR Study on 4-Azasteroid Derivatives and Precursors as Inhibitors of Prostate Cells Proliferation. 6th and 7th July, CICS-UBI Health Sciences Research Centre of University of Beira Interior, Covilhã. *XII Annual CICS-UBI Symposium* (Poster).

Publications not directly related with this thesis

1. Canário, C., Matias, M., Brito, V., Cruz-Vicente, P., Soeiro, P., Santos, A.O., Falcão, A., Silvestre & S., Alves, G. 10β-Hydroxyestra-1,4-diene-3,17-dione as Potential Antiproliferative Agent: *In Vitro* Biological Evaluation and *In Silico* Studies. *Nat. Prod. Res.* **36**(24), 6459-6463 (2022). https://doi.org/10.1080/14786419.2022.2039136
2. Canário, C., Matias, M., Brito, V., Pires, P., Santos, A.O., Falcão, A., Silvestre, S. & Alves, G. C-Ring Oxidized Estrone Acetate Derivatives: Assessment of Antiproliferative Activities and Docking Studies. *Appl. Sci.* **12**(7), e3579 (2022).
3. Canário, C., Matias, M., Brito, V., Santos, A.O., Falcão, A., Silvestre, S. & Alves, G. New Estrone Oxime Derivatives: Synthesis, Cytotoxic Evaluation and Docking Studies. *Molecules*. **26**(9), e2687 (2021). https://doi.org/10.3390/molecules26092687
4. Ramilo-Gomes, F., Addis, Y. Tekamo, I., Cavaco, I., Campos, D. L., Pavan, F. R., Gomes, C. S. B., Brito, V., Santos, A. O., Domingues, F., Luís, Â., Marques, M. M., Pessoa, J. C., Ferreira, S., Silvestre, S. & Correia, I. Antimicrobial and Antitumor Activity of S-Methyl Dithiocarbazate Schiff Base Zinc (II) Complexes. *J. Inorg. Biochem.* **216**, 111331 (2021). https://doi.org/10.1016/j.jinorgbio.2020.111331
5. Canário, C., Matias, M., Brito, V., Santos, A.O., Falcão, A., Silvestre, S. & Alves, G. $\Delta^{9,11}$-Estrone Derivatives as Potential Antiproliferative Agents: Synthesis, *In Vitro* Biological Evaluation and Docking Studies. *Comptes Rendus Chim.* **23**(2), 201–217 (2020). https://comptes-rendus.academie-sciences.fr/chimie/articles/10.5802/crchim.17/
6. Kolsi, L. E., Krogerus, S., Brito, V., Ruffer, T., Lang, H., Yli-Kauhaluoma, J., Silvestre, S. M. & Moreira, V. M. Regioselective Benzylic Oxidation of Aromatic Abietanes: Application to the Semisynthesis of the Naturally Occurring

Picealactones A, B and C. *ChemistrySelec*t **2**, 7008–7012 (2017). https://doi.org/10.1002/slct.201701477

7. Kiriazis, A., Aumüller, I. B., Arnaudova, R., Brito, V., Rüffer, T., Lang, H., Silvestre, S. M., Koskinen, P. J., Yli-Kauhaluoma, J. Nucleophilic Substitution of Hydrogen Facilitated by Quinone 2 Methide Moieties in Benzo[cd]azulen-3-ones. *Organic Letters*, **19**(8), 2030–2033 (2017). https://doi.org/10.1021/acs.orglett.7b00588

CHAPTER I

1. General Introduction

1.1. Overview on principal prostatic diseases and main therapeutical approaches

1.1.1. The prostate gland

The prostate is a male-specific hormone-responsive gland, located between the bladder and penis, surrounding the urethra, in the retroperitoneal space.[1] This gland is walnut-shaped and sized and it weighs about 15-20 g at the end of adolescence and requires androgenic hormones and an androgen receptor (AR) for normal growth and development.[2,3] Physiologically, the prostate has an important role in the male reproductive system, being responsible for the secretion of prostatic fluid, one of the components of semen. In this context, the prostate has five physiologic distinct roles: (1) duct for testicular sperm, (2) duct for seminar vesicular energetic material for sperm, (3) conditioning the nutrients of sperm, (4) formation of semen, and (5) duct for semen and sperm at ejaculation process.[4]

The prostate anatomy comprises three principal different zones: (1) central zone, (2) transitional zone, and (3) peripheral zone. Additionally, the prostate presents two other zones/regions, the anterior fibromuscular stroma and the periurethral gland region (**Figure 1**).[1,5–8]

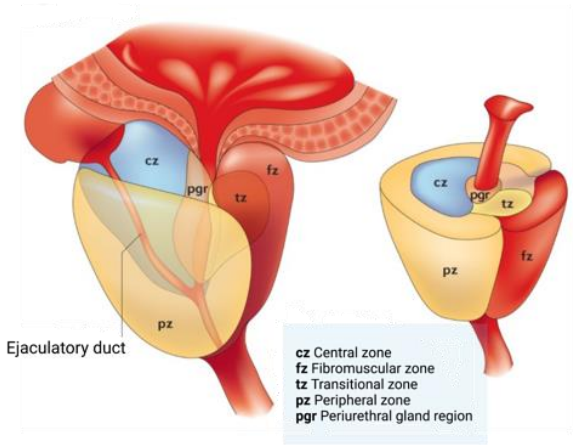

Figure 1. Zones and regions of the prostate. *Adapted from Reeves et al. (2016) and De Marzo e. al. (2007).*[1,9]

The central zone includes the whole base of the prostate and involves the ejaculatory ducts, comprising approximately 25 % of the total volume of the prostate. The transitional zone only represents 5 % of prostate volume and surrounds the proximal prostatic urethra. The peripheral zone represents the majority of prostate total volume, around 70 %, and surrounds the central and transitional zones. Relative to the histology, the prostate is mainly constituted by a glandular tissue with a basal layer of cuboidal epithelial cells covered by another layer of columnar secretory luminal cells, containing abundant fibromuscular stroma separating the individual glands. Moreover, several pathologies tend to occur in these specific zones of the prostate, including hyperplastic proliferative lesions (up to 20 %), mainly, in the transitional zone, and prostate cancers, mostly, in the peripheral zone (up to 70 %). In contrast, the central zone gives rise to only 1 to 5 % of prostate cancers.[7,10–12] The prostate is affected by three main pathologies: (1) prostatitis (inflammation), (2) benign prostatic hyperplasia (BPH), and (3) prostate cancer (PCa).[5] The next subsections will be focused on the BPH and PCa diseases, elucidating the pathophysiology, the role of the androgens in the development of these diseases, and the current main therapeutic approaches. On the other hand, the inflammation of prostate, prostatitis, will not be explored since it is out of the scope of the present thesis.

1.1.2. Benign prostatic hyperplasia

BPH is one of the most common urological male age-related diseases, affecting a majority of elderly men worldwide.[13–15] The prevalence of BPH increases significantly with increased age. An estimation revealed that 50 % of men have histologic evidence of BPH by age of 50 and 75 % by age of 80. Moreover, in around 40-50 % of these men, the disease becomes clinically relevant.[16,17] Several observational studies from Asia, Europe, and United States of America (USA) reported advanced age as the main risk factor for clinical BPH development and progression.[16,18,19] Additionally, genetics, diet and lifestyle may play an important role in BPH.[15] The occurrence in older men is also influenced by disorders such as diabetes, obesity, alcohol consumption, hyperlipidemia and lack of physical exercise.[20,21]

1.1.2.1. Pathophysiology

The disease BPH consists of a nodular hyperplasia, affecting the transitional and periurethral zones of the prostate, caused by an abnormal proliferative process of the prostate elements, namely stromal and epithelial cells, resulting in an enlarged prostate. BPH originates bladder outlet obstruction and compression, and it can result in a series of lower urinary tract symptoms (LUTS).[8,22–25] BPH is the most common etiology of

LUTS.[26] These symptoms include voiding symptoms such as incomplete bladder emptying sensation, straining to void, urinary hesitancy and a weak urinary flow rate. In addition, storage symptoms are also reported, such as nocturia, frequent urination, dysuria and urinary urgency.[27,28] Furthermore, BPH can lead to further complications such as sexual dysfunction, urinary incontinence, infection of the urinary tract, renal insufficiency and acute urinary retention.[29] Despite BPH is not a lethal disease, it affects considerably the quality of life of patients, causing anxiety, sleep disorders, and sexual problems.[24]

In BPH, the relative proportion of epithelial and stromal hyperplasia is highly variable. A study revealed that the individual cellular composition of the hyperplastic component of the prostate of men with clinical BPH oscillated in connective tissue, from 20.2 % to 59.3 %, in the epithelium, from 16.1 % to 56.1 %, in smooth muscle, from 4.3 % to 24.8 %, and in epithelial lumen from 5.3 % to 21.9 %.[22] Similarly, the level of prostatic enlargement is also highly variable.[30]

1.1.2.2. The role of androgens in the disease development

The prostate gland is an androgen-sensitive organ that needs proper androgen/AR signals for normal growth, function, and maintenance.[31,32] The prostate develops from the embryonic connective tissue, namely urogenital sinus mesenchyme (UGM) and an internal layer of urogenital sinus epithelium (UGE).[33] The initial step of prostate development in UGM involves the differentiation of fibroblasts and smooth muscle cells (SMCs), and in response to the UGM androgen/AR signals, UGE can grow into the surrounding stromal cells and develop into the prostate epithelial cells as part of the normal prostate development.[32] The capability of the UGM to induce epithelial growth and the developed epithelial cells suggests that the reciprocal developmental interactions between UGM and UGE might be controlled by androgen/AR signals, which are essential for the development of normal prostate.[34] AR is a member of a steroid and nuclear receptors superfamily that can be activated and translocated from cytoplasm to nucleus after binding the androgenic hormones testosterone or 5α-dihydrotestosterone (DHT).[32,35–37] Testosterone, mainly produced in the testes by Leydig cells (95 %) and in adrenal glands (5 %), is the natural ligand for the AR, entering in the prostate epithelial cells by passive diffusion and posteriorly converted into the more potent ligand DHT by steroid 5α-reductase (5AR) isoenzymes.[38,39] AR is expressed in epithelial and stromal tissues, in the prostate gland. The transactivated AR triggers the transcription, leading to the synthesis of specific proteins and cell proliferation (**Figure 2**).[31] Furthermore, epithelial AR and stromal AR can also function through epithelial-mesenchymal

transition (EMT) to influence prostate development. EMT is a process by which epithelial cells lose their cell-cell adhesion and gain migratory properties to become mesenchymal-like and/or mesenchymal stem cells.[32]

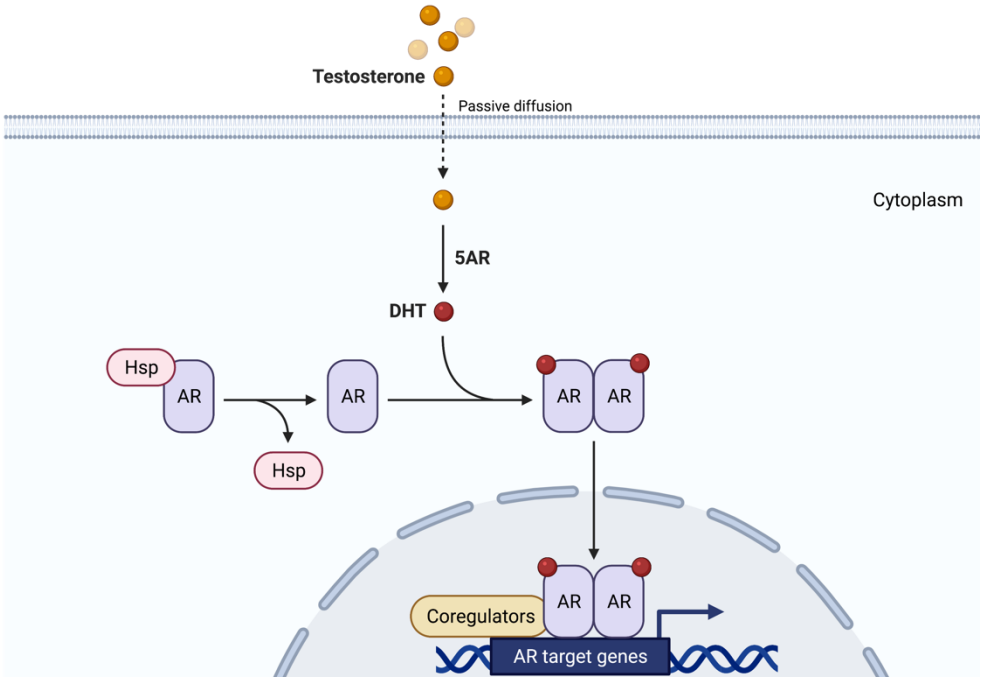

Figure 2. Androgen and androgen receptor (AR) signaling in the prostate cells. After testicular synthesis, testosterone is transported to target tissues and converted into 5α-dihydrotestosterone (DHT) by 5α-reductase (5AR). DHT binds to the ligand-binding pocket and promotes the dissociation of heat-shock proteins (Hsp) from the AR. Then, the AR translocates into the nucleus, dimerizes, and binds in the promoter region to the AR target genes, such as prostate-specific antigen (PSA) and transmembrane protease serine 2 (TMPRSS2).[37,40] Created with BioRender.com.

The enlargement of the prostate and the development of BPH producing clinical manifestations is dependent on androgens and several lines of evidence supporting this fact have been reported, based on experimental and clinical studies. Indeed, it has been well established that BPH does not develop in men castrated before puberty and males with hypopituitarism.[41,42] Moreover, this fact is supported by the fact that both medical and surgical castration have beneficial effects in BPH patients through the reduction in the levels of androgens.[43–46] An early study revealed that prostate nodule tissue in BPH is mainly constituted by stromal cells (88.4 %) and only by 9 % of epithelial cells, which suggests the relevance of these cells in BPH.[43]

The stromal androgens/AR signals may influence the development and progression of BPH via alteration of several growth factors in a paracrine and/or autocrine manner.[32] In this context, factors involved in the alteration of proliferation and differentiation of stem cell population, as well as factors involved in the EMT or inflammation and immune

tolerance, have been suggested to be directly or indirectly linked to the AR.[47] AR knockout animal models and recombination experiments revealed that androgens through AR in embryonic stromal cells are directly involved in prostate development via mesenchymal-epithelial interactions.[48] Consequently, targeting androgens/AR signals play a key role in the battle against the progression of BPH.[43] At this point, it is important to clarify the biosynthesis and metabolism of androgens to understand the molecules and macromolecules involved in these processes.

Androgens are essential in the expression of the male phenotype, having a crucial role during male sexual differentiation, development, and maintenance of secondary male characteristics and during the initiation and maintenance of spermatogenesis.[49] Testosterone and DHT are the two most important androgens of adult males. Testosterone is the major male androgen in circulation, while DHT is the principal androgen in tissues. In healthy adult men, 90% of the circulating levels of testosterone are secreted by the Leydig cells of the testes and 5-10% from the adrenal glands. In the circulation, about 44% of testosterone is firmly bonded to sex hormone-binding globulin, 54% is bonded loosely to albumin, and only 1-2% is in a free state. Unlike testosterone, only 25% of DHT in the circulation is secreted by the testes. Most DHT (65-75%) arises from the conversion of testosterone in the prostate, liver, and peripheral tissues through the action of 5AR, which has three isozymes, type 1, 2, and 3.[50–53] In men, the prostate is a major site of non-testicular production of DHT, which is derived primarily from testosterone. The simplified pathway of testosterone biosynthesis in Leydig cells (testes) and its metabolism within the prostate, as well as the enzymes involved are shown in **Figure 3**. The cytochrome P450 family of enzymes is responsible for metabolizing endogenous hormones and the respective biochemical intermediates. The enzyme CYP17A1 converts both pregnenolone and progesterone to dehydroepiandrosterone (DHEA) and androstenedione, respectively. CYP1B1 catalyzes the hydroxylation of testosterone to 6β-hydroxytestosterone (6-OHT), while 5AR type 2 is the main 5AR isozyme responsible for the conversion of testosterone to DHT, in the prostate cells. Moreover, inside the prostate, DHT can undergo further reduction to form 3β-androstanediol by the enzyme 3β-hydroxysteroid dehydrogenase or 3α-androstanediol by 3α-hydroxysteroid dehydrogenase. This last metabolite can be conjugated through the action of glucuronyl transferase in an irreversible reaction yielding 3α-androstanediol glucuronide, a terminal metabolite.[52–54] The inactivation of DHT in the prostate is important to determine the intracellular DHT concentration and it can be a potential modulator of androgenic activity in the prostate.[52]

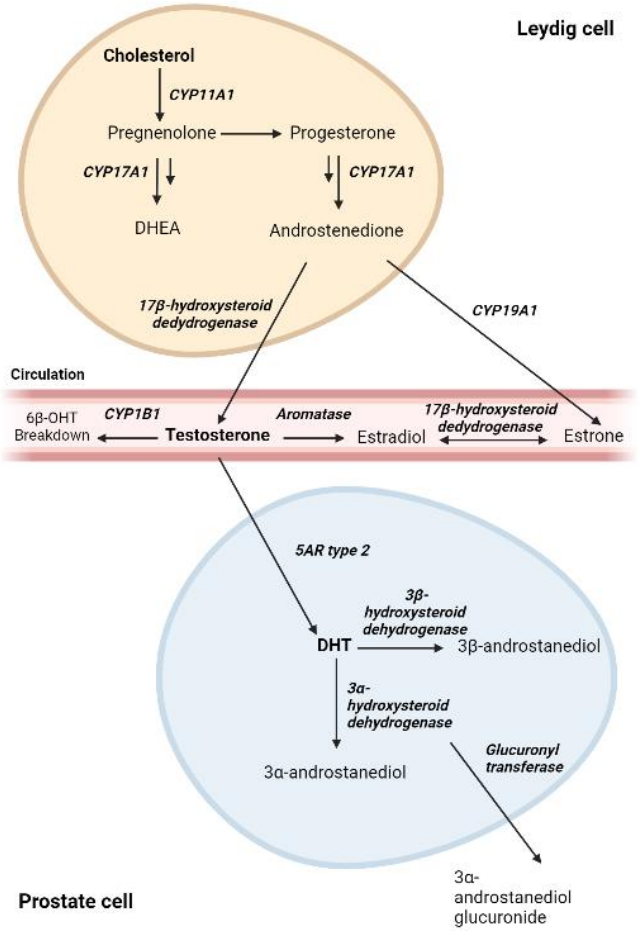

Figure 3. Simplified pathway of androgens biosynthesis and metabolism. *Adapted from Singh et al. (2005).*[54] Created with BioRender.com.

1.1.2.3. Therapeutic approaches

At the present, the primary goal for treating BPH is to have a positive impact on the disease by reducing the prostatic volume and, in the long-term, to reduce LUTS, discomfort and, improve urine flow rate. Ultimately, it is hoped that these effects translate into reduced lifetime risks of acute urinary retention and the need for BPH-related surgery, increasing significantly the quality of life of the patient.[24,55] The therapeutic approaches of BPH involve three different phases: (1) medical watchful waiting, (2) pharmacological treatment and, (3) surgical methods.[56,57] The selection of the procedure will depend on age, the type and severity of the symptoms, as well as on the size of the prostate gland.[24,56,58] The first stage, watchful waiting, is recommended for patients whose quality of life is not being influenced by LUTS, and includes dietary changes, physical exercise, education, and regular review of the patient's condition.[59] The drug therapy strategy is applied when the wait and watch approach becomes ineffective, particularly in men with severe LUTS. Then, it is necessary to administrate appropriate

medication. In this context, a variety of drugs is currently available: (1) α1-adrenergic antagonists (α1-blockers), (2) 5AR inhibitors (5ARIs), (3) muscarinic receptor antagonists (MRAs), (4) β3-adrenoreceptor agonists (β3-agonists), (5) phosphodiesterase type 5 inhibitors (PDE5Is) and, (6) plant extracts. Currently, the combination treatment featuring α1-adrenergic antagonists and 5AR inhibitors is a common approach.[24,57] Considering the surgical option, it is recommended for BPH patients with severe LUTS and other complications such as recurrent urinary tract infections, renal insufficiency, constant bladder stones formation, serious hematuria, or for patients that are reluctant to medication. The surgical methods include several different approaches: transurethral resection of the prostate (TURP), simple prostatectomy, laser enucleation, photoselective vaporization of the prostate (PVP), water-induced thermotherapy, microwave thermotherapy (TUMT), transurethral needle ablation (TUNA), transurethral prostate urethral lift (PUL), prostate artery embolization (PAE), transurethral incision of the prostate (TUIP), and transurethral vaporization of the prostate (TUVP).[60,61] These current therapeutic approaches are summarized in **Figure 4.**

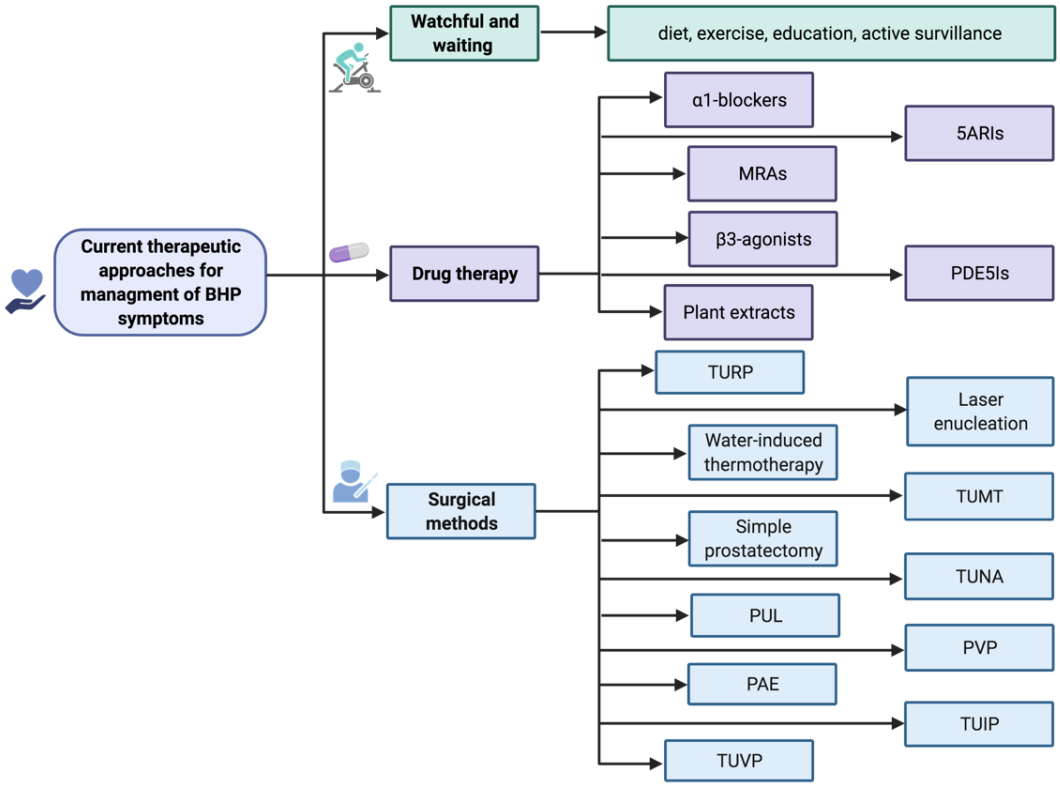

Figure 4. Current therapeutic approaches to treat and manage benign prostatic hyperplasia (BPH) symptomatology. Created with BioRender.com.

- **Pharmacological treatment**

In patients with mild to moderate LUTS symptoms and no clear indication for surgical intervention, the pharmacological approach is the most appropriate.[24,62,63] The advantages of drug therapy comprise the convenience for the patient, the avoidance of potential morbidity related to surgical methods, and the capacity to reverse the side effects of treatment if necessary.[64,65] On the other hand, the principal disadvantage of this strategy is the need for continued therapy to maintain the improvement in the patient's condition, with the risk of long-term costs and compliance issues.[65,66] As previously referred, the drugs clinically used for BHP treatment are α1-blockers, 5ARIs, MRAs, β3-agonists, PDE5Is, and plant extracts. The drugs approved by Food and Drug Administration (FDA) and European Medicines Agency (EMA) are summarized in **Figure 5**.

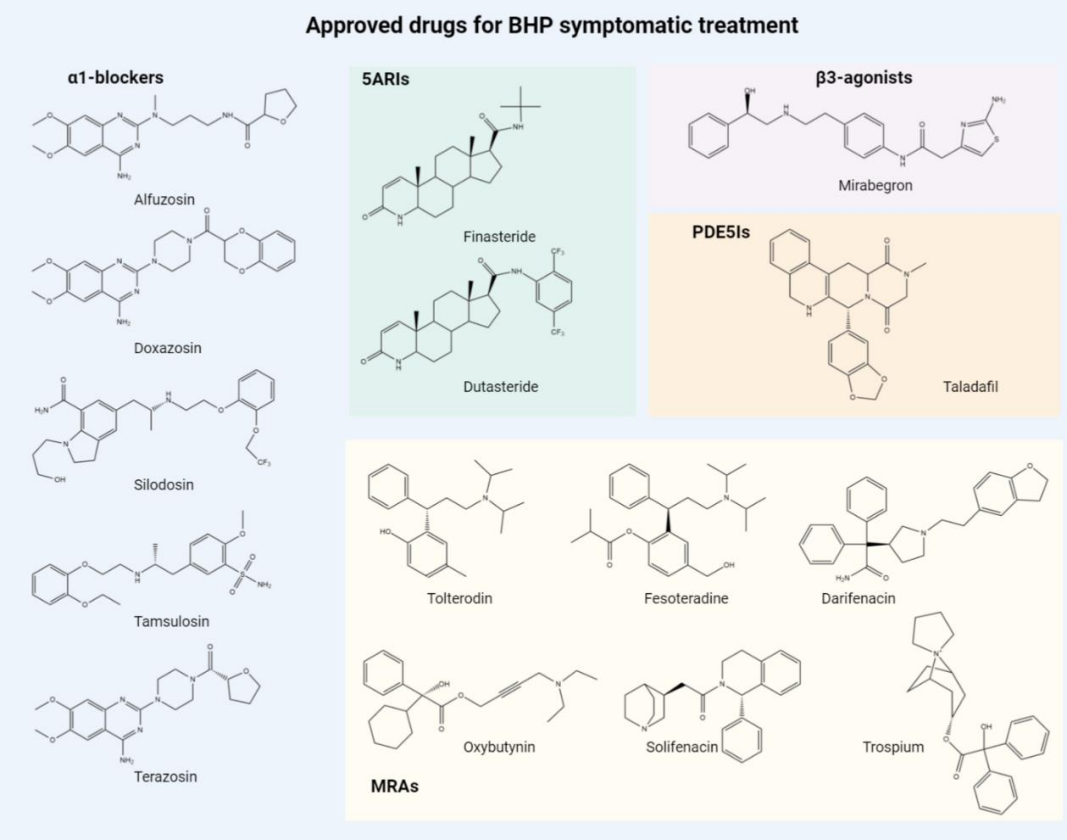

Figure 5. Current drugs approved by Food and Drug Administration (FDA) and European Medicines Agency (EMA) for benign prostatic hyperplasia (BPH) treatment. Created with ChemDraw and BioRender.com.

- **α1-Adrenergic Antagonists** (α1-blockers)

The α1-blockers are a family of bioactive molecules capable of binding and inhibiting type 1 α-adrenergic receptors, stopping smooth muscle contraction. α1-Adrenergic receptors are highly expressed in the smooth muscle of the prostate, bladder neck, and

urethra. Therefore, these inhibitors are useful in BPH treatment due to their capacity to cause relaxation of smooth muscle both in the bladder neck, urethra and prostate, reducing urethral resistance and relieving LUTS.[67–69] There are three distinct subtypes of α1-adrenergic receptors (α1A, α1B, and α1D), all distributed in different organs beside the prostate, such as the brain, heart, blood vessels, liver, kidney, and spleen. The receptors α1A and α1D are both important in smooth muscle contraction (and control of blood pressure), while the role of the α1B-adrenoceptors is less certain. Moreover, it is known that α1A blockade is responsible for BPH symptomatic management. However, in this context few selectivity studies of α1A-blockers have been reported.[70,71] Considering the wide distribution of these receptors, α1-blockers can lead to a range of side effects. These side effects include postural hypotension, asthenia, intraoperative floppy iris syndrome, abnormal ejaculation, and dizziness.[67] At the moment, there are five α1-blockers approved by the FDA and EMA for the treatment of BPH: silodosin, tamsulosin, alfuzosin, doxazosin, and terazosin.[24,72]

- **5AR Inhibitors** (5ARIs)

5AR is responsible for converting testosterone to DHT, promoting cell proliferation and consequently promoting the development of BPH. Considering this fact, 5AR has been studied as a target for the treatment of BPH.[73] The 5AR family includes 5AR type 1, 5AR type 2, and 5AR type 3, being the type 2 the most expressed in prostate tissue.[74] 5AR type 1 is expressed in non-genital skin, liver, and certain brain regions, and at lower levels in the prostate, genital skin, epididymis, seminal vesicles, testis, adrenal gland, and kidney. The type 2 isozyme is mainly expressed at the prostate, genital skin, epididymis, seminal vesicles, and liver.[39,51,75] More recently, the third type of 5α-reductase (5AR type 3) has been described and it is highly expressed in the pancreas and hormone-refractory prostate cancers. The expression of this isozyme was also described in prostate cancer cell lines.[76,77]

5ARIs, by inhibiting the conversion of testosterone, are capable of reducing DHT levels, shrinking the enlarged prostate, and preventing the progression of the disease.[78] There are two types of 5ARIs, type 2 selective inhibitors, as finasteride, and nonselective or dual inhibitors (inhibit type 1 and 2), as dutasteride. However, a study reported by Yamana and coworkers also showed the potential inhibition of 5AR type 3 by finasteride and dutasteride.[76] Chemically, finasteride and dutasteride are 4-azasteroids, being azasteroids a class of modified steroids which has been attracting researchers attention over the years.[79] Both drugs were clinically tested and were found to reduce LUTS to a significant extent, being the only 5ARIs approved until the moment.[80] In fact, clinical

studies carried out on BPH patients suggested that therapy with 5ARIs is an efficient approach for patients with moderate-to-severe symptoms and an enlarged prostate.[24] Finasteride and dutasteride not only improve the symptom score and urinary functions, but also retard the progression of BPH and reduce the risk of acute urinary retention and, consequently, the need for surgery.[81] Sexual adverse effects are the most common drug-related adverse effects and, usually, occur during the first year of treatment. In fact, the most common side effects include decreased libido, erectile dysfunction, and gynecomastia.[24,82] More recently, Diviccaro and coworkers performed *in vivo* studies to assess the effects of finasteride in the central nervous system.[83] This research was based on the appearance of several side effects also involving this system after discontinuation of the treatment with finasteride. Indeed, several studies, in addition to impaired sexual function, also reported high depression scores in patients and this condition was named post-finasteride syndrome.[84,85] The Diviccaro research suggested that finasteride treatment and withdrawal causes alterations in the hippocampus, corresponding with the appearance of depressive-like behavior.[83]

- **Muscarinic Receptor Antagonists** (MRAs)

Muscarinic cholinergic receptors are classified into five different subtypes (type 1 to type 5). Smooth muscle cells of the bladder, urothelium, and afferent nerves express mostly types 2 and 3, which play significant roles in the urethra and bladder. When these receptors are activated, the bladder muscles, namely the detrusor, contract, resulting in recurrent micturition and an augmented urgency to urinate.[86] The muscarinic receptor type 2 is more abundant in the bladder than type 3, however, the last one plays a more important role in bladder contractions.[87] Therefore, the development of MRAs emerged to improve storage symptoms in BPH patients. However, at the moment, the exact molecular mechanisms and binding/active sites are not yet well established.[88] Despite this, several MRAs have been developed and some of them were approved by the FDA and EMA to treat storage symptoms associated with LUTS and overactive bladder. These approved drugs include oxybutynin, tolterodine, fesoterodine, darifenacin, solifenacin, and trospium.[89] The side effects of these drugs include dry mouth, constipation, pruritus, micturition difficulties, nasopharyngitis, and dizziness, being dry mouth the most common effect.[90]

- **β3-Adrenoreceptor Agonists** (β3-agonists)

β-adrenoceptors includes β1, β2 and β3 subtypes.[91] In the human body, β3-adrenoceptors are mainly expressed in the gall bladder, heart, gastrointestinal tract, prostate, bladder, urothelium, and brain. The bladder detrusor muscle relaxation is

mediated principally by β3-adrenoceptors.[92] Considering this fact, β3-agonists were primarily developed to decrease detrusor tone, which promotes urine storage.[93] Currently, the only β3-agonist approved is mirabegron.[24] The treatment with this drug presents constipation, nasopharyngitis, headache, hypertension, and urinary tract infection as the most common side effects.[94] However, a more recent meta-analysis concluded that mirabegron is associated with a lower risk of side effects when compared with antimuscarinics or combination therapy with the same efficacy.[95]

- **Phosphodiesterase type 5 Inhibitors** (PDE5Is)

Phosphodiesterases constitute a group of eleven enzymes (type 1 to type 11) and phosphodiesterase type 5 (PDE5) is one of the most well-studied.[96] The enzyme PDE5 is found in the bladder detrusor muscle, vascular smooth muscle, prostate tissue, and ureters. PDE5Is were also developed with the purpose of relaxing the urinary smooth muscle and the bladder detrusor, ameliorating LUTS in BPH patients.[97,98] PDE5Is exert their action on the pathway of nitric oxide (NO), increasing NO released at neuronal-smooth muscle junctions.[99,100] Several molecules, like sildenafil, tadalafil, and vardenafil, have been reported as PDE5Is with efficacy on the improvement of LUTS in BPH patients, but only tadalafil was approved by FDA and EMA for the BPH treatment.[101] However, the treatment with tadalafil can cause side effects such as flushing, headache, back pain, indigestion, nasal congestion, and gastroesophageal reflux.[102] Despite this, the side effects related to PDE5Is seem to be moderate and well-tolerated by BPH patients, but the contraindications should be always considered at the prescription.[24]

- **Plant Extracts**

Herbal drug formulations are prepared using roots, seeds, pollen, bark, or fruits. The most relevant compounds found in plant extracts comprise phytosterols (e.g. ß-sitosterol), fatty acids, and lectins.[103] The *in vivo* effects and the precise mechanisms of action of plant extracts usually remain unclear, being the use of herbal medicines controversial and not yet recommended by the European Association of Urology (EAU) and by American Urological Association (AUA). Moreover, currently, the problems associated with the applied methods and the heterogeneity of clinical trials involving these products support this controversy.[24] Therefore, the adoption of a phytotherapeutic approach is dependent on the guidelines implemented by the health systems of each nation. In this context, this type of treatment has been prescribed mainly to patients with reluctance to accept standard medication due to the side effects. In Europe, the last data collection showed that plant extracts are not used in numerous countries, like Ireland, the United Kingdom, Denmark, Norway, Finland, and Sweden, and hardly used in

Portugal, Netherlands, Italy, Austria, and Greece. On the contrary, in Belgium, the prescription of herbal drugs, in comparison with other countries, is especially high.[61,104]

BPH treatment with herbal drugs involves extracts from several plants as *Saw palmetto*, *Cucurbita pepo L., Prunus africana*, *Urtica dioica L.*, and *Secale cereale L.*. Two of the most frequently prescribed and studied plant extracts are from *S. palmetto* and *C. pepo L.*.[105]

S. palmetto is derived from the berry of the dwarf palm tree. This plant extract (commercialized as Permixon™) is an effective dual inhibitor of 5AR isoenzyme activity (inhibits 5AR type 1 and 2) in the prostate. It was demonstrated that, unlike other 5ARIs, *S. palmetto* does not inhibit binding between activated AR and the steroid receptor-binding consensus in the promoter region of the PSA gene.[106,107] Nevertheless, it has no effect on the prostate volume or in the PSA test but slightly decreases the prostate epithelium. This herbal drug does not cause impotence, but it may aggravate chronic gastrointestinal disease.[108] A recent meta-analysis revealed that *S. palmetto* extract has an efficacy identical to the described for α1-blockers relative to the improvement in quality of life, LUTS symptoms, and in the maximum urinary flow. Furthermore, the inhibition of BPH progression using Permixon™ is equivalent to that achieved with treatment with 5ARIs during 6 months.[109]

C. pepo L. oil-free hydroethanolic extract (EFLA™940) is obtained from pumpkin seeds and its efficacy in the treatment of BPH patients has also been reported.[110–112] In a recent pilot study, Leibbrand and colleagues investigated the effects of EFLA™940 on BPH-related symptoms. For 12 weeks, significant effects were reported for International Prostate Symptom Score (IPSS), overall quality of life, and nocturia. This study suggested that the oil-free hydroethanolic pumpkin seed extract is a suitable herbal drug for improving BPH-related symptoms without the need for other medical treatment.[111] Although the precise action mechanisms underlying the effects of plant extracts on BPH patients have yet to be clarified, the studies already performed propose that this pharmacological action is related to anti-androgenic, anti-proliferative, anti-inflammatory, and anti-edema activities.[113–115]

- **Principal new drug candidates for BPH symptomatic treatment**

Currently, diverse drug candidates have been designed and developed for the treatment of symptoms associated with BPH. These new potential drugs include new α1-blockers, NO donating compounds, agonists/antagonists of vasopressin and tachykinin receptors, and selective cannabinoid receptor agonists (**Table 1**).[24,116]

Table 1. Relevant drug candidates that may led to beneficial outcomes in the treatment of symptoms associated with benign prostatic hyperplasia (BPH), mechanism of action, and respective references.

Drug candidate		Mechanism of action	Ref.
ID	**Molecular Structure**		
SNAP 6383	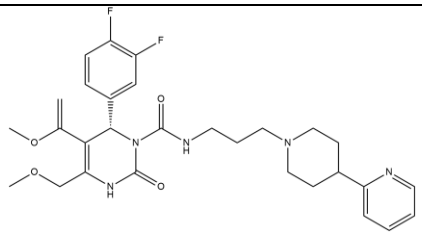	*α1A-blockage*	117,118,119
RS-17503	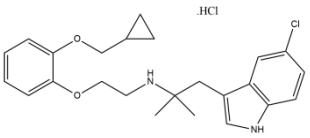		
S-nitroso-glutathione	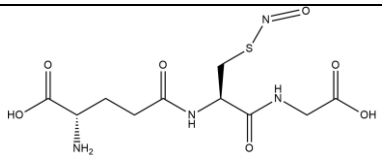	*NO donation*	120–122
S-nitrosocysteine	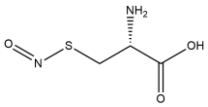		
SR 49059	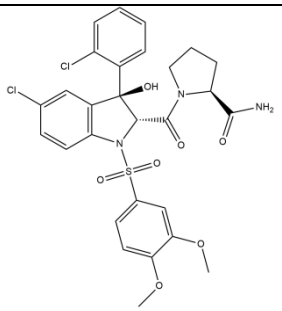	*Vasopressin v1a receptor antagonism*	123
L 659837	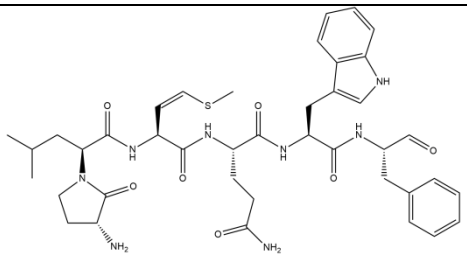	*Tachykinin (NK2) receptor antagonism*	124
CP 55940	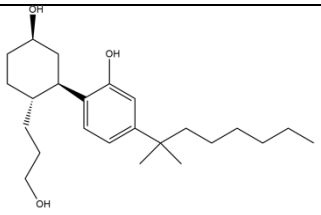	*Selective cannabinoid receptor agonism*	125–127

Pharmacological evidence indicated that activation of subtype α1A-receptor by norepinephrine in the bladder neck, prostate, and urethra has an important role in the manifestation of LUTS.[128] In addition, prostate selective α1A-blockers may provide better

efficacy in the treatment of BPH with fewer adverse effects, particularly regarding cardiovascular interferences.[129] Thus, the development of novel and selective antagonists comprise a relevant focus of investigation in the context of BPH management. Within the new molecules developed, it is relevant to highlight SNAP 6383 (Merck Research Laboratories, West Point, PA, USA) and RS-17503 (Roche Bioscience, Palo Alto, CA, USA). *In vitro* studies using animal and human prostate tissues demonstrated the high potency of SNAP 6383 (as known as L-771,668) on 1A subtype α-adrenergic receptor-mediated response. Furthermore, SNAP 6383 was found to have a potent effect on urethral pressure with minimal effect on blood pressure in animal models.[117,130] Similarly, RS-17503 has a selective and high affinity for α1A-adrenoceptor and is considered a potential drug for BPH treatment. Nevertheless, studies in isolated smooth muscle tissues of patients with LUTS showed that high concentrations of RS-17053 are needed to antagonize the tissue responses to norepinephrine.[118,119]

Other potential strategy includes drugs interfering with the NO/cyclic GMP signaling pathway since NO induces smooth muscle relaxation by activating the enzyme guanylyl cyclase, increasing the tissue levels of the second messenger molecule cyclic GMP.[116,131] Consequently, molecules capable of releasing NO (NO donors), as *S*-nitroso-glutathione (SGNO) and *S*-nitrosocysteine (SNC), have been studied *in vitro* to explore their potential to treat dysfunctions in the lower urinary tract. These experiments demonstrated that these NO donors are capable of increasing mean voided urine volume and maximum urinary flow rate by reducing the contraction of tissue strips isolated from the transitional zone of the prostate.[120,121] Vasopressin also plays a relevant role in the smooth muscle contraction in the prostate and urethra.[132] SR 49059, a vasopressin receptor subtype v1a antagonist, represents a potential candidate for BPH treatment.[116,123,133] In addition, targeting the effects of tachykinins (NK1, NK2, and NK3), endogenous neuropeptides acting through G-protein coupled receptors, have been taken into consideration in the treatment of urological diseases. *In vitro* experiments demonstrated that isolated tissues of the human prostate and urethra were contracted by an NK2 agonist (GR 64349) and this response was antagonized in the presence of an NK2 receptor antagonist, L 659 837.[124]

Lastly, evidence showed that the endocannabinoid system (receptors, respective ligands, and enzymes that control the levels of endocannabinoids) has an important role in the function of the human lower urinary tract.[125,126,134] In a healthy prostate gland, it was proven the existence of types 1 and 2 cannabinoid receptors in the nerves. On the contrary, in nodular hyperplasia, these receptors are rare or absent. Gratzke and

coworkers, using prostate specimens obtained from patients undergoing radical prostatectomy, studied the expression of the cannabinoid receptors (types 1 and 2) and the effects of CP 55940, an agonist of these receptors. This compound decreased nerve-mediated contractions of the prostate preparations. This research suggested a relevant role of cannabinoid receptors in mechano-afferent signaling and epithelial homeostasis in the human prostate, emerging as a novel therapeutic target for LUTS/BPH.[127] Despite the existence of these experimental data, none of these mentioned drugs have yet been tested in clinical studies.

Regarding the clinical trials involving drug therapy for BPH and according to the *ClinicalTrials.gov*, there are several ongoing studies that are presented in **Table 2** and explained bellow: (1) "Efficacy and safety of DKF-313 in patients with benign prostatic hyperplasia" (NCT04947631 – Phase 3), which aims to study the efficacy and safety of combination therapy of dutasteride and tadalafil; (2) "Evaluation of the effect of garcinia in combination with chromium on the clinical outcomes of patients with LUTS/BPH" (NCT04590534 – Phase 2); (3) "Study to evaluate the efficacy, safety and tolerability of vibegron in men with overactive bladder (OAB) symptoms on pharmacological therapy for benign prostatic hyperplasia (BPH)" (NCT03902080 – Phase 3); (4) "Evaluate the efficacy and safety of GV1001 in patients with benign prostatic hyperplasia (BPH)" (NCT04032067 – Phase 3), which goal is to test a 16-amino-acide peptide previously developed as a cancer vaccine, but GV1001 failed in clinical trials due to the lack of efficacy; (5) "Efficacy study of fedovapagon for nocturia in men with benign prostatic hyperplasia (BPH) (EQUINOC)" (NCT02637960 – Phase 2/3), and (6) "Efficacy and safety of combination therapy for treatment of overactive bladder in male patients with benign prostatic hyperplasia" (NCT02279615 – Phase 4), which pretends to study the efficacy and safety of a combination therapy of mirabegron and tamsulosin.[135,136] These trials are relative to drugs already tested and clinically used on monotherapy for BPH or tested for the treatment of other diseases, with exception of fedovapagon (also known as VA106483 and VT483). Fedovapagon (**Figure 6**) is a novel nonpeptidic drug that acts as a vasopressin V2 receptor agonist. This molecule was discovered by *Vantia Therapeutics* and currently is in Phase 2/3 of development for the treatment of nocturia caused by BPH.[137,138]

Table 2. Principal ongoing clinical trials with respect to drug therapy of benign prostatic hyperplasia (BPH).

Study	Clinical trial registry number	Phase
"Efficacy and safety of DKF-313 in patients with benign prostatic hyperplasia"	NCT04947631	3
"Evaluation of the effect of garcinia in combination with chromium on the clinical outcomes of patients with LUTS/BPH"	NCT04590534	2
"Study to evaluate the efficacy, safety and tolerability of vibegron in men with overactive bladder (OAB) symptoms on pharmacological therapy for benign prostatic hyperplasia (BPH)"	NCT03902080	3
"Evaluate the efficacy and safety of GV1001 in patients with benign prostatic hyperplasia (BPH)"	NCT04032067	3
"Efficacy study of fedovapagon for nocturia in men with benign prostatic hyperplasia (BPH) (EQUINOC)"	NCT02637960	2/3
"Efficacy and safety of combination therapy for treatment of overactive bladder in male patients with benign prostatic hyperplasia"	NCT02279615	4

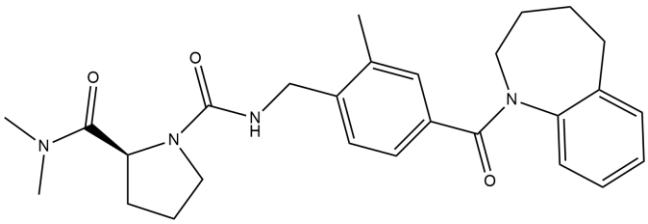

Figure 6. Molecular structure of fedovapagon, a vasopressin V2 receptor agonist developed to treat nocturia. Created with ChemDraw.

1.1.3. Prostatic cancer

Based on GLOBOCAN 2020, PCa is the most diagnosed type of cancer worldwide among men and is the fifth leading cause of cancer-related death (375,000 deaths) (**Figure 7**).[139,140] In particular, the European Cancer Information System estimated that in Portugal the PCa incidence per 100,000 persons per year was 136.5 and mortality was 41.6.[141] Worldwide, the incidence and mortality are correlated with increasing age, a well-established risk factor, as well as with the family history of this type of cancer and with some particular genetic mutations (*BRCA1* and *BRCA2*) and conditions, such as Lynch syndrome.[139,142,143] PCa can be classified as hereditary or sporadic, and most cases belong to the sporadic class.[144,145] Furthermore, in general, African American/Black males have

the highest incidence rates, supporting the importance of Western African ancestry in PCa risk.[146] Concerning the external risk factors, smoking, obesity, and some nutritional aspects may increase the risk of advanced PCa.[147] Worldwide, it is estimated that 2,235,568 new PCa cases will occur in 2040, which corresponds to a trend towards an increase in incidence (+ 58.1 %, compared with 2020). In addition, the same trend is observed relative to mortality, being estimated 720,661 deaths in 2040 (+ 92 %).[148]

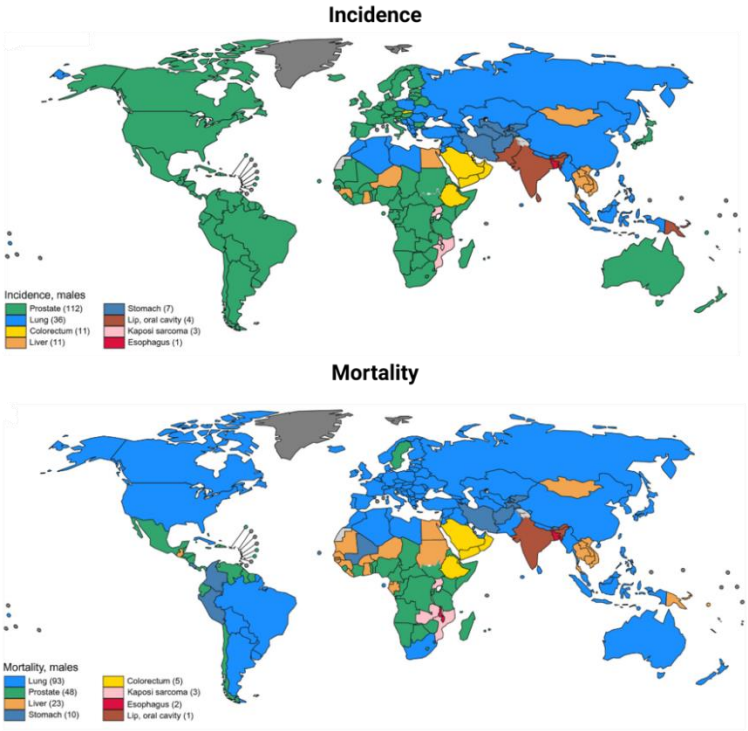

Figure 7. Incidence and mortality of most common type of cancer in each country among men in 2020. The cancer type with the most incidence in developed countries is prostate cancer (PCa) – **green** – (America, Europe, Africa, and Oceania), being the second deathliest behind lung cancer. *Adapted from Sung et al. (2020)*.[139]

1.1.3.1. Pathophysiology

PCa is a multifactorial disorder resulting from mutations in cancer susceptibility genes. The action of environmental agents that potency somatic genetic changes and other systemic or local factors including diet, hormones, and growth factors can result in undesired cell growth/cell survival.[149–151] Currently, it is well-established a relationship between chronic inflammation and several human cancers. Hence, cancer-related inflammation is considered a relevant point for diagnostic and therapeutic approaches.[152] Concerning PCa, it is also relevant to identify the potential triggers and mediators involved in prostatic inflammation and its implication in PCa risk and development. De Marzo and coworkers hypothesized that genetic factors, environmental influences (infectious agents, dietary carcinogens, hormonal imbalances, physical

trauma), and urine reflux cause prostate injury, leading to the development of chronic inflammation.[9] Consequently, chronic inflammation can result in the formation of lesions in epithelial prostate cells as known as proliferative inflammatory atrophy (PIA)., These lesions occur principally at the peripheral zone of the prostate, where PCa typically emerges.[9,153] Most of the PIA may show morphologic transitions to prostatic intraepithelial neoplasia (PIN) lesions, the precursor state of metastatic PCa.[154]

Histologically, prostate carcinoma comprises the accumulation of cancerous epithelial cells. Nevertheless, nonepithelial cells have also a relevant role in PCa initiation and progression, occurring significant modifications in epithelial and stromal cell sections.[154] The high-grade prostate PIN, the *in situ* carcinoma, is a precursor of metastatic PCa and appears in the peripheral regions of the prostate, unlike BPH which occurs almost exclusively within the transition zone. Moreover, morphologically, luminal epithelial cells present nuclear enlargement, nuclear crowding, an increased density of the cytoplasm, and increase in nucleolar size. Despite the decrease in the integrity of the basal cell layer, basal cells are present in PIN.[155] The transition from PIN to metastatic PCa comprises diverse histological modifications in invasive epithelial cells, presenting characteristics similar to luminal cells such as excessive ramification morphogenesis, loss of the basal cell layer, and cytologic atypia with increased nuclei and nucleoli.[154] Initially, PCa is confined to the prostate and at the initial diagnosis, the majority of tumors show an androgen-dependent cell proliferation profile. However, this disease tends to progress and metastasize, becoming independent of circulating androgens to growth, which usually corresponds to a lethal stage.[156] A wide range of studies was accomplished to identify the molecular causes that underlie the defects that may lead to the onset of cancer since they would provide rational targets for PCa prevention and treatment.[157,158] Microscopic analysis of prostate tissue by a pathologist is a requirement for PCa diagnosis, determining the stage after a prostatectomy (remotion of the prostate gland), and histological grading. In this context, the Gleason Score system, created by the pathologist Donald F. Gleason in 1966, is an important tool for the management of PCa.[159] This system depends on the architectural pattern of the tumor and the score results from the sum of the two most predominant growth patterns (**Figure 8**), being considered a simple and reasonably reproducible tool to apply. This scoring system was recently updated in 2015[160,161] and currently, it is one of the key parameters to be taken into consideration for therapy-planning for PCa patients.

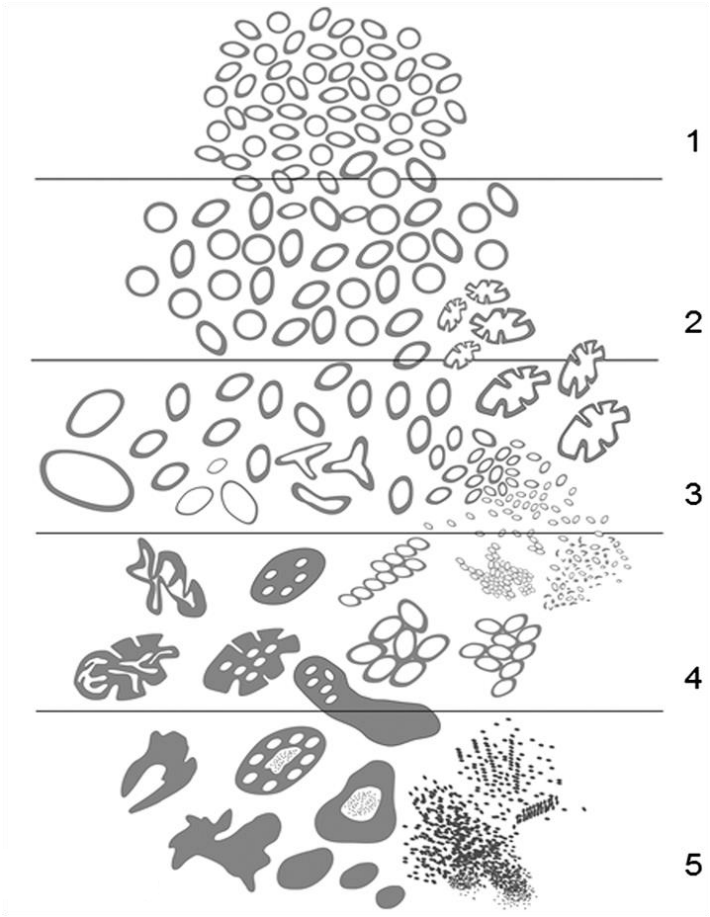

Figure 8. Gleason grading system currently applied. It was modified and implemented by the International Society of Urological Pathology, in 2015. Gleason patterns (1 to 5) correspond to different patterns of growth for prostatic adenocarcinomas. The Gleason score results from the sum of the two most common Gleason grades. *Retrieved from Shah and Zhou (2016).*[162]

Despite the high incidence of PCa and the well-known risk factors, the precise molecular mechanisms involved in the development and evolution of this disease remain to be fully elucidated. However, it is well known that androgens and even estrogens have an important role in PCa carcinogenesis.[163,164] Histological studies revealed a multistage initiation and progression of the neoplastic lesions.[165] Typically, a heterogeneous pattern of oncogenes activation occurs, and some candidate genes and activated pathways with a role in PCa initiation and progression to a more aggressive stage have been identified (**Figure 9**). Substantial evidence has suggested that the standard PCa model comprises several genetic and epigenetic events, namely: (1) low expression of glutathione S-transferase P1 (GSTP1) (2) downregulation of NKX3.1; (3) overexpression of hepsin; (4) frequent chromosomal rearrangement [e.g. ERG and transmembrane protease serine 2 (TMPRSS2)] and overexpression of ETS family proteins; (5) overexpression of Spink 1 (a secreted trypsin inhibitor); (6) loss of Fox P3; (7) loss of PTEN; (8) amplification and overexpression of *c*-Myc; (9) loss of EPHB2 (receptor tyrosine kinase for the ephrin-B

family of ligands); (10) loss of microRNA-101 (Mir-101), (11) overexpression of EZH2 and, (12) overexpression of AR.[154,166] In summary, an inflammatory lesion, PIA, is the early PCa precursor, and activation of c-Myc, telomere shortening, and inactivation of GSTP1 may initiate prostatic carcinogenesis.[167] Moreover, gene fusion comprising TMPRSS2, an androgen-regulated gene, and ETS family of transcription factor genes might contribute to the androgen dependence of PCa, and this fusion is present in about 60 % of PCas and in more than 20 % of PIN lesions.[168,169] Finally, it is well known that the loss of PTEN is related to the aggressiveness of PCa.[170,171]

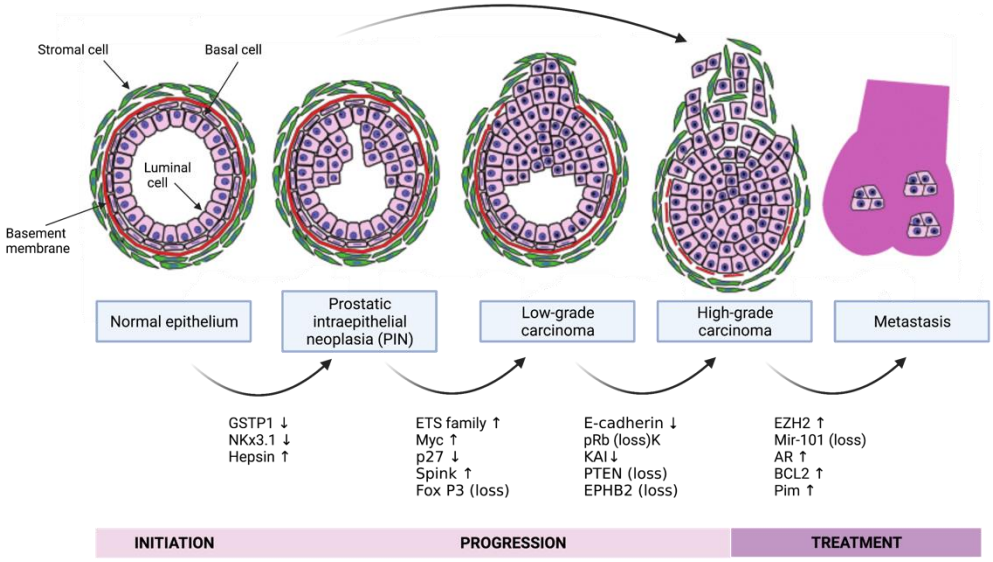

Figure 9. The standard model of the development and progression of prostatic cancer (PCa) based on genetic and epigenetic events. Overexpression of genes is shown with the arrow (↑), downregulation of expression with the arrow (↓) and, the deletion or inactivation of the tumor-suppressor genes is shown as (loss). *Adapted from Vasioukhin (2004) and Knudsen et. al (2010).*[154,166]

1.1.3.2. Steroidal requirements in prostate cancer

Although genetic and epigenetic differences between normal prostate and PCa can characterize the changes that occur in the progression from normal to malignant tissues, steroidal requirements have also an important role in the transition from normal prostate growth to tumor development. In fact, the androgen pathway is essential for the development and differentiation of the normal prostate.[172] In the disease development, the differentiation program driven by AR is instead appropriated through mechanisms that involve TMPRSS2-ETS translocations, which exploit the AR-regulated elements of TMPRSS2 to drive ETS family oncogenes.[169] These translocations occur early in localized disease and continue to sustain the ETS family oncogene expression in metastatic castration-resistant PCa, evident in part by expression analysis of circulating tumor cells.[173,174] Through this mechanism, AR and androgen-driven oncogene expression

probably remains critical for driving metastatic and castration-resistant disease, thereby implicating a continuous requirement for the androgen pathway.[163]

Hereditary deficiencies in three genes prevent or completely block normal prostate development. Loss-of-function mutations in the HSD17B3 gene, which encodes 17β-hydroxysteroid dehydrogenases (17β-HSD), reduce the conversion of 19-carbon-17-ketosteroids to their cognate 17β-hydroxysteroids, impairing the synthesis of testosterone in fetal testes, resulting in female external genitalia.[175] In addition, mutations in SRD5A2, which encodes the dominantly-expressed 5AR type 2 isozyme in the normal prostate that convert testosterone to DHT, cause pseudohermaphroditism and interfere with prostatic development, resulting in a hypoplastic prostate.[163] Lastly, AR mutations that block activation and transcription can affect the ligand-binding or DNA-binding domains, which also suppresses the normal prostate development.[176] These genetic deficiencies evidence the requirement of the two steps for DHT biosynthesis, as well as the requirement of its cognate nuclear receptor, for the development of normal prostate tissue.[163]

AR is a member of the nuclear receptor superfamily which includes the receptors of sex steroids (androgens, estrogens, and progestins), adrenal steroids (glucocorticoids and mineralocorticoids), vitamin D, retinoids, fatty acids, and thyroid hormones.[177,178] AR contains four different functional domains: the NH_2-terminal transactivation domain (A/B domain), the DNA-binding domain (C domain), a hinge region (D domain), and the ligand-binding domain (E domain). Deletion and mutational analyses of nuclear receptors in transfection experiments have identified two transcriptional functions: a ligand-independent NH_2-terminal activation function (AF-1), and a ligand-dependent function (AF-2) located in the ligand-binding domain.[178,179] In the cytoplasm, upon androgens binding, the androgen–AR complexes form homodimers, which constitute the active form of the transcription factor. The homodimers translocate into the nucleus and bind to androgen-responsive elements located on target genes, inducing transcription of genes for proteins such as PSA, which is clinically used for the detection and monitoring of PCa recurrence and progression.[178] In this process, an interaction between the NH_2 and COOH termini of the AR is important in stabilizing the bound ligand.[179,180] This NH_2/COOH interaction is facilitated by several AR coactivators, such as CBP, SRC-1, and ARA70.[181,182]

Although serum androgens alone do not significantly promote prostate carcinogenesis, androgen action and the AR functional status are believed to be relevant mediators of PCa development. Indeed, men castrated when young do not develop PCa. In addition,

androgens seem to increase the carcinogenic activity of genotoxic carcinogens via AR-mediated mechanisms.[182] It is known that androgens regulate proliferation, differentiation, and survival of prostatic epithelial cells, although some of these functions are also controlled by several membrane receptors, such as the epidermal growth factor (EGF) receptor.[183] Moreover, high levels of serum androgens in rats and humans induced by administration of anabolic steroids showed to increase cellular proliferation in the prostate.[178,184,185] Castration of adult male rats leads to a loss of 70 % of the prostate's secretory epithelial cells due to apoptosis.[186] Despite vascular endothelial cells of the prostate do not express AR, castration also induces apoptosis and degeneration of prostatic capillaries and constriction of larger blood vessels that precedes the appearance of apoptosis in prostatic epithelial cells.[178,187] Since androgens can regulate a subset of paracrine growth factors and thereby influence vascular survival, it is possible that castration initially changes growth factor production by prostatic stromal cells, resulting in a decreased vascular supply. Subsequently, the resulting reduction of blood flow, combined with decreased expression of other androgen-regulated proteins, might contribute to apoptosis of the secretory epithelia. Thus, prostatic cells have a wide range of responses to androgens, and the properties of the AR might play a relevant role in both the maintenance and homeostasis of normal prostatic epithelium and PCa development.[178]

Despite the high relevance of androgens in the prostate growth and function, and in PCa, estrogens also play an important role in this context. Indeed, estrogens have indirect systemic effects on the prostate, acting on the hypothalamus–pituitary–gonadal axis. Estrogens inhibit the release of gonadotropin-releasing hormone (GnRH) from the hypothalamus, blocking the release of luteinizing hormone (LH) from the pituitary.[164] Leydig cells, which are responsible for the production and secretion of testosterone, are dependent on LH. Consequently, exogenous estrogens affect the prostate by causing chemical castration/androgen deprivation, inducing prostatic epithelial apoptosis and generalized regression of this gland size.[188]

Estrogens act through estrogen receptors (ERs). Estrogen molecules diffuse through plasma membranes and bind to ERs found within the cytoplasm or nucleus where cofactors bind to the estrogen–ER complex, regulating transcription of specific target genes by binding to associated DNA regulatory sequences. There are two subtypes of ERs: ERα and ERβ.[189] The subtype β is highly expressed in prostatic epithelium in adulthood, while subtype α is predominantly expressed in adult prostatic stroma and to a lesser extent in the adult prostatic epithelium. Moreover, several studies have

demonstrated the presence of ERα in prostatic stromal cells during various stages of prostatic development and in prostatic pathogenesis.

Epidemiological and experimental studies established a relation between estrogens and PCa based on multiple evidences. In species susceptible to PCa (men and dogs), the 17β-estradiol (estrogen) to androgen ratio increases during aging when PCa manifests and is diagnosed. The raise in this ratio is temporally related to the development of BPH and PCa.[190,191] African Americans (highest incidence of PCa) have elevated levels of free plasma estradiol and testosterone.[192] In contrast, Caucasian Americans, Latino Americans, and Asian Americans (lower incidence of PCa) have reduced levels of serum estradiol and testosterone.[193] Furthermore, testosterone in combination with estradiol induces prostatic hyperplasia in dogs and induces PCa in rodent and human tissues.[190,191,194] The incidence of PCa is the highest in elderly men who have an increased estradiol/testosterone ratio.[195,196] The change in this ratio is often related with a decline in testicular function (reduced of testosterone production) and increased aromatase activity (estrogen production). Currently, the roles of aromatase and hence estrogen/ER signaling in prostatic carcinogenesis are being investigated.[164,197] Considering these evidences, targeting therapies toward the estrogen pathway may be a successful chemopreventive strategy for prostatic carcinogenesis.

1.1.3.3. Therapeutic approaches

There have been great advances in the treatment of PCa in the past 40 years. In 1985 in the USA, the five-year survival rate was 75 %, while in 2016, it was 98 % (this number is based on men diagnosed with PCa between 2010 and 2016 for all disease stages combined).[198,199] The treatment of PCa is selected based on the clinical stage, Gleason Score, and serum PSA levels (**Figure 10**).[10,200] The clinical stages comprise localized disease followed by the non-castrate rising PSA stage and the non-castrate metastatic stage. Usually, the castration-resistant stage is lethal.[201] Clinical staging describes the classification of cancer, and this is a piece of important information for treatment selection. Therefore, identifying a low-risk tumor can prevent a more invasive treatment, while identifying a high-risk tumor can encourage a more aggressive treatment approach.[198]

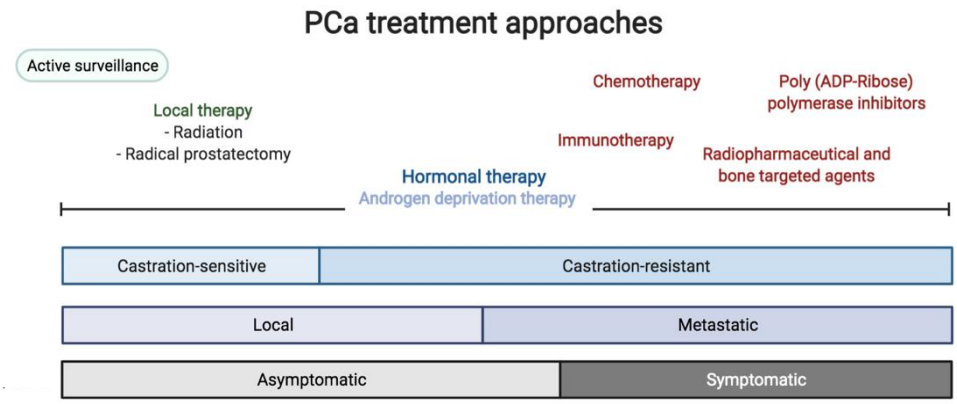

Figure 10. Treatment options for prostatic cancer (PCa). Created with BioRender.com.

- **Primary therapy**

Patients diagnosed with localized PCa have wide management options, comprising observational approaches as watchful waiting/active surveillance, radical prostatectomy, brachytherapy, and external beam radiation therapy.[202] The active surveillance approach has become a viable alternative to treatment and it involves close observation of a patient with frequent visits to a physician for a digital rectal exam, a PSA test, and, if necessary, a biopsy. If there is a change in the tumor characteristics, the patient may need to decide on a treatment. Active surveillance allows a patient to delay the treatment, thereby avoiding any side effects. Similar to BPH, the radical prostatectomy, i.e. the removal of the prostate gland and some surrounding tissue, is an option in localized PCa treatment with the same risks associated. This surgical method is most often recommended for men who have a life expectancy of at least 10 years or more.[203] Brachytherapy consists in placing radioactive seeds inside the prostate gland. This placement of the seeds affects the amount of radiation received by the tumor and other parts of the prostate. When developing a treatment plan, the aim is to deliver an appropriate amount of radiation to the tumor and to the tissue identified as at risk of cancer, while sparing healthy tissue. Brachytherapy carries risks including urinary problems and erectile dysfunction.[198]

For the treatment selection in localized PCa, several factors should be considered including: (1) specific side effects of different treatments, (2) possible comorbid conditions that may increase the severity of side effects or complications risk, (3) characteristics of cancer and the risk of progression without treatment, and (4) patient preferences. In the last two decades, radical prostatectomy and radiation therapy approaches for PCa have improved considerably, allowing a more effective local control of cancer, and reducing the appearance of side effects. More recently, the utility of hormonal therapy has also been demonstrated for localized PCa. Particularly, the

strongest evidence comprises the use of hormonal therapy in combination with radiation therapy.[204] However, the absence of comparative studies about the different therapeutic approaches makes it difficult for patients to choose a treatment that provides a clear advantage in terms of disease-free survival and quality of life. Considering this fact, patient preferences play an important role in a shared decision by patient and physician.[205]

- **Hormonal therapy in the treatment of metastatic disease**

Concerning mainly the metastatic disease, the androgen signaling axis is the major systemic treatment target, as depicted in **Figure 10**, through agents capable of restraining ongoing AR activation. Multiple approaches relative to hormone therapy have been employed in the management of PCa (**Figure 11)** and several drugs in this context have been approved for clinical use (**Table 3**).[10,206]

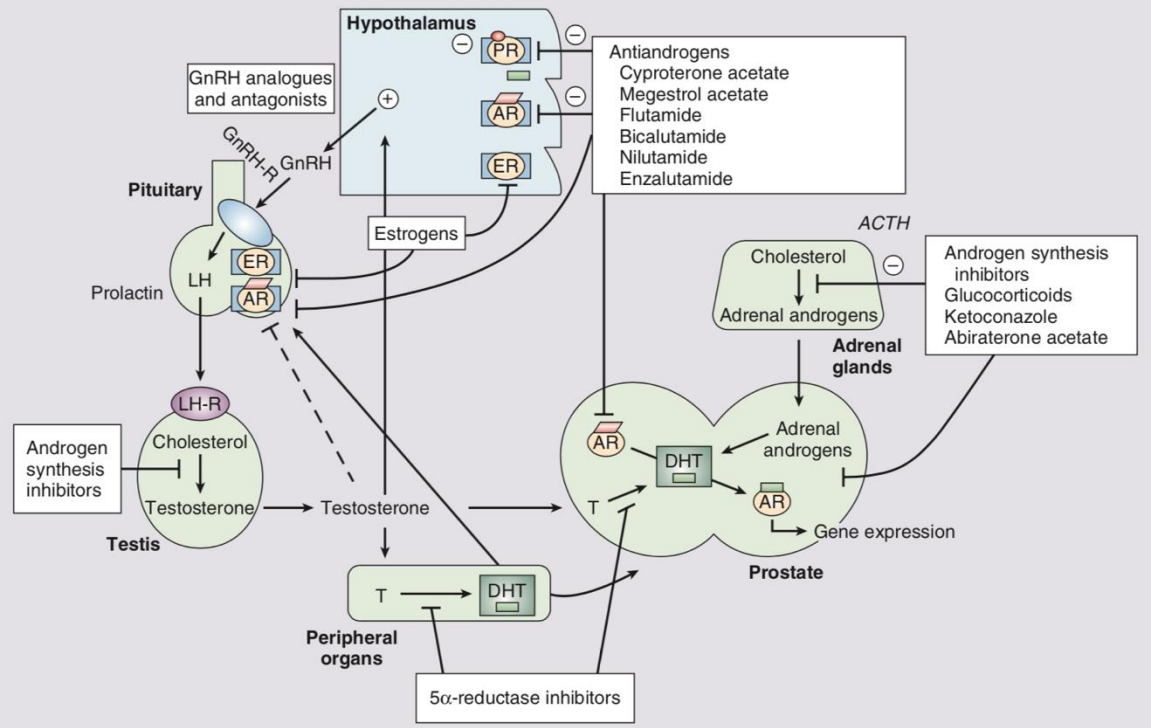

Figure 11. The hypothalamic-pituitary-gonadal axis and targets for hormonal therapy agents in prostatic cancer (PCa). ACTH= Adrenocorticotropic hormone, GnRH-R= GnRH receptor, LH-R= Luteinizing hormone receptor, PR = Progesterone receptor, T= Testosterone. *Adapted from Nelson et al. (2020).*[10]

The androgen deprivation therapy (ADT) comprises the reduction or blockade of gonadal androgen production and/or signaling, and has been a part of the standard care for patients with PCa since the 1970s.[207] Currently, this approach is accomplished through surgical castration and/or by medical castration. The surgical castration by bilateral orchiectomy is the most immediate method to reduce circulating testosterone by > 90% within 24h, and there is no risk of a paradoxical flare of the disease.[208] The first reversible

medical castration method was accomplished by administration of diethylstilbestrol (DES) – a semi-synthetic estrogen compound – in the 1940s.[207] Its anti-tumor effect is assigned to different actions on the PCa: (1) the negative feedback exerted on the hypothalamic–pituitary complex causes a decrease in luteinizing hormone secretion, decreasing androgen secretion; (2) DES increases the levels of sex hormone-binding globulin and pituitary prolactin secretion, decreasing testosterone production in the testes, and (3) DES also suppress the function of Leydig, inhibiting the secretion of androgenic steroids.[209] This effect decreases the secretion of testosterone. However, the Veterans Administration Cooperative Urological Research Group discovered that DES (at 5 mg/day) augmented cardiovascular and thrombogenic events. To reduce these side effects, lower doses of DES were administrated (1-3 mg/day) and consequently, fewer cardiovascular side effects were detected.[209,210] The discovery of gonadotropin-releasing hormone agonists and analogs, also called luteinizing hormone-releasing hormone (LHRH) agonists, efficacy similar to orchiectomy and DES and without increased cardiovascular and thromboembolic toxicity led to a loss of interest in DES.[211] Therefore, in the 1980s, DES stopped being clinically used and then was discontinued in most countries.[210]

GnRH agonists are capable of suppressing GnRH receptors and their actions, reducing the secretion of LH and follicle-stimulating hormone (FSH). Initially, GnRH agonists stimulate the pituitary gland which results in a temporary increase in the gonadotropins FSH and LH. Nevertheless, continued administration of the GnRH agonist desensitizes the pituitary gland, leading to a decrease in the secretion of gonadotropins and the production of sex hormones. As result, the testicular production of testosterone is decreased.[212] Currently, the GnRH agonists approved for the treatment of PCa are leuprolide, goserelin, and triptorelin. These agonists primarily trigger LH release by the pituitary, initiating a short-lived rise of serum testosterone levels which is frequently related to the symptomatic disease known as “flare” in men with widespread bone metastasis.[213] To prevent the appearance of this phenomenon, the administration of an estrogen or antiandrogen a week before and during the first weeks of GnRH agonist therapy is often an effective strategy.[214] In addition, GnRH antagonists (degarelix and relugolix) are also capable of suppressing testosterone levels more rapidly through direct inhibition of GnRH binding to its receptor, without initial stimulation of the GnRH receptor. This fact contributes to the absence of the “flare” phenomenon, being an approach frequently employed for advanced PCa treatment.[215] Generally, patients accept more easily GnRH therapy than bilateral orchiectomy (surgical castration).[10] Considering the other side effects of orchiectomy and GnRH agonists and antagonists,

they are very similar and can include: libido reduction, erectile dysfunction, testicles and penis atrophy, gynecomastia, osteoporosis, anemia, fatigue, weight gain and muscle mass loss, increased cholesterol levels, and depression.[216] In several patients with PCa, initially, ADT frequently leads to prolonged remission by decreasing the serum testosterone levels. However, eventually, an increase in serum PSA levels is detected despite adequate ADT. The failure of ADT indicates the appearance of novel signaling pathways usually driven by androgen-dependent mechanisms stimulating tumor progression and metastasis, despite the circulating androgen levels being at castration levels. Several mechanisms that possibly explain the tumor development in this disease stage, refereed as castration-resistant PCa (CRPC) have been determined. Despite these multiple mechanisms discovered, the AR stimulation remains the principal pathway.[217–219] In fact, until the moment, the studies have reported the importance of intratumoral androgen synthesis in CRPC progression, and ultimately, the lethality of this disease.[220]

In this context, a strategy to target the androgen signaling is the use of antiandrogens, a class of agents that interact straight with the AR to antagonize the correspondent transactivation of target gene transcription.[10,216] This class includes steroidal and nonsteroidal antiandrogens, presenting distinct pharmacological profiles. Steroidal antiandrogens (e.g. cyproterone acetate) are capable of decreasing testosterone levels and bind to other hormone receptors. On the other hand, nonsteroidal antiandrogens (e.g. flutamide, nilutamide, and bicalutamide) are more specific for AR.[216,221] Initially, antiandrogens were developed to be used in combination with medical castration (GnRH agonists and antagonists), a strategy known as combined androgen blockade (CAB). Theoretically, this approach aims to achieve a "complete" androgen blockade (completely eliminating androgens in the prostate tissue - intratumorally) through the reduction of androgen levels and neutralization of the propensity for adrenal androgen precursors (e.g. androstenedione and DHEA) to activate AR function.[222,223] Nevertheless, the increasing usage of antiandrogens as monotherapy was observed as a result of side effects of castration approaches, which have a negative impact on patients' quality of life. In fact, monotherapy with antiandrogens preserves gonadal function and, thus, improves the quality of life in terms of sexual function and bone demineralization.[224]

In men with PCa, the production of androgens by the adrenal glands (nongonadal source) or by cancer itself occurs in a significant manner, even in the castrate state. In this context, it has been considered that the levels of androgens produced by the adrenal glands are sufficient to activate the AR. In PCa, androgens can arise from two different pathways: (1) local conversion of adrenal precursors and (2) *de novo* synthesis through

the augmented expression of steroidogenic enzymes, such as CYP17.[225,226] Therefore, in clinical practice it is frequent the administration of high doses of ketoconazole, a CYP17 inhibitor, to antagonize this process. Interestingly, the treatment with this drug shows advantages for men with CRPC. In fact, several studies have demonstrated that ketoconazole treatment induced a ≥ 50 % PSA decline in 20–75 % of patients. In addition, the time to PSA progression ranged from 3 months to 14 months in patients receiving this drug.[227–229] Concerning the possible side effects, ketoconazole can cause elevated liver enzymes in blood tests (indicative of inflammation or damage), nausea, vomiting, gynecomastia, and a skin rash.[230] Since ketoconazole exhibits unselective inhibition toward CYP17, CYP11B1, CYP11B2, CYP11A1, and some hepatic CYP enzymes like CYP3A4, several drug interactions have been reported, as expected. This lack of selectivity also explains the verified side effects in the liver function.[231] More recently, a much more potent and selective CYP17 inhibitor than ketoconazole, abiraterone acetate, was developed and approved by FDA for clinical use. This drug is a pregnenolone analog and is principally used in the treatment of CRPC, considering the improvements in patients' survival in two randomized clinical trials. The side effects of abiraterone acetate, which are considered marginal, are hypokalemia, stigmata of secondary mineralocorticoid excess, and hypertension.[232–234]

Glucocorticoids have been used in the management of several tumor types, including metastatic CRPC, over the past three decades (e.g. prednisone and dexamethasone). These agents can suppress the secretion of adrenocorticotrophic hormone, resulting in lower expression of adrenal androgens. Consequently, a decline in PSA and in circulating tumor cells is observed.[235,236] While hydrocortisone and its derivatives, as prednisone, have both glucocorticoid and mineralocorticoid effects, dexamethasone is a more selective glucocorticoid receptor (GR) agonist.[237] Glucocorticoids are frequently administered in combination with chemotherapy agents for metastatic CRPC, also providing their anti-inflammatory and anti-emetic activities, which can suppress some aggressive therapy-related side effects.[238,239] However, their independent impact on patients' survival remains unclear, and unfavorable effects, such as osteoporosis and immunosuppression, complicate long-term use.[235] More recently, the high GR expression has been linked with resistance to enzalutamide therapy. Particularly, augmented GR expression was detected in enzalutamide-resistant tumors *in vivo* and in tumor biopsies from PCa patients treated with this drug.[240,241] In this context, the medical resistance that frequently emerges might be elucidated by the fact that AR can directly repress GR expression in PCa via a negative androgen response element in the GR promoter. Then, when AR signaling is blocked, the functional replacement of AR by GR can be a reasonable explanation.[242]

Table 3. Approved drugs for clinical use in prostate cancer (PCa) treatment targeting androgen signaling, and respective mechanism of action. Molecular structures were created with ChemDraw.

Approved drug		Mechanism of action
ID	**Molecular structure**	
Leuprolide	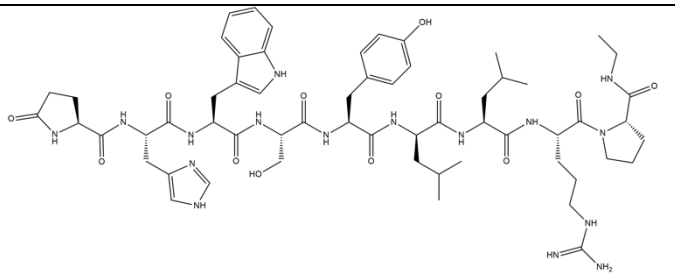	*GnRH agonist*
Goserelin	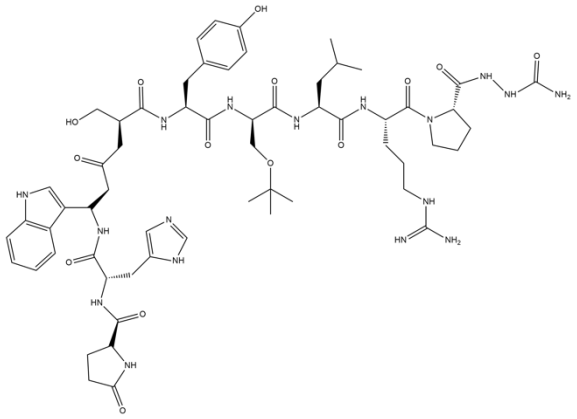	
Triptorelin	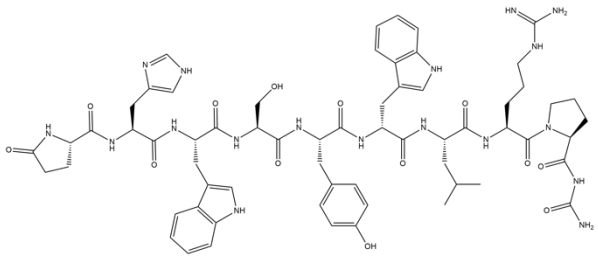	
Degarelix	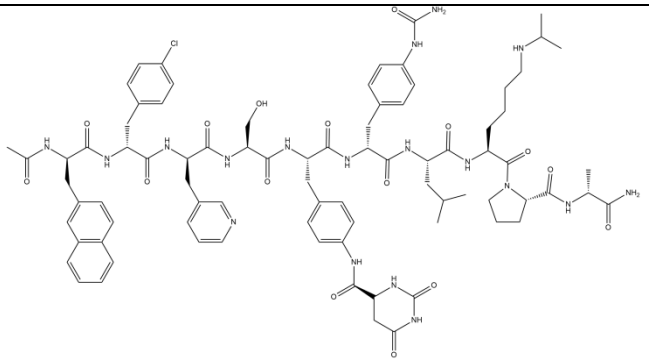	*GnRH antagonist*
Relugolix	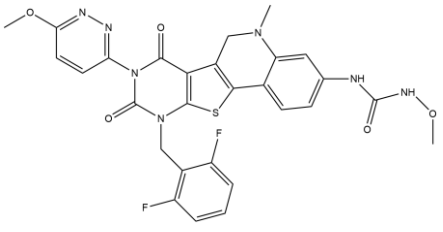	

Table 3. (Continuation).

ID	**Molecular structure**	**Mechanism of action**
Cyproterone acetate	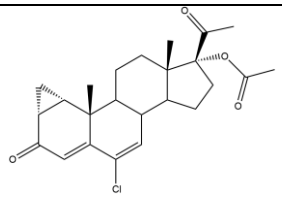	*Antiandrogen*
Megestrol acetate	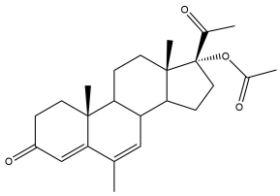	
Flutamide	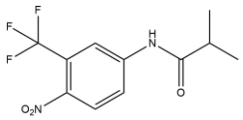	
Bicalutamide	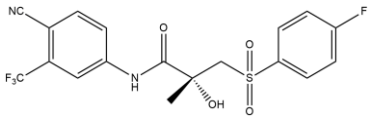	
Nilutamide	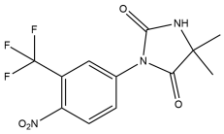	
Enzalutamide	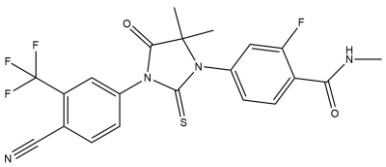	
Apalutamide	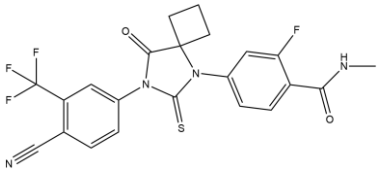	
Darolutamide	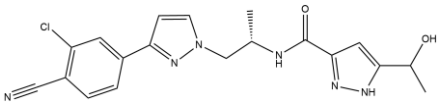	

Table 3. (Continuation).

ID	Molecular structure	Mechanism of action
Ketoconazole	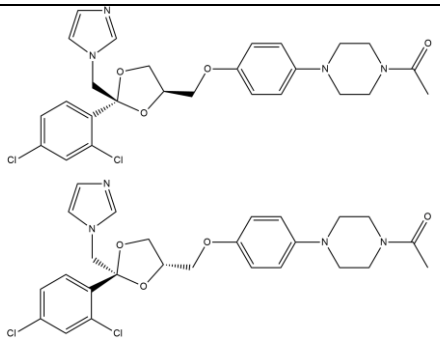	*Androgen synthesis inhibitor*
Abiraterone acetate	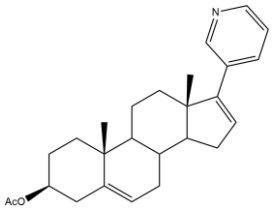	
Hydrocortisone	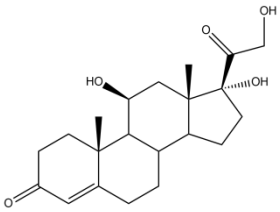	
Cortisone	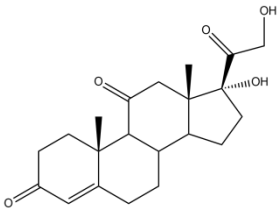	
Prednisone	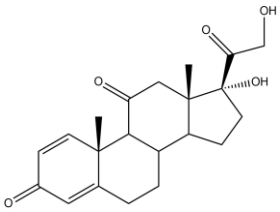	
Dexamethasone	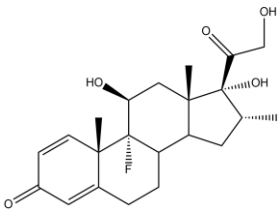	

Another apparently valid strategy targeting the androgen signaling axis would be the use of 5ARIs, since they inhibit the conversion of testosterone in DHT and, consequently, reduce the activation of the AR pathway. Considering this fact and the important role of androgens in the development of PCa, some researchers hypothesized that finasteride

could reduce PCa progression. Several studies have reported a 25 % reduction in PCa incidence in men receiving finasteride compared to a placebo.[243–245] Nevertheless, finasteride is not labeled for PCa treatment and it was rarely used for PCa prevention.[246] Although finasteride seems to reduce the incidence of PCa, an increase in the incidence of high-grade PCa compared to placebo was reported by the Prostate Cancer Prevention Trial (PCPT).[247] In the last decade, several studies have investigated the correlation between finasteride use and PCa, but they have shown contradictory results. Some studies reported that finasteride might reduce PCa risk and other different studies showed the contrary. In 2011, according to the information obtained from the trials PCPT and Reduction by Dutasteride of Prostate Cancer Events (REDUCE), the FDA made a safety announcement to healthcare professionals: "*The U.S. Food and Drug Administration (FDA) is informing healthcare professionals that the Warnings and Precautions section of the labels for the 5-alpha reductase inhibitor (5-ARI) class of drugs has been revised to include new safety information about the increased risk of being diagnosed with a more serious form of prostate cancer (high-grade prostate cancer). This risk appears to be low, but healthcare professionals should be aware of this safety information, and weigh the known benefits against the potential risks when deciding to start or continue treatment with 5-ARIs in men*".[248] More recently, a meta-analysis identified eight studies, including 54,335 cases of patients that used finasteride and 9197 patients who served as placebo controls and the results showed a significant correlation between finasteride use and high-grade PCa, corroborating the previous data.[249] Interestingly, some studies also reported that dutasteride, other 5AR inhibitor, can improve the prognosis of PCa patients, particularly with low-risk PCa.[250,251]

- **Chemotherapy for metastatic CRPC**

Relative to systemic chemotherapy drugs for the management of metastatic CRPC, only taxanes have demonstrated significant improvements in survival rates. Docetaxel and cabazitaxel (**Figure 12**), the taxanes approved for clinical use for metastatic CRPC treatment, led to the disruption of microtubule function, promoting apoptosis. However, the exact mechanism of action that occurs in PCa cells remains unclear. Concerning the side effects, the more frequent are neutropenic events, diarrhea, and fatigue/asthenia.[10,252–254] Therefore, glucocorticoids, as previously mentioned, are frequently administered in combination with these chemotherapeutic drugs, which help reducing these aggressive side effects.

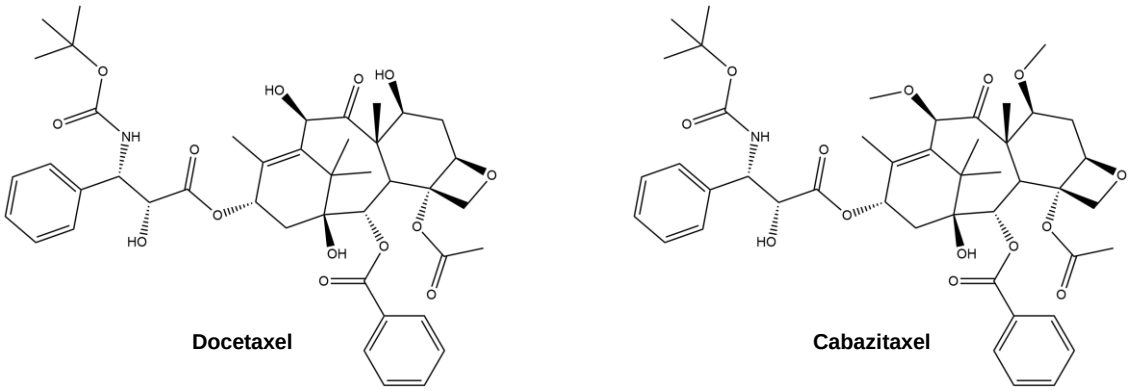

Figure 12. Drugs approved for clinical use in the chemotherapy of metastatic castration-resistant prostatic cancer (CRPC). Created with ChemDraw.

- **Other therapeutic approaches in the management of metastatic PCa**

There are other several strategies in the management of metastatic PCa such as immunotherapy with sipuleucel-T, the use of radiopharmaceuticals (e.g. radium-223) for symptomatic bone metastasis, and zoledronic acid/denosumab to prevent bone resorption.[255]

In general, cancer immunotherapy consists of the attempts to treat cancer through the activation of immune responses against malignant cells while overcoming tumor-induced tolerance. In this context, several PCa vaccine approaches have been endangered to early clinical development studies.[256] Currently and since 2010, sipuleucel-T, which is an autologous prostate-specific acid phosphatase-loaded antigen-presenting cell, is the only such treatment approved by the FDA based on the IMPACT trial.[10,257]

Patients with metastatic PCa are at high risk of skeletal complications, due to the increasing bone resorption and reduction of bone mineral density (osteopenia and/or osteoporosis) as a consequence of chronic ADT. Another reason is bone involvement in PCa which is very common. In fact, up to 75% of patients with metastatic PCa have this complication. Bone metastasis generally causes bone pain and more rarely hypercalcemia of malignancy appears, as well as other skeletal-related events, including pathologic fractures. In an attempt to treat these symptoms, radiation or surgery, or spinal cord compression are valid approaches.[10,255] Concerning radiopharmaceuticals, radium-223, an alpha emitter, was approved by FDA in 2013 to treat symptomatic bone metastasis in patients with CRPC and without presenting visceral metastasis, based on data obtained from the ALSYMPCA trial.[258]

For several years, to help the maintenance of skeletal integrity in patients with bone-metastatic PCa, intravenous bisphosphonates, such as zoledronic acid, have been used. The benefits of bisphosphonates were reported in a phase III study comprising men with metastatic CRPC and minimally symptomatic bone metastasis, in which zoledronic acid was compared against placebo.[259] Recently, immunotherapy using a monoclonal antibody capable of blocking the receptor activator of nuclear factor–κB (RANK) ligand, denosumab, was also approved by FDA for the prevention of skeletal-related events in bone-metastatic CRPC, based on the findings from a large randomized phase III trial.[260] Denosumab blocks the binding of RANK ligand to the respective receptor, inhibiting the osteoclastic activity and thus osteoclast-mediated bone resorption.[261]

More recently, a new class of agents emerged for the treatment of metastatic CRPC, namely the poly (ADP-ribose) polymerase (PARP) inhibitors. PARP is an enzyme involved in several mechanisms of DNA repair and may rescue cells with defects in homologous recombination. Consequently, the pharmacologic inhibition of PARP may lead to the apoptosis of cancer cells.[262] Currently, olaparib and rucaparib camsylate are the two drugs approved for clinical use in the treatment of metastatic CRPC (**Figure 13**).[263,264] In a clinical trial (NCT02987543), olaparib was associated with longer progression-free survival and improved response compared with enzalutamide or abiraterone. This trial was conducted in men with metastatic CRPC who had disease progression whereas receiving enzalutamide or abiraterone.[264] Concerning rucaparib, another clinical trial (NCT02952534) was performed to evaluate rucaparib also as a treatment for men with a metastatic CRPC related to a *BRCA*1 or *BRCA*2 gene modification who had received previous taxanes and ADT. Results showed that rucaparib has antitumor activity in patients with metastatic CRPC and a deleterious *BRC*1 and *BRCA*2 modification, with a manageable safety profile reliable with that described in other solid tumor types.[263]

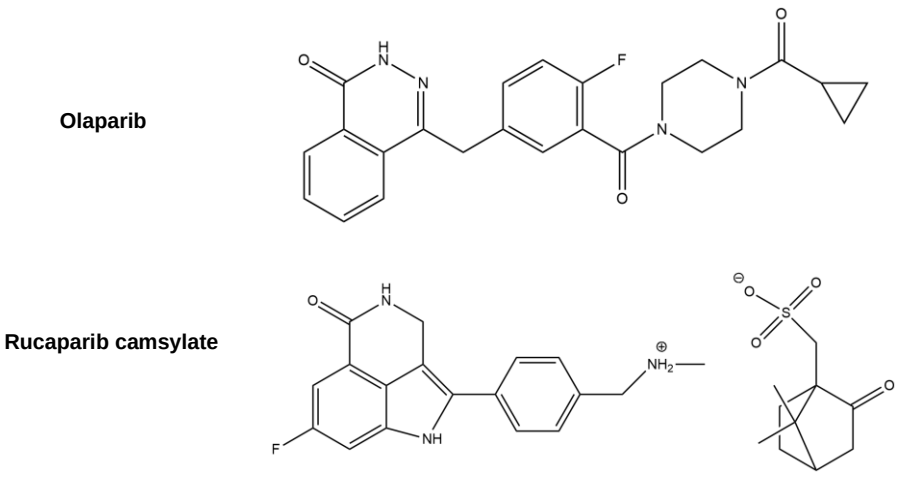

Figure 13. Poly (ADP-ribose) polymerase (PARP) inhibitors approved for clinical use in metastatic castration-resistant prostatic cancer (CRPC) treatment. Created with ChemDraw.

In summary, in the last years, the treatment of PCa has progressed considerably, with the development of drugs with different mechanisms of action improving outcomes and patients' quality of life.

- **Principal emerging drugs for PCa treatment**

The main strategy for treating PCa remains to target the AR signaling pathway. However, considering the elevated incidence of PCa and the disadvantages of the existing therapies, a considerable number of novel drugs are presently being studied worldwide. The discovery and development of new drugs has been markedly associated to a better understanding of the molecular mechanisms and signaling pathways in PCa. It is also important to mention that the clarification of the genetic factors involved in PCa progression is also essential to apply individualized and targeted therapy. In addition, despite the importance of drug discovery, it is also determinant the detection of PCa at an earlier stage to more efficiently prevent the progression of the disease, recurrence, and metastatic condition.[265]

Presently, several ongoing clinical trials aim the assessment of the efficacy and safety of new drugs to treat PCa, and the main examples are shown in **Table 4**. In addition to the described in this table, there are a significative number of clinical trials ongoing relative to combinatory therapy with already approved drugs, biomarkers, new radiopharmaceuticals (pharmaceutical drugs containing radioactive isotopes), and new diagnosis methods.[135]

Table 4. Principal ongoing clinical trials for novel agents in prostatic cancer (PCa) treatment. [a]

Drug	Mechanism of action	Clinical trial registry number	Phase
LAE001	Dual inhibitor of CYP17 and CYP11B2	NCT03843918	1/2
Nivolumab	PD1 blocker	NCT03637543	2
Avelumab		NCT03179410	2
ES414	Activator of T-cells	NCT02262910	1
Abemaciclib	Dual inhibitor of CDK4 and CDK6	NCT03706365	2/3
Capivasertib	AKT kinase inhibitor	NCT04493853	3
Atorvastatin	HMG-CoA reductase inhibitor	NCT04026230	3
HC-1119	AR inhibitor	NCT03850795	3

[a] PD1= Programmed cell death protein-1; CDK= Cyclin-dependent kinase; AKT= Protein kinase B; HMG-CoA= 3-Hydroxy-3-methylglutaryl-coenzyme A.

Concerning the earlier stages of drug discovery, numerous new molecular identities with potential anticancer activity against PCa, proven through *in vitro* and *in vivo* studies have been developed. Some relevant and more recent examples are shown in **Table 5**, and include steroidal, naproxen, and thiosemicarbazone-indole derivatives, and a prostate-specific membrane antigen-targeted monomethyl auristatin E conjugate. Interestingly, all of these potential drug candidates showed the capacity to reduce tumor volume in xenograft models.

Table 5. Examples of relevant compounds that may exert beneficial outcomes in the treatment of prostatic cancer (PCa), biological data, and respective references. Molecular structures created with ChemDraw. [a]

Drug candidate	Biological data	Ref.
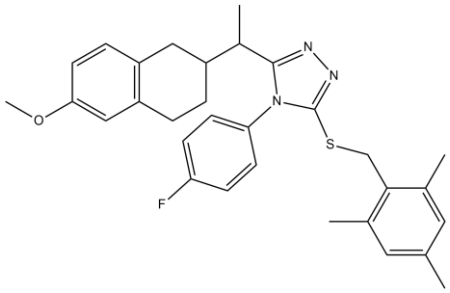 **SGK636**	*In vitro* - Antiproliferative activity: IC_{50} (DU-145)= 10.2 μM ; IC_{50}(LNCaP)= 2.21 μM - Induction of apoptotic genes including Bax, Caspase-3, Caspase-9 - Suppression of anti-apoptotic BcL-2 mRNA levels in LNCaP cells *In vivo* - Xenograft model (LNCaP): in male nude mice, SGK636 stopped the cancer development and invasion (55-70 %)	266
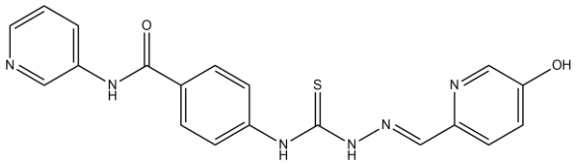 **Thiosemicarbazone-indole derivative**	*In vitro* - Antiproliferative activity: IC_{50}(PC3)= 0.054 μM - Induction of G1/S cycle arrest and apoptosis *In vivo* - Xenograft model (PC3): in mice, compound induced the reduction of tumor volume (43-54 %) - in mice, no significant toxicity was observed in the heart, liver, spleen, lungs, and kidney	267
Conjugate PSMA-Val-Cit-PAB-MMAE	*In vitro* - Antiproliferative activity: IC_{50}(PC3)= 29 nM; IC_{50}(22Rv1)= 27 nM *In vivo* - Xenograft model (22Rv1): in nude mice, the conjugate induced tumor growth inhibition (77-85 %) - Acute, chronic, and subchronic toxicities and pharmacokinetics studies have shown lower toxicity than MMAE (reference drug)	268

[a] MMAE= Monomethyl auristatin E; PSMA= Prostate-specific membrane antigen

Currently, *in silico* tools have been used as an important method to rationally design new potential drug candidates, and PCa context is not an exception. On the other hand,

computational drug repositioning methods using public databases are a promising and effective tool for discovering new applications for already existing drugs. In this ambit, Kim and coworkers predicted potential drug candidates to treat CRPC using a computational method that integrates available gene expression information of tumors from CRPC patients, drug-induced gene expression, and drug-response activity data. This study allowed to predict that sorafenib, olaparib, elesclomol, tanespimycin, and ponatinib may be active for the treatment of CRPC.[269] In another research, functional module genes, DNA methylations, core regulators, and potential drugs in primary PCa and CRPC were investigated through bioinformatic analyses. From these studies, exisulind and phosphodiesterase-4 inhibitors emerged as potential drugs for CRPC.[270] In summary, *in silico* studies constitute a new approach for scientists to clarify the potential molecular mechanisms of CRPC and important references for drug redirection and new drug development for PCa.

- **Could be 5ARIs potentially useful in the PCa treatment?**

After studies demonstrating the efficacy of using 5ARIs in prevention of PCa, the study of the use of these inhibitors in the treatment of PCa is the logical next step. At this moment, the efficacy and safety of 5ARIs in treating PCa have not been fully determined, and some controversial data were obtained, as described above. However, a more recent meta-analysis suggested that the use of 5ARIs in the PCa treatment can benefit patients with local and low Gleason score (≤ 7) PCa, especially in delaying the disease progression.[271] Moreover, the Therapy Assessed by Rising PSA (TARP) study was the first study to evaluate the effects of dutasteride and an antiandrogen in patients failing GnRH analogue. This research also aimed to elucidate the potential role of the dual 5ARI in rate reduction of progression in non-metastatic CRPC.[272] Although, the results of this study were not reported until the moment. Concerning to the localized disease, a more recent study, the Avodart After Radical Therapy for Prostate Cancer Study (ARTS), assessed the effect of dutasteride on PCa progression in patients with biochemical failure after radical therapy. From this study it was concluded that dutasteride delayed the progression of PCa. The safety and tolerability profile of dutasteride in these patients was generally consistent with previous experience.[251] Furthermore, several pre-clinical researches have demonstrated that inhibition of 5AR isoenzymes by finasteride or dutasteride can kill prostate cancer cells (LNCaP cells: hormone-dependent; PC-3: hormone-independent cells) and increase apoptosis *in vitro* and *in vivo*.[273–279] Considering all these facts, the research in this field still comprising a relevant focus of interest in the context of PCa treatment with promising outcomes.

1.2. Arylidenesteroids as bioactive molecules

Steroids are natural products that share a 17-carbon-atom skeleton and are composed of four fused rings: three cyclohexanes (A, B, and C rings) and one cyclopentane (D ring). The 17 carbons are numbered in ascending order from ring A until ending in ring D. Additional carbon atoms on steroids include angular methyl groups attached to C-13 and C-10 and alkyl substituents on C-17. Steroids vary on the attached functional groups, their position, and their configuration (**Figure 14**).[280,281] In the two-dimensional representation, the steroid scaffold seems planar and substituents on carbons of the steroid scaffold may be located either above or below the "plane" of the steroid. The stereochemistry of substituents is marked using the wedge–dash, indicating β-configuration (wedge) when substituents are above the plane, or α-configuration (dash) when substituents are below the plane. In consequence, the stereochemistry of the rings and the substituents on the steroid scaffold not only affects the biological activity of a given class of steroids, as well as their chemical reactivity to undergo further structural modifications (chemical synthesis).[281,282]

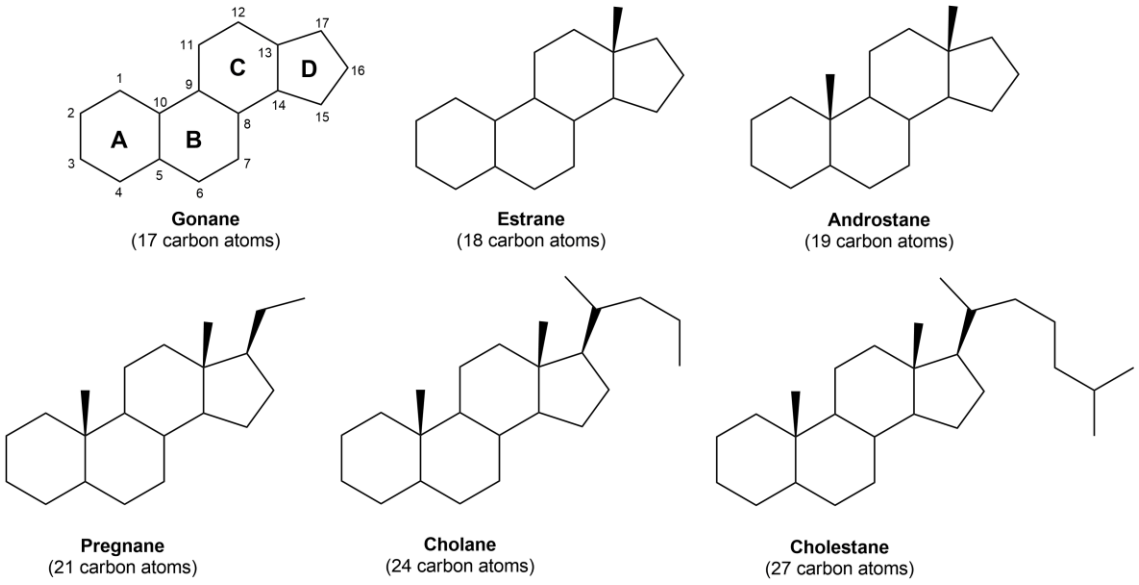

Figure 14. Chemical structure and numbering of the basic steroid skeleton (gonane), and classification of the main steroidal systems based on the number of carbons in the molecule. Created with ChemDraw.

This unique class of chemical products plays a crucial role in several biological processes, being the most important group of regulatory and signaling molecules. Steroids are widely found in animal and plant kingdoms, including in humans, and are biosynthesized from cholesterol via several enzyme-mediated transformations. Generally, steroids are lipophilic and readily enter cells, being able to interact with nuclear receptors as well as with membrane proteins. Therefore, they are associated with

most physiological functions and pathological conditions.[283] Moreover, steroid-based therapeutic drugs have called attention to the scientific academia and pharmaceutical industry for a long time due to their relatively low toxicity, less vulnerability to multi-drug resistance, and high bioavailability.[284–287]

Nowadays, steroidal derivatives constitute an important class of pharmaceutically active compounds for a large number of diseases, comprising brain tumors, breast and prostate cancers, osteoarthritis, adrenal insufficiencies, fungal and microbial infections, in addition to cardiovascular and autoimmune diseases.[288–293] Considering their relevance, several modified steroids have been synthesized and biologically evaluated, being verified that their relevant pharmacological properties depend on the structural features of the steroidal four-ring skeleton and side-chain.[284,294] In fact, even a minor structural change on the steroidal nucleus can lead to marked alterations in their physiological activity.[295] Thus, intending to improve their pharmacological properties and/or develop molecules with distinct bioactivities, structural alterations of steroids have been an important focus of research over the last decades.[296–299]

Arylidenosteroids represent one of the groups of modified steroids, which are the focus of the present section. In general, arylidene derivatives have been related to a wide range of pharmacological activities, such as anti-infective, antioxidant, anti-arrhythmic, anticancer and anti-inflammatory.[300–309] The general structure of these compounds includes a natural/synthetic core bearing an aryl group linked through an exocyclic double bond, which is usually part of an α,β-unsaturated ketone system. This system has an inherent chemical reactivity due to the simultaneous existence of electrophilic and nucleophilic points, which constitutes an important advantage. Therefore, these derivatives are especially useful in the preparation of several bioactive heterocyclic systems.[310–312] Considering the pharmacological interest of steroids and the biological and synthetic value of arylidene derivatives, it is not surprising that several studies involved the synthesis and biological evaluation of steroidal arylidenes, despite some potential problems of these compounds. In fact, in addition to the known possible hormonal effects, usually, these steroids have higher lipophilicity and the consequent risk of bioavailability problems. Moreover, the presence and inherent reactivity of their α,β-unsaturated ketone system can also be associated with potential toxicity problems, including mutagenesis and carcinogenesis.[311,312] Despite this, over the years, several arylidenosteroids have been explored, namely as hydroxysteroid dehydrogenases, aromatase, and 5AR inhibitors, as well as skeletal muscle relaxants, antimicrobial, neuroprotective, antiparasitic, and antiproliferative agents.[297,313–320] Additionally, other

research studies have reported their use as synthetic intermediates, principally in the preparation of aza-heterocycles with relevant potential applications.[321,322]

Considering the information in the literature, particularly those in the review published in the context of this thesis, steroidal arylidene derivatives (2- and 16*E*-arylideneandrostanes, 21*E*-arylidenepregnanes, and 16*E*-arylidenoestranes) with significant pharmacological activity, as well as their main chemical synthesis and applications as synthetic intermediates of relevant bioactive molecules will be discussed in this section.[323]

1.2.1. Synthetic approaches to prepare arylidenosteroids

Usually, arylidenosteroids are obtained through an aldol condensation between a steroid and an aldehyde. In this chemical reaction, an enol or enolate reacts with a carbonyl in the presence of an acid or base catalyst to form a β-hydroxyaldehyde or a β-hydroxyketone, followed by dehydration to afford a conjugated enone.[324] In particular, the reaction between an aldehyde/ketone capable of forming an enol/enolate and an aromatic carbonyl without an α-hydrogen (usually an aromatic aldehyde) is named by the well-known Claisen–Schmidt condensation. In steroids, this reaction has been principally performed in C-16 or C-21 positions and less often in C-2. Typically, the reactions to prepare arylidenosteroids occur at room temperature (r.t.), under basic catalysis, and the solvent is, in most cases, methanol (MeOH) or ethanol (EtOH) (**Figure 15**). The basicity of the reaction medium is usually conferred by sodium hydroxide (NaOH) or potassium hydroxide (KOH).[318,325–329] Nevertheless, depending on reaction substrate and reagents, the duration of the reaction and observed yields are extremely variable. In fact, according to the literature, these reactions can take between 1 to 48 h to be concluded and yields ranging from 23 to 98 % were described.[312,322,330,331] Androstane, pregnane, and estrane derivatives, namely DHEA, androstenedione, estrone, pregnenolone, and progesterone have been described as the main starting materials.

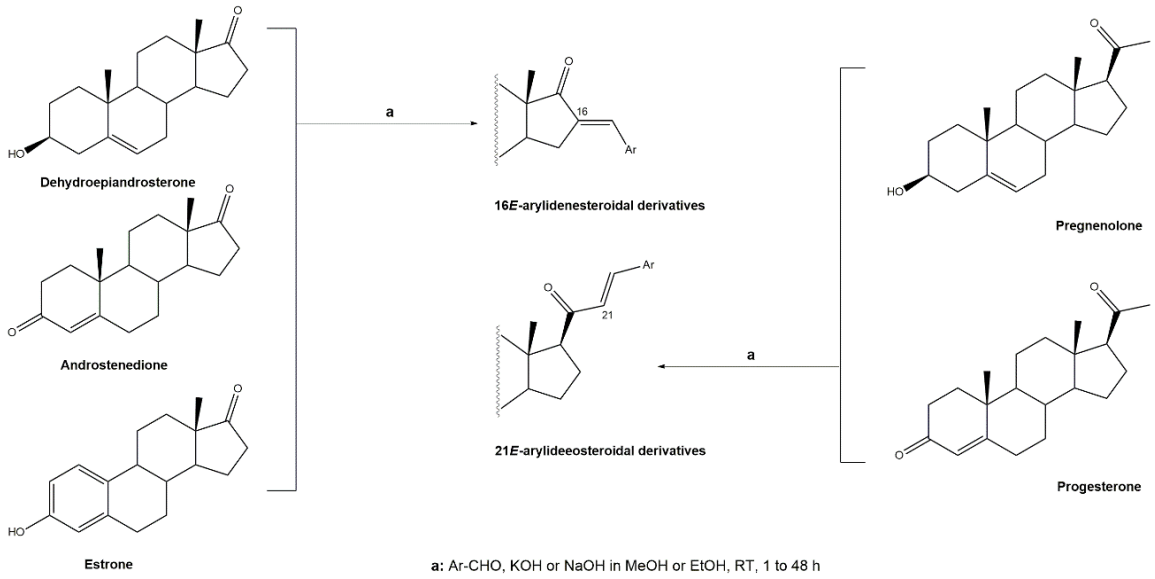

Figure 15. 16*E*- and 21*E*-Arylidenosteroids prepared by Claisen–Schmidt condensation. Created with ChemDraw.

Less often, the preparation of 2-arylidenosteroids from DHEA derivatives, DHT, and cholestanone was also described. The synthesis of these derivatives was based on the classical approach for aldol condensation, occurring at r.t. and under basic catalysis, using MeOH or EtOH as solvent.[311,332,333] Interestingly, over the last years, other synthetic strategies different from the classical reaction conditions have been explored. As a representative example, Guo et al. performed the same reaction using MeOH as solvent and NaOH as a base, however at higher temperatures, to afford excellent yields (91–95%) of the products.[317] Additionally, Huang et al. and Yu et al. applied a different strategy to prepare the corresponding aldol condensation products from 4-aza-androst-3,17-dione (**1**) and DHEA (**Figure 16**). In fact, as alternative for the use of NaOH or KOH, these authors used potassium fluoride on aluminum oxide (KF/Al_2O_3) as a recyclable basic catalyst and performed the reaction in EtOH under reflux temperature. Remarkably, shorter reaction times (1 h) were observed, and excellent yields of the products (90–94 %) were achieved.[321,334] This transformation was also performed using molecular iodine-loaded aluminum oxide (I_2-Al_2O_3) as heterogeneous catalyst and under microwave (MW) irradiation (**Figure 17**). These conditions allowed extremely short reaction times (5–7 min) and good yields of the products (79–85 %).[330] More recently, Mótyán and coworkers reported the synthesis of 16*E*-benzylidene-estrone-3-methyl ether derivatives by a MW-assisted (100 °C, 20 min) Claisen–Schmidt condensation, using EtOH as a solvent and KOH.[331]

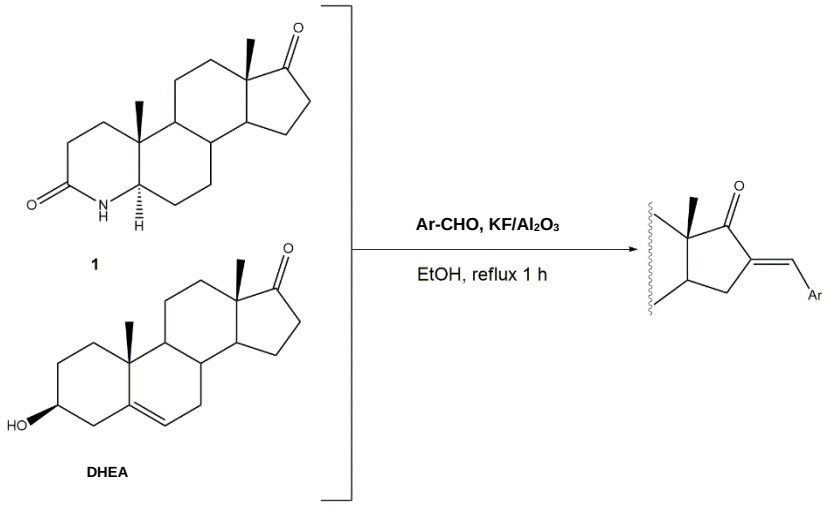

Figure 16. Synthesis of 16*E*-arylidenosteroids from **1** and dehydroepiandrosterone (DHEA), using KF/Al_2SO_3 or KF/Al_2O_3 as catalysts in EtOH, under reflux. Created with ChemDraw.

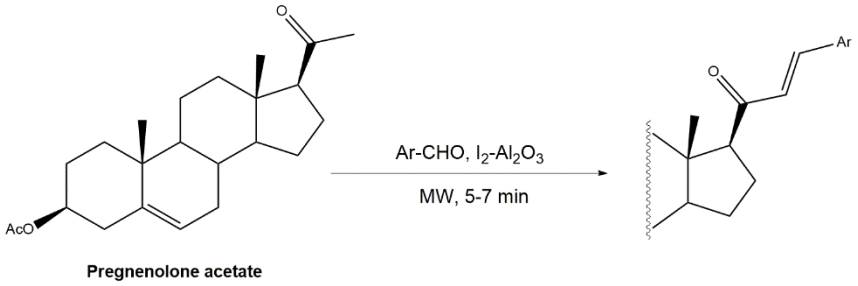

Figure 17. Synthesis of 21*E*-arylidenepregnenolone acetate derivatives catalyzed by I_2-Al_2O_3 under microwave (MW) irradiation [330]. Created with ChemDraw.

To our knowledge, the most unusual route to prepare steroidal arylidene derivatives was employed by Riebe and coworkers in the synthesis of 16*E*-arylidene-3-methoxyestrone derivatives from commercially available 3-methoxyestrone (**Figure 18**). Firstly, an enol intermediate using sodium methoxide and ethyl format in benzene and under reflux was prepared, followed by a reaction with formaldehyde in pyridine at room temperature. Then, a palladium-catalyzed Mizoroki–Heck reaction allowed the preparation of 16*E*-arylidenoestrane derivatives in fair to excellent yields (14–99 %), but strongly dependent on the electronic character of the aryl halide.[332]

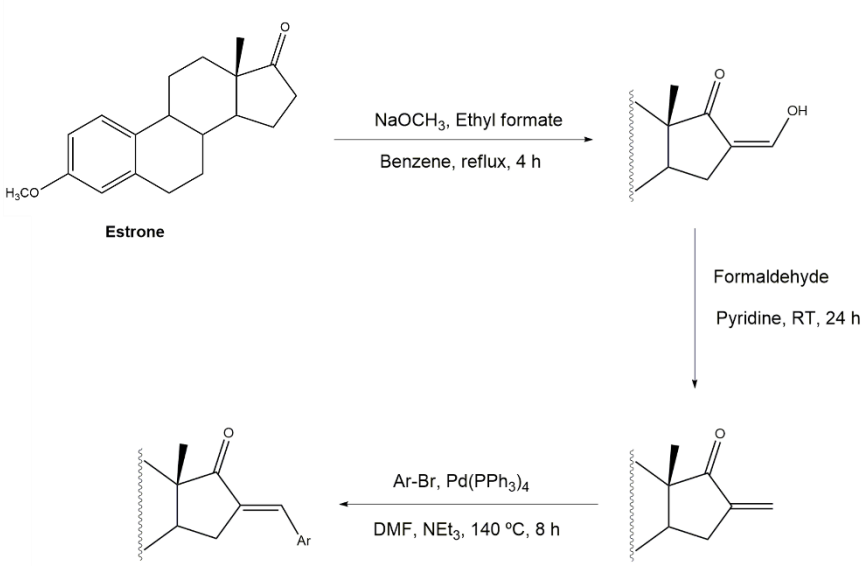

Figure 18. An alternative route to prepare 16*E*-arylidenoestrane derivatives by the employment of Mizoroki–Heck reaction [332]. Created with ChemDraw.

1.2.2. Bioactivity of 2- and 16*E*-arylideneandrostane derivatives

The 16*E*-arylideneandrostane backbone has appeared as an important template to develop potential anticancer agents. Among all distinct types of arylidene steroids, this is the most common. On the other hand, A-ring arylideneandrostane derivatives were also described but in a less frequency.[311,332,333] In addition to cytotoxic effects, some studies described other biological activities, such as aromatase inhibition, anti-inflammatory, neuroprotective and skeletal muscle relaxing activities, and tissue-selective AR modulator effects.[318,335,336] A selection of the most relevant 16*E*-arylidene-androstane derivatives is shown in **Table 6**. Frequently, these compounds presented better results than the respective positive controls in the biological experiments. When data for positive control is not present, the steroid with the best results is presented. Concerning relevant antiproliferative compounds, several arylideneandrostane derivatives, namely the steroids **2**–**7** (**Table 6**), have shown promising results.[296,333,335,337–339] In this context, Huang and coworkers described the cytotoxic effects of a series of novel DHEA derivatives bearing a modified *υ*-triazole ring at the C-16 position on different human cancer cells. Through the 3-(4,5-dimethylthiazol-2-yl)-2,5-diphenyltetrazolium bromide (MTT) colorimetric assay, the authors observed that steroid **2** (**Table 6**), which contains a 4-iodophenyl system attached to the triazole ring, displayed the highest antiproliferative activity in HepG2 and MCF-7 cells [half maximal inhibitory concentration (IC_{50}) of 9.10 and 9.18 μM, respectively]. Interestingly, these IC_{50} values are even lower than the estimated for the positive control 5-fluorouracil (5-

FU), an antineoplastic drug widely used in clinical practice to treat multiple solid tumors.[336] Furthermore, flow cytometry experiments in HepG2 cells demonstrated that steroid **2** exerted antiproliferative effects by arrest in the G2 phase and inducing apoptosis.[296] The androstane derivative **3** (**Table 6**), bearing a 3-chlorobenzylidene at C-16, and analogs were synthesized by Vosooghi et al. and their cytotoxicity was evaluated through the MTT assay. The results evidenced that this steroid **3** was the most potent, especially against KB and T47-D cells (IC_{50} values of 0.6 and 1.7 μM, respectively).[338] In another investigation, the amide androstane **4** with a chlorine atom attached to C-3 (**Table 6**) revealed potent antiproliferative effects against a panel of leukemia cell lines. In fact, the determined IC_{50} values for this steroid **4** against CCRF-CEM, K-562, RPMI-8226 and SR cells were 3.94, 2.61, 6.90, and 1.79 μM, respectively.[339] More recently, the synthesis and biological evaluation of ferrocenyl androstane conjugates was reported. The antiproliferative activity of these compounds was assessed and the steroid **5** (**Table 6**) was the most potent, being determined an IC_{50} of 1.2 μM in colon cancer HT-29 cells. This IC_{50} value is very relevant when compared with the positive control, cisplatin (Cis) (IC_{50}= 66 μM).[337] Besides *in vitro* experiments using cell lines, Chattopadhaya et al. also performed an *in vivo* cytotoxicity evaluation using a mouse model using the hollow fiber assay. In this study, interesting results were observed for the 3,4,5-trimetoxibenzylidene **6** (**Table 6**). In fact, for this steroid, a good score for inhibition of tumoral cells in the subcutaneous (S.C.) fiber implants (8/20) was determined, while for intraperitoneal (I.P.) fiber implants, the value significantly decreased (2/20).[335] In a very similar study, Bansal et al. synthesized and tested a series of 16*E*-arylideneandrostene derivatives bearing tertiary amine functionalities. Of these, the aminosteroid **7** (**Table 6**), possessing a diethylaminealkoxy group, was the most promising molecule with a score of 12 for I.P. and 8 for S.C. in the *in vivo* hollow fiber assay.[340]

Moreover, some arylidenosteroids have been described as aromatase inhibitors (AIs), particularly the 16*E*-arylideneandrostane derivatives **8**–**11** (**Table 6**). Aromatase is a cytochrome P450 enzyme (CYP19) that converts androgens into estrogens by an aromatization reaction. This enzyme plays a fundamental role in endocrine physiology and in estrogen-dependent tumors such as breast and endometrial cancers.[341] Thus, potent AIs have demonstrated to be clinically relevant in the treatment of the referred disorders. However, the adverse side effects of AIs used in clinical practice, such as muscle-skeletal pain, osteoporosis, and cardiovascular disease, are limiting and justify further research in this field.[342–346] In this context, the steroids **8**–**11** (**Table 6**) revealed potent aromatase inhibitory activity in *in vitro* assays. Noteworthy, the determined IC_{50}

values for the enzyme inhibition are considerably lower than the observed for aminoglutethimide, the positive control.[332,347–349]

Investigations to evaluate the potential of 16*E*-arylidene steroidal derivatives as neuroprotective agents for the treatment of Alzheimer's and Parkinson's diseases were also performed. In this scope, Singh et al. reported some interesting results, being the 4-aza-16*E*-pyridylene derivative **12**, prepared from DHEA (**Table 6**), the most promising. This compound was found to be a relevant neuroprotective agent, producing effects on TNF-α (a pro-inflammatory cytokine) levels in brain serum of rats comparable to the standard drug celecoxib (CEL), and better than for dexamethasone (DEX) (**Table 6**).[350]

Recently, Li and coworkers prepared 2-arylideneandrostene derivatives and evaluated their potential anti-inflammatory properties, including their effect on NO release by microglia BV-2 cells activated by lipopolysaccharide (LPS), as well as their cytotoxicity. Among all synthesized derivatives, steroids **13** and **14** (**Table 6**), presenting, respectively, 3-chloro- and 3,4,5-trimethoxyphenyl groups at the C-2 position, displayed the most relevant results. In fact, the calculated IC_{50} values for anti-inflammatory effect were 2.69 and 3.28 μM, respectively, which were lower than the positive control, minocycline (5.97 μM).[351]

Table 6. Representative examples of bioactive 2- and 16*E*-arylideneandrostane derivatives. Positive controls, when shown, are identified by the (+) symbol. Molecular structures created with ChemDraw. [a]

Compound	Bioactivity data			Ref.
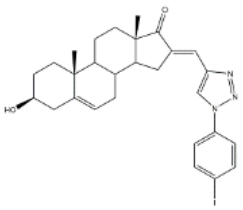 **2**	Antiproliferative activity (IC_{50} μM)			296
	Cell line	**2**	5-FU (+)	
	HepG2	9.10	10.59	
	MCF-7	9.18	28.11	
	Cell cycle arrest at G2 phase in HepG2			
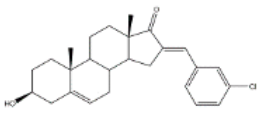 **3**	Antiproliferative activity (IC_{50}±SEM μM)			338
	Cell line	**3**	Etoposide (+)	
	KB	0.6±2.0	2.8±16.8	
	T47-D	1.7±14.8	1.2±8	
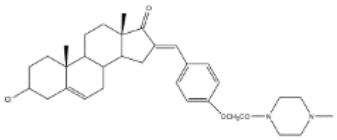 **4**	Antiproliferative activity (IC_{50} μM)			339
	Cell line	**4**		
	CCRF-CEM	3.94		
	K-562	2.61		
	RPMI-8226	6.90		
	SR	1.79		
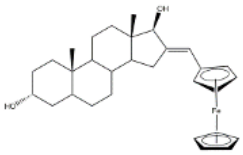 **5**	Antiproliferative activity (IC_{50} μM±SD μM)			337
	Cell line	**5**	Cis (+)	
	HT-29	1.2±0.4	66±2	
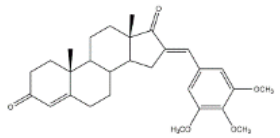 **6**	Cytotoxic activity – *in vivo* hollow fiber assay (score)			335
		6	Taxol (+)	
	I.P.	2	Data not	
	S.C.	8	shown	
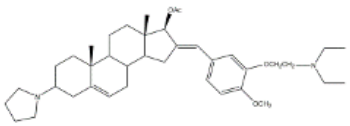 **7**	Cytotoxic activity – *in vivo* hollow fiber assay (score)			340
		7	Taxol (+)	
	I.P.	12	Data not	
	S.C.	8	shown	
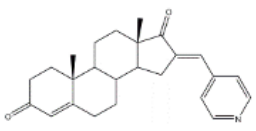 **8**	Aromatase inhibitory activity (IC_{50} μM)			348
	8	Aminoglutethimide (+)		
	5.2	28.5		
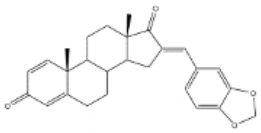 **9**	Aromatase inhibitory activity (IC_{50} μM)			348
	9	Aminoglutethimide (+)		
	6.4	28.5		

Table 6. (Continuation).

Compound	Bioactivity data			Ref.
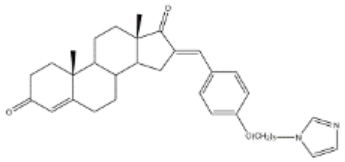 **10**	Aromatase inhibitory activity (IC_{50} μM)			349
	10	Aminoglutethimide (+)		
	4.4	28.5		
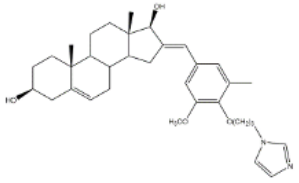 **11**	Aromatase inhibitory activity (IC_{50} μM)			349
	11	Aminoglutethimide (+)		
	2.4	28.5		
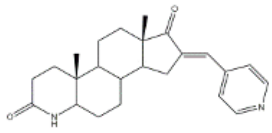 **12**	Anti-inflammatory activity TNF-α levels ($pg.mg^{-1}$protein±SD)			352
	12	CEL(+)	DEX(+)	
	88.6±1.8	68.2±1.1	89.6±2.0	
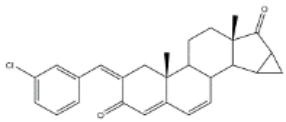 **13**	Anti-inflammatory activity (IC_{50} μM) (NO release of LPS-activated mouse microglial cell line BV2)			351
	13	Minocycline (+)		
	2.69	5.97		
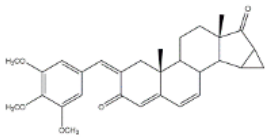 **14**	Anti-inflammatory activity (IC_{50} μM) (NO release of LPS-activated mouse microglial cell line BV2)			351
	14	Minocycline (+)		
	3.28	5.97		

[a] 5-FU=5-Fluorouracil, Cis= Cisplatin, I.P.= Intraperitoneal, S.C.= Subcutaneous, CEL= Celecoxib, DEX= Dexamethasone, LPS= Lipopolysaccharide.

Despite these promising results, other studies carried out with 2- and 16*E*-arylideneandrostrane derivatives described less relevant biological effects.[297,318,328,333,342,345] In addition, Semenenko and coworkers prepared 16*E*-arylidenedehydroepiandrosterones, as well as 2-arylidene derivatives of cholestanone, to be used as chiral dopants for cholesteric liquid crystal composition.[353] Another study reported the synthesis of a new series of quaternary ammonium salts of 16*E*-[4-(2-alkylaminoethoxy)-3-methoxybenzylidene]androstane derivatives as skeletal muscle relaxants. The biological results showed that these compounds produced varied degrees of muscle relaxant activity. However, they also inhibited acetylcholinesterase activity in low concentrations and therefore are not suitable for use as muscle relaxants.[316]

Additionally, Acharya and coworkers prepared new 16*E*-arylidene steroids linked to nitrogen mustards as hybrid compounds and evaluated their cytotoxic effects aiming to develop antileukemia agents. However, the specificity of these compounds towards leukemia cells remains unaffected and reduced potency was observed when compared to earlier reports for 16*E*-arylidene steroids.[339,340] Further studies suggested that these derivatives present different mechanisms of action in leukemia cells.[297] More recently, Brito et al. reported the synthesis and antiproliferative effects of novel 16*E*-arylidene-4-aza-androst-5-enes as prostate cell growth inhibitors. Despite their less potent antiproliferative effects in comparison with the positive control (5-FU), an interesting selectivity towards cancer cell lines was found for all aza-androstenes, presenting low cytotoxicity to non-tumoral human fibroblasts. Furthermore, molecular docking studies predicted that these 4-aza-androstene derivatives can interact with 5β-reductase, a surrogate of 5AR, and with other common targets of steroidal drugs, which can be important for further studies.[326]

1.2.3. Bioactivity of 21*E*-arylidenepregnane derivatives

Arylidenesteroidal derivatives of progesterone and pregnenolone and other similar pregnanes constitute a smaller group than arylideneandrostanes, and they have mainly been studied as potential antitumoral agents. The most potent arylidenepregnene derivatives reported are presented in **Table 7**. The steroids **15** and **16** were synthesized and tested by Banday et al. Their effects on tumoral cell proliferation were assessed through National Cancer Institute-60 Human Tumor Cell Lines Screen (NCI-60). This NCI-60 method involves 60 different human tumor cell lines, representing leukemia, melanoma, and cancers of the lung, colon, brain, ovary, breast, prostate, and kidney, to identify and characterize novel compounds with growth inhibition or killing of tumor cells. This method was designed to screen up to 3000 small molecules for potential anticancer activity in a short period of time.[354] The best results for molecules **15** and **16** were observed in HCT-15 and MCF-7 cell lines, respectively, being determined an IC_{50} value of 0.81 μM for compound **15** in HCT-15 cells, and an IC_{50} value of 0.60 μM for the 21*E*-arylidenepregnene derivative **16** in MCF-7 cells.[347] A more recent study described the synthesis of novel 4'-acylamino modified 21*E*-benzylidene steroidal derivatives and their cytotoxic activity. The toxicity of these steroids was assessed by a brine shrimp microtiter-plate method and by the MTT assay against HeLa and MCF-7 cells.[318,355] Within these arylidenosteroids, the 21*E*-4-(2-fluoro-benzamido)benzylidene derivative **17** (**Table 7**) seemed to be the most active. In fact, at a concentration of 30 $\mu g \cdot mL^{-1}$, this steroid originated a 58 and 64 % growth inhibition of HeLa and MCF-7 cells, respectively, and their toxicity against brine shrimp was considered weak (median lethal

concentration (LC_{50}) > 50 μg·mL^{-1}).[318] Interestingly, Abood and colleagues reported the synthesis and antimicrobial study of progesterone derivatives with arylidene groups at C-2 and C-21 positions. These compounds were tested using *Streptococcus pneumoniae* and *Staphylococcus aureus* as gram positive and *Pseudomonas aeruginosa* and *Escherichia Coli* as gram negative bacteria and their antifungal activity were studied against *Candida albicans* and *Aspergillus niger*. Ampicillin (AMP) (at 100 ng·mL^{-1}) was used as a standard drug (positive control). The obtained results indicated that compound **18**, at 100 ng·mL^{-1} (**Table 7**) originated an inhibition zone of *S. pneumoniae* and *S. aureus* proliferation (30 and 24 mm, respectively) larger than the standard drug (20 and 22 mm).[356]

Table 7. Examples of the most active 21*E*-arylidenepregnene derivatives. Positive controls, when shown, are identified by the (+) symbol. Molecular structures were created with ChemDraw. [a]

Compound	Bioactivity data		Ref.
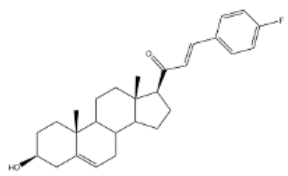 **15**	Antiproliferative activity (IC_{50} μM)		347
	Cell line	**15**	
	HCT-15	0.81	
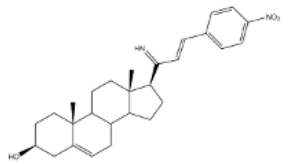 **16**	Antiproliferative activity (IC_{50} μM)		347
	Cell line	**16**	
	MCF-7	0.60	
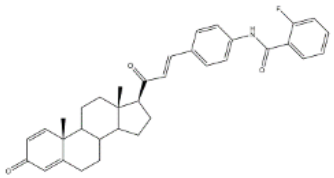 **17**	Antiproliferative activity Growth inhibition (%)		318
	Cell line	**17**	Cis (+)
	HeLa	58	99
	MCF-7	64	88
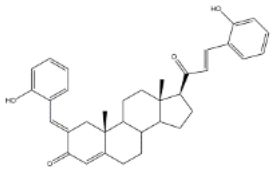 **18**	Antimicrobial activity Zone of inhibition (mm)		356
	Gram positive	**18**	AMP (+)
	Streptococcus pneumoniae	30	20
	Staphylococcus aureus	24	22

[a] Cis= Cisplatin, AMP= Ampicillin.

Moreover, novel 21*E*-benzylidene steroidal derivatives were synthesized from progesterone by Fan et al. These novel compounds were tested through MTT assay for

their cytotoxicity against brine shrimp and murine Lewis lung carcinoma (LLC) cells. In general, this series of new steroids showed weak cytotoxicity toward these cells.[355] Shan and coworkers also reported the preparation of 3β,7α,11α-trihydroxypregn-21-benzyliden-5-en-20-one derivatives and their cytotoxic activity. However, all these compounds showed a lower cytotoxic activity against EC109 cells than the positive control, oridonin.[357]

1.2.4. Bioactivity of 16*E*-arylidenoestrone and 16*E*-arylidenoestradiol derivatives

It is known that estrogenic hormones have an important contribution to estrogen-dependent diseases, being the majority of breast cancers primarily initiated and stimulated by estrogens.[358] In consequence, the structural modification of estrone and estradiol in different positions to obtain bioactive compounds has been a focus of intensive investigations. In this context, 16*E*-arylidenoestrone derivatives have also been prepared, and their bioactivity has been evaluated. For example, these arylidenes were studied as 17β-HSD type 1 inhibitors. This enzyme is responsible for the reduction of the 17-ketone group of estrone to afford 17β-estradiol, the most potent estrogen. Therefore, 17β-HSD type 1 represents a relevant therapeutic target in the treatment of estrogen-dependent cancers and endometriosis.[359–362] Thus, over the years, potent 17β-HSD type 1 inhibitors have been designed and synthesized. In addition, selectivity for 17β-HSD type 1 over other isoforms and the absence of estrogenic effects are of high relevance.[363] In this context, Allan et al. and Poirier et al. designed and prepared 16*E*-arylidenoestrone derivatives as 17β-HSD type 1 inhibitors, and promising results were achieved (**Table 8**). For instance, steroid **19** (**Table 8**), prepared by Poirier et al., exhibited a high inhibitory effect, with an IC_{50} of 3.4 μM, a value lower than the observed for the positive control, estradiol (7.3 μM).[315] In addition, Allan and coworkers modified estrone in different positions, namely C-6, C-16, and C-17, and the prepared structures were tested against 17β-HSD type 1 and type 2. Among all these derivatives, steroid **20** (**Table 8**) presented very relevant results. In fact, at 10 μM, this derivative led to a 72 % inhibition of 17β-HSD type 1 activity, while the 17β-HSD type 2 inhibition was only 13 %. This research group also verified that further modifications of steroid **20** led to a loss of selectivity.[364]

More recently, Wang et al. developed a new series of 16*E*-benzylidene-2-methoxyestradiol analogs. 2-Methoxyestradiol (2ME) is an endogenous estradiol metabolite that has been studied as an antitumor agent and some mechanisms of action for this compound have been explored. Interestingly, this steroid seems to mainly lead

to neoangiogenesis inhibition, microtubule disruption, and upregulation of the extrinsic and intrinsic apoptotic pathways.[365] In this scope, Wang and coworkers used 2ME as starting material for the synthesis of 16*E*-benzylidenestradiol derivatives and their potential antitumoral interest was assessed. Of these prepared compounds, steroid **21** (**Table 8**) showed potent antiangiogenic activity. Moreover, further studies suggested that this compound suppresses the tumor growth by about 50 % in human breast cancer (MCF-7) xenograft models without relevant side effects. The mechanistic studies suggested that steroid **21** targeted the epithelial to the mesenchymal transition process in MCF-7 cells and inhibited human umbilical vein endothelial cells (HUVEC) migration, contributing to angiogenesis interruption.[366]

Table 8. The most representative examples of active 16*E*-arylidenoestrone and -estradiol derivatives. Positive controls, when shown, are identified by the (+) symbol. Molecular structures were created with ChemDraw. [a]

Compound	Bioactivity data		Ref.
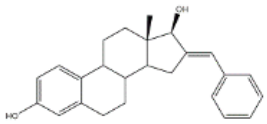 **19**	17β-HSD type 1 inhibitory activity (IC_{50} μM)		[315]
	19	Estradiol (+)	
	3.4	7.3	
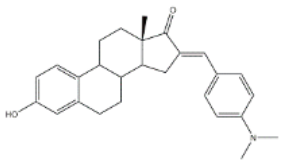 **20**	17β-HSD inhibitory activity (% at 10 μM)		[364]
	20		
	Type 1	Type 2	
	72	13	
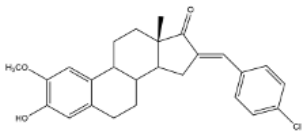 **21**	Tumor weight reduction (%) Human breast cancer (MCF-7) xenografts models		[366]
	21 (45 mg/kg/day)	2ME (+) (45 mg/kg/day)	
	About 50% Significative reduction compared with negative control	About 50% Significative reduction compared with negative control	

[a] 17β-HSD= 17β-Hydroxysteroid dehydrogenase, 2ME= 2-Methoxyestradiol.

Novel 16*E*-arylidenoestrone derivatives were synthesized, and their biological activity was assessed by Minu and coworkers. These compounds were studied at NCI for their antineoplastic activity against a 60-cell lines panel and have also been tested for their *in vitro* estrogenic and anti-estrogenic activities, but the results obtained were not as promising as observed in other previously reported studies. Additionally, the measured estrogen receptor (ER) binding affinity was also assessed, and the values determined

were low.[367] Recently, Canário et al. prepared $\Delta^{9,11}$-estrones as potential antiproliferative agents, including a 16*E*-benzylidene derivative. The effect of this compound on cell proliferation was assessed against several cell lines and it was verified that the introduction of a $\Delta^{9,11}$ double bond and a 16*E*-benzylidene group in estrone lead to an increase of the cytotoxic activity against the hormone-dependent breast cancer cells MCF-7 and T47-D, with IC_{50} values of 25.14 and 25.06 μM, respectively. However, when compared to 5-FU, as the positive control, this compound showed to be less potent (IC_{50}= 1.71 and 0.54 μM, respectively).[368]

1.2.5. Relevance of steroidal arylidene derivatives as synthetic intermediates of bioactive compounds

In addition to their biological activity, steroidal arylidenes are also versatile synthetic intermediates in the preparation of other bioactive structures. In fact, these steroids have been used in the introduction of diverse chemical groups present in bioactive compounds, such as oximes, hydroxyl and hydrazones, and are particularly useful in several heterocyclization reactions.[347,369–371] In this context, over the years, a large number of bioactive heterocyclic steroidal derivatives have been synthesized, and some of them are already being clinically used.[232,372] Interestingly, diverse heterocyclic compounds, including arylpyrazolines and pyrazoles, arylpyrimidines, oxindoles, pyridones and pyridines as well as spiro-pyrrolidines were prepared from arylidenosteroids.[298,310,322,327,331,334,356,371,373–383]

Frequently, pyrazolines are prepared from steroidal arylidenes (**Figure 19**). A common strategy to synthesize C-17 pyrazolinyl derivatives is the heterocyclization of 21*E*-arylidenepregnenolones in the presence of hydrazine hydrate ($NH_2NH_2{\cdot}H_2O$) in glacial acetic acid (AcOH) under reflux during approximately 2 h.[39,310,382] Diverse approaches to obtain 16,17-pyrazolinyl steroids from 16*E*-arylidenedehydroepiandrosterone derivatives have also been described (**Figure 19**). Thus, different androstane-*N*-acylated pyrazolines were prepared in the presence of $NH_2NH_2{\cdot}H_2O$ in AcOH or propionic acid at reflux temperature after 2–9 h.[51,384,385] In addition, Singh et al. reported the synthesis of pyrazolinylandrostanes by using only $NH_2NH_2{\cdot}H_2O$ in 1,4-dioxane under reflux for 5 h. Moreover, the reaction of these 16*E*-arylideneandrostanes with phenylhydrazine hydrate in anhydrous MeOH under reflux during 12 h afforded the corresponding phenylpyrazolinyl substituted derivatives.[384] Furthermore, Naggar et al. synthesized estrone-*N*-substituted pyrazolines from 16*E*-arylidenoestrones by condensation with methylhydrazine or phenylhydrazine in refluxing dioxane for 5 h.[374] It is important to stress that the information about the stereochemistry of 16,17-pyrazolinyl steroids is not

always clear. Indeed, some authors indicated that C-C bond between C-16 and C-5′ is β.[384,385] On the other hand, the study reported by El-Naggar and coworkers do not present any information about the stereochemistry of these compounds.[374]

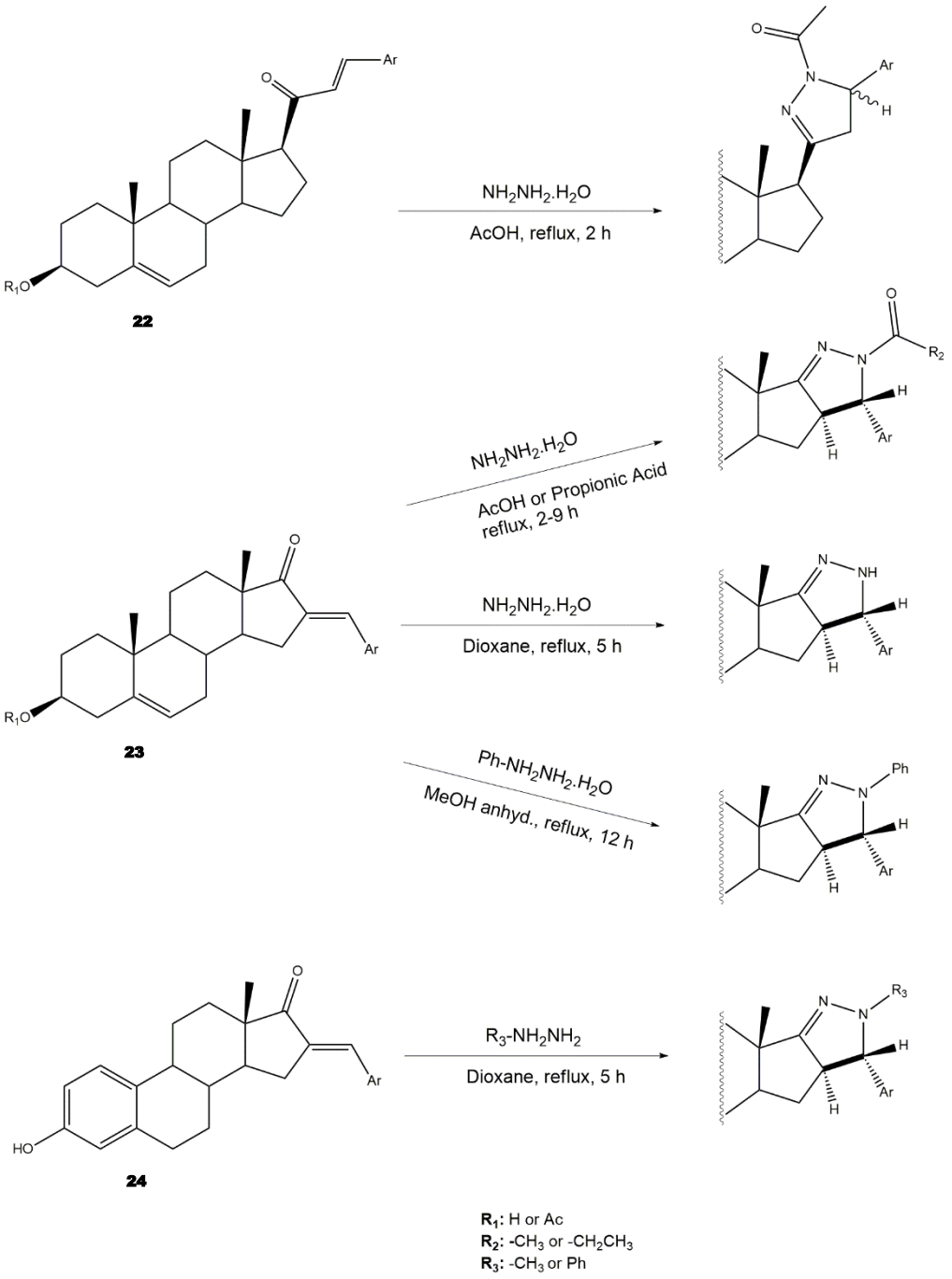

Figure 19. Synthetic routes for preparation of steroidal arylpyrazolines from 16*E*- and 21*E*-arylidenesteroids. Created with ChemDraw.

The synthesis of steroidal arylpyrimidines and pyridines from 16*E*- and 21*E*-arylidenesteroids was also described (**Figure 20**). Ke et al. described the preparation of

steroidal[17,16-*d*]pyrimidines using **23** as starting material and guanidine nitrate under basic catalysis and reflux during 1 h[327] In addition, Huang et al. reported the synthesis of steroidal[17,16-*d*]triazolopyrimidines using 3-aminotriazole, again using a basic catalyst at reflux during 30 h.[321] Furthermore, 2'-aminopyrimidines and 2'-cyanoiminopyrimidines were prepared from 16*E*-arylidenoestrone derivatives using guanidine hydrochloride or 2-cyanoguanidine and sodium ethoxide in EtOH, and the mixture was refluxed for 4-6 h.[377] Different steroidal pyridines were also synthesized from 21*E*-arylidenosteroids in the presence of malononitrile and sodium ethoxide, at reflux temperature for 8 h, in a single reaction. Interestingly, sodium ethoxide acted as a bifunctional species, being simultaneously the ethoxy source and the promoter of reactions between α,β-unsaturated ketones and malononitrile.[376]

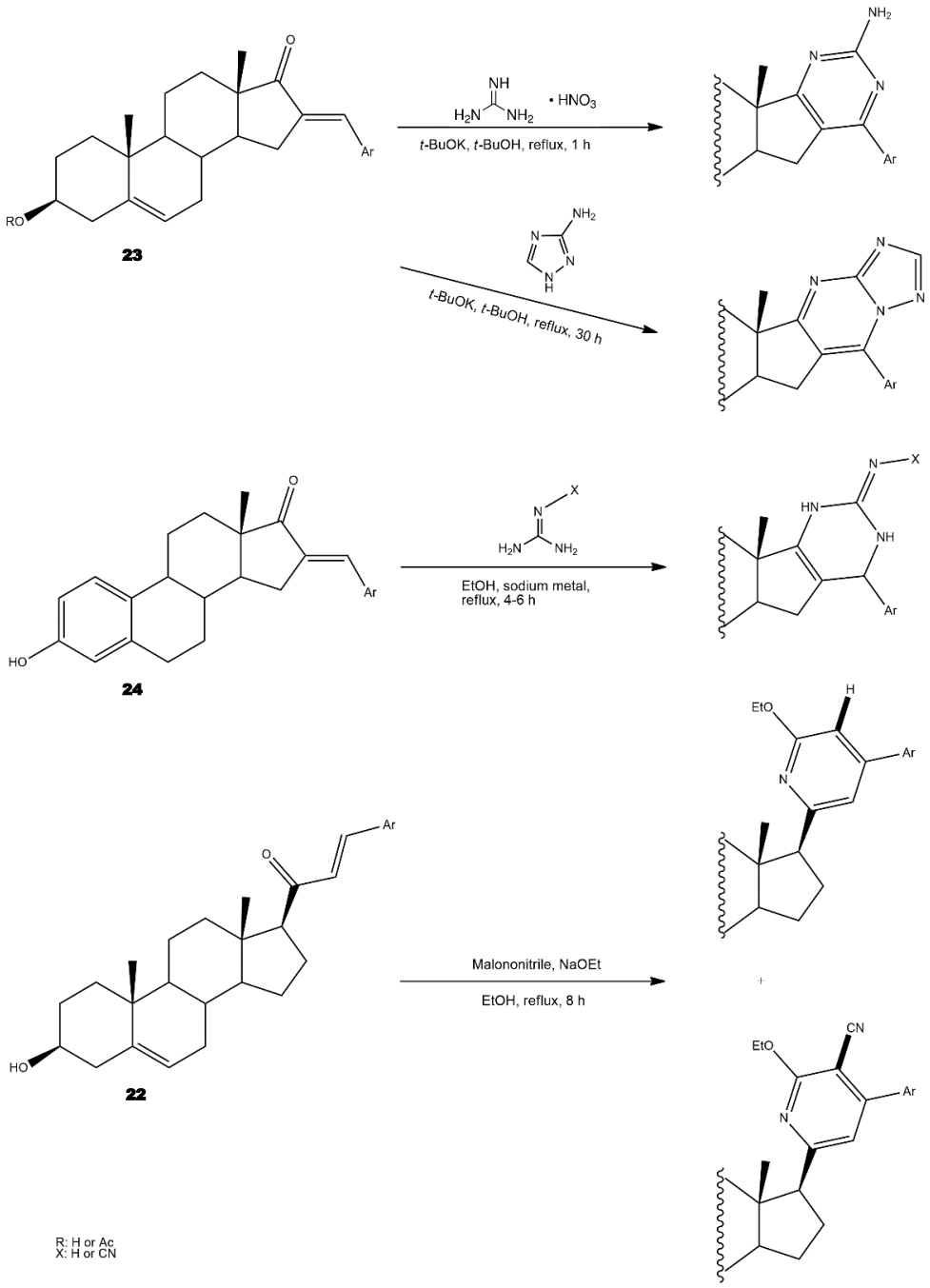

Figure 20. Different pathways to synthesize steroidal arylpyrimidines and pyridines from 16*E*- and 21*E*-arylidenesteroids. Created with ChemDraw.

The preparation of steroidal spiro-oxindoles and spiro-pyrrolidines from arylidenosteroids was reported by Yu et al. and Gavaskar et al. (**Figure 21**). In this context, a series of novel steroidal spiro-pyrrolidinyl oxindoles was obtained through a 1,3-dipolar cycloaddition of azomethine ylides generated from the decarboxylative condensation of isatin and sarcosine. For this, the arylidenosteroids **24** were mixed with isatin and sarcosine in 1,4-dioxane/MeOH (1:1) and this reactional mixture was left

under reflux for 5 h to afford the referred products in excellent yields.[334] More recently, Gavaskar and coworkers reported a 1,3-dipolar cycloaddition to synthesize novel steroidal dispiropyrrolidine heterocycles. This reaction occurred through an azomethine ylide generated from 1,2-phenylenediamine, ninhydrin, sarcosine, and a 16*E*-arylidenoestrone derivative in the ionic liquid *N*-(1-acryloyl)-*N*-(4-cyclopentyl)piperazinium phosphate, previously synthesized by this group, at 120 °C.[379,386]

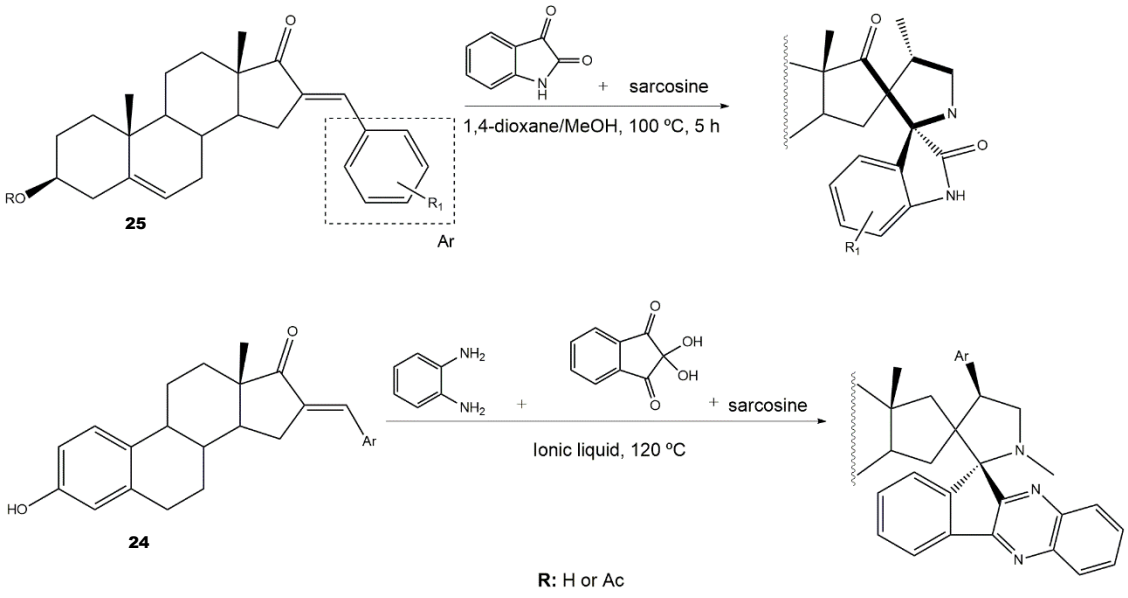

Figure 21. Synthesis of steroidal spiro-oxindoles and spiro-pyrrolidines from 16*E*-arylidenesteroids.[331,381] Created with ChemDraw.

The most promising and representative steroidal heterocyclic derivatives prepared from arylidenesteroids that have been reported are presented in **Table 9**. Most of these final heterocyclic products have been developed and evaluated as antiproliferative and anti-inflammatory agents, as well as aromatase and 5AR inhibitors. Of these, steroid **26** has relevant antiproliferative effects, as very low IC_{50} values (0.24 and 0.25 μM, respectively) against HT-29 and HCT-15 cells were determined.[310] In addition, pyrimidine **27** has also exhibited interesting antiproliferative effects against HepG2, Huh-7, and SGC-790 cells, presenting IC_{50} values (5.41, 5.65 and 10.64 μM, respectively) lower than the determined for the positive control. Moreover, the steroids **28**–**32** were evaluated as potential 5AR inhibitors, and some interesting results were obtained (**Table 9**). Compound **28** presented relevant 5AR type 1 inhibitory effects in comparison with finasteride (IC_{50} values are 14.5 μM and 21.6 μM, respectively), whereas derivatives **29**–**32** revealed potent 5AR type 2 inhibitory effects. Of these, pyrazolines **31** and **32** showed the most promising results (the IC_{50} values for 5AR type 2 inhibition were 7.3 and 8.2 nM,

respectively), while **29** and **30** presented lower inhibitory activity for 5AR type 2 (the determined IC_{50} were 13.90 and 14.20 μM, respectively).[373,382] Steroid **33** (**Table 9**) also showed to be a potential antiproliferative agent against NCI-H460 and HeLa cells, presenting good IC_{50} values (10.30 and 12.50 μM, respectively). Particularly, in HeLa cell line, this compound led to cell cycle arrest at the S phase.[298] Yu and coworkers also reported some molecules with interesting results for antiproliferative activity, namely the steroidal spiro-pyrrolidinyl oxindoles **34**–**36**, synthesized from DHEA (**Table 9**). Particularly, pyrazolidine **34** showed good antiproliferative activity against SMMC-7721 (IC_{50}= 4.30 μM) and MCF-7 (IC_{50} = 2.06 μM) cells, being more potent than positive control (5-FU) [334]. Steroid **35** also presented relevant results in SMMC-7721 and MGC-803 cell lines (the determined IC_{50} were 6.05 and 5.79 μM, respectively). In addition, flow cytometry studies demonstrated that this compound caused cellular early apoptosis and cell cycle arrest at the G2/M phase in a concentration and time-independent mode. Additionally, compound **36** showed to be the most potent derivative in SMMC-7721 cells (IC_{50}= 0.71 μM).[334] Steroid **37** (**Table 9**) also stood out from novel pregnenolone derivatives synthesized by Choudhary et al., presenting an interesting effect against MDA-MB 231 cells (the determined IC_{50} value for antiproliferative activity was 0.91 μM). In addition, it was showed that steroid **37** is more potent than the positive control, doxorubicin (DOX) (IC_{50}= 1.23 μM).[371]

Mitchell and coworkers synthesized 16-substituted 4-azasteroids as tissue-selective AR modulators, using 16*E*-arylideneandrostane derivatives as synthetic intermediates. Generally, this class of steroids displayed potent AR binding and agonist activity. Of these novel molecules, **38** (**Table 9**) showed the most promising results, exhibiting an osteoanabolic and tissue-selective profile in ovariectomized (OVX) and orchiectomized (ORX) rat models. In OVX rats (models with bone loss that simulate estrogen deficiency), the main evaluated parameter was bone formation rate (BFR) and it was reported as a percentage of the DHT effect at a standard dose. On the other hand, the selectivity was assessed by measuring the effects on ventral prostate (VP) and seminal vesicles (SV) through ORX male rat models. Interestingly, compound **38** exhibited a BFR of 120 %, relative to DHT, an increase in the VP of 3 % and a 21 % of increase in SV weight, confirming its tissue selectivity (**Table 9**).[387] Furthermore, the preparation and biological evaluation of a new series of 16*E*-arylidene substituted steroidal oximes from 16*E*-arylideneandrostanes was also reported.[335,388] In this context, Chattopadhaya et al. used the hollow fiber assay to assess the antitumor interest of novel 16*E*-arylideneandrostane oxime derivatives.[335] Interestingly, the oxime **39** presented the best

result, exhibiting a good score for inhibition of tumoral cells in the S.C. fiber implants (4/20) and for I.P. fiber implants (6/20) (**Table 9**).

Moreover, Dubey and coworkers also synthesized 16*E*-benzylidene substituted steroidal oximes from 16*E*-arylideneepiandrosterone derivatives.[388] These compounds were evaluated for *in vitro* antineoplastic activity at NCI against three cell lines. Within these oximes, the 3β-hydroxy derivative **40** (**Table 9**) was found as the most potent. In fact, in the three cell lines tested, NCI-H460 (lung), MCF-7 (breast) and SF-268 (central nervous system), this oxime **40** showed negative values for the percentage of cell growth (−44, −44, and −79, respectively) (**Table 9**).[388] In addition, the same authors also reported the preparation of 16*E*-benzylidene substituted 3,17-dioximinoandrostene derivatives as anticancer agents and interesting results were obtained.[389] These steroids were also biologically tested at NCI against the same three cell lines. Of these, compound **41** showed to be the most active dioxime against the tumoral cells, presenting the lowest percentage values for cell growth in NCI-H460, MCF-7, and SF-268 cells (−11, 5, and −8, respectively) (**Table 9**).

Table 9. The most representative active heterocyclic steroidal derivatives obtained from arylidenosteroids. Positive controls, when shown, are identified by the (+) symbol. Molecular structures were created with ChemDraw. [a]

Compound	Bioactivity data			Ref.
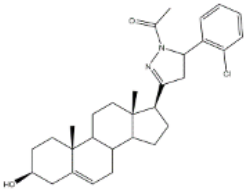 **26**	Antiproliferative activity (IC_{50} μM)			310
	Cell line	**24**		
	HT-29	0.24		
	HCT-15	0.25		
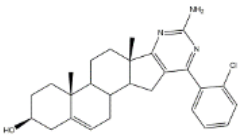 **27**	Antiproliferative activity (IC_{50} μM)			327
	Cell line	**25**	5-FU (+)	
	HepG-2	5.41	>100	
	Huh-7	5.65	>95	
	SGC-790	10.64	>100	
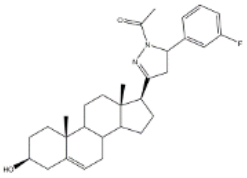 **28**	5AR type 1 inhibition (IC_{50} ±SEM μM)			382
	26	Finasteride (+)		
	14.50±0.48	21.6±0.62		

Table 9. (Continuation).

Compound	Biological data	Ref.
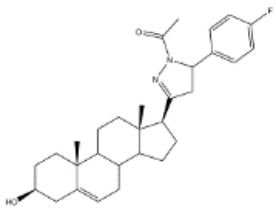 **29**	5AR type 2 inhibition (IC_{50} ±SEM μM) **27**: 13.90±0.75; Finasteride (+): 15.4±0.58	382
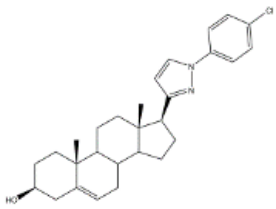 **30**	5AR type 2 inhibition (IC_{50} ±SEM μM) **28**: 14.20±0.75; Finasteride (+): 15.4±0.58	382
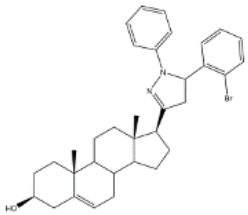 **31**	5AR type 2 inhibition (IC_{50} ±SEM nM) **29**: 7.30±0.62; Finasteride (+): 2.4±0.15	373
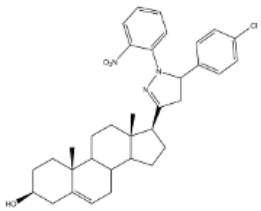 **32**	5AR type 2 inhibition (IC_{50} ±SEM nM) **30**: 8.20±0.55; Finasteride (+): 2.4±0.58	373
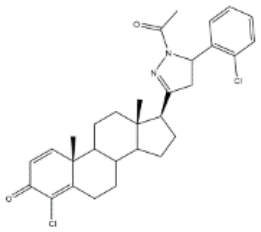 **33**	Antiproliferative activity (IC_{50} μg.mL^{-1}) Cell line / **31** / 5-FU (+) / Cis(+) NCI-H460: 10.30 / 2.48 / 0.699 HeLa: 12.50 / 0.887 / 2.03 Cell cycle arrest at S phase in HeLa cells	298

Table 9. (Continuation).

Compound	Biological data			Ref.
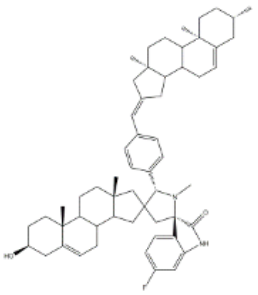 **34**	Antiproliferative activity (IC_{50} μM)			334
	Cell line	**32**	5-FU (+)	
	SMMC-7721	4.30	9.78	
	MCF-7	2.06	7.54	
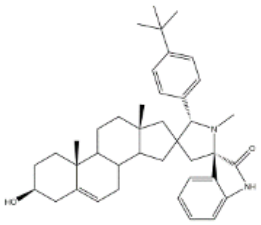 **35**	Antiproliferative activity (IC_{50}±SEM μM)			334
	Cell line	**33**	5-FU (+)	
	SMMC-7721	6.05±0.48	9.78±0.99	
	MGC-803	5.79±0.76	6.92±0.35	
	Cell cycle arrest at G2/M phase in MGC cells			
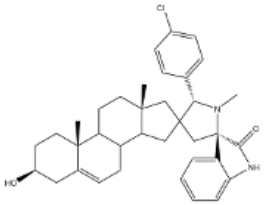 **36**	Antiproliferative activity (IC_{50}±SEM μM)			334
	Cell line	**34**	5-FU (+)	
	SMMC-7721	0.71±0.11	9.78±0.99	
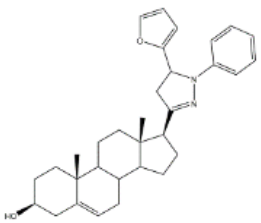 **37**	Antiproliferative activity (IC_{50} μM)			371
	Cell line	**35**	DOX (+)	
	MDA-MB 231	0.91	1.23	
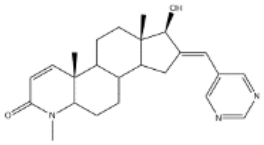 **38**	Osteoanabolic activity and tissue-selectivity (% of the effect of DHT)			390
	OVX	**36**	DHT	
	BRF	120	100	
	ORX			
	VP	3	100	
	SV	21	100	
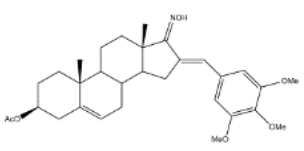 **39**	Cytotoxic activity – *in vivo* hollow fiber assay (score)			335
		37	Taxol (+)	
	I.P.	4	Data not shown	
	S.C.	6		

Table 9. (Continuation).

Compound	Biological data		Ref.
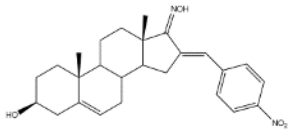 **40**	Antiproliferative activity Cell growth (%)		388
	Cell line	**38**	
	NCI-H460	−44	
	MFC-7	−44	
	SF-268	−79	
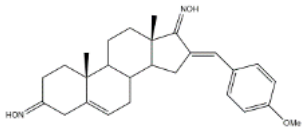 **41**	Antiproliferative activity Cell growth (%)		389
	Cell line	**39**	
	NCI-H460	−11	
	MCF-7	5	
	SF-268	-8	

[a] 5AR= 5α-Reductase, 5-FU= 5-Fluorouracil, Cis= Cisplatin, DOX= Doxorubicin, OVX= Ovariectomized, ORX= Orchiectomized, DHT= 5α-Dihydrotestosterone, I.P.= Intraperitoneal, S.C.= Subcutaneous.

Considering all previous information, steroids represent a relevant group of natural, semi-synthetic, and synthetic compounds with distinguished functions. In the last three decades, a significant number of steroidal arylidene derivatives have been synthesized and screened for a variety of biological activities and used as synthetic intermediates, mainly to obtain bioactive heterocyclic steroids. Within these, several arylidenosteroids have shown significant antiproliferative activity when compared to reference compounds. In addition to this cytotoxic activity, a considerable number of 16*E*-arylideneandrostane derivatives were also studied as ARIs with promising results, and a few 16*E*-arylidenoestrone derivatives were studied as 17β-HSD type 1 inhibitors. Moreover, steroidal arylidene derivatives have also emerged as very important synthetic intermediates to obtain steroidal heterocycles as arylpyrazolines and pyrazoles, arylpyrimidines and pyridines, spiro-oxindoles, and spiro-pyrrolidines, among other bioactive systems. Within these, arylpyrazoline derivatives stand out as potential 5AR inhibitors and antiproliferative agents.[323] Interestingly, arylidenesteroids, despite being relevant and essential synthetic intermediates of heterocyclic compounds with important 5AR inhibitory activity, they have not yet been studied as 5ARIs per se, representing a huge gap on research in this context.

In summary, due to the straightforward synthesis of arylidenosteroids and their bioactivity, as well as the inherent chemical reactivity of α,β-unsaturated ketones, useful in the preparation of other derivatives, this class of compounds has been of high interest in the last years.

1.3. Drug discovery and development process

Historically, until the 20th century, medicines mostly comprised herbs and potions. However, in the middle of the 19th century, the first efforts to isolate and purify the active principles of those medicines were attempted. Since that time, numerous naturally occurring drugs have been found and the respective structures determined. Later, from these natural products, several analogs have been synthesized to improve bioactivity. A considerable part of this work was based on trial and error; however, the results revealed some general principles behind rational drug design. Although there was an important component of trial and error involved in the drug discovery and development process, a pattern started to be established. More recently, medicinal chemistry has suffered a revolutionary modification namely with the rapid advances in the biological sciences which allowed a much better understanding of physiology and pathology at cellular and molecular levels. Consequently, most research projects in this field (pharmaceutical industry and/or academia) start with target identification and design of compounds capable of interacting with that target, producing the desired response. A clarification of the structure and function of the target, and the knowledge of the action mechanism of the potential drug is essential to the success of this approach.[391,392] Nowadays, a typical drug discovery and development process comprise several imperative stages: (1) drug discovery, which involves target identification and validation, and basic research; (2) preclinical phase; (3) clinical phase, which includes clinical trials; (4) regulatory phase, and (5) post-surveillance stage after drug approval (**Figure 22**).[393] In the next subsections, drug discovery, including unmet medical needs, target selection and validation, hit-to-lead process, and lead optimization will be discussed. Furthermore, preclinical and clinical phases, approval and post-market monitoring, and other points relevant to drug discovery and development will also be described.

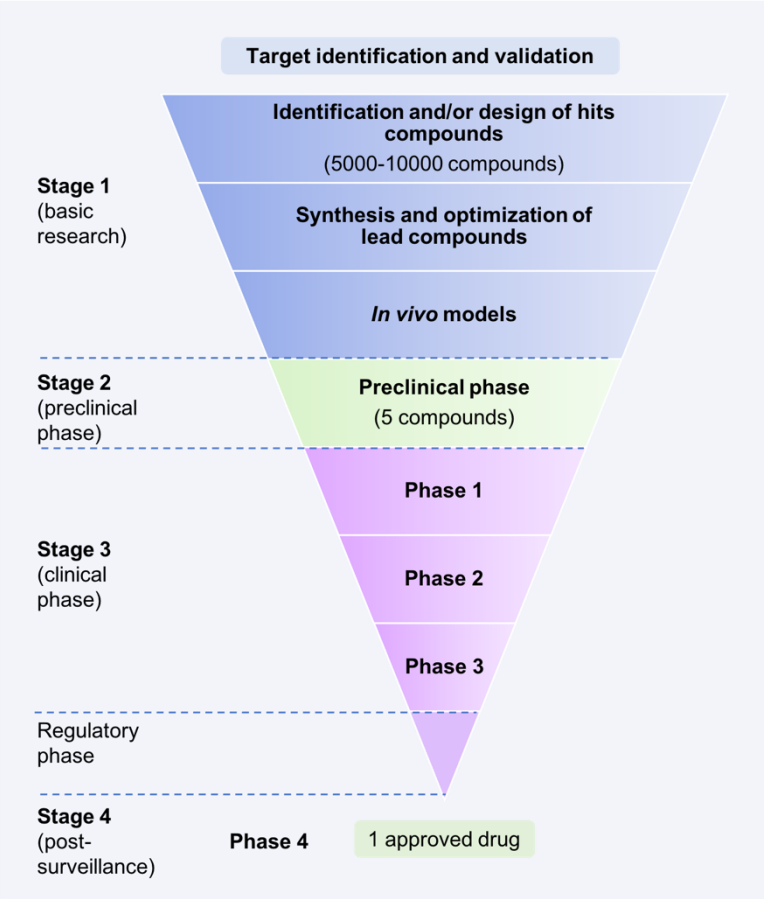

Figure 22. Overview of drug discovery and development process: drug discovery, preclinical and clinical trials. *Adapted from Gallego et al. (2021).*[393]

1.3.1. Drug discovery

The drug discovery stage aims to identify a small synthetic molecule or a large biomolecule for wide-ranging evaluation as a potential drug candidate. Generally, the actual drug discovery process comprises identification of disease and its unmet medical need, target selection and validation, *in vitro* assay development followed by high throughput screening (HTS) of compound libraries against the selected target. The purpose of *in vitro* assays and HTS implementation is to identify hits. Posteriorly, these hits are optimized to generate lead compounds that exhibit acceptable potency and selectivity considering the biological target. Additionally, lead compounds should demonstrate efficacy in animal models of disease. Afterward, the lead compounds are usually further optimized to increase their efficacy and pharmacokinetics (PK) properties before they can advance in the drug development process.[391,392]

- **Unmet medical needs, target identification and validation**

To start a drug discovery process it is mandatory the selection of a medical condition whose therapy outcomes are not satisfactory by currently existing medical treatments. This lack of a satisfactory medical treatment for a determined disease is named an unmet medical need. The methods to recognize the unmet medical need involve (1) market analysis, (2) inputs from relevant specialists in a therapeutic area, (3) feedback from health professionals, and (4) information provided in scientific conferences. Furthermore, it is crucial the understanding of disease epidemiology, etiology and current therapeutic approaches, and their deficiencies drive a careful gap analysis and thereby to facilitate the selection of medical needs in a particular disorder.[392] For the pharmaceutical industry, the relevance of economic factors is a key-point for disease selection. Indeed, the research and development of a new drug candidate involve massive investment and companies must ensure a good financial return on this investment. Another important point in drug discovery investigation is the focus on diseases with high prevalence (e.g. depression, ulcers, obesity, flu, cancer, and cardiovascular disorders) in the developed countries, due to the capacity of this market to pay new drugs. On the other hand, a lower number of investigations have been carried out regarding the diseases of developing countries. However, when the impact of these diseases crosses borders and affects developed countries, mainly Western society, the pharmaceutical industry becomes more interested. In summary, choosing which disease to combat is usually a matter for a company's market strategists and science becomes important at the next stage.[391]

The next stage is the identification and characterization of a target with a relevant role in the disease and thus with potential therapeutic interest. Following the target identification, the characterization of its molecular mechanisms is a fundamental step. The main characteristics of a good target are (1) efficacy, (2) safety, (3) meeting clinical and commercial requirements, and (4) being "druggable".[394] The concept of "druggable" target comprises its accessibility to the presumed drug (a small molecule or larger biologicals) and upon binding induces a biological response measurable both *in vitro* and *in vivo*.[395] Therefore, bioactive compounds (small or large molecules) exert their activity and consequently led to a quantifiable clinical response by interacting with a naturally existent molecular structure, the target. The most common targets include, for instance, enzymes, receptors, DNA, RNA, metabolites, substrates, transport proteins, and ribosomes.[396] Generally, targets can be classified as established or novel targets. Established targets have been scientifically demonstrated to have an exact physiological

and pathophysiological role. On the other hand, the role of novel targets is turning out to be clear and elucidated through advancing research.[392]
There are several approaches to target identification, such as data mining using bioinformatics (identifying, selecting, and prioritizing potential disease targets), genetic association (e.g. analysis of genetic polymorphisms and their relation with the disease), expression profile (changes in mRNA/protein levels), phenotypic analysis (*in vitro* cell-based mechanistic studies), and functional screening (knockdown, knockout or using target-specific tools).[394,397]

Concerning the so-called phenotypic analysis approach, compounds/antibodies are assessed in cell-based experiments and/or animal models of disease to identify molecules that led to an anticipated phenotype modification. This may comprise an alteration in the *in vitro* expression of a single or several proteins or achieving a desired pharmacological response *in vivo*. After the identification of a bioactive compound, its molecular target is then determined by genetic approaches, including expression cloning techniques, *in silico* studies and/or by chemical proteomics-based approaches, such as affinity chromatography, activity-based protein profiling, and label-free techniques.[392,398]

The genetic association is also considered a valid method for target identification, wherein genetic variants, such as single nucleotide polymorphisms (SNPs), related to the risk of acquiring/developing a disease, are identified.[392] Additionally, genome-wide association studies that investigate the complete human genome for a large number of SNPs at a time, to identify variants that occur in the majority of patients with a complex disease, have been a helpful strategy in target selection.[399]

The next essential step is target validation to prove that it is relevant to the disease and that modulating it will have the desired outcome. This step depends on having relevant, physiologically realistic disease models and phenotypic assays. There are several approaches towards validation, comprising *in vitro* assays for modulating gene expression *in vitro* and *in vivo*, as well as the use of monoclonal antibodies, genetic manipulation of target genes, chemical genomics, and proteomics.[394,400,401] The use of monoclonal antibodies is an excellent strategy for target validation since they can interact with a larger region of the target molecule surface, which allows a better discrimination between closely related targets and often provides superior affinity. Small molecules, in contrast with antibodies, usually interact with the more conserved active site of a target, while antibodies can be selected to bind to exclusive epitopes.

Consequently, this specificity is the basis for their lack of "off-target" toxicity, which constitutes a major advantage over small molecule drugs.[395] The "off-target" effect refers to adverse effects as a result of modulation of other targets.[402] Nevertheless, antibodies are not capable of crossing cell membranes, limiting the target class principally to the cell surface and secreted proteins.[395]

Concerning genetic manipulation, the use of genetically modified animals for target validation is an attractive methodology, allowing the analysis of the phenotypic consequences of gene manipulation. Development of knockout and knock-in models, conditional mutant gene-targeted, and transgenic animal models are examples of genetically modified animals.[403] However, genes can generate several isoforms of a protein which may have distinct functions, and variations in proteins can also be a consequence of post-translational modifications, which constitute a limitation of the genetic approach in target validation. To overcome this limitation, proteomics, which purposes the modulation of the activity of the target protein itself, emerged in the past two decades as an improved approach to target validation.[404]

- **Hit-to-lead process and lead optimization**

Following target identification and validation, the hit identification and lead discovery represent the next important step in the drug discovery pipeline. A "hit" molecule is a compound that presents the desired activity in a screening assay (usually *in vitro*) which is confirmed upon retesting. Thereby, the hit compound is a starting point for a forward medicinal chemistry optimization.[395]

The current pipeline to discover hit compounds is a data-driven process, based on bioactivity data obtained, frequently, from HTS. Usually, this method uses libraries of up to a million drug-like compounds, which may be directly and quickly evaluated against the target, using a biochemical or a cell-based assay, and then it is also necessary to perform secondary assays to confirm the site of action of compounds.[405] HTS involves complex laboratory automation, and can even be performed without prior data of the nature of the molecule with potential bioactivity. In this context, fragment-based drug design is a more focused strategy which consists of the evaluation of libraries of compounds with small molecular weights at high concentrations, and the hits are defined as compounds that although can present weak activity shows efficient binding to the target. Then, structural fragments of the hits can be used as building blocks for the synthesis of more potent and drug-like compounds.[406] After this, a more specialized focused screening approach can also be performed, using tissue-based assays looking for a response aligned with the final desired *in vivo* effect.[395] It is important to mention that

the cost of obtaining new hit compounds through the HTS methodology is relatively high. Consequently, quantitative structure-activity relationship (QSAR) modeling has been playing a crucial role in ranking and prioritizing compounds for synthesis and/or biological evaluation, using pharmacophores and molecular modeling to conduct a virtual screening (VS) of compound databases and empirical data available in literature.[392,407,408] QSAR models can be applied not only in hits identification but also in hit-to-lead optimization (**Figure 23**). In the hit-to-lead optimization, a favorable balance between potency, selectivity, and PK and toxicological parameters should be accomplished through some optimization phases to develop a novel, safe, and effective drug. Since the synthesis or biological evaluation of compounds is not needed before computational assessment and analysis, QSAR constitutes a labor-, time-, and cost-effective approach to finding compounds with desired biological properties. Therefore, QSAR is broadly applied in pharmaceutical industries, universities, and research centers all around the world.[409]

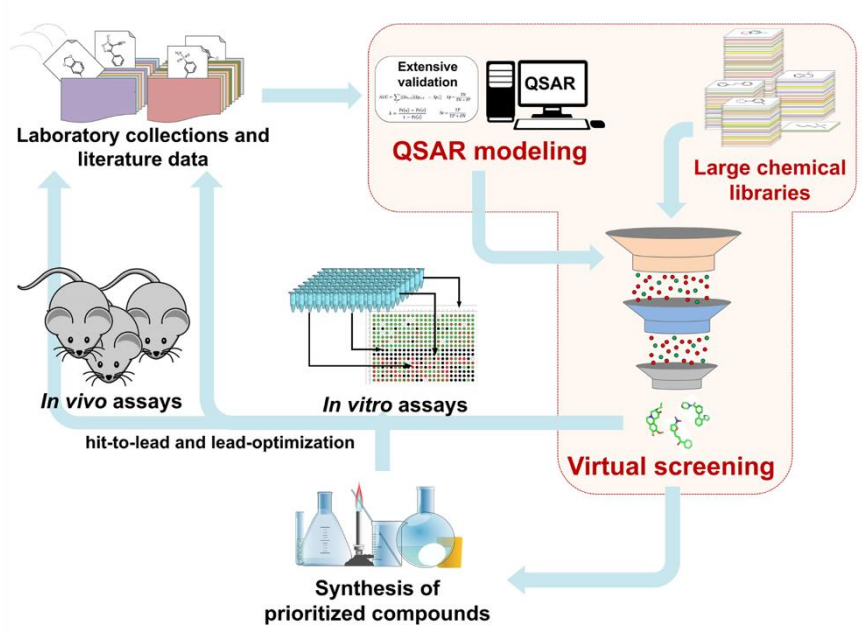

Figure 23. Scheme of quantitative structure activity relationship (QSAR)-based virtual screening (VS) approach in hit discovery. *Adapted from Neves et al. (2018).*[407]

The hit compounds can be further explored as possible lead compounds and then optimized. Generally defining, the "hit" is a compound which has the desired activity in a screening and whose activity is confirmed upon retesting, while the "lead" is defined as the most promising structure among hit compounds with elevated and proved potency in biological assays (*in vitro* and *in vivo*) that express the target mechanism. Furthermore, the lead compound presents profiles of safety and PK that usually have to

be upgraded. Hence, its potential is established by a whole range of properties beyond its activity. The lead is characterized based on several physicochemical (e.g. solubility) and biological/pharmacological (e.g. target binding affinity, permeability, metabolic stability) properties. These characteristics are known to be crucial in drug candidates, namely absorption, distribution, metabolism, and excretion (ADME) profile.
In this context, as the most preferred route for administration of a drug is oral, the new drug candidate in development should obey the Lipinski rule of 5. This rule emphasizes that a compound is more likely to be membrane-permeable and absorbed by the body if it matches the following principles: (1) its molecular mass is less than 500, (2) its *logP* (a measure of lipophilicity) is less than 5, (3) the number of hydrogen bond donors is less than 5, and (4) the number of hydrogen bond acceptors is less than 10.[410] In summary, the quality of a lead compound is dictated by an entire range of properties beyond its activity in a binding assay, and usually, these properties are more challenging to optimize than the primary biological activity.[411]

After lead identification, their activity, selectivity and toxicity, as well as PK properties are optimized in an iterative and multifactorial process, leading to the selection of a suitable candidate for further improvement in the drug discovery and development process.[411,412] It is imperative the demonstration of a direct correlation between concentrations of the compound in plasma with its pharmacodynamic (PD) effect. Furthermore, a dose-linear exposure is preferable, as the compounds which do not exhibit such behavior have limited clinical utility, especially if they have a narrow therapeutic window. Studies for metabolites identification and characterization are also conducted during this stage as they may affect the compound efficacy, be active and present toxicity. In addition, active metabolites may be considered new exploratory lead structures for further investigation. Medicinal chemistry studies are not complete once a preclinical candidate has been identified. The researchers also initiate an effort on a backup strategy to identify substitute compounds if some failures of the drug candidate in preclinical and clinical development exist.[392]

1.3.2. Preclinical and clinical trials

- **Preclinical drug development**

Once a drug candidate is selected, an extensive set of preclinical development studies are performed and the results obtained are crucial in the decision-making process to determine the progression or not for the clinical (human) studies. These complex studies are designed to support its approval by the regulatory bodies to move the candidate into a clinical study by submission of an Investigational New Drug (IND) application. All the

information assembled about the candidate in terms of efficacy, toxicity, PK, PD, and pharmaceutical properties will be part of this application. To obtain this information, several investigations have to be accomplished, namely, safety pharmacology and toxicology studies in animals and other activities related to chemistry, manufacturing, and control (CMC) such as formulation development, stability studies, quality control measures, and comprehensive recommended clinical protocols for initiating clinical studies.[392] A drug candidate is considered suitable for clinical tests if it binds selectively to the target receptor site, stimulates the desired functional response of the target, and if it has adequate bioavailability and biodistribution to cause the desired responses in animals. In addition, the drug candidate must also pass a formal toxicity assessment in animals. Due to the incidents of unpredicted human toxicity that occurred in the last decades, the regulatory agencies and public demands for the safety of new candidates have become extremely strict, and safety issues are also determinant.[413]

The types of preclinical studies are *in vitro*, *ex vivo,* and *in vivo*. These studies have to be performed under good laboratory practices (GLP), defined by medical product development regulations, for preclinical laboratory studies, by FDA and EMA. *In vitro* and *ex vivo* studies are comparatively fast, simple, and cost-efficient approaches to preclinical testing. These studies can be carried out in cells, tissues, and organs, or focus on particular cell components such as proteins or other biological macromolecules, and they allow a tight control and monitoring of experimental settings.[414] Through these assays, it is possible to observe the activity of the new drug candidate upon diverse features, such as the induction of cell death and proliferation, modifications in gene expression, alterations in the protein profile, and changes in cell cycle.[415–418] In addition, *in vitro* and *ex vivo* studies have potential to provide mechanistic insights. However, these models represent isolated cells and tissues that may not behave as they would within the body. Therefore, further sophisticated and advanced preclinical models are required to more accurately establish the safety profile of the candidate before its transition to clinical trials.[414] At this stage, *in vivo* experiments emerge as the following logical step, since they consider the complete organism based on animal models. Animal testing is tightly regulated in most countries and, consequently, authorization from local ethical review boards is mandatory to guarantee that no unnecessary harm is provoked to animals under study.[419] As expected, controlling experimental settings is more problematic for *in vivo* studies due to the complexity of the living organism. Then, compounds may behave differently from what is estimated based on results obtained in the previous assays.[414] The selection of proper animal models depends on multiple criteria and requirements. Understanding of species-specific physiology, the

resemblance considering the target organ, metabolic pathways, and regulatory, financial, and ethical aspects are essential aspects to consider in this selection. *In vivo* studies are frequently performed in rodent and non-rodent models. Mice, rats, and dogs are among the most recurrently used animals, while primates (e.g., monkeys) are used occasionally and typically for larger molecules.[420] Among these animal models, one of the most popular and used in pharmaceutical testing is the mouse, due to the genomic similarity. In fact, 99% of all mouse genes overlap with those of humans. However, it is important to be aware of some species-specific differences namely in host immune response, and tumor heterogeneity that may modify therapeutic outcomes. Differences in PK and PD among species are also not insignificant and consequently, mouse models frequently offer poor predictive power regarding clinical efficacy. Nevertheless, the absence of better alternatives makes mouse models the gold standard, mainly concerning cancer-targeting drugs.[421]

Preclinical evaluation of a new drug candidate is expensive, labor exhaustive, and time-consuming. In consequence, the deep impact related to the time and costs expended with this developmental phase on the potential return on investment should not be a reason to accelerate the establishment of the necessary preclinical information. The acceleration of the process can result in an unsafe initial trial in patients. In fact, the time and effort expended in the preclinical phase can determine the outcome of the project.[422]

- **Clinical trials**

Clinical drug development has permission to begin if the IND application is approved. Clinical trials generally constitute the longest part of the drug development process, and also represent the major single current expenditure. Typically, clinical studies are categorized in clinical trials of Phase 1, Phase 2, and Phase 3. Posteriorly, Phase 4 studies take place after the drug is approved for marketing.[392,423] The overall aims of these phases of clinical trials are relatively similar, although the design of these trials can be considerably distinctive.

In general, Phase 1 studies are performed to evaluate the safety and tolerability of a new medicinal product and are typically conducted on a small number of healthy volunteers (20 to 180). This trial often represents the first human exposure to the new drug and it usually lasts about 2 years. PK (ADME) and PD parameters are monitored. In addition, the maximum tolerated dose (MTD) is determined, and these trials are usually single-blind studies. Furthermore, they intend to decrease potential risk to future study patients

while providing satisfactory data to facilitate the design of scientifically valid Phase 2 studies.[392,424,425]

Then, the Phase 2 trial is the first study that confirms safety and establishes efficacy benchmarks of the new drug in patient volunteers (ideally 100 to 300), and also usually lasts about 2 years.[424,425] However, phase 2 studies can have several purposes such as the acquirement of dose-response relationship data and determination of dosing regimen (e.g. ideal dose, frequency of administration). Generally, these trials are randomized and could be single- or double-blind trials. The majority of clinical drug candidates fail in this phase mainly due to the lack of efficacy and/or safety issues.[392]

Phase 3 trial comprises a large-scale clinical study (1,000 to 3,300 patient volunteers), which aim is to confirm the effectiveness and safety results from previous investigations. Phase 3 studies are conducted for 2 to 4 years at multiple sites and compare the investigational new drug with the best current treatment or standard of care in a particular disease. Moreover, the safety is also evaluated in a larger pool to possibly the detection of less common or long-term related side effects. These trials are randomized, controlled and double-blinded, with multiple study arms, and are the most expensive and complex studies. Furthermore, Phase 3 trials also assess different subpopulations, drug dosages, formulations, and monitor potentially important drug interactions. Then, if the results obtained are favorable, all data is collected and compiled into a dossier and a New Drug Application (NDA) is filed for regulatory approval to license the drug.[392,426]

1.3.3. Approval and post-market monitoring

After filling and submitting an NDA to the regulatory agencies, the review and approval can take 1 to 2 years.[424] Once the drug is approved, Phase 4 (post-marketing monitoring) starts and this is considered the real test as the new medicinal product is tested in the real world for the first time. This phase comprises the monitoring of side effects (pharmacovigilance) and evaluation of drug efficacy/safety (entire user population).[424,426] Phase 4 has also significant implications and involves modification on drug labeling, contraindications, interactions, and even withdrawal if a relevant problem is detected.[392] In fact, the new medicinal product launch is a milestone in drug development. In summary, the surveillance of spontaneously reported adverse events continues as long as a product is marketed, and Phase 4 in that sense never ends.[427]

1.3.4. Other approaches and concepts in drug discovery and development

Despite the increasing investments in research infrastructures by the pharmaceutical industry and technological innovations, efforts to raise the number of molecular identities coming through the drug development process have mostly been unsuccessful [428]. One of the reasons for this lower (than expected) number of innovative drugs can be related to the one-drug-one target paradigm. In addition, the contribution of multiple targets in complex diseases requires a simultaneous modulation (e.g. Alzheimer's disease, cancer) [429]. To achieve this type of modulation, either the use of different or the single multiple-targeting agents can be valid strategies. The last option constitutes a considerable challenge for medicinal chemists. To increase the number of potential new drugs, other approaches and concepts in drug discovery and development have arisen in the past years, and some of these approaches will be presented in this section.

In the last two decades, molecular docking has arisen as an important and now is a well-established *in silico* structure-based method widely used in drug discovery process. Docking simulations allow the identification of novel compounds with potential therapeutic interest, predicting ligand-target interactions at a molecular level, or delineating structure-activity relationships (SAR). Initially, this tool was developed to help understanding the mechanisms of molecular recognition between small and macromolecules. However, uses and applications of docking in drug discovery have changed over the last years.[430] Nowadays, docking studies is also widely employed to assist several drug discovery tasks, such as the identification of novel chemical scaffolds within large libraries of compounds, to perform *in silico* target fishing and profiling for drug repositioning, polypharmacology, and prediction of adverse effects.[431–435] In fact, molecular docking can be considered an extremely versatile tool. Moreover, docking simulations has been successfully embedded within automated workflows for the screening of large libraries of compounds and targets. In summary, the possibilities offered by docking in combination with other approaches are important to reduce time and costs in both the development of clinical candidates with better safety profiles and for the identification of novel applications of already known drugs.[430]

Network pharmacology has emerged as a new paradigm in drug discovery, aiming to understand drug actions and interactions with multiple targets. To systematically catalog the molecular interactions of a drug molecule in a living cell, this approach uses computational power (**Figure 24**).[436,437] This strategy also attempts to discover new drug leads and targets, and repurpose existing drug molecules for different diseases, allowing an unbiased clarification of mechanisms of action as well as systematic prediction of effective therapeutic combinations.[438] However, network pharmacology still requires some guidance in the selection of the right type of targets and new scaffolds of drug molecules. Thus, traditional knowledge can play a crucial role in this process of formulation discovery and repurposing existing drugs. Indeed, this approach opens up new therapeutic alternatives, and also intents the improvement of safety and efficacy of existing medications.[437]

Figure 24. Map of interactions of human polypharmacology showing the relationship between proteins in the chemical space. Two proteins are interacting in chemical space (edge) if both bind one or more compounds within a defined difference in binding energy threshold. The number of proteins in this network is 486 (nodes), with 3,636 polypharmacology interactions (edges). *Adapted from Paolini et al. (2006) and Hopkins et al. (2008).*[436,439]

Repositioning already approved drugs for new indications, also referred to as repurposing, is another approach frequently used. The main advantage of this approach is the possibility of passing forward the preclinical safety studies and Phase 1 trials, which represents a time-cost saving for the pharmaceutical industry.[392,440,441] For instance, drug repurposing is one of the key tools in the investigation for drugs in the early fight against

Covid-19. In this context, remdesivir and dexamethasone were found to display improvements in clinical endpoints in hospitalized patients.[442,443] Remdesivir (Veklury®) for COVID-19 treatment was approved by EMA in July 2020.[444] Initially, remdesivir, developed by Gilead Sciences, emerged to treat infections caused by RNA-based viruses, including Ebola. Additional ongoing clinical trials will clarify the efficacy of the repurposing of other approved drugs against COVID-19.[445]

An alternative and a relatively new approach towards drug discovery is the allosteric modulation of drug targets. Nowadays, a high number of drugs change the action of enzymes, receptors, transporters, and other molecules through direct binding in the active sites of these macromolecules. Nevertheless, active site configuration is similar in numerous proteins playing associated functions, leading to an inferior specificity of a drug for the desired target. In consequence, adverse side effects may appear and the need for a new strategy in drug discovery is emerging based on the binding of the drugs to sites away from the active sites (allosteric sites). In summary, the major benefit of this approach is that the allosteric sites might be exclusive, which allows for selective targeting, and consequently, the target-specific adverse side effects reported decrease.[446]

Natural products have been considered a valuable source of leads for drug discovery. However, structural modifications are required to increase their physicochemical properties to generate derivatives for structure-activity relationship acquisition of data, which constitute a challenging process. In order to exploit the full potential in the generation of innovative drugs from natural products, new strategies have been under development based on more recent innovations in technology, as the use of computation. These approaches allow a fast identification of novel bioactive natural products, derivatives, and structure elucidation have opened on the drug discovery process in this context.[447,448] In this context, the two main distinct complementary approaches that have been applied are the classical pharmacology, known as phenotypic drug discovery, and reverse pharmacology, designated target-based drug discovery. In the phenotypic drug discovery, the main focus is the function, being compounds screened to find those that modify the phenotype. For instance, extracts or compounds are assessed against cell lines in a quantitative measurement of one or more cellular parameters. The disease state and the action mechanism will be identified after this process. In target-based drug discovery, the gene that codes for a protein target involved in the disease is identified and then, compounds are screened based on the affinity binding against the respective target using computation methods. The active compounds found *in silico* need to be posteriorly checked in tissues and whole organisms (*in vitro* and *in vivo*). Complex and

advanced high-content phenotypic drug screenings using cell lines representative of a disease have been developed. *In vivo* assays usually include the use of organisms as fruit fly, zebrafish or mouse are commonly used for phenotypic screenings. On the other hand, target-based approach mainly benefits from the advances and evolution of science in the fields of biochemistry, structural biology, chemistry, genomics and technology.[448–450]

More recently, the pharmaceutical industry is also investing in the discovery and development of biologics or biologically derived medicinal products, such as monoclonal antibodies, polypeptides, hormones, growth factors, interferons, interleukins, and vaccines. The production of these medicinal products requires recombinant DNA processes. In general, their mechanism of action involves targeting either a genotype or a protein target. Nevertheless, the production of these drugs is expensive, complex, and being mainly proteins they have the potential for immunogenicity. Usually, the patients under this therapeutic are those for which the conventional therapies do not work or for whom no therapeutic options exist.[392,451]

Concerning early phase drug development, microdosing is a very useful strategy, increasing productivity in the research process. This methodology involves the administration of a subpharmacologically active dose of the drug in humans, and exploratory PK data is studied. Until the moment, evidence suggests that microdosing is a reliable predictive tool of human PK, principally in combination with physiologically based modeling. Microdosing is also applied to study drug-drug interactions, polymorphism, and assessing drug concentrations overtime at the site of action. This phase is also mentioned as Phase 0 and regulatory agencies concede approval for its execution without a complete preclinical safety report. The drug candidates presenting poor PK properties are not selected for further investigations and development.[392,452]

Lastly, crowd sourcing is an emerging approach to indorse cooperation of academic and industrial sectors in the early stages of drug discovery, taking advantage of the respective complementary expertise.[453] It is expected that this type of collaboration could support the improvement of research and development productivity in the pharma/biotech industry, using the internet as the main platform.[454,455] The collaboration of these two sectors is schematically resumed in **Figure 25**. In general, academic researchers conduct investigations to clarify the mechanistic related to fundamental biologic processes, aiming to produce therapeutic benefits. These findings indirectly contribute to advances as the industry requests new projects and targets from basic/fundamental research. Moreover, discoveries are shared with the industry through presentations and

publications, and the acquisition of patents licenses. The industry is mainly responsible for the identification of new drug candidates, subsequent validation work, and regulatory affairs.[456]

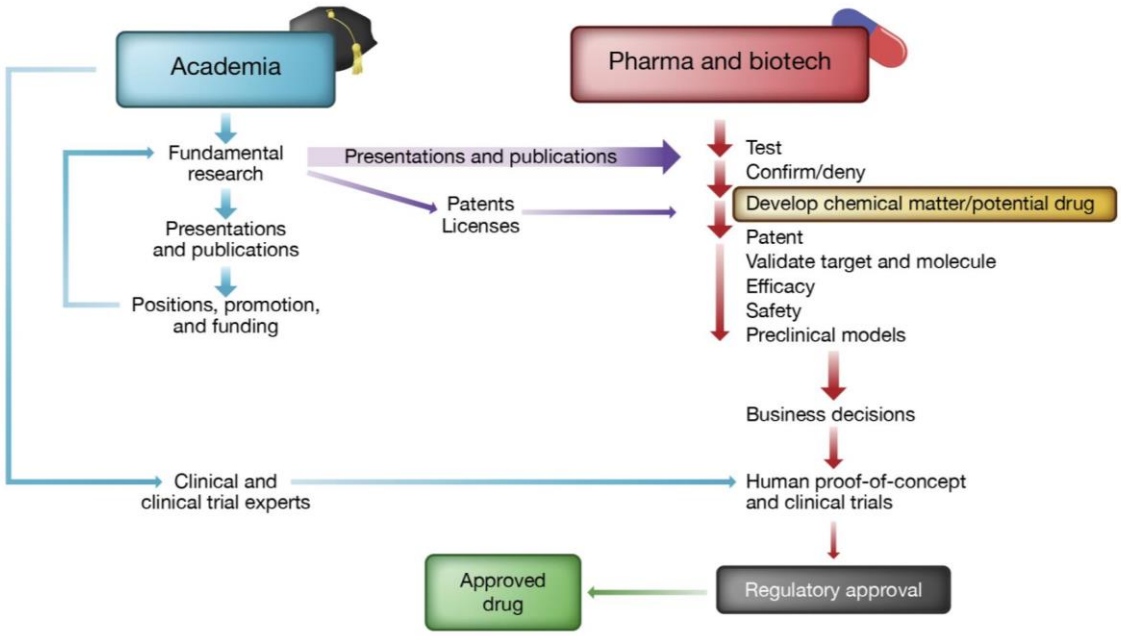

Figure 25. Role of collaboration between academia and pharma/biotech industries in drug discovery and development. *Adapted from Flier et al. (2019).*[456]

In conclusion, advances in technologies and the appearance of all these approaches have been a significant impact on the effectiveness of the discovery and development of safe and efficient new medicinal products by researchers. Despite this progress, the pharmaceutical industry remains under pressure, considering costs, pricing, and risks related to the drug discovery and development process. Nevertheless, the constant elevated unmet medical needs (e.g. rare diseases, neglected diseases) will continue to stimulate the innovation generated by pharma/biotech industries in collaboration with academia, public-private partnerships, and precompetitive research to achieve an efficient disease treatment. In addition, advances in computing tools to aid drug discovery have also enabled the selection of focused screens more successfully. Lastly, it is important to highlight the relevance of intellectual property protection in supporting pharmaceutical research and development.

1.4. Objectives of this thesis

The importance of pharmacological therapy in the management of prostatic disorders such as BPH and PCa is unquestionable. In addition, the use of 5ARIs in BPH treatment constitutes a relevant and frequently applied approach. Moreover, the use of ADT and/or chemotherapeutic agents in PCa patients is usually inevitable. Considering the unmet medical needs in this context, it is well established that the 5ARIs in the market (e.g. finasteride) exhibit relatively low potency and have several adverse side effects that decrease markedly the patients' quality of life. Furthermore, the effect of these drugs in the PCa prevention and treatment is controversial since finasteride, despite reduce the incidence of PCa, seems to induce the increase in the incidence of high-grade PCa compared to placebo. On the other hand, studies showed that treatment and management with 5ARIs can benefit patients with local and low Gleason score PCa, especially in delaying the disease progression. Considering the available evidence, targeting 5AR still seems a valid and logical strategy for the management of both prostatic disorders: BHP and PCa in a hormone-dependent stage.

Since the hormone steroids play crucial roles in the pathophysiology and the treatment of the referred diseases, the chemical modification of steroids remains an interesting field of investigation for novel drug candidates. Thus, in the literature, arylidenesteroids, a class of modified steroids, have been reported with important antiproliferative activity and also with potential 5AR inhibitory activity since they are relevant synthetic intermediates of compounds with this bioactivity. Moreover, arylidenesteroids have not yet been studied as 5ARIs *per se*, which constitutes a clear gap and a pertinent opportunity of research in this context.

In this scope, the principal goal of the present doctoral project was the preparation of novel steroidal arylidene derivatives potentially useful in prostatic diseases, presenting inhibitory capacity against 5AR and/or antiproliferative properties against tumoral cells. In conclusion, this work aimed the discovery of hit compounds for further development in the context of BPH and PCa.

To achieve this purpose, the following specific objectives were outlined for the execution of the present doctoral work (**Figure 26**):

1. **Chemical synthesis.** Rational design, synthesis, purification, and structural characterization (NMR, m.p., IR, HRMS) of new series of steroidal arylidene derivatives modified in the A and B rings.

2. ***In vitro* screening of antiproliferative activity of the synthesized compounds.** Assessment of the effect on cell proliferation of newly synthesized compounds through MTT assay. The assays will be carried out against several cell lines, tumoral (hormone-dependent and independent cells) and non-tumoral (e.g. LNCaP: human prostatic carcinoma cell line androgen-dependent; PC-3: cell line androgen-independent initiated from a bone metastasis of a grade IV prostatic adenocarcinoma; MCF-7: epithelial cell line isolated from the breast tissue of a patient with metastatic adenocarcinoma; PNT1A: normal human prostatic cell line). For the steroidal derivatives with the greatest potency to reduce cell proliferation, the values of inhibitory concentration at 50% will be estimated (IC_{50}).
3. ***In vitro* characterization of the most promising steroidal derivatives effects.** In addition to cell proliferation studies, through complementary biological techniques, characterization of the effect on cells of compounds identified in the previous task with higher antiproliferative activity (e.g. measure of caspases activity, cell and nuclei morphologic characterization).
4. ***In silico* studies.**
    a. *3D-QSAR studies*. Clarify the relationship between the structure of some synthesized compounds and precursors and its effects on proliferation of androgen-dependent (LNCaP) and androgen-independent (PC-3) prostate cell lines by building a three-dimensional quantitative structure–activity relationship (3D-QSAR) model applying the software Open3DQSAR.
    b. *Molecular docking simulations*. Evaluation and prediction of the affinity and potential interactions between novel compounds and several proteins which are known targets of steroidal drugs currently used in the treatment of BHP, PCa, and also breast cancer (5AR type 2, AR, ERα, and CYP17A1).
5. ***In vitro* screening of 5AR inhibitory activity of the novel steroidal arylidene derivatives.** Assessment of enzymatic activity in mouse liver microsomes by HPLC-DAD through the measurement of testosterone levels (need of partial method validation). The IC_{50} values of the most active compounds will be determined.

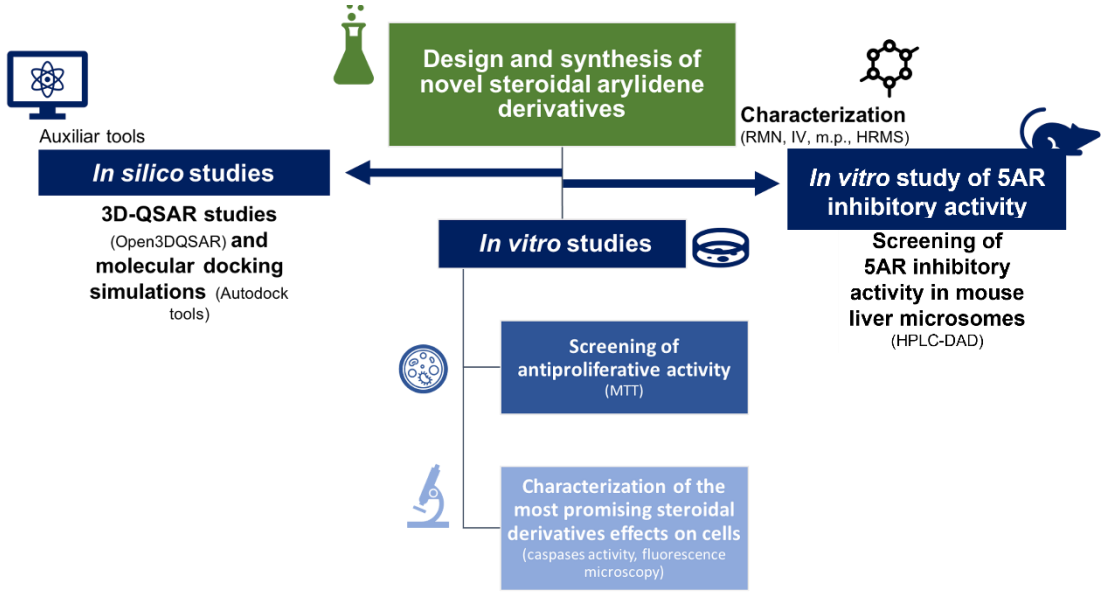

Figure 26. Flowchart of specific objectives of the present doctoral project (3D-QSAR= Three-dimensional quantitative structure-activity relationship, 5AR= 5α-Reductase).

CHAPTER II

2. Development of new azasteroids with potential interest in prostatic diseases

2.1. Studies on 4-aza-arylidene derivatives as cell growth inhibitors

2.1.1. Introduction

Azasteroidal compounds target a diversity of biological processes and therefore are potential candidates for the treatment of a large group of diseases, including breast cancer, PCa, BPH, osteoporosis, and autoimmune diseases.[457–460] More specifically, 4-azasteroids were extensively explored over the years as inhibitors of the conversion of testosterone to DHT by 5AR.[31] Currently, finasteride and dutasteride are the only 4-azasteroids approved for BPH treatment (**Figure 27**). However, as described in the previous chapter, several drug-related adverse effects were reported, namely comprising interferences in sexual function, which can significantly limit their use. Additionally, considering the risk of interactions with other drugs and several contraindications, there is still a need to develop more potent and selective drugs for this purpose.[461]

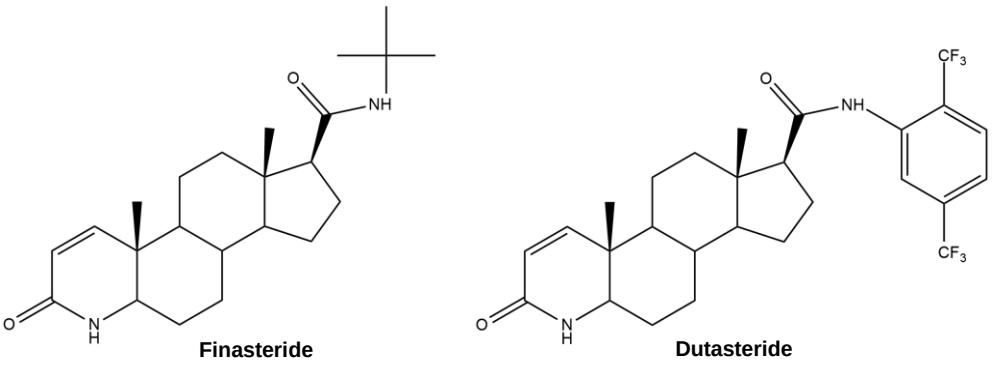

Figure 27. 5α-Reductase inhibitors (5ARIs) approved for clinical use in the treatment of benign prostatic hyperplasia (BPH). Created with ChemDraw.

5ARIs have also been evaluated for their potential use as chemopreventive and therapeutic agents against PCa since that all isoforms of this enzyme are present in PCa tissues at increased levels. For example, a research study reported the synthesis of 4-azasteroidal purine nucleoside analogs and their evaluation as antitumor agents in MCF-7 and PC-3 cell lines, and some of these compounds exhibited potent antiproliferative effects against PCa cells.[462–464] In the context of anticancer agents, within the natural,

semisynthetic, and synthetic steroidal derivatives with high antitumor interest, several examples can be highlighted.[31,465] For example, some 17(*E*)-picolinylidene androstanes were described as potential inhibitors of prostatic and breast cancer cell growth. Interestingly, their antiproliferative activity against PC-3 cells was correlated with the antiproliferative effect observed with abiraterone and the predicted CYP17A1 binding affinities.[460] Among other explored chemical modifications, the insertion of a 16-arylidene group into the steroid structure is also associated with significant cytotoxic effects in several cell lines, being considered a relevant pharmacophore for anticancer activity.[329,335,340,348] On the other hand, pregnane derivatives have also emerged as potential antitumoral agents, with very promising observed results being.[298,310,318,347,357,371,382] Considering this, Banday and colleagues reported the synthesis of novel benzylidene pregnenolone derivatives and their antiproliferative effects against a panel of human cancer cell lines. This research allowed the discovery of very potent compounds, especially against HCT-15 and MCF-7 cells.[382] Consequently, all these facts support the association between the introduction of an arylidene group at C-16 (androstanes) or C-21 (pregnanes) positions of steroid skeleton with important cytotoxic effects in several cell lines, being considered a relevant pharmacophore for anticancer activity.[316,329,335,339,340,348]

Bearing in mind all these facts, the general aim of my dissertation project for the obtention of the Master's degree in Medicinal Chemistry was the preparation of new 4-azasteroidal derivatives starting from testosterone and progesterone, modified at C-16 and C-21 with aromatic and heteroaromatic rings and the evaluation of their effects on different cell lines. In addition, their mode of interaction with estrogen receptor α (ERα), AR, CYP17A1, and 5BR was also studied by *in silico* molecular docking.[326,466] Considering the interesting data obtained from the dissertation project, it was decided to continue and carry out further studies. Therefore, the new results obtained are presented in this section, comprising cell proliferation effects in the PC-3 cell line, characterization of the cytotoxic effect of the most potent steroidal derivatives, and molecular docking simulations with 5AR, whose three-dimensional structure was recently unveiled.[467] In addition, 3D-QSAR studies were also performed to clarify the relationship between the structure of these 4-azasteroid derivatives and precursors with their effects on the proliferation of LNCaP and PC-3 cells, androgen-dependent and independent prostatic cancer cell lines, respectively.

2.1.2. Results and discussion

2.1.2.1. *In vitro* biological studies

2.1.2.1.1. Screening of cell proliferation effects

The effects of previously synthesized azasteroids **VB 4a-g** and **VB 7a-g**, and synthetic precursors and intermediates (testosterone, progesterone, **VB 1**, **VB 2**, **VB 3**, **VB 5**, and **VB 6**) on the proliferation of PC-3 cells were examined by the MTT proliferation colorimetric assay. These compounds were prepared (**Figure 28**) in the context of Master's dissertation, and their effects were firstly evaluated against other cell lines (LNCaP, T47-D, and NHDF).[326,466] In the context of the present thesis, the PC-3 cell line was used as a model of androgen-independent PCa to further assess the selective cytotoxicity of these steroids. Due to the structural similarities between the prepared azasteroidal derivatives and finasteride, this drug was also included in this study, as well as testosterone, progesterone, and DHT, allowing the comparison of the effect on cell proliferation with the novel compounds. Furthermore, 5-fluorouracil (5-FU), clinically used as an antitumor agent, was also included in the assay as a positive control.

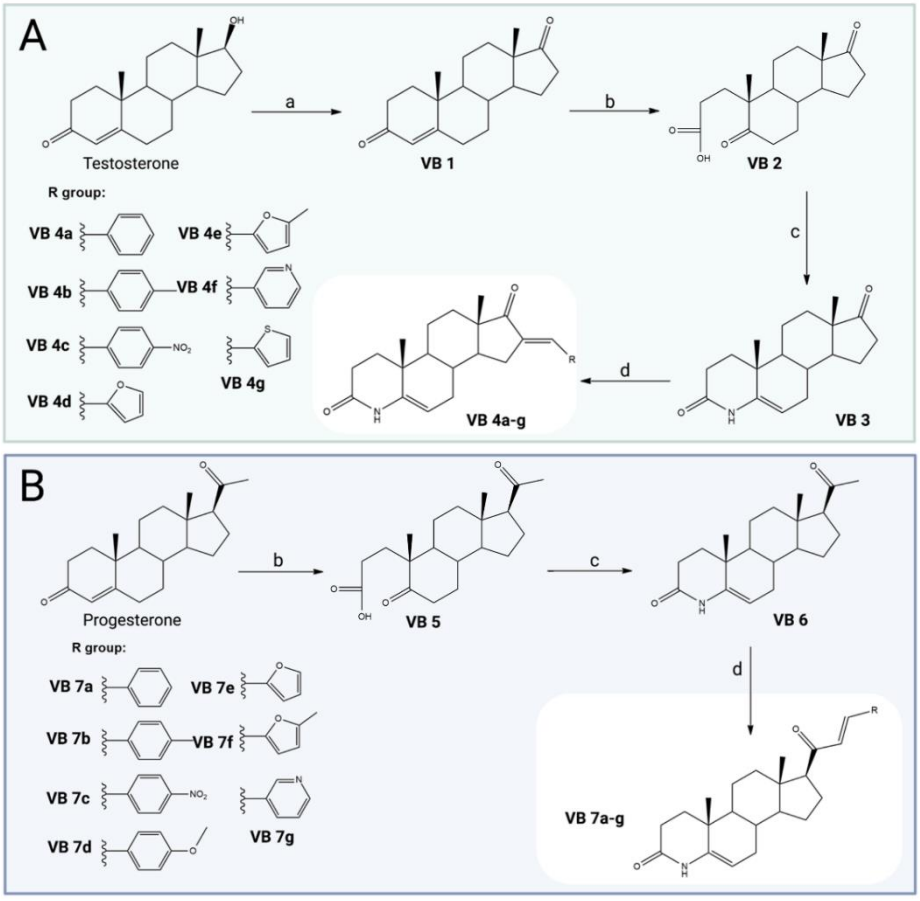

Figure 28. Preparation of novel 4-azasteroids from testosterone (**A**) and progesterone (**B**), and respective R group. Reactional conditions: **a**) PCC, DCM, r.t., 3 h; **b**) $NaIO_4$, $KMnO_4$, Na_2CO_3, *i*-PrOH, reflux, 3 h; **c**) ammonium acetate, GAA, reflux, 4 h; **d**) KOH, aldehyde, EtOH, r.t., 12-24 h.[326,466] (PCC= Pyridinium chlorochromate, DCM= Dichloromethane, GAA= Glacial acetic acid). Created with ChemDraw and BioRender.com.

Primarily, PC-3 cells were exposed to all compounds at 30 μM, during 72 h, in a screening assay, similarly which was performed by other authors [326,468–470]. Following this preliminary evaluation, concentration-response studies were performed for the most antiproliferative prepared compounds (% cell proliferation < 50) and 5-FU, and the half-maximal inhibitory concentration (IC_{50}) of the selected compounds were determined. Screening results are shown in **Figure 29** and the determined IC_{50} values are shown in **Table 10**. The IC_{50} was calculated for compounds **VB 4a**, **VB 7a, VB 7b, VB 7c** and **VB 7g**. Interestingly, steroids **VB 7c** and **VB 7g** showed to be the most potent compounds in PC-3 cells, presenting very close values, 3.29 and 3.64 μM, respectively. Considering these results, compounds **VB 7c** and **VB 7g** appeared to be promising candidates for more advanced studies.

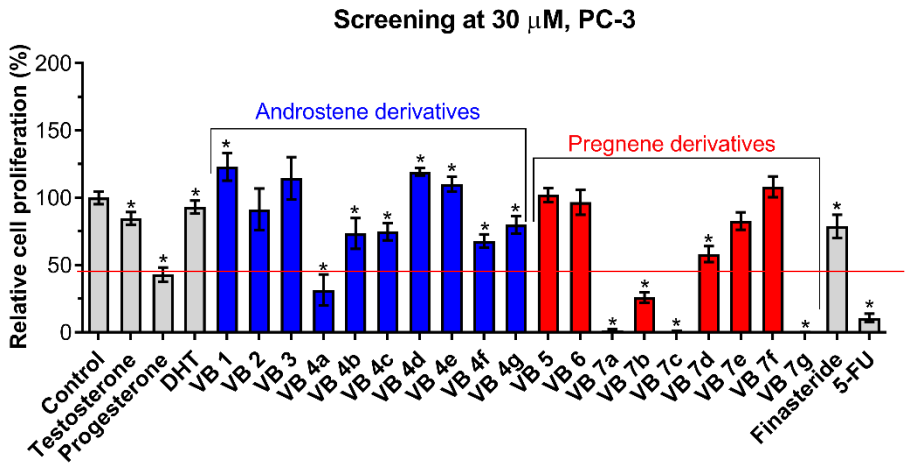

Figure 29. Screening MTT screening results. Relative cell proliferation of PC-3 cells exposed to the compounds previously synthesized, substrates, DHT, finasteride, and 5-FU for 72 h at a concentration of 30 μM. The cell proliferation was determined by the MTT assay, spectrophotometrically quantifying formazan at 570 nm. Data are expressed as a percentage of cell proliferation in comparison with the negative control and are indicated as mean±SD and are representative of at least two independent experiments. *$p< 0.05$ *vs* the control (the Student *t*-test). (DHT= 5α-Dihydrotestosterone, 5-FU= 5-Fluorouracil).

Table 10. Estimated IC_{50} values for various compounds in PC-3 cell line. [a]

Compound	PC-3		Compound	PC-3	
	IC_{50}	r^2		IC_{50}	r^2
VB 4a	22.63	0.98	**VB 7g**	3.64	0.98
VB 7a	12.60	0.96	**Finasteride**	>100	-
VB 7b	25.94	0.98	**5-FU**	2.30	0.96
VB 7c	3.29	0.99			

[a] The cells were treated at various concentrations (0.01, 0.1, 1, 10, 50, and 100 μM) for 72 h. and the IC_{50} values were calculated by sigmoidal fitting. The data shown are representative of at least two independent experiments. The coefficient of determination (r^2) is indicative of how closely the sigmoidal curve generated can be fitted with nonlinear regression statistics for the cell lines and incubation periods tested.

However, to proceed to further studies, a general analysis considering the MTT results on all cell lines was required (**Appendix 1**, **Tables Ap 1** and **Ap 2**). Overall, from this analysis, and despite the relevant results observed in PC3 cells, it was concluded that steroid **VB 7g** showed to be the most potent on T47-D cell line (IC_{50}= 1.33 μM). This cell line, obtained from human breast carcinoma, is hormone-dependent, being sensitive/responsive to estrogen via ERα.[471] Consequently, more advanced studies to characterize the effect of **VB 7g** on T47-D cells were performed.

2.1.2.1.2. Characterization of the cytotoxic effect

In a previous study in the context of the Master's dissertation, the 21*E*-pyridinyl derivative, **VB 7g**, showed to be the most potent of the evaluated azasteroids on T47-D cells, presenting a determined IC_{50}=1.33 μM.[466] In order to evaluate the cytotoxic effect when these cells are exposed to this compound, it was performed a fluorescence microscopy study after Hoechst 33342 – a nucleus marker – propidium iodide (PI) – a cell death marker – staining. For this, after 24, 48, and 72 h of treatment with **VB 7g** at 20 μM, cells were observed through optical microscopy and then stained for fluorescence microscopy observation. The photographs obtained are shown in **Figure 30** and it can be verified that those cells exposed to **VB 7g** seem to have a higher PI staining than positive and negative controls. On the other hand, it is possible to observe several morphological modifications over time when cells are exposed to **VB 7g** and also to 5-FU, being these alterations more drastic when cells are treated with the azasteroid. These modifications are mainly characterized by the roundness of cells and by the decrease of the cell area and volume. In addition, the ratio of PI/Hoechst 33342 staining is presented in **Figure 31**. Untreated cells are considered the negative control of the experiment, while 5-FU was used as the positive control. Interestingly, cells treated with **VB 7g** showed a significant increase of the PI/Hoechst 33342 staining ratio at 24, 48, and 72 h (**Figure 31**). The positive control, 5-FU, led to a significant increase only after 72 h of incubation. These results indicate that cells incubated with **VB 7g** since an early time of treatment are losing viability and are significantly dying when compared to negative and positive controls.

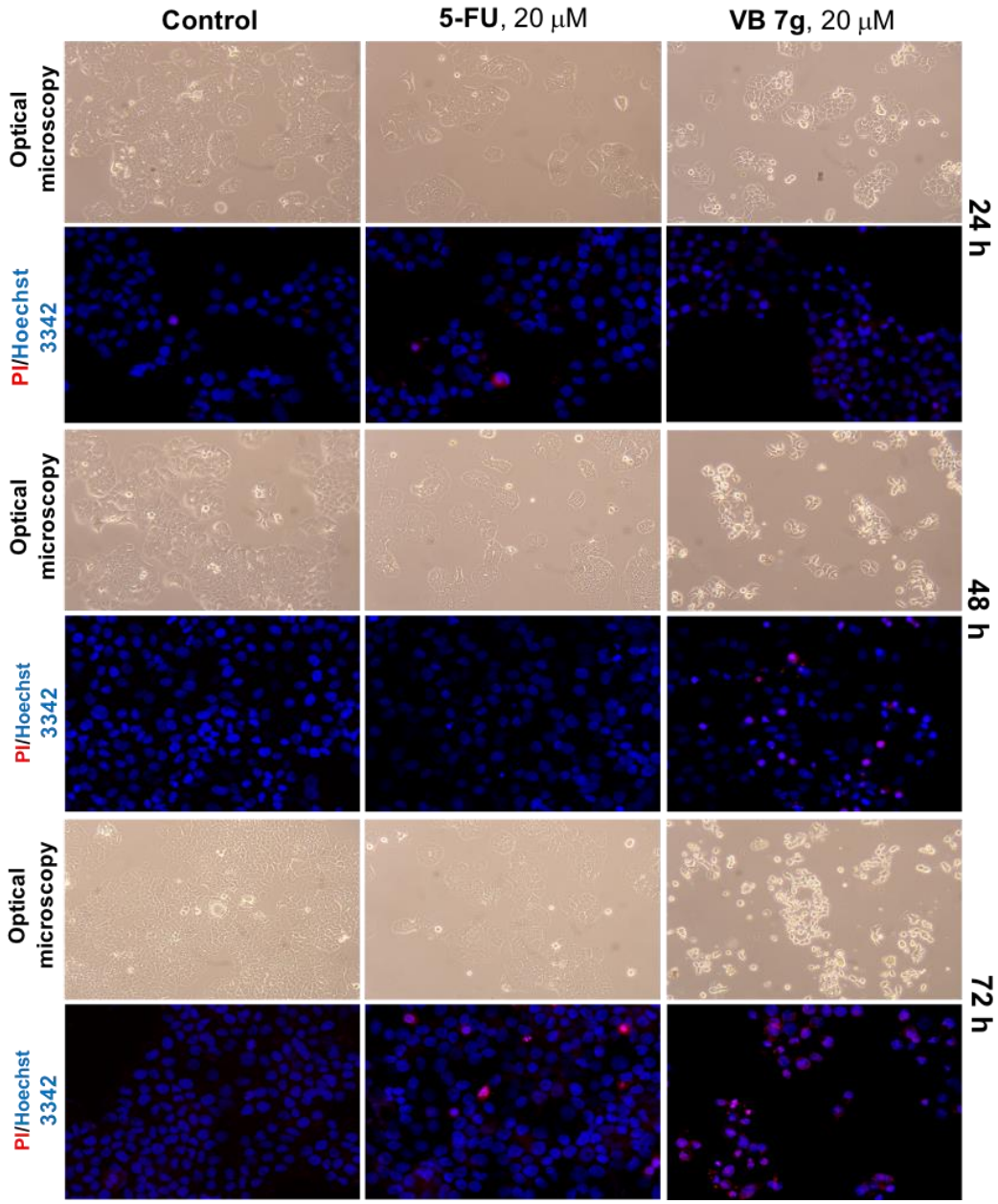

Figure 30. PI/Hoechst 33342 staining results. T47-D cells were incubated for 24, 48, and 72 h with 5-FU and **VB 7g** at 20 μM. Untreated cells are considered the control of the experiment. Cells were visualized in an Optical microscope Olympus CKX41 coupled to a digital camera (Olympus SP-500UZ) and in an Axio Imager A1 microscope (fluorescence). The resulting images were treated in ImageJ software. (PI= Propidium iodide, 5-FU= 5-Fluorouracil).

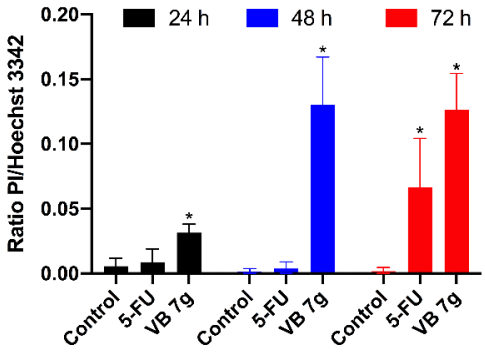

Figure 31. Ratio of PI/Hoechst 33342 staining results. T47-D cells were incubated during 24, 48, and 72 h with 5-FU and **VB 7g** at 20 µM. Untreated cells are considered the control of the experiment. Cells were visualized in an Axio Imager A1 microscope and the resulting images were treated in ImageJ. Data are representative of at least two experiments. *p< 0.05 compared to control. (PI= Propidium iodide, 5-FU= 5-Fluorouracil).

Moreover, to quantify the morphological changes in cell nuclei after **VB 7g** incubation, nuclei were stained with Hoechst 33342 and the nuclear morphology was assessed with ImageJ software (**Figure 32-A**). In this context, the **VB 7g**-incubated cultures showed a significant decrease in the nuclear area after all incubation periods. The decrease in cell nuclei due to DNA loss is an indicator of apoptosis and this correlation was evidenced by Eidet et al..[472] In **Figure 32-B**, the results of nearest neighbor analysis (NND) of T47-D cells when treated with the testing compound is shown. The NND is measured to assess the cell nuclei distribution and is defined as the distance between the centroid of each nucleus and its closest one. This analysis was employed to evaluate if the treatment (5-FU and **VB 7g**) caused changes in cell distribution. Interestingly, cells treated during 48 and 72 h with 5-FU and **VB 7g** showed to have different distances, which means a more aleatory cellular placement. The literature points out that these results are in agreement with the occurrence of apoptosis, which seems to cause a more unequal cell spacing.[472]

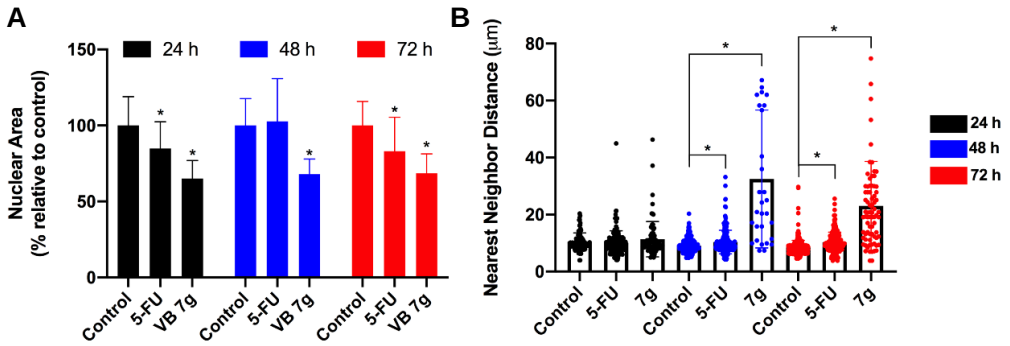

Figure 32. (**A**) T47-D nuclear area of cells untreated (control) and cells treated with 5-fluorouracil (5-FU) and **VB 7g** at 20 µM, incubated 24, 48, and 72 h; (**B**) Nearest neighbor analysis of T47-D cells with the same conditions referred previously. Data are indicated as mean±SD and are representative at least two independent experiments. *p< 0.05 compared to control.

Lastly, in **Figure 33**, nuclei with a morphology coincident with the observed in apoptotic cells are indicated with red arrows, presenting a circular and pyknotic form. To explore the possible mechanism of apoptotic death in T47-D cells, the caspase-9 activity was measured using a Caspase-Glo kit from Promega, looking for evidence of caspase-dependent apoptosis. It is known that caspase-9 has an important role in the intrinsic or mitochondrial pathway of apoptosis death mechanism.[473] In this experiment, cells were exposed for 48 h to DOX at 10 μM, as the positive control, and to **VB 7g** at 10 and 20 μM, and the results obtained are shown in **Figure 34**. After 48 h of treatment, significant elevation in caspase-9 activity was observed in cells treated with DOX and with both concentrations of **VB 7g**, which is relevant evidence that this compound triggers the apoptotic mechanism of cell death.

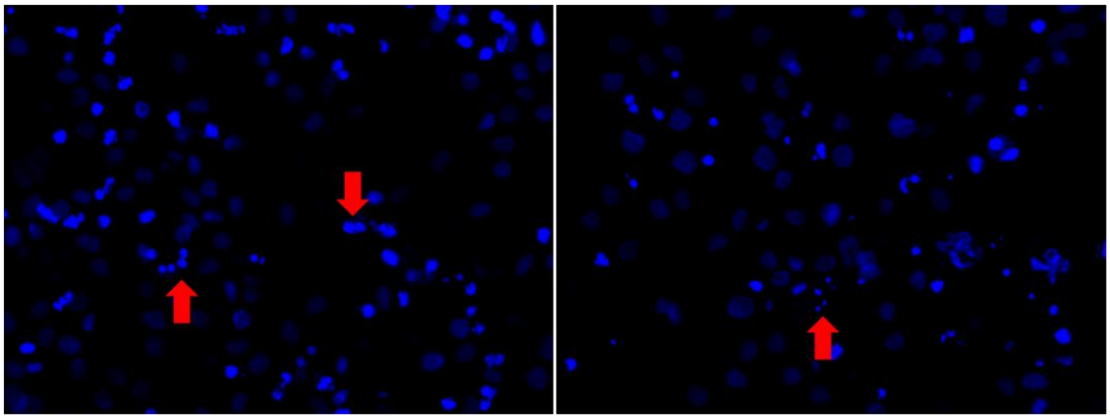

Figure 33. T47-D cells stained with Hoechst 33342, after treatment with **VB 7g** during 72 h. Pyknotic cells with circular morphology are indicative of apoptosis.

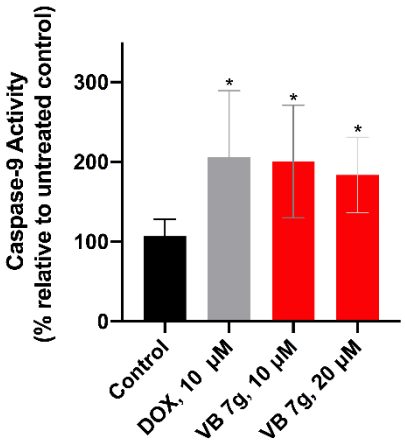

Figure 34. T47D caspase-9 activity results. Cells were treated for 48 h with doxorubicin (DOX) at 10 μM, as the positive control, and **VB 7g** at 10 and 20 μM, and the results are relative to untreated cells (control). The activity of caspase–9 was evaluated using a Caspase-Glo kit from Promega. Data are indicated as mean±SD and are representative at least two independent experiments. *p< 0.05 compared to control.

2.1.2.2. *In silico* studies

2.1.2.2.1. Molecular docking studies

An *in silico* study was performed using molecular docking simulations with vina executable. The principal aim was to assess the affinity and the existence of potential interactions between these new compounds and 5AR type 2, complementing the studies with other steroidal targets already performed in the context of the Master's dissertation (**Appendix 1, Table Ap 3**). Moreover, the assessment of 5AR inhibitory activity was an important propose of the dissertation. Therefore, the docking simulations were executed for each 4-azasteroidal derivatives **VB 4a-g** and **VB 7a-g** against 5AR type 2. Three-dimensional structural coordinates of this enzyme were obtained from the protein data bank (PDB) and molecular docking was performed using the program AutoDockTools. To validate the docking method, simulations were carried out between crystallized ligand/drugs with the respective macromolecule and the control re-docking simulation was able to reproduce the ligand-enzyme interaction geometries presented in the respective crystal structure with a root-mean-square distance (RMSD)≤ 2.0 Å (**Appendix 2, Table Ap 4**). The value of RMSD obtained from the re-docking simulation between finasteride (co-crystallized ligand) and 5AR type 2 was 0.78 Å, complying with the requirement for the method validation. Based on the control docking simulation (with finasteride), predicted binding energies < –11.90 kcal.mol^{-1} were considered to be significant.

The results of docking simulations can be seen in **Table 11**. As can be observed, potential strong binding energies for almost all compounds for the active site of 5AR type 2 were predicted. In addition, androstene derivatives (**VB 4a-g**) seemed to have higher affinity than pregnene derivatives (**VB 7a-g**). Therefore, these results showed that there is the possibility that these steroids can potentially interact with the 5AR type 2 and possibly act as 5ARIs, which can be explained by the fact these are 4-azasteroids. Moreover, the results revealed that all novel derivatives have affinity energy values similar to the finasteride, the control. The principal interactions between the macromolecules and the best-scored derivatives in molecular docking simulations were also analyzed. Through the analysis of these interactions, it is possible to conclude that the amide group in A-ring can be essential in establishing polar interactions with the different amino acids of studied proteins. Additionally, in **Chapter IV**, these interactions will be further explored in the context of experimentally determined 5AR inhibition.

Table 11. Predicted binding energies of previously prepared 4-azasteroids (**VB 4a-g** and **VB 7a-g**) calculated from molecular docking against 5α-reductase (5AR) type 2. The binding energy of ligand, finasteride (in yellow), present in the X-ray crystal structure was calculated by re-docking.

Compound	5AR type 2 *Autodock binding energy (kcal.mol^{-1})*	Compound	5AR type 2 *Autodock binding energy (kcal.mol^{-1})*
Finasteride	−11.9	**VB 7a**	−11.8
VB 4a	−12.9	**VB 7b**	−12.0
VB 4b	−13.2	**VB 7c**	−11.7
VB 4c	−12.7	**VB 7d**	−11.6
VB 4d	−12.2	**VB 7e**	−11.1
VB 4e	−12.3	**VB 7f**	−11.2
VB 4f	−12.7	**VB 7g**	−11.7
VB 4g	−12.1		

2.1.2.2.2. 3D-QSAR analysis

To better understand the relationship between the structure/properties of these steroidal derivatives and their effect on LNCaP and PC-3 cells proliferation, a three-dimensional quantitative structure-activity relationship (3D-QSAR) model was built using the open-source software Open3DQSAR.[474] This method is frequently used as a tool to clarify and eventually predict biological activities of new molecules, as an optimizer of existing lead compounds, or simply to help the analysis of structure-activity relationship data.[409,475,476] Mainly, this ligand-based approach is usually applied using results from enzymatic assays. However, some authors have also successfully applied it to results achieved in cell proliferation studies.[477,478] The present 3D-QSAR model was built using a set of steroidal molecules: testosterone, progesterone, DHT, **VB 1-3**, **VB 4a-g**, **VB 5-6**, **VB 7a-g**, and finasteride, being formed a training dataset of 16 compounds and a test dataset of 6 derivatives. The respective biological data reported previously by us relative to the cell proliferation (%) of LNCaP and PC-3 cells treated with 30 μM of compounds was also added to the input file (**Table 12**).[326,466]

Table 12. Biological data/input for three-dimensional quantitative structure-activity relationship (3D-QSAR) study: relative cell proliferation (%) of LNCaP and PC-3 cells incubated with compounds synthesized, precursors, 5α-dihydrotestosterone (DHT), and finasteride, during 72 h of exposition at 30 μM. [a]

Compound	LNCaP	PC-3	Compound	LNCaP	PC-3
Testosterone	117.5±19.8	84.7±4.7	**VB 4g**	54.3±6.7	79.9±6.4
Progesterone	64.3±9.1	42.9±5.4	**VB 5**	96.4±13.6	102.1±5.2
DHT	141.2±12.0	93.1±4.9	**VB 6**	58.3±18.3	96.7±9.3
VB 1	98.3±6.5	123.1±10.3	**VB 7a**	6.5±5.3	1.4±1.0
VB 2	129.9±22.0	91.4±15.6	**VB 7b**	62.7±8.9	25.9±3.8
VB 3	99.2±15.9	114.6±15.7	**VB 7c**	5.2±0.6	0.7±0.4
VB 4a	49.9±10.6	31.5±11.6	**VB 7d**	88.0±15.5	58.2±5.9
VB 4b	26.1±10.6	73.5±11.5	**VB 7e**	85.3±6.7	82.7±6.5
VB 4c	19.3±12.9	74.8±6.3	**VB 7f**	88.9±17.7	108.1±7.8
VB 4d	90.9±4.9	119.4±2.8	**VB 7g**	0.7±0.1	0.1±0.1
VB 4e	60.8±6.6	110.2±5.4	**Finasteride**	88.5±2.4	78.8±8.7
VB 4f	66.9±12.2	67.9±5.0			

[a] The results are express as mean±SD and are representative of at least two independent experiments.

The present study was accomplished based on the described firstly by Emmerich and coworkers, and posteriorly by Catarro et al., applying the modifications required.[478,479] Initially, the step and overall size influence of the grid box was established to be 0.5 and 5.0 Å respectively, leading to the best results of training and test sets r^2 as well as to the internal cross-validation q^2 (data not shown). Moreover, the best method for internal cross-validation, comparing the leave-one-out (LOO) and leave-many-out (LMO) approaches were settled. Simultaneously, the best method to use the experimental data input, using percentages of relative cell proliferation, was also selected. From these analyzes, the LOO method and the use of relative cell proliferation led to the best results for correlation between the experimental results and the predicted ones by the constructed method (**Figure 35**, **Table 13**). Considering these premises and although the biological data are related to cells proliferation and not to specific targets, robust 3D-QSAR models were obtained. In case of LNCaP cells, the built model presented a high r^2 of 0.98 and a q^2 for the LOO of 0.96, a value relatively close to obtained for the test set (r^2= 0.86) (**Table 13**). On the other hand, considering PC-3 cells, the final model exhibited a r^2 of 0.96 and a q^2 for the LOO of 0.75, which is also a close value to the r^2 obtained for the test set (r^2= 0.81) (**Table 13**). In conclusion, these two models not only showed to possess a relatively high predictive capacity, but also showed a relative high prediction precision.

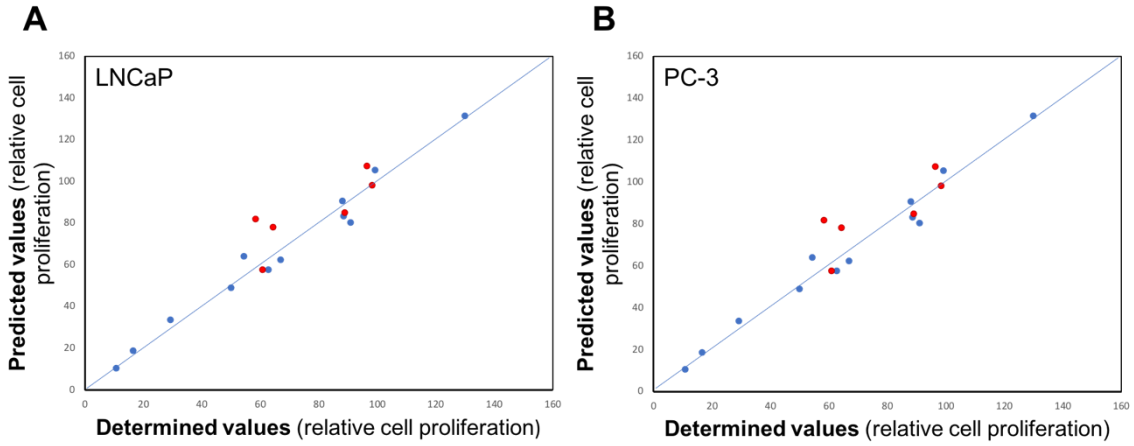

Figure 35. Predicted *vs.* determined values of relative cell proliferation of LNCaP (**A**) and PC-3 (**B**) cells for training set (**blue**) and test set compounds (**red**).

Table 13. Statistical parameters of final three-dimensional quantitative structure-activity relationship (3D-QSAR) models for percentage of cell (LNCaP and PC-3) proliferation and respective logarithms methods of input data. [a]

LNCaP				PC-3			
Group	**Method**	**Parameter**	**Value**	**Group**	**Method**	**Parameter**	**Value**
Train (N=17)	Percentage of proliferation	**q^2_{LOO}**	0.96	**Train** (N=17)	Percentage of proliferation	**q^2_{LOO}**	0.75
		$SDEP_{LOO}$	8.23			$SDEP_{LOO}$	22.48
		q^2_{LMO}	0.32			q^2_{LMO}	0.32
		$SDEP_{LMO}$	4.23			$SDEP_{LMO}$	4.23
		r^2	0.98			r^2	0.96
		SDEC	5.42			SDEC	7.41
Test (N=6)	Percentage of proliferation	r^2	0.86	**Test** (N=6)	Percentage of proliferation	r^2	0.81
		SDEP	19.61			SDEP	24.86

[a] SDEP=Standard deviation error in prediction, SDEC= Standard deviation error in calculation, LOO= Leave-one-out, LMO= Leave-many-out.

The model based on % of LNCaP cell proliferation after exposure to compounds at 30 μM during 72 h revealed that, at a steric level, the position of bulky groups of 16*E*-4-aza-androstrene derivatives is ideal, favoring the decrease of the cell proliferation (**Figure 36-A** - yellow). However, the position of aromatic ring substituent of bulky groups on the 21*E*-4-azapregnene derivatives is less favorable concerning the pretended reduction of cell proliferation (**Figure 36-A** - green). In addition, with respect to the electrostatic effects, partial positively charged groups seemed to be beneficial in the region of the double bond on the B-ring, and in the region of the aromatic ring attached to the D-ring of 16*E*-4-aza-androstrene derivatives (**Figure 36-B** - **blue**). The partial negative charges observed, especially in the region of aromatic ring attached to the D-ring of 21*E*-4-azapregnene derivatives, are also favored (**Figure 36-B** - **red**).

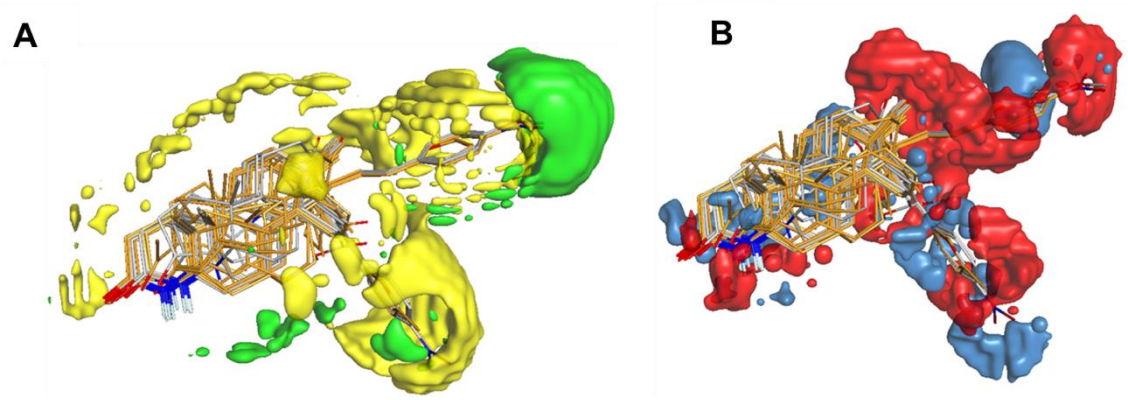

Figure 36. PLS coefficient contour maps of the 3D-QSAR model with all superposed compounds (LNCaP). **(A)** Steric effects. **Green** (0.0015): bulky groups are prohibited, **yellow** (−0.003): bulky groups are favored. **(B)** Electrostatic potential. **Blue** (0.001): groups with positive partial charges are favored, **red** (−0.001): groups with negative partial charges are favored. (Favored= favors a decrease in cell proliferation). (PLS= Partial least squares, 3D-QSAR= Three-dimensional quantitative structure-activity relationship).

Concerning the model based on % of PC-3 cell proliferation after exposure to compounds at 30 μM for 72 h, the analysis of the obtained results was more difficult, since the images obtained are quite ambiguous. From this analysis, relative to the steric effects, it seems that the position of bulky groups on the D-ring is, in general, favorable, principally when aromatic rings attached to the D-ring are *p*-substituted (**Figure 37-A** - yellow). Regarding the electrostatic effects, partial positively charged groups seemed to be often beneficial in the region of the aromatic ring attached to the D-ring, mainly in the case of pregnene derivatives (**Figure 37-B** - **blue**). The partial negative charges observed are especially favored in the case of androstene derivatives (**Figure 37-B** - **red**).

The results suggested that the antiproliferative activity against both cell lines seems to be mainly depending on bulkiness nature of arylidene groups. In accordance with these results, prior to the future design and preparation of novel steroidal analogs with potential antiproliferative activity against prostatic tumoral cells, their 3D structure must be taken in consideration. Indeed, the 3D-QSAR models, based on empirical data, are capable of simulate the experimental results robustly, constituting a valuable tool as a guide in the rational drug design. Nevertheless, it is important to be awareness that these studies use structures with minimized energies that cannot be exactly the biologically *in vitro* active conformation.

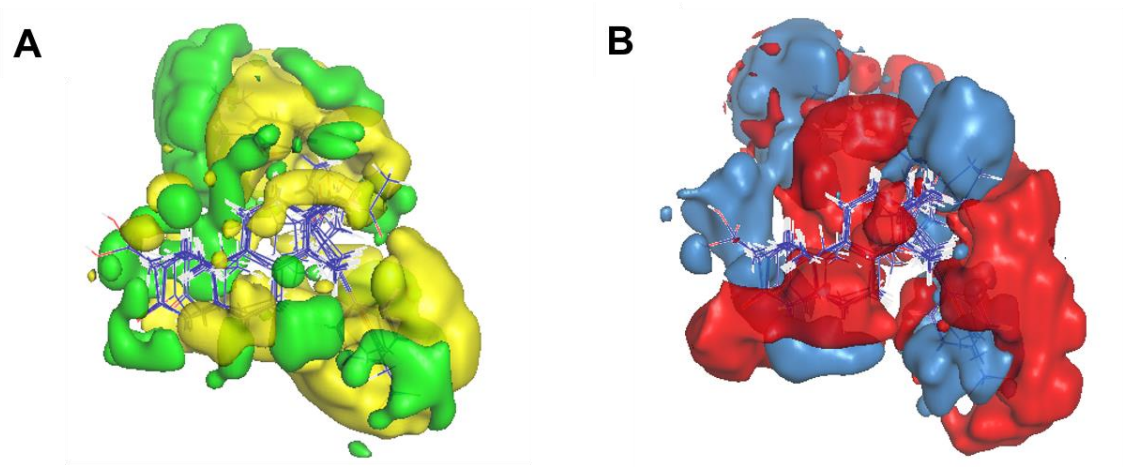

Figure 37. PLS coefficient contour maps of the 3D-QSAR model with all superposed compounds (PC-3). **(A)** Steric effects. **Green** (0.0015): bulky groups are prohibited, **yellow** (−0.003): bulky groups are favored. **(B)** Electrostatic potential. **Blue** (0.001): groups with positive partial charges are favored, **red** (−0.001): groups with negative partial charges are favored. (Favored= favors a decrease in cell proliferation). (PLS= Partial least squares, 3D-QSAR= Three-dimensional quantitative structure-activity relationship).

2.1.3. Experimental section

2.1.3.1. General remarks

Finasterida Tetrafarma 5 mg was purchased from *Tetrafarma e Produtos Farmacêuticos, Lda*, Portugal, and finasteride was extracted from the tablets.[480] The NMR spectra acquired showed that this compound was extracted with high purity. All tested compounds were synthesized and characterized according the previous work reported by our group, during the development of the project for obtention of the Master's degree.[326,466]

2.1.3.2. Biological studies

2.1.3.2.1. Cell culture

PC-3 and T47-D cells were obtained from American Type Culture Collection (ATCC, Manassas, VA, USA) and were cultured in 75 cm^2 culture flasks at 37 ºC in a humidified air incubator with 5 % CO_2. PC-3 and T47-D cells, which were used in passages 25^{th} to 28^{th} and 10^{th} to 15^{th}, respectively, were cultured in RPMI 1640 medium (Sigma–Aldrich, Inc., St. Louis, MO, USA) with 10 % fetal bovine serum (Sigma – Aldrich, Inc.) and 1 % of the antibiotic mixture of 10,000 U/mL penicillin G and 100 mg/mL of streptomycin (Sp, Sigma–Aldrich, Inc.). The medium was renewed every 2–3 days until cells reach nearly the confluence state. When cells reach approximately 90 to 95 % confluence, they were detached gently by trypsinization (trypsin–EDTA solution, 0.125 g/L of trypsin and 0.02 g/L of EDTA). Before each experiment, viable cells were counted, in a Neubauer

chamber by a trypan blue exclusion assay and adequately diluted in the appropriate complete cell culture medium.

2.1.3.2.2. MTT cell proliferation assay

All the stock solutions were previously prepared by dissolving compounds in dimethyl sulfoxide (DMSO; Sigma–Aldrich, Inc.) at 10 mM and stored at 4 °C. From these solutions, the several diluted compounds solutions in different concentrations were freshly prepared in a complete culture medium before each experiment. The maximum DMSO concentration in final solutions (<1 %) does not interfere with the cell viability (data not shown). After reaching a near confluence state, PC-3 cells were trypsinized and counted by the trypan blue exclusion assay, and then 100 µL of cell suspension/well with an initial density of 2×10^4 cells/mL were seeded in 96-well culture plates (Nunc, Apogent, Denmark) and left to adhere for 48 h. After cells adherence, the medium was replaced by several solutions of the compounds in the study (30 µM for preliminary studies and 0.01, 0.1, 1, 10, 50, and 100 µM for concentration-response studies) in the appropriate medium for approximately 72 h. 5-FU and finasteride were used as positive controls and untreated cells were used as the negative control. Each experiment was performed in quadruplicate and independently performed at least two times. The in vitro antiproliferative effects were evaluated by the MTT assay (Sigma–Aldrich, Inc.). For this, after the incubation period, the medium was removed and 100 µL of phosphate buffer saline (NaCl 137 mM; KCl 2.7 mM, Na_2HPO_4 10 mM, and KH_2PO_4 1.8 mM in deionized water and pH adjusted to 7.4) were used to wash the cells. Then, 100 µL of the MTT solution (5 mg/mL) was prepared in the appropriate serum-free medium and was added to each well, followed by incubation for 4 h at 37 °C. Thereafter, the MTT containing medium was removed and the formazan crystals were dissolved in DMSO. Then the absorbance was measured at 570 nm using a microplate spectrophotometer BIO-RAD xMarkTM. Cell viability values were expressed as percentages relative to the absorbance determined in the cells used as negative controls.

2.1.3.2.3. Fluorescence microscopy

To access the effects of compound **VB 7g** in T47-D cells, fluorescence microscopy assays with Hoechst 33342 (Thermo Fisher Scientific, Inc., Walthman, MA, USA) and PI (Sigma–Aldrich, Inc.) staining were performed. T47-D cells were seeded at 2×10^4 cells/mL in a 24-well culture plate containing circular coverslips of 10 mm diameter, in a complete culture medium. After 48 h, cells were incubated during 24, 48, and 72 h, with 5-FU at 20 µM, as the positive control, compound **VB 7g** at 20 µM, and untreated cells were used as a negative control. Ended the incubation period, cells were observed

in an optical microscope Olympus CKX41 (Olympus, Tokyo, Japan) coupled to a digital camera (Olympus SP-500UZ). Then, cells were incubated with 20 μL/per well of a solution of PI (1 mg/mL) in PBS for 25 min at 37 °C, in the dark. The medium was removed, and the cells were fixed with formalin 4 % at r.t. for 15 min. Cells were washed three times with PBS and then they were incubated with 30 μL/per coverslip of Hoechst 33342 (1:500) for 10 min. After incubation, cells were washed three times with PBS. Coverslips were mounted on a drop of Dako fluorescence mounting medium (Agilent Technologies, Santa Clara, CA, USA) on a microscope slide and visualized in a Zeiss Axio Imager A1 microscope (Carl Zeiss, Göttingen, Germany) with the 40 × objective.

2.1.3.2.4. Cell nuclear morphology and distribution analysis using ImageJ

The nuclear measurements were achieved by converting 16-bit photomicrographs of Hoechst 33342-stained nuclei, in different conditions, into 8-bit images and then these images were autothresholded to binary photos using the default method "Make binary" function of ImageJ (v. 1.49). Cell nuclei that are touching were separated and fragments were discarded based on the area through the "Analyze Particle" function. This function also provides several information pretended as nuclear area, circumference, and form factor [472]. In addition, the "Nearest Neighbor Distance" was determined. This function allows measuring the distance between each cell nucleus and the nearest ones.

2.1.3.2.5. Caspase-9 activity assay

The caspase-9 activity was evaluated using the Promega Caspase-Glo 9 assay (Promega, Madison, WI, USA). T47-D cells were seeded in a 96 multiwells plate at a density of 4×10^4 cells/mL. After 48 h, cells were treated with the positive control, DOX, at 10 μM and the cells were also treated with 10 and 20 μM of **VB 7g**, during 48 h. The assay was performed at the end of treatment, following the instructions provided by the manufacturer. Data are representative of at least two experiments.

2.1.3.2.6. Statistical analysis

The data are expressed as a mean±standard deviation (SD) and differences between groups were considered statistically significant when $p< 0.05$. The determination of IC_{50} was done by sigmoidal fitting analysis considering a 95 % confidence interval. All data shown are representative of at least two independent experiments.

2.1.3.3. *In silico* studies

2.1.3.3.1. Molecular docking

2.1.3.3.1.1. Preparation of protein and ligands

The three-dimensional structural coordinates for 5AR type 2 (5AR type 2 PDB ID: 7BW1) was obtained from Protein Data Bank (www.rcsb.org). The coordinates of the co-crystallized ligand and water molecules were deleted using the software Chimera (v. 1.10.1) and histidine charges were defined to match the physiologic environment, and the final structures were saved in PDB format. Then non-polar hydrogens were merged in AutoDockTools (v. 1.5.6) from The Scripps Research Institute.[481] Kollman and Gasteiger partial charges were added. Lastly, the prepared structures were converted from the PDB format to PDBQT for posterior utilization in the docking simulations. All ligands were constructed using Chem3D Pro software (v. 12.0, Cambridge ChemBioOffice 2010, Perkin Elmer). Energy minimization and geometry optimization (MMFF94 force field: 500 steps of conjugate gradient energy minimization followed by 500 steps of steepest descent energy minimization with a convergence setting of 10×10^{-7}) were performed with Avogadro (v. 1.0.1) and the final structures were saved as a PDB file format. Then, the ligands were completely prepared, choosing torsions and the structures were converted from PDB format to PDBQT, in AutoDockTools.

2.1.3.3.1.2. Grid map parameters

Autodock grid maps were calculated for each macromolecule using AutoGrid4, based on the active site coordinates of each protein crystal structure. The size of all grid boxes was 40×40×40 with 0.375 Å of spacing. Maps were calculated for each atom type in each ligand along with an electrostatic and desolvation map using a dielectric value of −0.1465.

2.1.3.3.1.3. Method validation and molecular docking simulations

Molecular docking simulations were conducted using the Lamarckian genetic algorithm and empirical free energy scoring function.[481] The maximum number of energy evaluations was 2,500,000 and the GA population size was 150. A total of 15 hybrid GA-LS runs were performed for each simulation. The results of molecular docking were visualized in the PyMol program (v. 1.3, The PyMol Molecular Graphics System, Schrödinger, LLC – www.pymol.org), built to educational use. All docking simulations performed to validate the method, using the ligands present in crystal structures, were able to reproduce the ligand-protein interaction geometries. For the docking process to

be considered successful, the RMSD value between ligand conformations (docked ligand and crystalized ligand) has to be less than 2.0 Å.

2.1.3.3.2. 3D-QSAR modeling

2.1.3.3.2.1. Biological data and molecular structures compilation

The data set for the 3D-QSAR analysis comprised 23 steroidal compounds described in our previously reported study and Master's dissertation, including synthetic precursors (testosterone and progesterone), synthetic intermediates, and finasteride.[326,466] 2D ligands were built with ChemBio Draw Ultra 12.0 and the energy of their 3D conformation was minimized in the MMFF94s force field with ChemBio 3D Pro v. 12.0. Then, the structures were compiled into an SDF file format with the BIOVIA Discovery Studio v. 16.1 software (Dassault Systems, Paris, France), and the experimental data relative to cell proliferation in the preliminary screening at 30 μM in the LNCaP and PC-3 cells were also added to this file.

2.1.3.3.2.2. Molecular alignment and calculation of field descriptors and PLS regression

Subsequent alignment of the 23 structures under study was performed in the Open3DALIGN software based on the structure of the compound with better results of cell proliferation percentage for each cell line, separately. After the alignment, molecular interactions fields (MIFs) regarding Van-der-Waals interactions (the steric field) and the electrostatic field were calculated by using a grid box around the molecules with a 0.5 Å step size and a 5.0 Å margin, in Open3DQSAR v. 2.x. Both MIFs were pretreated with max/min cutoff (level= ±30), zeroing (level= 0.05), standard deviation cutoff (level= 0.1), N-level variable elimination and block unscaled weighting (BUW), with 6 compounds randomly assigned to the test set. The PLS method was used to correlate the MIFs with the biological data and the model was further improved using the processes of smart region definition (SRD) to variables grouping, and the fractional factorial design (FFD) method to select a subset of variables whose impact on cross-validated q^2 is favorable. For the internal cross-validation were used the LMO and LOO methods. Finally, to assess the generated QSAR model quality, the test dataset was used to predict the percentage of cell proliferation. The PLS coefficient contour maps of the MIFs from the 3D-QSAR model were visualized using PyMol, with illustration of the different surfaces at blue, red, green and yellow, of electrostatic positive (0.001), electrostatic negative (–0.001), steric field positive (0.015) and steric field negative (–0.03), respectively.

CHAPTER III

3. Novel 16*E*-arylidene-5α,6α-epoxyepi-androsterone derivatives: synthesis, *in vitro* biological evaluation and *in silico* studies

3.1. Introduction

In the previous chapter, interesting results were described in relation to 4-aza-androstanes and -pregnanes. Thus, considering the aims of this doctoral project, the rational design, synthesis, purification and structural characterization, as well as biological evaluation of new series of functionalized azasteroidal arylidene derivatives were planned. In this context, the introduction of heterocyclic rings in these steroids to explore the known reactivity of the arylidene group was considered. Hence, a great number of attempts to synthesize novel 3-, 6-, and 4-azasteroidal derivatives, including with heterocycles fused or attached to the D-ring were accomplished (**Appendix 3**). However, despite the remarkable effort, these synthetic methodologies revealed to be unfeasible in the context of this doctoral project, and steroidal derivatives with the desired modifications were not successfully prepared. Thus, alternative approaches to synthesize novel steroids with potential interest in prostatic disorders were explored.

In this ambit, considering the importance of arylidenesteroids previous described in Introduction, and the proven mastery in the synthesis of these compounds, as well as the smooth reactional conditions associated with it, it was decided to modify 16*E*-arylidenedehydroepiandrosterone derivatives to obtain a new series of steroids.[323,326] Indeed, steroidal arylidene derivatives have been mainly reported as 17β-HSD type 1 inhibitors, as well as anti-inflammatory and antiproliferative agents.[315,338,349,351,366] Additionally, the most active arylidenesteroids usually comprise heteroatoms or halogens on their structures.[323] Within this group 16*E*-arylideneandrostane derivatives have been reported as potent anticancer agents, being potentially useful in the treatment of leukemia, breast and prostatic cancers and brain tumors.[338] This fact also contributed to choose an androstane, DHEA, as starting material at the present work.

On the other hand, epoxysteroids emerged as a class of steroids with interesting bioactivity. For example, 5α,6α-epoxycholesterol, an oxysterol, exhibits several

biological activities, including regulation of cell proliferation and cholesterol homeostasis.[482] Additionally, other epoxysteroids have been reported in the literature as potential neuroprotective agents, 5ARIs, and antiproliferative agents.[320,483–485] In this scope, Chávez-Riveros and coworkers reported the synthesis and identification of pregnenolone derivatives as inhibitors of isozymes of 5AR, that included an epoxysteroid, the 21(*p*-fluoro)benzoyloxy-5α,6α-epoxy-3β-hydroxypregn-16-en-20-one derivative, which presented an IC_{50} value against 5AR type 2 of 179 nM.[486] Moreover, Pérez-Ornelas et al. also described the synthesis and biological evaluation (*in vitro* and *in vivo* effects) of new potential steroidal 5ARIs. This study carried out with 5AR enzyme from hamster and human prostate showed that several steroidal compounds, including the 3β-acetoxy-5α,6α-epoxypregn-16-ene-20-one derivative, exhibited much higher 5AR inhibitory activity, as indicated by the IC_{50} values than the present by finasteride. In addition, the comparison of the weight of the hamster's prostatic gland indicated that the epoxysteroid had a comparable weight decrease as finasteride.[487] Considering these facts, the modification on different 16*E*-arylidenedehydroepiandrosterones consisted on the stereoselective epoxidation of $\Delta^{5,6}$, affording new 16*E*-arylidene-5α,6α-epoxyepiandrosterone derivatives.

The present chapter describes the synthesis and biological evaluation of novel 16*E*-arylidene-5α,6α-epoxyepiandrosterone derivatives. A battery of several exploratory *in vitro* assays was performed including MTT cell proliferation assay, immunocytochemistry assay with Ki67, fluorescence microscopy observation after PI staining, and analysis of cell nuclear morphology and distribution using ImageJ software, in order to verify the effects of these novel steroidal derivatives in cell proliferation. Furthermore, the possible interaction with the most important steroidal targets, in this context, was studied through molecular docking simulations.

3.2. Results and discussion

3.2.1. Chemical synthesis

The preparation of novel 16*E*-arylidene-5α,6α-epoxyepiandrosterone derivatives has been carried out as depicted in **Figure 38**. Firstly, the synthesis of 16*E*-arylidene-desydroepiandrosterone derivatives (**VB 8a-m**) was achieved through a crossed-aldol condensation, named as Claisen-Schmidt reaction, by mixing DHEA and different aromatic aldehydes in EtOH with an aqueous solution of KOH (50 %). After 2-24 h at room temperature the intermediate products were obtained in very good to excellent yields (71–95 %) – **Table 14**.[326] In proton NMR spectra, the presence of the peak relative to the vinylic proton is clear. Since this type of intermediates are already described in the

literature, a basic structural characterization (^{1}H NMR spectra acquisition and m.p. determination) was performed to confirm their successful preparation.[317,321,327,335,338,389]

Then, based on a procedure described by Carvalho et al., the new epoxysteroids were obtained from **VB 8a-m** by a stereoselective reaction with the peroxyacid magnesium monoperoxyphthalate (MMPP).[482] Overall, epoxidation of steroids with *trans-anti-trans* ring fusions generally leads to the formation of the α-epoxide. This fact can be explained by the preference of the attack by the reagent on the α-side of the steroid scaffold since the β-side is shielded by the two angular methyl groups at C-10 and C-13.[488] Despite the 5α,6α-epoxysteroids have generally been obtained by oxidation with the most common peroxyacid 3-chloroperoxybenzoic acid (*m*-CPBA), MMPP emerged as an advantageous alternative, considering its higher stability in the solid state and safety in handling. In addition, this peroxyacid can be produced and commercialized at a lower cost, and the respective work-up procedures are relatively easy due to its water solubility.[482,489–491] Moreover, MMPP is more selective than *m*-CPBA considering the obtention of α-epoxides, leading to significantly higher values of α/β epoxide ratios.[482,492] To improve this ratio in final products **VB 9a-m**, a recrystallization with methanol was performed and only very small amounts of the β-epoxide (< 2 %) could be detected in ^{1}H NMR spectra for some of these epoxysteroids. The duplication of peaks that allowed this conclusion are mainly relative to the signals of the methylene groups 18-CH_3 and 19-CH_3. In addition, the doublet relative to 6-CH is also distinct for the α- (≈ 3.1 ppm) and β-epoxides (≈ 2.9 ppm).

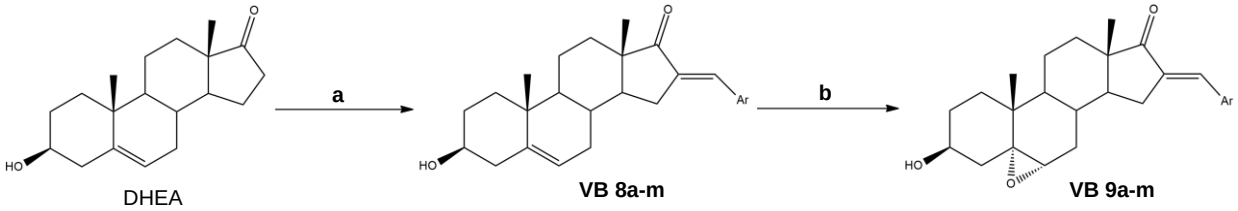

Figure 38. Synthetic route to prepare novel 16*E*-arylidene-5α,6α-epoxyepiandrosterone derivatives (**VB 9a-m**). Reagents and conditions: **a**) aldehyde, aq. sol. KOH 50 %, EtOH, r.t., 2-24 h; **b**) MMPP, DCM/water, 5 °C, 24-30 h. (MMPP= Magnesium monoperoxyphthalate, DCM= Dichloromethane). Created with ChemDraw.

In general, these novel 16*E*-arylidene-5α,6α-epoxyepiandrosterone derivatives (**VB 9a-m**) were synthesized in reasonable global yields (30–86 %) – **Table 14**. Interestingly, discrepant yields were achieved for these steroidal derivatives, suggesting different reactivity considering the substituent present at C-16 (aromatic group). Relative to structural characterization, with exception of epoxide **VB 9a,** steroidal epoxides **VB 9b-**

m are new synthetic molecules and respective high resolution mass spectra acquisition (HRMS) was mandatory, as well as IR and ^{13}C NMR spectra.[493] In proton spectra of these new molecules, it can be observed the presence of 6-CH peak at ≈2.9 ppm instead of ≈5.4 ppm (6-CH peak of substrate – **VB 8a-m**), proving the epoxide formation at this position. Moreover, peaks of carbon spectra and data acquired from mass spectra corroborates the 16*E*-arylidene-5α,6α-epoxyepiandrosterone derivatives formation.

Table 14. Corresponding Ar-CHO groups, intermediates (**VB 8a-m**) and final products (**VB 9a-m**) with respective global yields. Molecular structures created with ChemDraw.

Ar-CHO	Intermediate product	Final product	Global yield (%) [a]
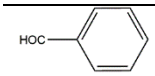	VB 8a	**VB 9a**	69
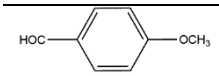	VB 8b	**VB 9b**	30
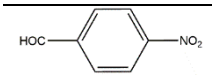	VB 8c	**VB 9c**	86
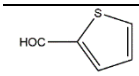	VB 8d	**VB 9d**	58
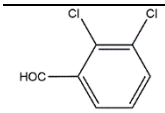	VB 8e	**VB 9e**	76
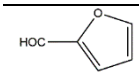	VB 8f	**VB 9f**	86
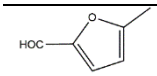	VB 8g	**VB 9g**	79
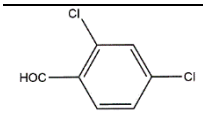	VB 8h	**VB 9h**	85
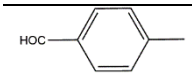	VB 8i	**VB 9i**	65
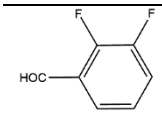	VB 8j	**VB 9j**	58
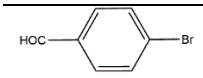	VB 8k	**VB 9k**	69
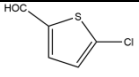	VB 8l	**VB 9l**	86
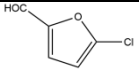	VB 8m	**VB 9m**	65

[a] Global yield after the two synthetic steps from dehydroepiandrosterone (DHEA).

3.2.2. Biological evaluation

3.2.2.1. Antiproliferative activity

The effects of the epoxysteroids **VB 9a-m** on the proliferation of non-tumoral cells and tumoral cells were assessed by the MTT proliferation colorimetric assay. PNT1A (normal prostate cells) and NHDF (normal human dermal fibroblasts) were used as models of non-tumoral cells. As models of androgen-dependent and androgen-independent, prostatic cancer were used LNCaP and PC-3 cell lines, respectively. MCF-7 cell line are estrogen-responsive breast cancer cells. In a first assay, cells were exposed to all of these new steroidal derivatives at the concentration of 10 and 50 μM for 72 h. Moreover, 5-FU was also introduced in the assay as a clinically used antitumor positive control. The results of this preliminary study are depicted in **Figure 39** (full data presented on the **Appendix 4**, **Table Ap 5**).

From this preliminary study, compounds **VB 9f** and **VB 9g** seemed to not display a strong effect in cell proliferation against tumoral cell lines (relative cell proliferation ≥ 50 % at both concentrations), being apparently more cytotoxic against non-tumoral cells (NHDF and PNT1A), principally steroid **VB 9g**. On the other hand, steroids **VB 9a**, **VB 9e**, **VB 9h**, **VB 9i**, **VB 9k**, **VB 9l**, and **VB 9m** showed strong effects on cell proliferation, principally at 50 μM (relative cell proliferation ≤ 50 %), against all cell lines. In addition, at 50 μM almost all compounds (**VB 9a**, **VB 9e**, **VB 9h**, **VB 9f**, **VB 9k**, and **VB 9l**) had a strong effect on proliferation of PC-3 cells, causing a decrease on cell proliferation clearly higher than 75 % relative to the control. Similarly, steroidal derivatives **VB 9e**, **VB 9h**, **VB 9i**, **VB 9k**, **VB 9l**, and **VB 9m** at 50 μM, also produced a decrease on LNCaP cell proliferation higher than 75 %. However, at 10 μM, the same compounds in the same cell line seemed to have no relevant effects. Interestingly, in MCF-7 cell line, treatment with steroids **VB 9e** and **VB 9h** at 50 μM produced a cell proliferation of nearly 0 % relative to the control. Generally, compounds these epoxides seemed to be the most potent compounds, having significative effects in all cell lines. In summary, after this preliminary screening assay, there is no doubt that steroid **VB 9e** produced the most significant effect in cell proliferation, mainly in MCF-7 cells at the two tested concentrations (10 and 50 μM). In fact, in addition to causing a decrease close to 100 % in cell proliferation at 50 μM, it also caused a decrease around 75 % at 10 μM.

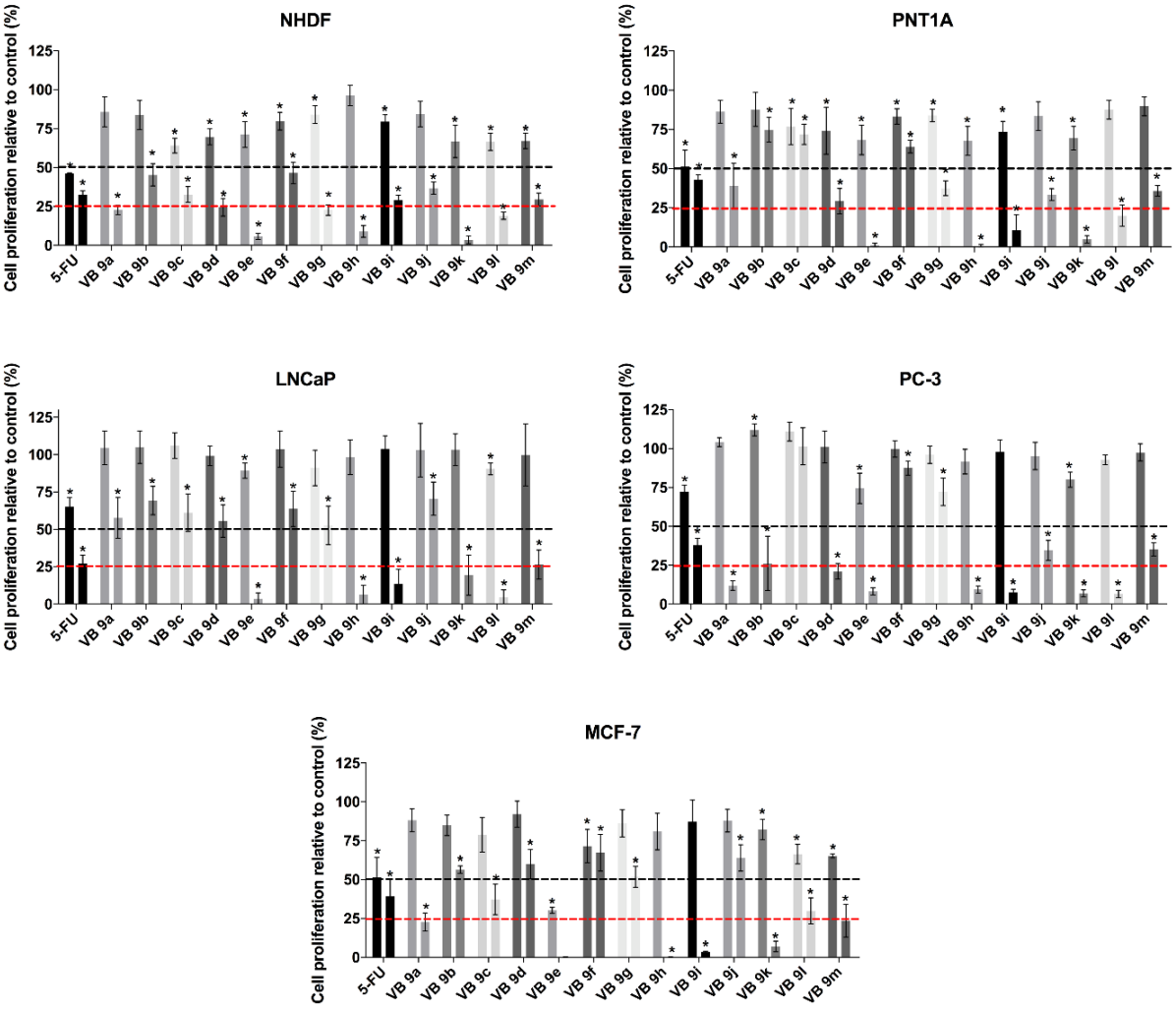

Figure 39. Results of preliminary studies of cell viability at two concentrations, 10 and 50 μM in NHDF, PNT1A, LNCaP, PC-3 and MCF-7 cell lines. The effect of all the synthesized final products, during 72 h, was evaluated and 5-fluorouracil (5-FU) was used as positive control. Data are indicated as mean±SD and are representative at least two independent experiments. *p< 0.05 in relation to a negative control (Student's t-test).

After this preliminary evaluation, concentration–response studies were performed for the most antiproliferative compounds (relative proliferation relative to control < 50 % at 10 μM or < 25 % at 50 μM) and 5-FU in all cell lines. The IC_{50} values were estimated by treating cells with solutions of tested compounds at 0.01, 0.1, 1, 10, 50 and 100 μM for 72 h. Considering the non-tumoral cells, IC_{50} values were determined for all compounds to more deeply verify the selectivity of these epoxides, not only concerning their potential antitumoral interest. The results obtained are shown in **Table 15**, and some relevant points can be highlighted. Steroids **VB 9a**, **VB 9b**, and **VB 9j** presented some selectivity for PC-3 cells, comparing the IC_{50} values among non-tumoral cell and PC-3. Relative to compound **VB 9d**, the IC_{50} values are lower in non-tumoral cells [IC_{50}(NHDF)= 29.65 μM; IC_{50}(PNT1A)= 29.56 μM) than in PC-3 (IC_{50}= 37.56 μM]. Regarding the androgen-

dependent cell line, LNCaP, a relative selectivity can be observed for steroid **VB 9m**, with an interesting IC_{50} value (15.80 μM), lower than the observed against the other cell lines. Finally, the lowest values were determined in MCF-7 cells, particularly for epoxide **VB 9e** which is the most potent steroid (IC_{50}= 3.47 μM) identified in the present study. In addition, this value is lower than determined to 5-FU, the positive control (IC_{50}= 6.30 μM), being the only case concerning tumoral cells. Furthermore, the determined IC_{50} values against non-tumoral cells are higher than the observed for MCF-7 cells. Consequently, this compound was selected to further studies in order to better understand the potential mechanisms underlying the cytotoxicity observed.

Table 15. Estimated IC_{50} values (μM) for final compounds and 5-fluorouracil (5-FU) in non-tumoral cells: NHDF and PNT1A, and in tumoral cells: LNCaP, PC-3, and MCF-7.

Compound	NHDF		PNT1A		LNCaP		PC-3		MCF-7	
	IC_{50}	r^2	IC_{50}	r^2	IC_{50}	r^2	IC_{50}	r^2	IC_{50}	r^2
5-FU	6.34	0.95	6.48	0.95	9.43	0.95	21.20	0.97	6.30	0.90
VB 9a	39.52	0.94	33.12	0.96	27.37	0.95	17.02	0.99	42.67	0.84
VB 9b	39.27	0.96	54.52	0.94	-	-	20.06	0.99	-	-
VB 9c	32.33	0.92	>100	-	-	-	-	-	20.82	0.83
VB 9d	29.65	0.94	29.56	0.84	-	-	37.56	0.98	-	-
VB 9e	18.69	0.97	12.75	0.94	12.83	0.98	19.03	0.99	3.47	0.94
VB 9f	49.96	0.92	56.63	0.92	-	-	-	-	-	-
VB 9g	23.44	0.94	46.33	0.93	-	-	-	-	-	-
VB 9h	14.95	0.96	14.41	0.99	15.02	0.98	44.46	0.99	14.46	0.90
VB 9i	28.34	0.96	13.27	0.98	19.29	0.98	13.97	0.99	18.68	0.93
VB 9j	33.43	0.86	56.46	0.95	-	-	-	-	-	-
VB 9k	15.98	0.93	15.33	0.98	36.88	0.88	14.52	0.98	14.52	0.92
VB 9l	16.62	0.85	15.58	0.99	11.34	0.97	43.76	0.97	21.82	0.92
VB 9m	18.40	0.83	19.47	0.95	15.80	0.93	-	-	56.90	0.92

Generally, comparing the antiproliferative activity of these new steroidal 5α,6α-epoxides with 16*E*-arylidenedehydroepiandrosterone derivatives already described in the literature, it can be observed that epoxysteroids seem to have higher antiproliferative activity against tumoral cell lines.[296,317,335,338] For instance, Vosooghi and colleagues prepared and evaluated against tumoral cell lines by MTT assay the intermediate products herein named as **VB 8a** and **VB 8h**, and these steroids presented IC_{50} values against T47-D cells (breast cancer) > 100 μM. On contrary, the corresponding epoxysteroids (**VB 9c** and **VB 9h**, respectively) exhibited lower IC_{50} values against MCF-7 cells (also from breast cancer): IC_{50}(**VB 9c**)= 20.82 μM and IC_{50}(**VB 9h**)= 14.46 μM.[338] Despite this, few 16*E*-arylidenedehydroepiandrosterone derivatives with interesting cytotoxicity can also be highlighted. For example, Huang and colleagues reported the

cytotoxic effects of a series of these DHEA derivatives on different human cancer cells. These authors observed that the most potent of this series, which contains a 4-iodophenyl system attached to a triazole ring (bonded at C-16), displayed the highest antiproliferative activity in HepG2 and MCF-7 cells (IC_{50}= 9.10 and 9.18 μM, respectively).[296] Moreover, in other study it was showed that the DHEA derivative bearing a 3-chlorobenzylidene at C-16 was the most potent against KB (nasopharyngeal epidermoid carcinoma) and T47D cells (IC_{50} values of 0.6 and 1.7 μM, respectively).[338] Considering all these results chemical modifications on these compounds to improve the bioactivity are rationally justified.

3.2.2.2. Characterization of effects on cell proliferation

Considering the results of MTT proliferation assay in which **VB 9e** exhibited the most potent effect (IC_{50}= 3.47 μM) in MCF-7 cell line, a panel of more specific biological experiments with this derivative was accomplished. This set of biological evaluation methodologies included immunocytochemistry assay, PI incorporation, and analysis of cell nuclear morphology and distribution using ImageJ software.

The immunocytochemistry technique is based on the evaluation of the expression of protein antigens in the cell via specific combination of antibodies and target molecules. In the present study, the expression of Ki67 was assessed in MCF-7 cells after 48 h of treatment with 5-FU, as positive control, and **VB 9e** at 1 and 10 μM. 5-FU was included in the assay due to its capacity to induce apoptosis. 5-FU is an analogue of uracil, and consequently it rapidly enters the cell through the same facilitated transport mechanism. Then, 5-FU is converted intracellularly into active metabolites: fluorodeoxyuridine monophosphate, fluorodeoxyuridine triphosphate and fluorouridine triphosphate. These active metabolites are able to disrupt RNA synthesis and inhibit the action of thymidylate synthase, leading the cell to apoptosis.[336] The monoclonal antibody Ki67 detects a human nuclear antigen that is present in proliferating cells but absent in quiescent cells.[494,495] Ki67 is a labile, nonhistone nuclear protein that is related to the cell cycle. It is expressed in proliferating cells during mid G1 phase, increasing in level through S and G2, and peaking in the M phase of the cell cycle. It is rapidly catabolized at the end of the M phase, and is undetectable in resting (G0 and early G1) cells.[496,497] In addition, this marker is commonly used to stratify good and poor prognostic categories in invasive breast cancer.[498,499] In a parallel study, MCF-7 cells were staining with PI and the percentage of PI-positive cells was measured after treatment with 5-FU and **VB 9e** at same conditions of immunocytochemistry assay. The fluorescent exclusion dye PI is widely used as an important dye in tissue culture systems and labels the nucleus in dying

cells with compromised plasma membrane.[500,501] This method has proved to be particularly useful in studying cell death *in vitro*.[502,503]

The results of percentages of Ki67-positive cell and of PI-positive cells (% relative to control) obtained are shown in **Figure 40**. Additionally, representative photomicrographs of MCF-7 cells after Hoechst-33342/Ki67 and Hoechst-33342/PI staining are presented at **Figure 41**. From these experiments, it was observed that 5-FU and **VB 9e,** at 10 μM, induced a statistically significant decrease on Ki67-positive relative to control in a very similar manner ($p< 0.0001$). Moreover, at 1 μM, none of the compounds significantly affected the percentage of Ki67-positive cells when compared to the control. In relation to PI staining, again at the lowest concentration, no significant effect was observed on the percentage of PI-positive cells relatively to the negative control. On the contrary, at 10 μM, both compounds showed to significantly increment the percentage of PI-positive cells. However, compared with 5-FU ($p< 0.05$), the effect of **VB 9e** is statistically more significant ($p< 0.0001$), increasing about 3 times more the percentage of PI incorporation than the positive control.

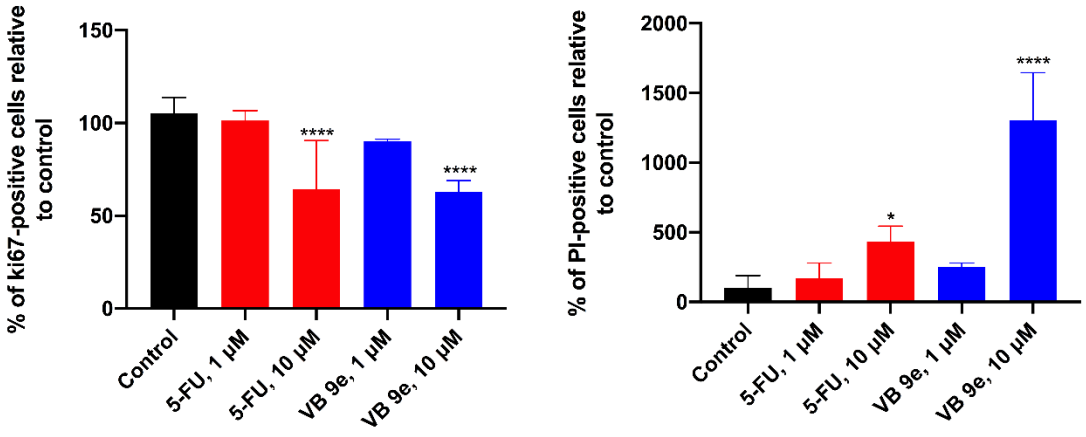

Figure 40. Results of Ki67 (**A**) and PI (**B**) staining in MCF-7 cells after treatment with 5-FU, as positive control, and **VB 9e** at concentrations 1 and 10 μM, during 48 h. Data are indicated as means±SEM and are representative at least two independent experiments. *$p< 0.05$, ****$p< 0.0001$ in relation to the negative control (ordinary one-way ANOVA test). (PI= Propidium iodide, 5-FU= 5-fluorouracil).

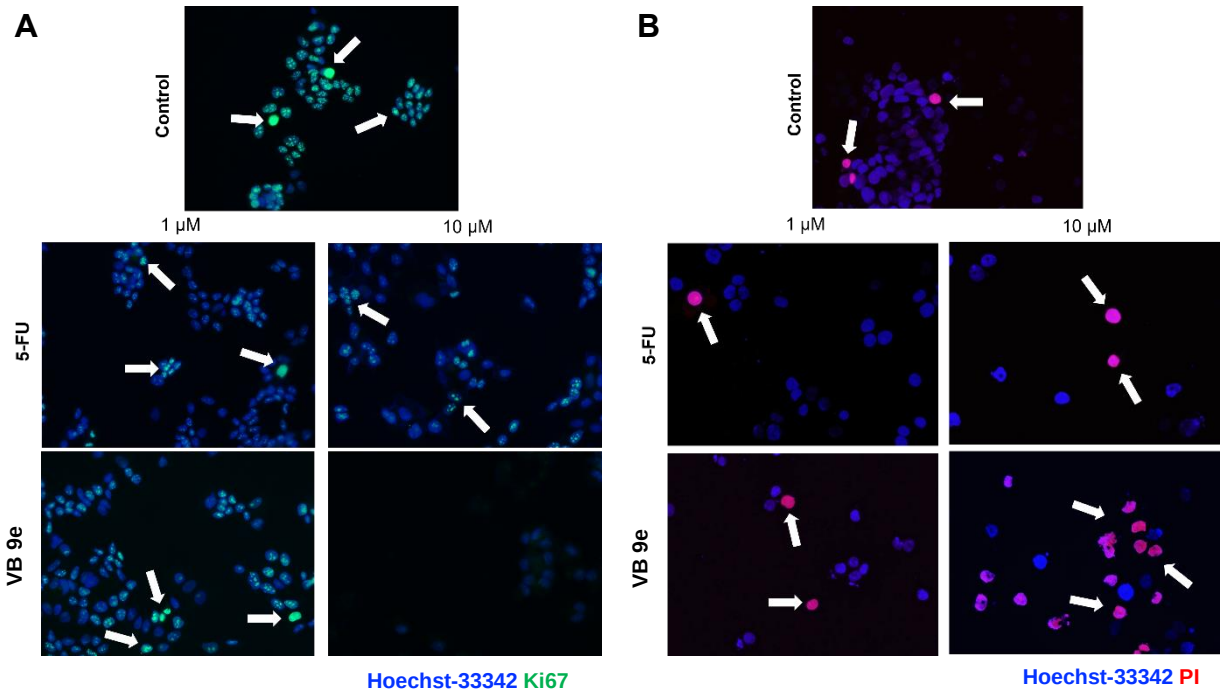

Figure 41. Representative photomicrographs of MCF-7 cell line after (**A**) Hoechst-33342/Ki67 and (**B**) Hoechst-33342/PI staining. Cells were treated with 5-FU, as positive control, and **VB 9e** at 1 and 10 μM, during 48 h. (PI= Propidium iodide, 5-FU= 5-fluorouracil).

Additionally, considering cellular morphologic features associated to apoptosis/necrosis, in apoptosis cells preserves the organelles and cell membrane for some time whereas the nucleus undergoes early degeneration. On the other hand, in necrotic cells, the nucleus stays relatively intact while the cell membrane and organelles show early degeneration.[504] Usually, cap-shaped chromatin margination is one of the first signs of apoptosis, as well as cytosol condensation, pyknosis and cell membrane blebbing. Then, the nucleus develops several dense and circular micronuclei, which are released to the extracellular space. Lastly, the cells split into numerous apoptotic bodies. *In vitro*, the late stage of necrosis presented by apoptotic cells is usually characterized by early cell membrane damage. Nevertheless, pyknotic and fragmented cell nuclei are not common in necrosis.[504–506] Thus, these distinctive modifications in nuclear morphology during apoptosis can be used as markers of this cell death cell mechanism. In this study, bearing in mind the research reported by Eidet and coworkers, the nuclear area (NA) and cell distribution through the NND were analyzed as the main indicators of apoptosis.[472]

The results of this study are shown in **Figure 42**. Interestingly, after exposure with **VB 9e** at both tested concentrations, the NA of MCF-7 cells decreased significantly (p< 0.0001) relatively to control (**Figure 42-A**). Moreover, this effect is more drastic for the epoxide **VB 9e** than the observed for 5-FU, the reference. In relation to NND

measurement, it was constated a similar effect when cells were treated with 5-FU and the steroid at 1 and 10 μM (**Figure 42-B**). Therefore, the cell distribution analysis indicated a more random distribution with nuclei more spaced after 48 h of incubation with tested compounds. In this context, Eidet and coworkers demonstrated in a study the relation between activation of apoptosis and more uneven cell spacing.[472] In conclusion, the results obtained from this more specific experiments constitute a strong indication of the possibility of **VB 9e** triggering the apoptotic cell death pathway. However, other studies should be performed to confirm this hypothesis.

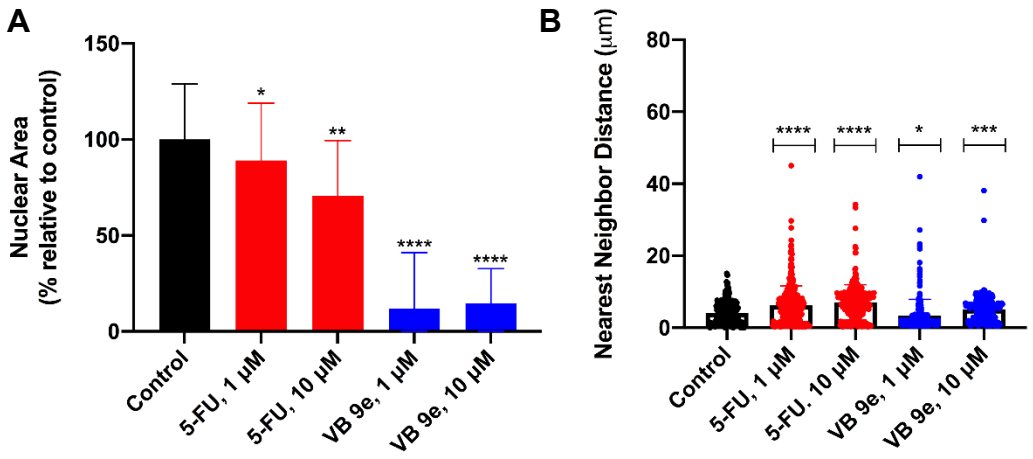

Figure 42. (**A**) MCF-7 nuclear area of cells untreated (control) and cells treated with 5-fluorouracil (5-FU) and **VB 9e** at 1 and 10 μM, incubated during 48 h; (**B**) Nearest neighbor analysis of MCF-7 cells in the same conditions referred previously. Data are indicated as mean±SD and are representative at least two independent experiments. *$p< 0.05$, **$p< 0.01$, ***$p< 0.001$, ****$p< 0.0001$ compared to control (unpaired two tailed Student's *t*-test).

3.2.3. Molecular docking studies

To evaluate the potential affinity of these novel compounds to several proteins an *in silico* study using molecular docking simulations was accomplished. This study aimed to verify the existence of potential interactions between these novel epoxysteroids and proteins which are known to interact with steroids. Thus, these simulations were performed against known targets of steroidal drugs currently used in the treatment of breast cancer, BPH, and PCa, namely, 5AR, ERα, AR, CYP17A1, and aromatase. The protein targets were selected according to the following criteria: (1) a high-resolution X-ray crystal structure is available in complex with a steroidal drug or other ligand and (2) the protein is a target of clinically approved steroid-based anticancer drugs in the treatment of hormone-dependent breast cancer or PCa. Moreover, 5AR was included in this assay since the use of 5ARIs, including steroidal drugs (e.g. finasteride), comprise the main strategy in the treatment and management of BPH. Three-dimensional structural coordinates of protein receptors were obtained from the protein databank (PDB) and

molecular docking was performed using the program AutoDockTools. This study was performed for each derivative, **VB 9a-m**, against all mentioned targets. Firstly, the docking method validation was mandatory, and simulations were carried out between crystallized ligands/drugs with the respective proteins. From this validation study, it was observed that all control redocking simulations were able to reproduce the ligand–protein interaction geometries presented in the respective crystal structures with a RMSD < 2.0 Å. On the basis of the control redocking simulations, predicted binding energies are analyzed in comparison with the value observed for the control. 5AR was co-crystalized with NADP-DHF adduct, and thus the redocking study was performed with 5AR complexed with this adduct. However, an additional simulation only with finasteride and 5AR was achieved to posteriorly compare with the novel epoxysteroids. The predicted binding energies of steroids **VB 9a-m** are shown in **Table 16**, and some relevant binding energies can be observed. In general, considering the lowest affinity energies, the tested steroids exhibited higher affinity to 5AR and to CYP17A1, and very low affinity to ERα and AR. Regarding the results against 5AR, interestingly, with exception of compound **VB 9d**, all epoxysteroids have equal or lower energies than the control, finasteride. These results showed that there is a possibility of these synthesized final products to be potential 5AR inhibitors. Moreover, when the molecular docking was performed with CYP17A1 it was observed that when compared with abiraterone, the affinity of the tested compounds is generally very similar. These interesting values can be suggestive that these steroidal derivatives can also have relevant interactions with this relevant target, which is important on androgen signaling pathway in PCa.[507,508] On the other hand, the values obtained against ERα and AR are clearly indicative of the absence of relevant interactions between these targets and the novel epoxysteroids, being energies values significantly higher than the control. Given the typical selectivity problem of this type of compounds, this result is interesting. Lastly, regarding the results against aromatase, it was observed that all compounds, with exception of steroid **VB 9h**, generated affinity energies higher than the redocking values, suggesting lower affinity than androstenedione (the co-crystallized ligand). Despite epoxide **VB 9h** exhibiting slightly higher than androstenedione, but probably this difference is not significant to improve the bioactivity. In addition, after the visualization and study of the potential interactions between **VB 9h** and aromatase in Discovery Studio software, it was observed that the most relevant interactions to the enzyme activity are mostly absent.

Table 16. Molecular docking results, including redocking energy values, obtained by vina executable. Lowest affinity energies are indicated in Kcal.mol^{-1}. All new compounds were tested with the most significant steroidal targets. [a]

Compound	5AR type 2	ERα	AR	CYP17A1	Aromatase
VB 9a	−12.5	−1.5	−3.3	−10.2	−9.8
VB 9b	−12.4	−2.3	1.8	−10.2	−8.0
VB 9c	−12.7	−0.7	2.4	−10.5	−8.2
VB 9d	−11.8	−0.6	−3.9	−9.8	−9.7
VB 9e	−12.7	−1.5	−1.7	−11.0	−8.3
VB 9f	−11.9	−2.1	−5.8	−9.8	−9.6
VB 9g	−12.4	−2.1	−2.4	−10.3	−8.8
VB 9h	−13.7	1.2	0.0	−10.3	−10.2
VB 9i	−12.7	−1.5	0.6	−10.5	−8.5
VB 9j	−13.0	−1.4	−3.1	−10.8	−8.8
VB 9k	−12.5	−0.3	0.7	−10.5	−8.0
VB 9l	−11.9	−1.5	−0.5	−10.1	−8.3
VB 9m	−12.4	−2.3	−1.6	−10.3	−8.8
Finasteride	−11.9	-	-	-	-
Estradiol	-	−10.4	-	-	-
DHT	-	-	−11.2	-	-
Abiraterone	-	-	-	−10.2	-
Androstenedione	-	-	-	-	−10.1

[a] 5AR= 5α-reductase, ERα= estrogen receptor α, AR= androgen receptor, CYP17A1= steroid 17α-hydroxylase/17,20 lyase, DHT= 5α-dihydrotestosterone.

3.3. Experimental section

3.3.1. General remarks

Reagents and solvents were purchased from standard sources and were purified and/or dried whenever necessary using standard procedures before use. The reactions were performed under magnetic stirring using Heidolph plates. Thin layer chromatography (TLC) analysis was performed using 0.20 mm Al-backed silica-gel plates (Macherey-Nagel 60 F254, Duren, Germany) and after elution plates were visualized under UV radiation (254 nm) in a CN-15.LC UV chamber. Then, the revelation step using an ethanol/sulfuric acid (95:5) mixture followed by heating at 120 °C was performed. Finally, the steroid derivatives were isolated by simple evaporation of solvents using a rotary vacuum drier from Büchi (R-215). Melting points were measured by a Büchi Melting Point B-540 (Büchi, Switzerland). Attenuated total reflectance IR spectra were collected using a Thermo Scientific Nicolet iS10, smart iTR, equipped with a diamond attenuated total reflectance crystal. For IR data acquisition, each solid sample was placed onto the crystal and the spectrum was recorded. An air spectrum was used as a reference in absorbance calculations. The sample spectra were collected at room temperature in the 4000-600 cm^{-1} range by averaging 16 scans at spectral resolution of 2 cm^{-1}. ^{1}H NMR

and ^{13}C NMR spectra were recorded using a Bruker Avance 400 MHz spectrometer (^{1}H NMR at 400.13 MHz and ^{13}C NMR at 100.62 MHz) and were processed with the software TOPSPIN (v. 3.1) (Bruker, Fitchburg, WI). Deuterated chloroform ($CDCl_3$) was used as a solvent for all samples. Chemical shifts are reported in parts per million (ppm) relative to TMS or solvent as an internal standard. Coupling constants (*J* values) are reported in hertz (Hz) and splitting multiplicities are described as s= singlet, d= doublet, t= triplet, combinations of above, or m= multiplet. ESI-TOF mass spectrometry was performed by the microanalysis service using a QSTAR XL instrument.

3.3.2. Chemical synthesis

General procedure to obtain the synthetic intermediates 16*E*-arylidene-dehydroepiandrosterone derivatives (VB 8a-m)

To an ethanolic solution of DHEA (43.2 mg, 1.5 mmol) and aldehyde (1.8 mmol) was added an aqueous solution of KOH 50 % (800 μL) and the reaction was stirred for 4-24 h at r.t..

The reaction mixture was worked up first by adding cold water to induce precipitation and then filtering and washing to give the 16*E*-arylidene-dehydroepiandrosterone derivatives **VB 8a-m**.[317,322,327,335,338,388]

*16E-Benzylidene-3β-hydroxyandrost-5-en-17-one (**VB 8a**)*

White powder (89 %); m.p. 179-180 °C; ^{1}H NMR ($CDCl_3$, 400 MHz) δ: 0.91 (3H, s, 18-CH_3), 1.00 (3H, s, 19-CH_3), 3.51-3.42 (1H, m, 3-CH), 5.33 (1H, s, 6-CH), 7.39-7.27 (4H, m, H_{ar}+H_{vin}), 7.47 (2H, d, *J*= 7.2 Hz, H_{ar}).

*16E-(4'-Methoxybenzylidene)-3β-hydroxyandrost-5-en-17-one (**VB 8b**)*

White powder (91 %); m.p. 207-208 °C; ^{1}H NMR ($CDCl_3$, 400 MHz) δ: 0.95 (3H, s, 18-CH_3), 1.06 (3H, s, 19-CH_3), 3.56-3.46 (1H, m, 3-CH), 3.82 (3H, s, 4'-OCH_3), 5.38 (1H, s, 6-CH), 6.92 (2H, d, *J*= 8.9 Hz, H_{ar}), 7.38 (1H, s, H_{vin}), 7.48 (2H, d, *J*= 8.8 Hz, H_{ar}).

*16E-(4'-Nitrobenzylidene)-3β-hydroxyandrost-5-en-17-one (**VB 8c**)*

White powder (93 %); m.p. 250-251 °C; ^{1}H NMR ($CDCl_3$, 400 MHz) δ: 0.98 (3H, s, 18-CH_3), 1.06 (3H, s, 19-CH_3), 3.57-3.47 (1H, m, 3-CH), 5.38 (1H, s, 6-CH), 7.43 (1H, s, H_{vin}), 7.64 (2H, d, *J*= 8.5, H_{ar}), 8.24 (2H, d, *J*= 8.6 Hz, H_{ar}).

*16E-(Thiophen-2'-ylmethylene)- 3β-hydroxyandrost-5-en-17-one (**VB 8d**)*

White powder (91 %); m.p. 216-218 °C; ^{1}H NMR ($CDCl_3$, 400 MHz) δ: 0.93 (3H, s, 18-CH_3), 1.05 (3H, s, 19-CH_3), 3.57-3.47 (1H, m, 3-CH), 5.39 (1H, s, 6-CH), 7.10 (1H, m, H_{ar}), 7.31 (1H, d, *J*=3.5, H_{ar}), 7.49 (1H, d, *J*= 5.1 Hz, H_{ar}), 7.60 (1H, s, H_{vin}).

*16E-(2',3'-Dichlorobenzylidene)-3β-hydroxyandrost-5-en-17-one (**VB 8e**)*

White powder (95 %); m.p. 137-138 °C; ^{1}H NMR ($CDCl_3$, 400 MHz) δ: 1.01 (3H, s, 18-CH_3), 1.08 (3H, s, 19-CH_3), 3.60-3.50 (1H, m, 3-CH), 5.39 (1H, s, 6-CH), 7.27 (1H, d, *J*= 8.8 Hz, H_{ar}), 7.50-7.40 (2H, m, H_{ar}), 7.75 (1H, s, H_{vin}).

*16E-(Furan-2'-ylmethylene)-3β-hydroxyandrost-5-en-17-one (**VB 8f**)*

White powder (93 %); m.p. 184-185 °C; ^{1}H NMR ($CDCl_3$, 400 MHz) δ: 0.92 (3H, s, 18-CH_3), 1.04 (3H, s, 19-CH_3), 3.57-3.46 (1H, m, 3-CH), 5.39 (1H, s, 6-CH), 6.50-6.47 (1H, m, H_{ar}), 6.62 (1H, d, *J*= 3.4 Hz, H_{ar}), 7.19-7.16 (1H, m, H_{ar}), 7.54 (1H, s, H_{vin}).

*16E-[(2'-Methylfurane)methylene]-3β-hydroxyandrost-5-en-17-one (**VB 8g**)*

Orange powder (88 %); m.p. 139-140 °C; ^{1}H NMR ($CDCl_3$, 400 MHz) δ: 0.91 (3H, s, 18-CH_3), 1.04 (3H, s, 19-CH_3), 3.58-3.46 (1H, m, 3-CH), 5.39 (1H, s, 6-CH), 6.09 (1H, s, H_{ar}), 6.54 (1H, d, *J*= 3.14 Hz, H_{ar}), 7.13 (1H, s, H_{vin}).

*16E-(2',4'-Dichlorobenzylidene)-3β-hydroxyandrost-5-en-17-one (**VB 8h**)*

Yellow powder (93 %); m.p. 192-199 °C; ^{1}H NMR ($CDCl_3$, 400 MHz) δ: 1.01 (3H, s, 18-CH3), 1.09 (3H, s, 19-CH3), 3.60-3.50 (1H, m, 3-CH), 5.39 (1H, s, 6-CH), 7.30 (1H, d, *J*= 8.32 Hz, H_{ar}), 7.49 (2H, d, *J*= 8.46 Hz, H_{ar}), 7.71 (1H, s, H_{vin}).

*16E-(4'-Methylbenzylidene)-3β-hydroxyandrost-5-en-17-one (**VB 8i**)*

Yellow powder (71 %); m.p. 229-231 °C; ^{1}H NMR ($CDCl_3$, 400 MHz) δ: 0.96 (3H, s, 18-CH_3), 1.05 (3H, s, 19-CH_3), 2.36 (3H, s, 4'-CH_3), 3.57-3.47 (1H, m, 3-CH), 5.38 (1H, s, 6-CH), 7.20 (2H, d, *J*= 7.93 Hz, H_{ar}), 7.45-7.39 (3H, m, H_{ar}+H_{vin}).

*16E-(2',3'-Difluorobenzylidene)-3β-hydroxyandrost-5-en-17-one (**VB 8j**)*

Yellow powder (81 %); m.p. 140-141 °C; ^{1}H NMR ($CDCl_3$, 400 MHz) δ: 0.96 (3H, s, 18-CH_3), 1.04 (3H, s, 19-CH_3), 3.55-3.45 (1H, m, 3-CH), 5.35 (1H, s, 6-CH), 7.19-7.06 (2H, m, H_{ar}), 7.26 (1H, d, *J*= 7.34 Hz, H_{ar}), 7.56 (1H, s, H_{vin}).

*16E-(4'-Bromobenzylidene)-3β-hydroxyandrost-5-en-17-one (**VB 8k**)*

Yellow powder (89 %); m.p. 219-220 °C; ^{1}H NMR ($CDCl_3$, 400 MHz) δ: 0.95 (3H, s, 18-CH_3), 1.06 (3H, s, 19-CH_3), 3.37-3.46 (1H, m, 3-CH), 5.37 (1H, s, 6-CH), 7.39-7.32 (3H, m, H_{ar}+H_{vin}), 7.52 (2H, d, *J*= 8.09 Hz, H_{ar}).

*16E-[(5'-Chlorothiophen-2'-yl)methylene]-3β-hydroxyandrost-5-en-17-one (**VB 8l**)*

Beige powder (94 %); m.p. 216-217 °C; ^{1}H NMR ($CDCl_3$, 400 MHz) δ: 0.92 (3H, s, 18-CH_3), 1.05 (3H, s, 19-CH_3), 3.60-3.44 (1H, m, 3-CH), 5.39 (1H, s, 6-CH), 6.92 (1H, d, *J*= 3.54 Hz, H_{ar}), 7.08 (1H, d, *J*= 3.54 Hz, H_{ar}), 7.44 (1H, s, H_{vin}).

*16E-[(5'-Chlorofuran-2'-yl)methylene]-3β-hydroxyandrost-5-en-17-one (**VB 8m**)*

Orange powder (90 %); m.p. 160-161 °C; ^{1}H NMR ($CDCl_3$, 400 MHz) δ: 0.96 (3H, s, 18-CH_3), 1.09 (3H, s, 19-CH_3), 3.62-3.52 (1H, m, 3-CH), 5.43 (1H, s, 6-CH), 6.31 (1H, d, *J*= 3.36 Hz, H_{ar}), 6.64 (1H, d, *J*= 3.36 Hz, H_{ar}), 7.11 (1H, s, H_{vin}).

General procedure to obtain the 16*E*-arylidene-5α,6α-epoxyepiandrosterone derivatives (VB 9a-m)

The substrate **VB 8a-m** (0.5 mmol) was dissolved in 4.5 mL of DCM. To this solution, MMPP (13.6 mg) and 250 µL of distillated water were added, and the reactional mixture was stirred at room temperature for 24 h.

After the reaction is complete, the mixture was filtered, and the organic solvent was removed under reduced pressure. The white solid was dissolved in diethyl ether, and it was washed with an aqueous solution of Na_2SO_3 10%, with a saturated $NaHCO_3$ solution and brine. The organic portion was dried with anhydrous Na_2SO_4, filtered, and dried under reduced pressure. The resultant crude was recrystallized from methanol to afford steroids **VB 9a-m**.

*16E-Benzylidene-3β-hydroxy-5α,6α-epoxyandrostan-17-one (**VB 9a**)*

White powder (78 %); m.p. 207-208 °C; IR (cm $^{-1}$): 1628, 1725, 2859, 2943, 3190. ^{1}H NMR ($CDCl_3$, 400 MHz) δ: 0.90 (3H, s, 18-CH_3), 1.11 (3H, s, 19-CH_3), 2.95 (1H, d, *J*= 4.4 Hz, 6-CH), 3.94-3.84 (1H, m, 3-CH), 7.42-7.32 (4H, m, H_{ar}+H_{vin}), 7.51 (2H, d, *J*= 8.1 Hz, H_{ar}). ^{13}C NMR ($CDCl_3$, 101 MHz) δ: 14.28, 15.29, 15.99, 20.06, 27.90, 29.24, 31.07, 31.20, 32.37, 35.14, 39.76, 42.84, 47.41, 49.95, 58.70, 65.69, 65.87, 68.57, 128.71, 129.30, 130.33, 135.28, 135.58, 209.20.

*16E-(4'-Methoxybenzylidene)-3β-hydroxy-5α,6α-epoxyandrostan-17-one (**VB 9b**)*
White powder (33 %); m.p. 248-252 °C; IR (cm $^{-1}$): 1600, 1725, 2859, 2935, 3517. ^{1}H NMR ($CDCl_3$, 400 MHz) δ: 0.88 (3H, s, 18-CH_3), 1.10 (3H, s, 19-CH_3), 2.94 (1H, d, *J*= 4.4 Hz, 6-CH), 3.82 (3H, s, 4'-$COCH_3$), 3.95-3.84 (1H, m, 3-CH), 6.92 (2H, d, *J*= 8.8 Hz, H_{ar}), 7.36 (1H, s, H_{vin}), 7.47 (2H, d, *J*= 8.7 Hz, H_{ar}). ^{13}C NMR ($CDCl_3$, 101 MHz) δ: 14.34, 15.99, 20.07, 27.92, 29.08, 29.23, 31.08, 31.22, 32.38, 35.15, 39.79, 42.87, 47.30, 50.04, 55.37, 58.73, 65.71, 68.60, 114.24, 128.27, 132.11, 133.08, 133.20, 160.53, 209.37. HRMS (ESI-TOF) m/z: $[M + H]^+$ Calcd for $C_{27}H_{34}O_4$ 422.2457; Found 422.2575.

*16E-(4'-Nitrobenzylidene)-3β-hydroxy-5α,6α-epoxyandrostan-17-one (**VB 9c**)*
White powder (92 %); m.p. 257-258 °C; IR (cm $^{-1}$): 1513, 1717, 2234, 2859, 2937, 3333. ^{1}H NMR ($CDCl_3$, 400 MHz) δ: 0.91 (3H, s, 18-CH_3), 1.10 (3H, s, 19-CH_3), 2.95 (1H, d, *J*= 4.3 Hz, 6-CH), 3.94-3.84 (1H, m, 3-CH), 7.42 (1H, s, H_{vin}), 7.63 (2H, d, *J*= 8.8 Hz, H_{ar}), 8.24 (2H, d, *J*= 8.8 Hz, H_{ar}). ^{13}C NMR ($CDCl_3$, 101 MHz) δ: 14.21, 15.99, 20.03, 27.88, 29.18, 29.26, 31.06, 31.15, 32.36, 35.12, 39.73, 42.82, 47.56, 49.70, 58.57, 65.66, 68.53, 123.92, 130.38, 130.66, 139.57, 141.91, 147.55, 208.28. HRMS (ESI-TOF) m/z: $[M + H]^+$ Calcd for $C_{26}H_{31}NO_5$ 437.2202; Found 437.2250.

*16E-(Thiophen-2'-ylmethylene)-3β-hydroxy-5α,6α-epoxyandrostan-17-one (**VB 9d**)*
White powder (64 %); m.p. 191-192 °C; IR (cm $^{-1}$): 1670, 1707, 2869, 2942, 3169. ^{1}H NMR ($CDCl_3$, 400 MHz) δ: 0.86 (3H, s, 18-CH_3), 1.10 (3H, s, 19-CH_3), 2.96 (1H, d, *J*= 4.4 Hz, 6-CH), 3.95-3.85 (1H, m, 3-CH), 7.13-7.08 (1H, m, H_{ar}), 7.31 (1H, d, *J*= 3.4 Hz, H_{ar}), 7.49 (1H, d, *J*= 5.0 Hz, H_{ar}), 7.58 (1H, s, H_{vin}). ^{13}C NMR ($CDCl_3$, 101 MHz) δ: 13.41, 14.98, 18.45, 19.04, 26.86, 28.17, 30.14, 31.38, 34.09, 38.73, 41.84, 46.78, 48.69, 57.69, 64.66, 67.56, 70.58, 124.92, 126.90, 128.68, 131.41, 132.27, 138.86, 207.92. HRMS (ESI-TOF) m/z: $[M + H]^+$ Calcd for $C_{24}H_{30}O_3S$ 398.1916; Found 398.1985.

*16E-(2',3'-Dichlorobenzylidene)-3β-hydroxy-5α,6α-epoxyandrostan-17-one (**VB 9e**)*
White powder (80 %); m.p. 135-136 °C; IR (cm $^{-1}$): 1626, 1715, 2247, 2856, 2943, 3398. ^{1}H NMR ($CDCl_3$, 400 MHz) δ: 0.89 (3H, s, 18-CH3), 1.07 (3H, s, 19-CH3), 2.89 (1H, d, *J*= 4.5 Hz, 6-CH), 3.90-3.80 (1H, m, 3-CH), 7.21 (1H, t, *J*= 7.9, H_{ar}), 7.36 (1H, d, *J*= 7.8 Hz, H_{ar}), 7.41 (1H, d, *J*= 7.8 Hz, H_{ar}), 7.67 (1H, s, H_{vin}). ^{13}C NMR ($CDCl_3$, 101 MHz) δ: 14.19, 15.98, 20.02, 27.86, 28.81, 29.22, 31.06, 31.17, 32.36, 35.36, 35.12, 39.74, 42.78, 47.71, 49.74, 58.61, 65.66, 68.53, 126.91, 127.87, 129.41, 130.60, 133.67, 133.92, 136.06, 138.80, 208.09. HRMS (ESI-TOF) m/z: $[M + H]^+$ Calcd for $C_{26}H_{30}Cl_2O_3S$ 460.1772; Found 460.1716.

*16E-(Furan-2'-ylmethylene)-3β-hydroxy-5α,6α-epoxyandrostan-17-one (**VB 9f**)*

Yellow powder (92 %); m.p. 175-177 °C; IR (cm $^{-1}$): 1692, 1708, 2870, 2944, 3162. ^{1}H NMR ($CDCl_3$, 400 MHz) δ: 0.85 (3H, s, 18-CH_3), 1.10 (3H, s, 19-CH_3), 2.99 (1H, dd, *J*= 15.84, 6.5 Hz, 6-CH), 3.94-3.84 (1H, m, 3-CH), 6.48 (1H, m, H_{ar}), 6.66 (1H, d, *J*= 3.4 Hz, H_{ar}), 7.16 (1H, t, *J*= 2.2 Hz, H_{ar}), 7.54 (1H, s, H_{vin}). ^{13}C NMR ($CDCl_3$, 101 MHz) δ: 14.38, 15.98, 20.08, 27.91, 28.71, 29.20, 31.07, 31.17, 32.39, 35.14, 39.78, 42.88, 47.53, 49.52, 58.79, 65.75, 68.58, 112.37, 115.81, 119.73, 133.08, 144.80, 152.20, 209.24. HRMS (ESI-TOF) m/z: $[M + H]^+$ Calcd for $C_{24}H_{30}O_4$ 382.2244; Found 382.2260.

*16E-[(5'-Methylfuran-2'-yl)methylene]-3β-hydroxy-5α,6α-epoxyandrostan-17-one (**VB 9g**)*

Orange powder (90 %); m.p. 153-154 °C; IR (cm $^{-1}$): 1578, 1624, 1708, 2869, 2942. ^{1}H NMR ($CDCl_3$, 400 MHz) δ: 0.80 (3H, s, 18-CH_3), 1.05 (3H, s, 19-CH_3), 2.30 (3H, s, 5'-CH_3), 2.91 (1H, d, *J*= 4.4 Hz, 6-CH), 3.90-3.80 (1H, m, 3-CH), 6.05 (1H, d, *J*= 3.3 Hz, H_{ar}), 6.49 (1H, d, *J*= 3.3 Hz, H_{ar}), 7.06 (1H, s, H_{vin}). ^{13}C NMR ($CDCl_3$, 101 MHz) δ: 14.10, 14.42, 15.99, 20.08, 27.91, 28.67, 29.17, 31.04, 31.18, 32.38, 35.14, 39.75, 42.88, 47.51, 49.65, 58.84, 60.43, 65.84, 68.59, 109.01, 117.51, 119.99, 131.35, 150.74, 155.53, 209.40. HRMS (ESI-TOF) m/z: $[M + H]^+$ Calcd for $C_{25}H_{32}O_4$ 396.2300; Found 396.2297.

*16E-(2',4'-Dichlorobenzylidene)-3β-hydroxy-5α,6α-epoxyandrostan-17-one (**VB 9h**)*

Yellow powder (91 %); m.p. 140-141 °C; IR (cm $^{-1}$): 1582, 1628, 1720, 2245, 2860, 2937, 3418. ^{1}H NMR ($CDCl_3$, 400 MHz) δ: 0.90 (3H, s, 18-CH_3), 1.09 (3H, s, 19-CH_3), 2.92 (1H, d, *J*= 4.4 Hz, 6-CH), 3.94-3.84 (1H, m, 3-CH), 7.29-7.25 (1H, m, H_{ar}), 7.46-7.39 (2H, m, H_{ar}), 7.66 (1H, s, H_{vin}). ^{13}C NMR ($CDCl_3$, 101 MHz) δ: 14.19, 15.98, 20.02, 27.84, 29.20, 31.03, 31.16, 32.35, 35.13, 39.71, 42.77, 47.63, 49.80, 58.62, 60.43, 65.70, 68.55, 127.01, 129.97, 130.47, 135.32, 136.46, 138.25, 208.16. HRMS (ESI-TOF) m/z: $[M + H]^+$ Calcd for $C_{26}H_{30}Cl_2O_3S$ 460.1572; Found 460.1605.

*16E-(4'-Methylbenzylidene)-3β-hydroxy-5α,6α-epoxyandrostan-17-one (**VB 9i**)*

Pallid yellow powder (92 %); m.p. 228-230 °C; IR (cm $^{-1}$): 1608, 1631, 1714, 2861, 2943, 3227. ^{1}H NMR ($CDCl_3$, 400 MHz) δ: 0.84 (3H, s, 18-CH_3), 1.06 (3H, s, 19-CH_3), 2.32 (3H, s, 4'-CH_3), 2.89 (1H, d, *J*= 4.3 Hz, 6-CH), 3.90-3.80 (1H, m, 3-CH), 7.15 (12H, d, *J*= 7.7 Hz, H_{ar}), 7.34 (3H, m, H_{ar}+H_{vin}). ^{13}C NMR ($CDCl_3$, 101 MHz) δ: 14.30, 15.98, 20.06, 21.49, 27.87, 29.22, 31.03, 31.19, 32.37, 35.13, 39.75, 40.88, 42.40, 42.86, 49.99, 58.76, 65.79, 68.54, 129.47, 130.37, 132.72, 133.38, 134.60, 139.71, 209.45. HRMS (ESI-TOF) m/z: $[M + H]^+$ Calcd for $C_{27}H_{34}O_3$ 406.2507; Found 406.2557.

*16E-(2',3'-Difluorobenzylidene)-3β-hydroxy-5α,6α-epoxyandrostan-17-one (**VB 9j**)*

Yellow powder (71 %); m.p. 140-141 °C; IR (cm $^{-1}$): 16301, 1720, 2933, 3225, 3370, 3549. ^{1}H NMR ($CDCl_3$, 400 MHz) δ: 0.89 (3H, s, 18-CH_3), 1.09 (3H, s, 19-CH_3), 2.92 (1H, d, *J*= 4.4 Hz, 6-CH), 3.92-3.82 (1H, m, 3-CH), 7.18-7.05 (1H, m, H_{ar}), 7.22 (1H, d, *J*= 6.1 Hz, H_{ar}), 7.53 (1H, s, H_{vin}). ^{13}C NMR ($CDCl_3$, 101 MHz) δ: 14.19, 15.95, 20.03, 27.85, 29.09, 29.20, 30.99, 31.15, 32.33, 35.13, 39.68, 42.80, 47.60, 49.56, 58.70, 65.84, 68.50, 117.79, 117.99, 120.73, 123.85, 124.18, 124.75, 125.80, 138.79, 208.33. HRMS (ESI-TOF) m/z: $[M + H]^+$ Calcd for $C_{26}H_{30}F_2O_3$ 428.2163; Found 428.2239.

*16E-(4'-Bromobenzylidene)-3β-hydroxy-5α,6α-epoxyandrostan-17-one (**VB 9k**)*

Yellow powder (77 %); m.p. 192-193 °C; IR (cm $^{-1}$): 1586, 1637, 1715, 2861, 2942, 3226. ^{1}H NMR ($CDCl_3$, 400 MHz) δ: 0.86 (3H, s, 18-CH_3), 1.08 (3H, s, 19-CH_3), 2.92 (1H, d, *J*= 4.4 Hz, 6-CH), 3.90-3.80 (1H, m, 3-CH), 7.30 (1H, s, H_{vin}), 7.33 (1H, d, *J*= 8.5 Hz, H_{ar}), 7.50 (2H, d, *J*= 8.5 Hz, H_{ar}). ^{13}C NMR ($CDCl_3$, 101 MHz) δ: 14.23, 15.97, 20.06, 27.86, 29.21, 30.95, 31.17, 32.40, 35.17, 39.68, 42.80, 47.49, 49.82, 58.74, 65.86, 69.40, 123.54, 131.62, 131.91, 132.02, 134.42, 136.20, 209.04. HRMS (ESI-TOF) m/z: $[M + H]^+$ Calcd for $C_{26}H_{31}BrO_3$ 470.1456; Found 470.1471.

*16E-[(5'-Chlorothiophen-2'-yl)methylene]-3β-hydroxy-5α,6α-epoxyandrostan-17-one (**VB 9l**)*

Beige powder (91 %); m.p. 119-120 °C; IR (cm $^{-1}$): 1680, 1709, 2245, 2859, 2933, 3288. ^{1}H NMR ($CDCl_3$, 400 MHz) δ: 0.82 (3H, s, 18-CH_3), 1.07 (3H, s, 19-CH_3), 2.94 (1H, d, *J*= 4.4 Hz, 6-CH), 3.90-3.80 (1H, m, 3-CH), 6.90 (1H, d, *J*= 3.9 Hz, H_{ar}), 7.05 (1H, d, *J*= 3.9 Hz, H_{ar}), 7.40 (1H, s, H_{vin}). ^{13}C NMR ($CDCl_3$, 101 MHz) δ: 14.39, 15.95, 19.99, 27.85, 28.66, 29.17, 30.95, 31.14, 32.35, 35.15, 39.69, 42.85, 47.81, 49.68, 58.73, 65.84, 68.43, 125.58, 127.16, 131.82, 133.40, 134.56, 138.65, 208.75. HRMS (ESI-TOF) m/z: $[M + H]^+$ Calcd for $C_{24}H_{39}ClO_3S$ 432.1525; Found 432.153.

*16E-[(5'-Chlorofuran-2'-yl)methylene]-3β-hydroxy-5α,6α-epoxyandrostan-17-one (**VB 9m**)*

Pallid orange powder (72 %); m.p. 185-187 °C; IR (cm $^{-1}$): 1624, 1710, 2246, 2850, 2940, 3400. ^{1}H NMR ($CDCl_3$, 400 MHz) δ: 0.80 (3H, s, 18-CH_3), 1.05 (3H, s, 19-CH_3), 2.92 (1H, d, *J*= 4.2 Hz, 6-CH), 3.90-3.80 (1H, m, 3-CH), 6.23 (1H, d, *J*= 3.4 Hz, H_{ar}), 6.54 (1H, d, *J*= 3.4 Hz, H_{ar}), 6.70 (1H, s, H_{vin}). ^{13}C NMR ($CDCl_3$, 101 MHz) δ: 14.31, 15.94, 18.44, 20.05, 27.88, 28.60, 29.16, 31.05, 32.40, 35.13, 39.77, 42.87, 47.53, 49.49, 58.46, 58.79, 65.74, 68.58, 109.23, 117.55, 118.67, 133.48, 139.19, 151.73, 208.98. HRMS (ESI-TOF) m/z: $[M + H]^+$ Calcd for $C_{24}H_{29}ClO_4$ 416.1754; Found 416.1785.

3.3.3. Biological evaluation

3.3.3.1. Cell culture

LNCaP, PC-3, MCF-7, PNT1A, and NHDF cells were obtained from American Type Culture Collection (ATCC; Manassas, VA, USA) and were cultured in 75 cm^2 culture flasks at 37 °C in a humidified air incubator with 5 % CO_2. LNCaP, PC-3, and PNT1A cells, which were used in passages 21st to 28th, 23rd to 27th and 3rd to 7th, respectively, were cultured in RPMI 1640 medium (Sigma-Aldrich, Inc. St. Louis, USA) with 10 % fetal bovine serum (FBS; Sigma-Aldrich, Inc. St. Louis, USA) and 1 % of the antibiotic mixture of 10,000 U/mL penicillin G and 100 mg/mL of streptomycin (Sp, Sigma-Aldrich, Inc. St. Louis, USA). MCF-7 cells were cultured in DMEM medium (Sigma-Aldrich, Inc. St. Louis, USA) supplemented with 10 % fetal bovine serum (FBS; Sigma-Aldrich, Inc. St. Louis, USA) and 1 % of antibiotic/antimycotic (10,000 U/mL penicillin G, 100 mg/mL streptomycin and 25 μg/mL amphotericin B: Ab, Sigma-Aldrich, Inc. St. Louis, USA) and these cells were used in passages 15th to 20th. Finally, NHDF cells were cultured in RPMI 1640 medium supplemented with 10 % FBS, 2 mM *L*-glutamine, 10 mM HEPES, 1 mM sodium pyruvate and 1 % of the antibiotic/antimycotic Ab and these cells were used in passages 10th to 14th. For all cell types, the medium was renewed every 2 days until cells reach nearly the confluence state. When cells reach approximately 90-95 % confluence, they were detached gently by trypsinization (trypsin-EDTA solution: 0.125 g/L of trypsin and 0.02 g/L of EDTA). Before of each experiment, viable cells were counted, in a Neubauer chamber by a trypan-blue exclusion assay and adequately diluted in the appropriate complete cell culture medium.

3.3.3.2. Preparation of compounds solutions

All tested compounds were dissolved in DMSO (Sigma-Aldrich, Inc. St. Louis, USA) in a concentration of 10 mM and stored at 4 °C. From the mother-solutions, the diluted solutions of the compounds, in different concentrations, were prepared in the respective complete culture medium before each experiment. The maximum level of DMSO concentration in the studies was 1 % and previous studies demonstrated that this concentration has no relevant effects on cell proliferation (data not shown).

3.3.3.3. MTT cell proliferation assay

After reaching a confluence state, cells were trypsinized and counted by the trypan-blue exclusion assay and then cells were seeded with an initial density of 2×10^4 cells/mL in 96-well culture plates (Nunc, Apogent, Denmark) and left to adhere and grow for 48 h. Subsequently, the medium was removed, and the cells were treated with diluted compounds solutions (10 and 50 μM for preliminary studies and 0.01, 0.1, 1, 10, 50 and

100 μM for concentration-response studies) for 72 h. 5-FU was used as positive control and untreated cells were used as the negative control. At the screening studies, in tumoral lines, compounds presenting cell proliferation relative to control lower than 50 %, at 10 μM, or below 25 %, at 10 μM, were selected to concentration-response studies. Each experiment was performed in quadruplicate and independently performed at least two times. The *in vitro* antiproliferative effects were evaluated by the MTT assay (Sigma-Aldrich, Inc. St. Louis, USA). After the incubation period, the medium was removed and 100 μL of phosphate buffer saline (PBS, NaCl 137 mM; KCl 2.7 mM, Na_2HPO_4 10 mM and KH_2PO_4 1.8 mM in deionized water and pH adjusted to 7.4) were used to wash the cells. Then 100 μL of the MTT solution (5 mg/mL) was prepared in the appropriate serum-free medium and was added to each well, followed by incubation for 4 h at 37 °C. Hereafter, the MTT containing medium was removed and the formazan crystals were dissolved in DMSO. Then the absorbance was measured at 570 nm using a xMarkTM microplate spectrophotometer from BIO-RAD Laboratories. Cell viability values were expressed as percentages relatively to the negative control.

3.3.3.4. Immunocytochemistry assay

MCF-7 cells were trypsinized and counted by the trypan-blue exclusion assay and then cells were seeded with an initial density of 3×10^4 cells/mL in 24-well culture plates (Nunc, Apogent, Denmark) containing circular coverslips of 10 mm diameter. Following seeding (48 h), cells were treated with a 1 and 10 μM concentrations of 5-FU, as positive control, and **VB 9e** for 48 h. Untreated cells were used as a negative control. After this period, photograph shots were acquired at an optical microscope coupled with a digital camera (**Appendix 5**, **Figure Ap 12**). Subsequently, the medium was removed, and cells were fixed with were fixed with 4 % formalin (15 min, r.t.). After fixation, cells were washed three times with PBS, permeabilized and blocked for non-specific binding sites for 1 h with 0.5 % Triton X-100 and 6 % BSA. Cells were incubated at 4 °C with 30 μL/coverslip of primary antibody, rabbit polyclonal anti-Ki67 (1:50, Abcam Plc.), prepared in 0.3 % BSA and 0.1 % Triton X-100, during 24 h. Then, cells were washed three times with PBS and incubated for 1 h, r.t., with 30 μL/coverslip of a solution containing the secondary antibody, Alexa Fluor 488 donkey anti-rabbit (1:200, Life Technologies), and the nuclear marker Hoechst-33342 (1:500, Life Technologies) prepared in PBS. Lastly, the coverslips were washed three times with PBS and mounted on a drop of the fluoroshield mounting medium (Abcam, Plc.) on a microscope slide and left dry for 24 h. Photomicrographs were taken using an Axio Imager A1 microscope (Carl Zeiss, Göttingen, Germany) with the 40× objective. The staining procedure and the visualization was performed in the dark.

3.3.3.5. Propidium iodide incorporation

After 48 h of being seeded at the same conditions explained in the previous section (2.2.4), MCF-7 cells were treated with the steroidal derivative **VB 9e** and 5-FU at 1 and 10 μM and maintained in culture for 48 h. Untreated cells were also used as a negative control. Subsequently, cells were incubated with 20 μL/per well of a propidium iodide solution (PI; 1 mg/mL in PBS; Sigma-Aldrich Co. LLC) for 25 min at 37 ºC, in the dark. Then, the medium was removed, and the cells were fixed with 4 % formalin at r.t. for 15 min. Cells were washed three times with PBS and incubated with 30 μL/per coverslip of Hoechst-33342 (1:500) for 10 min (in the dark). After incubation, cells were washed three times with PBS. Coverslips were mounted on a drop of the fluoroshield mounting medium on a microscope slide, left dry for 24 h, and then visualized in a Zeiss Axio Imager A1 microscope with the 40× objective.

3.3.3.6. Analysis of cell nuclear morphology and distribution using ImageJ

The nuclear measurements were achieved by converting 16-bit photomicrographs of Hoechst 33342-stained nuclei, in different studied conditions, into 8-bit images. Then, these imagens were autothresholded to binary photos using the default method "Make binary" function of ImageJ (v. 1.49) software (NIH Image, Bethesda, MD, USA). Cell nuclei that are touching were separated and fragments were discarded on the basis of area through "Analyze Particle" function. This function also provides several information as nuclear area, circumference and form factor [472]. Furthermore, the "Nearest Neighbor Distance" was determined. This function allows to measure the distance between each cell nucleus and the nearest ones, providing information about cell distribution.

3.3.3.7. Statistical analysis

The MTT results are representative of at least two independent experiments (N ≥ 2), comprising each one four replicates (n = 4). The data are expressed as mean±standard deviation (SD). The analysis of immunocytochemistry and cell nuclear morphology and distribution experiments were performed at the border of the coverslips, where cells formed a pseudo monolayer. The experiments were performed in at least two independent cultures (N ≥ 2, n =2) and the results are expressed as mean ± standard error of mean (SEM). All statistical significances were determined with GraphPad Prism 6 software (GraphPad, San Diego, CA, USA) by using ANOVA followed by Dunnett's or Bonferroni's test or unpaired two tailed Student's t-test. Differences between groups were considered statistically significant for a p-value lower than 0.05 (p< 0.05).

3.3.4. Molecular docking

3.3.4.1. Preparation of macromolecules and ligands

The 3D structural coordinates of 5AR type 2 (PDB ID: 7BW1), ERα (PDB ID: 1A52), AR (PDB ID: 2AMA), CYP17A1 (PDB ID: 3RUK) and aromatase (PDB ID: 3EQM) were retrieved from Protein Data Bank site (www.rcsb.org). The coordinates of the co-crystalized ligands and water molecules were deleted using the software Chimera (v. 1.10.1) and histidine charges were defined to match physiologic environment and the final structures were saved in PDB format. Then, non-polar hydrogens were merged in AutoDockTools (v. 1.5.6) from The Scripps Research Institute.[509] Kollman and Gasteiger partial charges were added in the same software. Lastly, the prepared structures were converted from the PDB format to PDBQT. All ligands were drawn using Chem3D Pro (v. 12.0) software (by Cambridge ChemBioOffice 2010). Then the energies were minimized, and the geometry was optimized (MMFF94 force field: 500 steps of conjugate gradient energy minimization followed by 500 steps of steepest descent energy minimization with a convergence setting of 10×10^{-7}) with the software Avogadro (v. 1.0.1) and the final structures were saved as PDB file format. The ligands were completely prepared choosing torsions and the structures were converted form PDB format to PDBQT, in AutoDockTools.

3.3.4.2. Grid map parameters

The grid parameters were determined using AutoDockTools based on the coordinates of the ligand crystallized of each complex macromolecule-ligand, namely NADP-DHF, estradiol, DHT, abiraterone and androstenedione, with the respective macromolecule. The grid box was centered on the ligand with the following coordinates: 5AR type 2 coordinates were x= −27.450, y= 15.112, z= 31.795; ERα coordinates were x= 90.36, y= 13.681, z= 72.011; AR coordinates were x= 27.603, y= 1.834, z = 4.722; CYP17A1 coordinates were x= 27.256, y= −0.978, z= 33.104 and aromatase coordinates were x= 86.071, y= 54.241, z= 46.085. The size of the grid box was 20 × 20 × 20 with a spacing of 1.0 Å.

3.3.4.3. Method validation and molecular docking simulations

Scoring functions are essential for molecular docking performance. In order to verify those functions, it is necessary to validate the docking performance of AutoDock Vina. This step is required to verify the performance by analysis of the difference between the real and best-scored conformations. For the docking process to be considered successful, the root-mean-square distance (RMSD) value between those two conformations must be

less than 2.0 Å. In this case, the validation method was performed by re-docking 5AR type 2 with NADP-DHF adduct, ERα with estradiol, AR with DHT, CYP17A1 with abiraterone and aromatase with androstenedione. Low RMSD values were obtained for all cases, which means that the docking process was reliable and validated. After ligands and protein preparation, as well as method validation, molecular docking was performed by AutoDock Vina executable, which uses an iterated local search global optimizer. The parameter exhaustiveness of the performed experiments was defined as 15. The results of molecular docking were visualized in Discovery Studio Visualizer (v. 5.0) program from BIOVIA and in PyMol (v. 1.1) software.

CHAPTER IV

4. Synthesis, antiproliferative activity and *in silico* studies of new series of steroidal 3β,5α,6β-triols and 4-ene-3,6,17-triones

4.1. Introduction

In the past two decades, high attention has been given to non-azasteroids as 5ARIs to overcome the main side effects of clinical approved 4-azasteroids.[24,81] In this context, for oxidized steroids, beyond the steroidal epoxides already explored in the previous chapter, interesting results were also observed. Progesterone, 16-dehydropregnenolone, and DHEA derivatives emerged as the main oxidized steroidal compounds modified at rings A and B (e.g. steroidal 3,6-diones) with relevant 5AR inhibitor activity, and thus potentially useful in prostatic disorders.[486,487,510,511] However, information about the antiproliferative effects of these derivatives in tumoral cells, principally in prostatic cell lines, is practically non-existent. Consequently, an opportunity of research in this ambit is, in fact, quite evident. In this scope, a recent study achieved by Chávez-Riveros and colleagues described the synthesis and cytotoxic effect of pregnenolone derivatives with two α,β-unsaturated ketones at C-3 and C-6 and. Among the prepared and evaluated compounds, the α,β-unsaturated diketone analogs with a benzoic acid ester moiety (**Figure 43-A**) and with a 4-fluorinated benzoic acid ester moiety (**Figure 43-B**) exhibited exciting results against PC-3 cells, inhibiting the proliferation by ≈ 58 and ≈ 98 %, respectively, at 50 μM.[483] Considering this interesting result, further studies of the effects on tumoral cells proliferation of steroidal oxidized derivatives at rings A and B are, in fact, promising. In addition, the same research group reported in other study the assessment of the effects of the oxidized (*p*-fluoro)benzoyloxy 21-esters of pregnenolone as inhibitors of 5AR type 1 and 2. In this scope, *in vitro* and *in vivo* experiments were performed, and results showed that 21(*p*-fluoro)benzoyloxypregna-4,16-diene-3,6,20-trione had the capacity to *in vitro* inhibit the activity of both isozymes, being a dual 5ARI (**Figure 43-B**). Moreover, this compound also displayed *in vivo* activity since when administrated in combination with testosterone to castrated hamsters, it significantly decreased the weight of the prostate and seminal vesicles. In contrast, the derivative

21(*p*-fluoro)benzoyloxy-5α-hydroxypregna-16-en-3,6,20-trione exhibited selective inhibition of 5AR type 2 (**Figure 43-C**).[486]

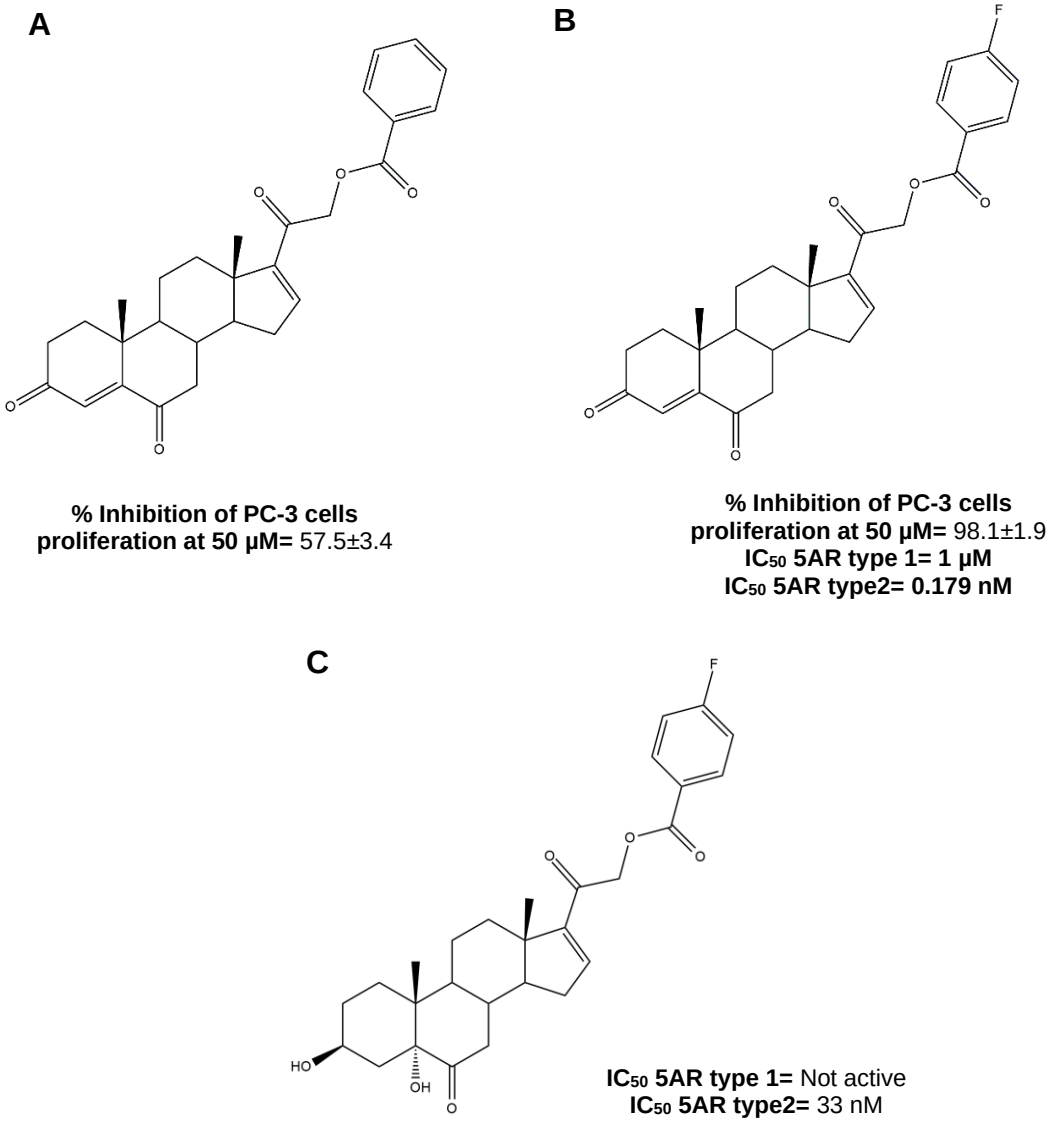

Figure 43. Representative examples of oxidized pregnenolone derivatives with relevant antiproliferative activity against PC-3 cells and/or with important 5α-reductase (5AR) inhibitory activity. (**A**) 21-benzoyloxypregna-4,16-diene-3,6,20-trione, (**B**) 21(*p*-fluoro)benzoyloxypregna-4,16-diene-3,6,20-trione and (**C**) 21(*p*-fluoro)benzoyloxy-5α-hydroxypregn-16-en-3,6,20-trione derivatives and respective percentage (%) of inhibition of PC-3 cell proliferation at 50 μM and/or IC_{50} values against 5AR type 1 and 2. Created with ChemDraw.

In the previous chapter, several 16*E*-arylideneandrost-5-ene derivatives were stereoselectively epoxidized at C5=C6. Then, a set of studies to clarify their effects on cells proliferation were performed and some promising results were observed. Consequently, considering the importance of oxidized steroids even as potential 5ARIs and the possibility of modifying the synthesized epoxysteroids **VB 9a-m**, it was decided to prepare new series of steroidal 3β,5α,6β-triols and 4-ene-3,6,17-triones considering

the most active steroidal epoxides accordingly to the results reported in **Chapter III**. Similar to the described in the last chapters, these new compounds were also subject to a set of biological assays to evaluate their effects on cell proliferation. In addition, the affinity of these steroids against main targets of steroids were assessed in silico.

4.2. Results and discussion

4.2.1. Chemical synthesis

The preparation of new series of steroidal 3β,5α,6β-triols and 4-ene-3,6,17-triones was achieved as shown in **Figure 44**. The six most potent epoxysteroids (with relevant effect on proliferation of tumoral cells) described in the previous chapter were used as starting material in this synthetic pathway (**VB 9a**, **VB 9e**, **VB 9h**, **VB 9i**, **VB 9l**, and **VB 9m**) to obtain steroidal 3β,5α,6β-triols. Based on the simple and effective procedure described by Bernardo-Otero et al., initially, the synthesis of new steroidal 3β,5α,6β-triols (**VB 10a-f**) was accomplished by mixing the correspondent substrate, the aforementioned epoxysteroids, with perchloric acid ($HClO_4$) in acetone/water at r.t. for approximately 5 h.[512] The desired *trans*-diols (5α-OH and 6β-OH) were obtained in excellent yields (82–95 %) – **Table 16.** The opening of 5,6-epoxides, independently of their stereochemistry, as expectable is stereoselective affording 5α,6β-vicinal diols. The steric hindrance, resulting from the presence of the two angular groups (C-10 and C-13) on the steroid nucleus (substrate of reaction), leads to a *trans*-diaxial hydroxylation.[513] Although there are alternative procedures reported for the synthesis of trihydroxysteroids with very good yields, such as the one-pot synthesis from 3β-hydroxy-Δ^5-steroids (using MMPP in combination with an acidic catalyst) or the use of a bismuth (III) as a catalyst, the use of $HClO_4$ at very smooth conditions (r.t. and safe solvents) revealed to be the most appropriate in the present context.[488,513,514] Considering the availability of substrates (**VB 9** series) and reagents/solvents required for this approach in the laboratory, and the high yields also reported, this classic procedure using $HClO_4$ was selected.[512]

Applying the same criteria, to obtain new compounds with the arylidene group of the most potent epoxysteroids, the 16*E*-arylidene-3β-hydroxyandroste-5-en-17-ones **VB 8a**, **VB 8e**, **VB 8h**, **VB 8i**, **VB 8l**, **VB 8m** were oxidized in one step to afford the respective $\Delta^{4,5}$-unsaturated 3,6,17-triones.[515–517] Based on the procedure described by Denancé et al., the oxidation was accomplished using PPC reagent in DCM at r.t. under inert atmosphere (N_2) for 24 h.[515] Then, the crude resultant containing the respective steroidal triketone (**VB 11a-f**) was purified by column chromatography (2:1 AE/PE 40-60 ˚C). These products were synthesized in reasonable yields (53–70 %) in accordance with the

reported in the literature, with exception of **VB 11a** (20 %) (**Table 17**).[515,517] Probably, this low and unexpected yield is related to the purification step, where some of the product is invariably lost. In relation to the procedure applied, this synthetic approach using PCC as the oxidant agent in DCM constitute an advantage method since it afforded in one-step the desired final products. In contrast, some alternative procedures described this oxidation in multiple steps, which leads to lower global yields, and the use of less safe reagents (e.g. pyridine).[483,487]

All synthesized compounds were examined by means of m.p., IR and NMR spectroscopy and the new described steroids (**VB 10a-f** and **VB 11a-f**) were subjected to HRMS analysis. The NMR spectral assignments for the steroids were based on previously reported data from similar steroids.[483,518] From the proton NMR spectra analysis, the formation of steroidal triols **VB 10a-f** was proved by the presence of a signal relative to 6-CH at ≈ 4.03 ppm, which presents lower deviation than the 6-CH of the epoxysteroids (≈ 2.90 ppm). After oxidation of **VB 8a**, **VB 8e**, **VB 8h**, **VB 8i**, **VB 8l**, **VB 8m** with PCC and purification of respective products **VB 11a-f**, the vinylic proton peak of 4-CH appeared as a singlet at ≈ 6.15 ppm and, it was also observed the absence of the signals correspondent to 3-CH and 6-CH protons. Concerning the triketones, carbon NMR spectra clearly showed the formation of the ketone groups at C-3 and C-6, presenting new two peaks with high deviation at around 199 and 200 ppm.

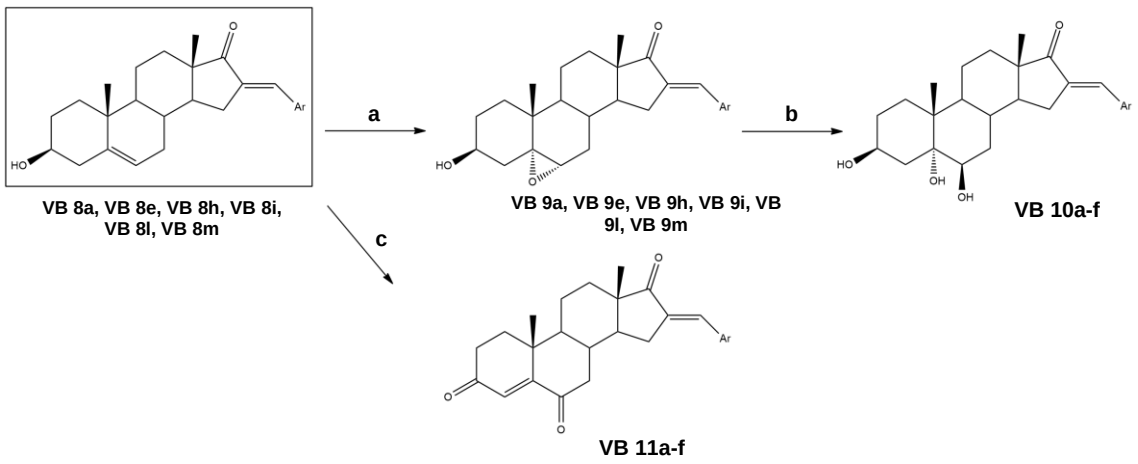

Figure 44. Synthetic pathway to obtain new steroidal 3β,5α,6β-triols (**VB 10a-f**) and 4-ene-3,6,17-triones (**VB 11a-f**). Reagents and conditions: **a)** MMPP, DCM/water, 5 ˚C, 24-30 h; **b)** $HClO_4$, acetone/water, r.t., 5 h; **c)** PCC, DMC, r.t., N_2, 24 h. (PCC= Pyridinium chlorochromate, DCM= dichloromethane). Created with ChemDraw.

Table 17. Corresponding Ar-CHO groups, steroidal 3β,5α,6β-triols (**VB 10a-f**) and final products 4-ene-3,6,17-triones (**VB 11a-f**) with respective yields. Molecular structures created with ChemDraw.

Ar-CHO	3β,5α,6β-triols	Yield (%)[a]	4-ene-3,6,17-triones	Yield (%)[b]
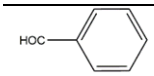	**VB 10a**	82	**VB 11a**	20
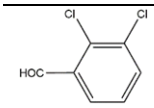	**VB 10b**	94	**VB 11b**	58
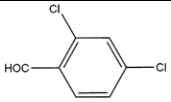	**VB 10c**	95	**VB 11c**	60
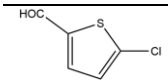	**VB 10d**	88	**VB 11d**	57
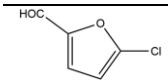	**VB 10e**	91	**VB 11e**	70
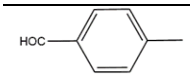	**VB 10f**	94	**VB 11f**	53

[a] This yield is only representative of the reaction of epoxide opening.
[b] This yield is only representative of the reaction of oxidation with PCC.

4.2.2. Biological evaluation

4.2.2.1. Antiproliferative activity

Similar to **Chapter II**, the assessment of the synthesized compounds' effects on proliferation of tumoral and non-tumoral cell lines (NHDF, PNT1A, LNCaP, PC-3, and MCF-7) was primarily performed via MTT assay (full data presented on the **Appendix 4**, **Table Ap 6**). Firstly, cells were exposed to steroids **VB 10a-f** and **VB 11a-f** at the concentration of 10 and 50 μM for 72 h. As previously, 5-FU was included in the assay as a clinically used antitumoral agent (positive control). In **Figure 45** are shown the results of this preliminary study.

After the preliminary study, it was observed that compounds **VB 10a**, **VB 10d**, **VB 10e**, and **VB 10f** did not display considerable effect in NDHF proliferation at the two tested concentrations. In the other hand, PNT1A cells seemed to be generally more sensitive to these steroids than NHDF, showing statistically significant decrease in proliferation compared to control in almost all cases. In general, a stronger effect on non-tumoral cell proliferation is observed at the higher concentration.

Comparing these results with the study reported by Chávez-Riveros et al., described in the **Introduction** of this chapter, some of them should be highlighted.[483] The referred research work reported two steroidal triones (within four triones) with important cytotoxic effect at 50 μM against PC-3 cells, inhibiting the proliferation by ≈ 58 and ≈ 98

%. At the same conditions, the triones reported in this thesis were all capable (with exception of **VB 11d**) of reduce cell proliferation at least by 50 %. For a more precise and correct comparation of the potency, the IC_{50} of compounds reported by Chávez-Riveros and coworkers should have been determined.

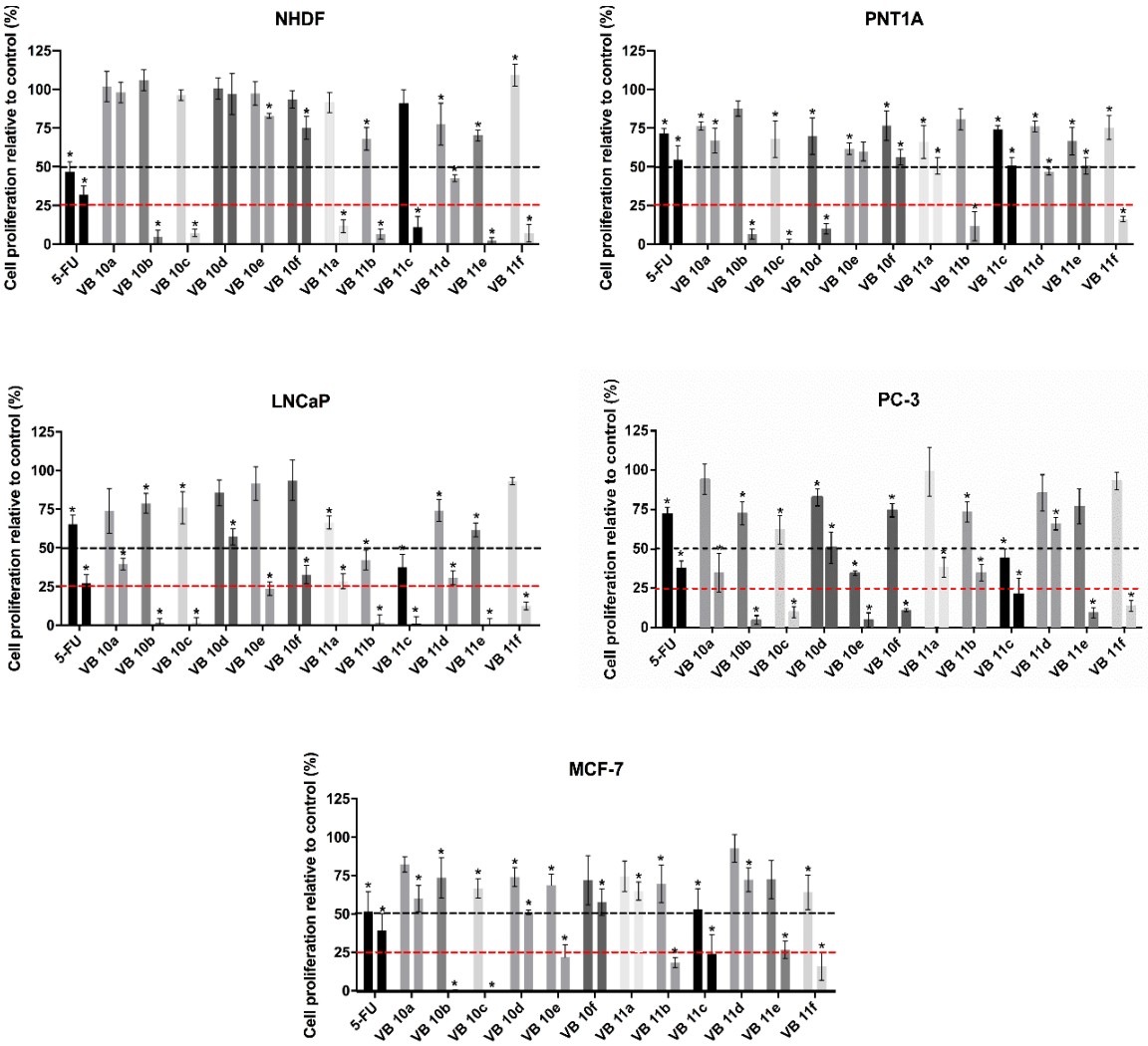

Figure 45. Results of preliminary studies of cell viability at two concentrations, 10 and 50 μM in NHDF, PNT1A, LNCaP, PC-3 and MCF-7 cell lines. The effect of all the synthesized final products, during 72 h, was evaluated and 5-fluorouracil (5-FU) was used as positive control. Data are indicated as mean±SD and are representative at least two independent experiments. **p*< 0.05 in relation to a negative control (Student's *t*-test).

Relative to prostate cells, LNCaP seemed to be more sensitive to these new compounds mainly to steroidal 4-ene-3,6,17-triones **VB 11b** and **VB 11c**. However, **VB 10b** and **VB 10c,** steroidal 3β,5α,6β-triols, also presented interesting effects at 50 μM (percentage of proliferation relative to control ≤ 25 %). On the other hand, the response of PC-3 cells to the treatment with these derivatives is more heterogeneous. Nevertheless, it is possible

observe that principally compounds **VB 10b**, **VB 10c**, **VB 10e**, **VB 10f**, **VB 11c**, **VB 11e,** and **VB 11f** exhibited strong effects on PC-3 proliferation at the higher concentration (percentage of proliferation relative to control ≤ 25 %). Lastly, **VB 10b** and **VB 10c** were the most potent compounds against MCF-7 cells at 50 μM, causing a percentage of relative cell proliferation near to 0 %. On the contrary, **VB 10a**, **VB 10d**, **VB 10f**, **VB 11a**, and **VB 11d** revealed weak effects on cell proliferation. In this case, the profile of the effect on this cell line of tested compounds with the same R group is similar.

Considering the results of the preliminary evaluation, concentration–response studies were performed for the most antiproliferative compounds (relative cell proliferation < 50 % at 10 μM or/and < 25 % at 50 μM) and 5-FU in all cell lines, in the same conditions described in the previous chapter (0.01, 0.1, 1, 10, 50 and 100 μM, 72 h). Considering the non-tumoral cells, IC_{50} values were determined for all compounds. The estimated values of IC_{50} are shown in **Table 18**, and some interesting results can be observed. Compound **VB 11c** in addition to the demonstrated selectivity for tumoral cells, is the most potent compound in LNCaP cell line, being the only compound with an IC_{50} value (6.48 μM) lower than the positive control [IC_{50}(5-FU) = 9.43 μM]. Against LNCaP, compound **VB 11b** also showed an interesting IC_{50} value (7.85 μM), however higher than the observed with 5-FU. Furthermore, compound **VB 10e** exhibited a clear selectivity for PC-3 cells, presenting its lowest IC_{50} value (6.96 μM) in this cell line and being also the most potent in comparison with other tested steroids. Concerning to MCF-7 cell line, all compounds exhibited estimated IC_{50} values significantly higher than the positive control (IC_{50}= 6.30 μM).

Table 18. Estimated IC_{50} values (μM) of **VB 10a-f**, **VB 11a-f** and 5-fluorouracil (5-FU) in non-tumoral cells: NHDF, PNT1A and in tumoral cells: LNCaP, PC-3, and MCF-7.

Compound	NHDF		PNT1A		LNCaP		PC-3		MCF-7	
	IC_{50}	r^2	IC_{50}	r^2	IC_{50}	r^2	IC_{50}	r^2	IC_{50}	r^2
5-FU	6.34	0.95	83.40	0.92	9.43	0.95	3.30	0.98	6.30	0.90
VB 10a	>100	-	97.74	0.86	-	-	44.44	0.99	-	-
VB 10b	41.84	0.94	40.82	0.99	40.38	0.95	18.18	0.99	19.71	0.96
VB 10c	29.23	0.99	26.83	0.99	25.49	0.99	14.06	0.99	18.28	0.95
VB 10d	60.37	0.96	21.02	0.94	-	-	-	-	-	-
VB 10e	82.17	0.94	67.14	0.96	45.68	0.96	6.96	0.98	45.98	0.95
VB 10f	66.60	0.92	88.29	0.92	-	-	27.02	0.97	-	-
VB 11a	47.18	0.87	45.98	0.96	15.65	0.94	-	-	-	-
VB 11b	29.78	0.97	18.10	0.96	7.85	0.99	-	-	22.05	0.81
VB 11c	34.17	0.97	47.56	0.93	6.48	0.99	9.79	0.99	16.03	0.96
VB 11d	43.31	0.85	50.31	0.96	-	-	-	-	-	-
VB 11e	17.24	0.98	48.17	0.98	11.88	0.99	18.19	0.98	24.06	0.92
VB 11f	33.18	0.92	35.10	0.97	29.36	0.99	33.08	0.99	26.90	0.92

4.2.2.2. Characterization of effects on cell proliferation

Bearing in mind the results of the MTT proliferation assay, the effects of the most potent compounds, **VB 10e** (IC_{50}= 6.48 μM) and **VB 11c** (IC_{50}= 6.96 μM), were assessed through several experiments in PC-3 and LNCaP cells, respectively. Firstly, in an attempt to obtain some evidence regarding the cell death mechanism, the analysis of changes in nuclear morphology and cell distribution was performed using ImageJ software. As explained in **Chapter III**, cell death can be categorized as apoptotic or necrotic or both, presenting distinct morphological characteristic.[504,519] Consequently, considering the characteristic changes in nuclear morphology during apoptosis, morphological features can be used as indicators of activation of programmed cell death. In the present study, the nuclear area (NA) and cell distribution through the nearest neighbor distance (NND) were analyzed as the main indicators of apoptosis.[472] Thus, LNCaP and PC-3 cells were treated with the tested compounds and positive control (5-FU) at 20 μM, for 24, 48, and 72 h. After these different periods, microphotographs were taken using an optical microscope, and a basic analysis of the cells morphology and density was performed. (**Figures 46** and **47**).

From this basic observation with optical microscope, it can be verified that exposure of LNCaP cells to **VB 11c** caused similar effects to 5-FU, the positive control, over time, including the morphological modifications and density (**Figure 46**). Under untreated conditions, these adherent cells present an epithelial morphology, and grow as single cells

and loosely attached clusters.[520] After exposure to compounds, these modifications are mainly characterized by the roundness of cells, the decrease of the cell area and volume, and the presence of pyknotic cells. At 24 h of exposure of both compounds, the alterations in cells were already detected. As expected, these alterations were more drastic at 72 h of exposure. Interestingly, no evidence of debris indicative of necrosis was observed in all tested conditions Concerning this preliminary evaluation and the morphological cells modifications observed, the hypothesis of cell death by apoptosis triggered by **VB 11c** was raised.

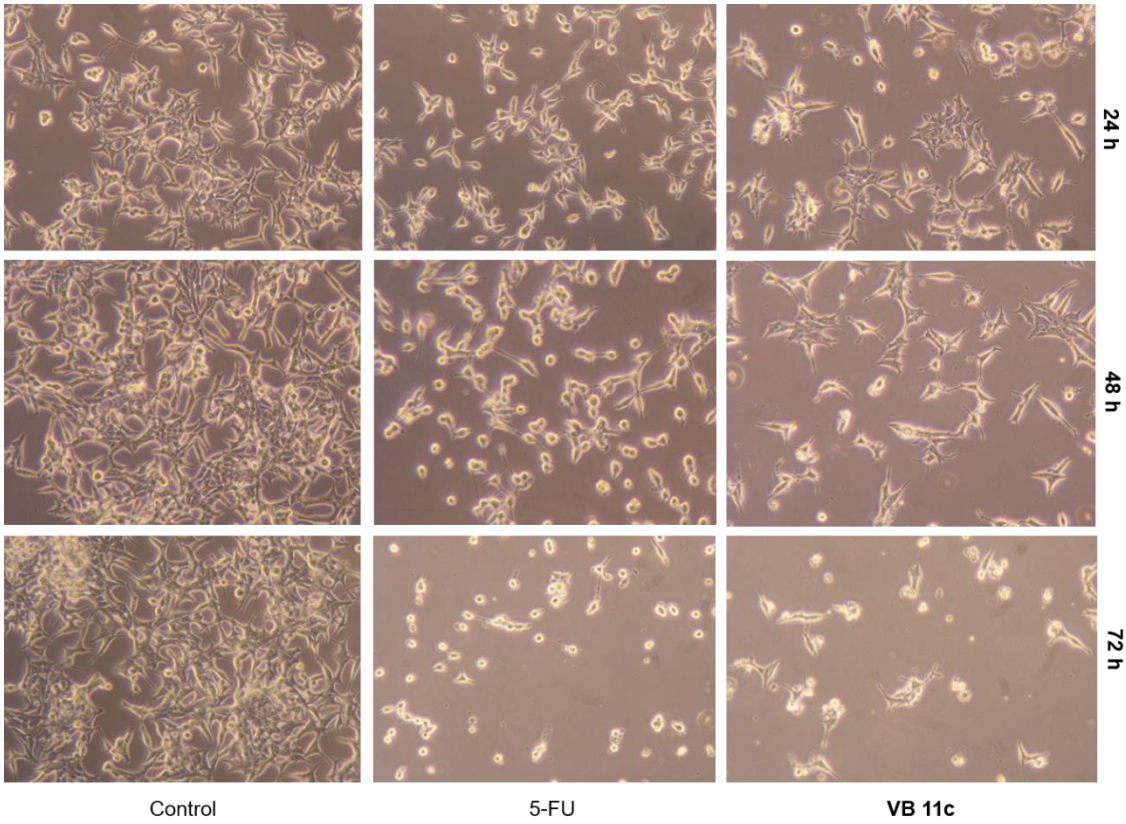

Figure 46. Microphotographs taken after incubation of LNCaP cells with 5-fluorouracil (5-FU) and **VB 11c** at 20 μM (24, 48, and 72 h). Untreated cells are considered the control of the experiment. Cells were visualized in an Optical microscope Olympus CKX41 coupled to a digital camera (Olympus SP-500UZ) (zoom 100 ×).

PC-3 adherent cells are characterized by an epithelial morphology, similarly to LNCaP cells.[521] Relative to the microscopic observation of PC-3 cells, morphologic alterations at different assay conditions are less evident than the observed in LNCaP cells. Additionally, when cells were treated with **VB 10e** and 5-FU the cellular density is apparently lower than the observed in untreated cells (control) after 48 and 72 h of incubation (**Figure 47**). Furthermore, exposure to **VB 10e** after these two periods seemed to cause less cellular density than the positive control. Nevertheless, no

morphological changes seemed to occur at the different tested conditions comparing with the control.

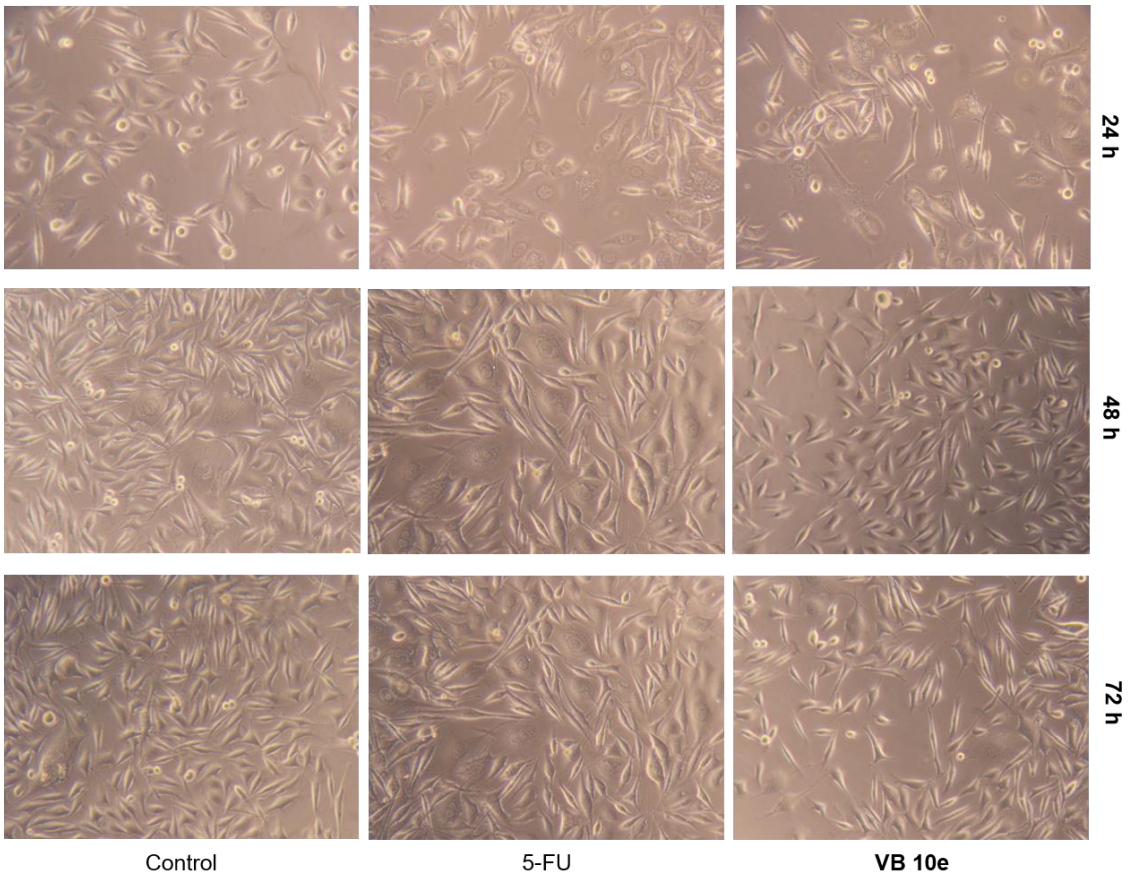

Figure 47. Microphotographs taken after incubation of PC-3 cells with 5-fluorouracil (5-FU) and **VB 10e** at 20 μM (24, 48, and 72 h). Untreated cells are considered the control of the experiment. Cells were visualized in an Optical microscope Olympus CKX41 coupled to a digital camera (Olympus SP-500UZ) (zoom 100 ×).

After the microphotographs were taken, cells were fixed, incubated with the nuclei marker, Hoescht-33342, treated, and visualized in a Axio Imager A1 microscope using a fluorescent filter. Then, photomicrographs were taken and processed in ImageJ software to quantitatively assess the nucleus morphology and cell distribution through the measure of NA and NND. The results obtained with LNCaP and PC-3 cell lines are depicted in **Figures 48** and **49**, respectively. After incubation with **VB 11c**, LNCaP cells presented NA values significantly lower than the control at 48 and 72 h of exposure (**Figure 48-A**). Additionally, comparing with the positive control, 5-FU, this NA reduction is statistically more significant. On the contrary, after 24 h of incubation, no significant differences in NA values were observed for both tested compounds. On the other hand, the NND analysis, as expected, showed a cell distribution significantly more spaced, indicating a lower cellular density after exposure of LNCaP cells to 5-FU and **VB**

11c for 48 and 72 h. Comparing to 5-FU, the effects relative to untreated control were more drastic when cells were incubated with the steroidal derivative (48 h, $p< 0.001$; 72 h, $p< 0.0001$). From this result, the hypothesis of cell death by apoptosis becomes more probable.

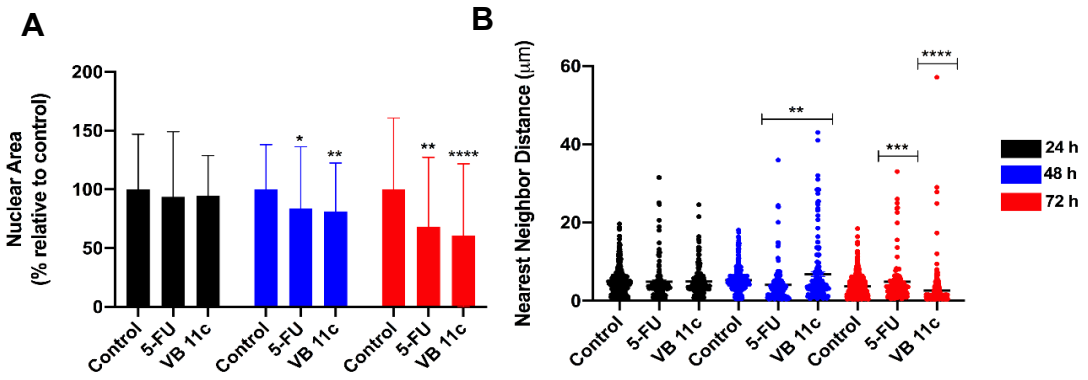

Figure 48. (**A**) LNCaP nuclear area of cells untreated (control) and cells treated with 5-fluorouracil (5-FU) and **VB 11c** at 20 µM, incubated during 24, 48, and 72 h; (**B**) Nearest neighbor analysis of LNCaP cells in the same conditions referred previously. Data are indicated as mean±SD and are representative at least two independent experiments. *$p< 0.05$, **$p< 0.01$, ***$p< 0.001$, ****$p< 0.0001$ compared to control (unpaired two tailed Student's *t*-test).

Relatively to PC-3 cells, it was verified that no statistically significant differences were observed in NA measurement after treatment with **VB 10e** and 5-FU over time (**Figure 49-A**). On the other hand, concerning the NND analysis, while 5-FU caused a significant increase in the NND only after 48 and 72 h of exposure, **VB 10e** triggered this increasing also at 24 h of incubation with PC-3 cells (**Figure 49-B**). This result is indicative of lower cellular density, corroborating the information acquired from the observation at the optical microscope. Overall, these results suggested that probably **VB 10e** caused proliferation inhibition instead of triggering a cell death mechanism.

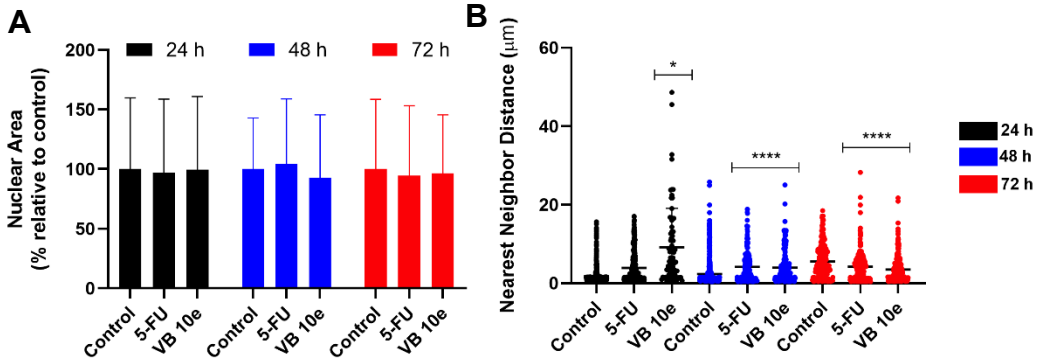

Figure 49. (**A**) PC-3 nuclear area of cells untreated (control) and cells treated with 5-fluorouracil (5-FU) and **VB 10e** at 20 µM, incubated during 24, 48 and 72 h; (**B**) Nearest neighbor analysis of PC-3 cells in the same conditions referred previously. Data are indicated as mean±SD and are representative at least two

independent experiments. *p< 0.05, **p< 0.01, ***p< 0.001, ****p< 0.0001 compared to control (unpaired two tailed Student's t-test).

Considering the previous results and looking for evidence of caspase-dependent apoptosis, the caspase 3/7 activity was evaluated using a Caspase-Glo kit from Promega to explore the possible mechanism of apoptotic death triggered by **VB 11c** in LNCaP cells. It is well known that caspases 3 and 7 have a crucial role in the apoptotic mechanism as effectors/executioner caspases. An executioner caspase, once activated, is able to cleave and activate other effector caspases, accelerating the response loop of caspase activation.[522–524] In this experiment, cells were exposed for 72 h to DOX at 5 μM and 5-FU at 20 μM, as positive controls, and to **VB 11c** at 10 and 20 μM, and the results obtained are shown in **Figure 50**. After 72 h of exposure, significant increase in caspase 3/7 activity was detected in cells treated with DOX, 5-FU and with both concentrations of **VB 11c**. Interestingly, DOX and **VB 11c** at 20 μM produced a very similar effect on caspase 3/7 activity, increasing the activity almost 5 times in comparison with control. These results constitute strong evidence that this steroid triggers the apoptotic mechanism of cell death in tested conditions.

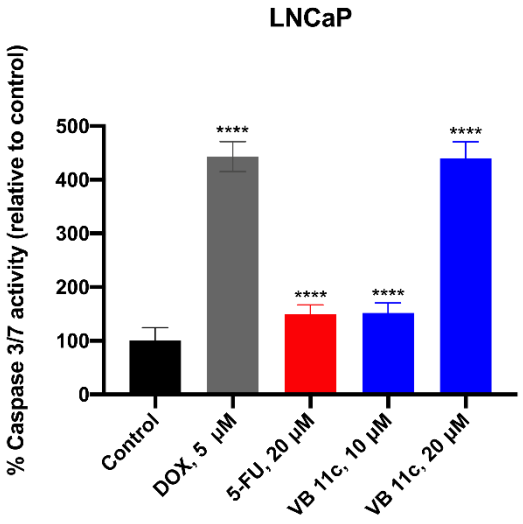

Figure 50. Assessment of apoptosis: Caspase-Glo® 3/7 assay results after 72 h of treatment with **VB 11c** at concentrations 10 and 20 μM, in LNCaP cells. Data are shown as mean percentage of caspase 3/7 activity referred to the untreated control (100 %)±SD. DOX and 5-FU were used as positive control. **** p< 0.001 (Student's t-test), N=2, n=4. (DOX= Doxorubicin, 5-FU= 5-Fluorouracil).

Bearing in mind all the results obtained from the biological evaluation, these oxidized steroids, 3β,5α,6β-triols and 4-ene-3,6,17-triones, constitute an important class of potential antiproliferative agents. Since the lack of biological studies in this context is evident, the investment on these compounds as a source of antitumor agents must be definitely carried out, comprising an interest field of new research projects.

4.2.3. Molecular docking studies

Similar to the previous chapter, these novel steroidal derivatives were subjected to an *in silico* analysis to understand the potential affinity with the most relevant targets of steroids (5AR type 2, ERα, AR, CYP17A1, and aromatase) in the context of this doctoral project. The molecular docking simulations were performed using vina executable, after the method validation (RMSD redocked of co-crystallized ligands < 2.0 Å).

The results obtained for lowest affinity energies (Kcal.mol^{-1}) for steroidal derivatives **VB 10a-f** and **VB 11a-f** against the mentioned targets are shown in **Table 19**. Overall, compounds exhibited high affinity to CYP17A1, presenting lowest affinity energies inferior to abiraterone (–10.3 Kcal.mol^{-1}). In addition, the affinity of steroidal 4-ene-3,6,17-triones are generally higher than the observed for 3β,5α,6β-triols. This suggested a strong possibility of establishment of important interactions between tested steroidal derivatives, especially steroidal triones, and this enzyme, which could be interesting considering the relevance of CYP17A1 in androgen signaling pathway. In contrast, poor affinity was observed with respect to simulation results against ERα and AR, which is clearly suggestive of the lack of important interactions between these targets and tested steroids. Similar to epoxysteroids, these data are pertinent due to the known risk of selectivity problems for steroidal compounds. Moreover, considering the results against 5AR, the energy values were more heterogeneous, though, in general, compounds presented affinity to these targets with values close to the ones of respective reference compound/drug. These molecular docking simulations evidenced the possibility of these new compounds interact with 5AR, not discarding the hypothesis of acting as 5ARIs. In relation to aromatase, steroidal 4-ene-3,6,17-triones exhibited higher affinity than triols, presenting energy values lower than the reference, androstenedione. Interestingly, a steroidal trione, 4-androstene-3,6,17-trione (4-AT), was already described as an irreversible inhibitor of aromatase activity.[525] Thus, the eventual interaction with aromatase could also be interesting since its inhibition constitutes a therapeutic approach in the treatment of metastatic breast cancer.[342]

Table 19. Molecular docking results, including redocking energy values, obtained by vina executable. Lowest affinity energies are indicated in Kcal.mol^{-1}. Novel compounds were tested against the most significant steroidal targets. [a]

Compound	5AR type 2	ERα	AR	CYP17A1	Aromatase
VB 10a	−11.1	−4.6	−2.9	−11.3	−9.4
VB 10b	−11.5	−0.6	−4.6	−10.3	−10.4
VB 10c	−11.0	−0.8	−1.6	−10.3	−9.9
VB 10d	−10.1	−1.3	−2.6	−10.5	−9.2
VB 10e	−10.6	−1.5	−4.6	−10.5	−9.2
VB 10f	−10.7	−2.0	−1.6	−10.5	−9.6
VB 11a	−11.3	−5.7	−3.2	−12.1	−11.3
VB 11b	−11.8	−5.3	−0.5	−12.2	−12.1
VB 11c	−12.4	−6.2	−2.9	−11.4	−11.3
VB 11d	−11.2	−4.5	−3.2	−11.2	−11.1
VB 11e	−10.8	−4.6	−1.9	−11.4	−11.0
VB 11f	−10.8	−5.0	−4.3	−11.5	−11.0
Finasteride	−11.9	-	-	-	-
Estradiol	-	−10.4	-	-	-
DHT	-	-	−11.2	-	-
Abiraterone	-	-	-	−10.2	-
Androstenedione	-	-	-	-	−10.1

[a] 5AR= 5α-reductase, ER= estrogen receptor α, AR= androgen receptor, CYP17A1= steroid 17α-hydroxylase/17,20 lyase, DHT= 5α-dihydrotestosterone.

4.3. Experimental section

4.3.1. General remarks

The general remarks to be considered are already described at **Chapter III**, **section 3.3.1.**, page 111.

4.3.2. Chemical synthesis

General procedure to obtain steroidal 3β,5α,6β-triols (VB 10a-f)

The substrates **VB 9a**, **VB 9e**, **VB 9h**, **VB 9i**, **VB 9l**, and **VB 9m** previously synthesized (0.5 mmol) were dissolved in 11.33 mL of acetone. To this solution, $HClO_4$ (206 μL) and 1.442 mL of distilled water were added, and the reactional mixture was stirred at r.t. for approximately 5 h.

After the reaction is complete, it was added 120 mL of AE and the organic phase was washed with brine and with a saturated $NaHCO_3$ solution. The organic portion was dried with anhydrous Na_2SO_4, filtered, and dried under reduced pressure to afford the final products **VB10a-f**.

*16E-Benzylidene-3β,5α,6β-trihydroxyandrostan-17-one (**VB 10a**)*

White powder (82 %); m.p. 172-174 ºC; IR (cm $^{-1}$): 1626, 1705, 2862, 2937, 3426. ^{1}H NMR ($CDCl_3$, 400 MHz) δ: 0.91 (3H, s, 18-CH_3), 1.17 (3H, s, 19-CH_3), 3.54 (1H, s, 3-CH), 4.04 (1H, m, 6-CH), 7.16 (2H, d, *J*= 7.2 Hz, H_{ar}), 7.31 (4H, m, H_{ar}+H_{vin}). ^{13}C NMR ($CDCl_3$, 101 MHz) δ: 14.61, 16.76, 20.48, 29.31, 29.71, 30.84, 31.64, 32.27, 32.67, 33.61, 38.64, 40.82, 45.89, 47.74, 49.08, 67.52, 75.88, 76.06, 128.69, 129.25, 130.32, 133.11, 135.61, 135.94, 209.72. HRMS (ESI-TOF) *m/z*: $[M + H]^+$ Calcd for $C_{26}H_{34}O_4$ 411.2535; Found 411.2525.

*16E-(2',3'-Dichlorobenzylidene)-3β,5α,6β-trihydroxyandrostan-17-one (**VB 10b**)*

Yellow solid (94 %); m.p. 210-211 ºC; IR (cm $^{-1}$): 1629, 1708, 2854, 2934, 3443. ^{1}H NMR ($CDCl_3$, 400 MHz) δ: 0.89 (3H, s, 18-CH_3), 1.08 (3H, s, 19-CH_3), 3.75-3.85 (1H, m, 3-CH), 4.21 (1H, d, *J*= 5.5 Hz, 6-CH), 7.45 (1H, t, *J*= 7.9 Hz, H_{ar}), 7.50 (1H, s, H_{vin}), 7.69 (2H, t, *J*= 7.8 Hz, H_{ar}). ^{13}C NMR ($CDCl_3$, 101 MHz) δ: 14.54, 16.70, 20.46, 28.99, 29.87, 31.55, 31.91, 32.40, 33.97, 38.59, 41.27, 45.22, 48.03, 48.81, 66.14, 66.82, 74.35, 74.83, 127.39, 128.74, 129.42, 131.34, 132.44, 135.91, 140.80, 208.55. HRMS (ESI-TOF) *m/z*: $[M + H]^+$ Calcd for $C_{26}H_{32}Cl_2O_4$ 479.1756; Found 479.1745.

*16E-(2',4'-Dichlorobenzylidene)-3β,5α,6β-trihydroxyandrostan-17-one (**VB 10c**)*

White solid (95 %); m.p. 249-250 ºC; IR (cm $^{-1}$): 1466, 1582, 1633, 1709, 2854, 2939, 3441. ^{1}H NMR ($CDCl_3$, 400 MHz) δ: 0.88 (3H, s, 18-CH_3), 1.07 (3H, s, 19-CH_3), 3.75-3.85 (1H, m, 3-CH), 4.55 (1H, s, 6-CH), 7.45 (1H, s, H_{vin}), 7.51 (1H, d, *J*= 8.2 Hz, H_{ar}), 7.73 (2H, t, *J*= 8.7 Hz, H_{ar}). ^{13}C NMR ($CDCl_3$, 101 MHz) δ: 14.53, 16.69, 20.44, 29.12, 29.89, 31.56, 31.92, 32.41, 33.98, 38.58, 45.22, 47.94, 48.85, 66.14, 74.34, 74.83, 126.21, 128.11, 129.78, 131.93, 132.35, 134.81, 135.70, 140.25, 208.56. HRMS (ESI-TOF) *m/z*: $[M + H]^+$ Calcd for $C_{26}H_{32}Cl_2O_4$ 479.1756; Found 479.1748.

*16E-[(5'-Chlorothiophen-2'-yl)methylene]-3β,5α,6β-trihydroxyandrostan-17-one (**VB 10d**)*

Pallid yellow solid (91 %); m.p. 226-227 ºC; IR (cm $^{-1}$): 1423, 1636, 1702, 2862, 2933, 3435. ^{1}H NMR ($CDCl_3$, 400 MHz) δ: 0.83 (3H, s, 18-CH3), 1.09 (3H, s, 19-CH3), 3.82 (1H, m, 3-CH), 4.03 (1H, m, 6-CH), 7.27 (1H, d, *J*= 4.0 Hz), 7.44 (1H, s, H_{vin}), 7.47 (1H, d, *J*= 4.0 Hz, H_{ar}). ^{13}C NMR ($CDCl_3$, 101 MHz) δ: 14.78, 16.71, 20.45, 28.96, 29.81, 31.55, 31.95, 32.43, 33.95, 38.60, 45.31, 47.97, 48.76, 66.14, 74.38, 74.85, 124.83, 128.58, 133.01, 133.48, 134.89, 136.42, 139.01, 208.58. HRMS (ESI-TOF) *m/z*: $[M + H]^+$ Calcd for $C_{24}H_{31}ClO_4S$ 479.1756; Found 479.1748.

*16E-[(5'-Chlorofuran-2-yl)methylene]-3β,5α,6β-trihydroxyandrostan-17-one (**VB 10e**)*

Beige powder (94 %); m.p. 190-192 ºC; IR (cm $^{-1}$): 1484, 1558, 1617, 1715, 2860, 2934, 3338. ^{1}H NMR ($CDCl_3$, 400 MHz) δ: 0.74 (3H, s, 18-CH_3), 0.99 (3H, s, 19-CH_3), 3.73 (1H, m, 3-CH), 4.13 (1H, d, *J*= 5.5 Hz, 6-CH), 4.46 (1H, d, *J*= 4.1 Hz, H_{ar}), 6.62 (1H, d, *J*= 3.5 Hz, H_{ar}), 6.91 (1H, s, H_{vin}), 6.93 (1H, d, *J*= 3.8 Hz, H_{ar}). ^{13}C NMR ($CDCl_3$, 101 MHz) δ: 14.70, 16.70, 20.48, 28.96, 29.79, 31.53, 31.94, 32.91, 34.03, 38.61, 41.30, 45.31, 47.69, 48.57, 66.16, 74.39, 74.85, 110.51, 118.01, 118.87, 134.67, 138.07, 151.94, 208.77. HRMS (ESI-TOF) *m/z*: $[M + H]^+$ Calcd for $C_{24}H_{31}ClO_5$ 435.1938; Found 435.1930.

*16E-(4'-Methylbenzylidene)-3β,5α,6β-trihydroxyandrostan-17-one (**VB 10f**)*

White solid (88 %); m.p. 199-202 ºC; IR (cm $^{-1}$): 1618, 1703, 2863, 2931, 3414. ^{1}H NMR ($CDCl_3$, 400 MHz) δ: 0.85 (3H, s, 18-CH_3), 1.09 (3H, s, 19-CH_3), 2.34 (3H, s, 4'-CH_3), 3.75-3.86 (1H, m, 3-CH), 4.21 (1H, d, *J*= 5.7 Hz, 6-CH), 7.24 (1H, s, H_{vin}), 7.27 (2H, d, *J*= 7.9 Hz, H_{ar}), 7.52 (2H, d, *J*= 7.9 Hz, H_{ar}). ^{13}C NMR ($CDCl_3$, 101 MHz) δ: 14.68, 16.71, 20.51, 21.50, 29.43, 29.85, 31.54, 32.04, 32.40, 33.99, 38.57, 41.29, 45.34, 47.53, 49.15, 66.19, 74.39, 74.84, 129.93, 130.76, 132.18, 132.92, 136.01, 139.68, 209.18. HRMS (ESI-TOF) *m/z*: $[M + H]^+$ Calcd for $C_{27}H_{36}O_4$ 425.2691; Found 425.2681.

General procedure to obtain steroidal 4-ene-3,6,17-triones (VB 11a-f)

A solution of substrates **VB 8a**, **VB 8e**, **VB 8h**, **VB 8i**, **VB 8l**, and **VB 8m** (0.5 mmol) and PCC (750 mg) in DCM (10 mL) was stirred at r.t. under inert atmosphere (N_2) for 24 h. The reaction was monitored by TLC.

After completion, the mixture was filtered with celite, and washed with diethyl ether. The solvents were removed under reduced pressure and the steroid was purified through a chromatographic column (2:1 AE/PE) to afford the corresponding products **VB 11a-f**.

*16E-Benzylidene-androst-4-ene-3,6,17-trione (**VB 11a**)*

Pallid yellow solid (20 %); m.p. 218-220 ºC; IR (cm $^{-1}$): 1630, 1675, 1711, 2869, 2952. ^{1}H NMR ($CDCl_3$, 400 MHz) δ: 0.96 (3H, s, 18-CH_3), 1.17 (3H, s, 19-CH_3), 6.15 (1H, s, 4-CH), 7.35 (3H, m, H_{ar}), 7.41 (1H, s, H_{vin}), 7.46 (2H, d, *J*= 7.5 Hz, H_{ar}). ^{13}C NMR ($CDCl_3$, 101 MHz) δ: 14.38, 17.68, 20.27, 29.02, 31.02, 33.35, 33.92, 35.42, 39.79, 45.60, 47.35, 49.71, 50.94, 126.02, 128.84, 129.66, 130.39, 134.15, 134.63, 135.18, 160.12, 199.15, 201.02, 208.19. HRMS (ESI-TOF) *m/z*: $[M + H]^+$ Calcd for $C_{26}H_{28}O_3$ 389.2166; Found 389.2107.

*16E-(2',3'-Dichlorobenzylidene)-androst-4-ene-3,6,17-trione (**VB 11b**)*

Beige solid (58 %); m.p. 246-247 ºC; IR (cm $^{-1}$): 1624, 1679, 1720, 2859, 2948. ^{1}H NMR ($CDCl_3$, 400 MHz) δ: 1.02 (3H, s, 18-CH_3), 1.20 (3H, s, 19-CH_3), 6.18 (1H, s, 4-CH), 7.24 (1H, t, *J*= 7.9 Hz, H_{ar}), 7.36 (1H, s, H_{vin}), 7.46 (1H, d, *J*= 7.9 Hz, H_{ar}). ^{13}C NMR ($CDCl_3$, 101 MHz) δ: 14.27, 17.76, 20.23, 28.72, 30.99, 33.33, 33.90, 35.42, 39.76, 45.53, 47.65, 49.51, 50.87, 126.09, 127.86, 130.25, 130.96, 133.72, 134.03, 135.69, 137.86, 159.94, 199.03, 200.80, 207.05. HRMS (ESI-TOF) *m/z*: [M + H]$^+$ Calcd for $C_{26}H_{26}Cl_2O_3$ 457.1337; Found 457.1328.

*16E-(2',4'-Dichlorobenzylidene)-androst-4-ene-3,6,17-trione (**VB 11c**)*

Beige solid (60 %); m.p. 208-210 ºC; IR (cm $^{-1}$): 1624, 1679, 1720, 2859, 2948, 3441. ^{1}H NMR ($CDCl_3$, 400 MHz) δ: 0.97 (3H, s, 18-CH_3), 1.16 (3H, s, 19-CH_3), 6.14 (1H, s, 4-CH), 7.24 (1H, d, *J*= 8.5 Hz, H_{ar}), 7.30 (1H, s, H_{ar}), 7.67 (1H, s, H_{vin}). ^{13}C NMR ($CDCl_3$, 101 MHz) δ: 14.28, 17.69, 20.23, 28.82, 30.98, 33.32, 33.90, 35.41, 39.76, 45.53, 47.56, 49.54, 50.88, 126.08, 127.16, 129.07, 130.06, 131.94, 135.70, 136.50, 137.30, 159.96, 199.05, 200.79, 207.09. HRMS (ESI-TOF) *m/z*: [M + H]$^+$ Calcd for $C_{26}H_{26}Cl_2O_3$ 457.1337; Found 457.1329.

*16E-[(5'-Chlorothiophen-2-yl)methylene]-androst-4-ene-3,6,17-trione (**VB 11d**)*

Pallid yellow solid (70 %); m.p. 160-161 ºC; IR (cm $^{-1}$): 1605, 1626, 1679, 1710, 2860, 2938. ^{1}H NMR ($CDCl_3$, 400 MHz) δ: 0.92 (3H, s, 18-CH_3), 1.16 (3H, s, 19-CH_3), 6.15 (1H, s, 4-CH), 6.89 (1H, d, *J*= 4.0 Hz, H_{ar}), 7.10 (1H, d, *J*= 4.0 Hz, H_{ar}), 7.42 (1H, s, H_{vin}). ^{13}C NMR ($CDCl_3$, 101 MHz) δ: 14.50, 17.61, 20.23, 28.56, 30.94, 33.22, 33.90, 35.39, 39.75, 45.52, 49.37, 50.97, 126.03, 126.26, 127.31, 132.28, 132.77, 135.08, 138.29, 160.06, 199.17, 200.89, 207.63. HRMS (ESI-TOF) *m/z*: [M + H]$^+$ Calcd for $C_{24}H_{25}ClO_3S$ 429.1291; Found 429.1281.

*16E-[(5'-Chlorofuran-2-yl)methylene]-androst-4-ene-3,6,17-trione (**VB 11e**)*

Pallid orange solid (53 %); m.p. 220-221 ºC; IR (cm $^{-1}$): 1423, 1613, 1678, 2249, 2861, 2944, 3366. ^{1}H NMR ($CDCl_3$, 400 MHz) δ: 0.93 (3H, s, 18-CH_3), 1.18 (3H, s, 19-CH_3), 6.18 (1H, s, 4-CH), 6.26 (1H, d, *J*= 3.4 Hz, H_{ar}), 6.59 (1H, d, *J*= 3.4 Hz, H_{ar}), 7.05 (1H, s, H_{vin}). ^{13}C NMR ($CDCl_3$, 101 MHz) δ: 14.45, 17.68, 20.28, 28.52, 30.96, 33.31, 33.93, 35.45, 39.79, 45.67, 47.44, 49.29, 50.98, 109.36, 118.22, 119.25, 126.05, 132.39, 139.73, 151.41, 160.10, 199.10, 201.16, 207.91. HRMS (ESI-TOF) *m/z*: [M + H]$^+$ Calcd for $C_{24}H_{25}ClO_4$ 413.1519; Found 413.1508.

*16E-(4'-Methylbenzylidene)-androst-4-ene-3,6,17-trione (**VB 11f**)*

Pallid brown solid (57 %); m.p. 270-271 ºC; IR (cm $^{-1}$): 1636, 1682, 1722, 2864, 2946. ^{1}H NMR ($CDCl_3$, 400 MHz) δ: 0.95 (3H, s, 18-CH_3), 1.17 (3H, s, 19-CH_3), 2.33 (3H, s, 4'-CH_3), 6.15 (1H, s, 4-CH), 7.17 (2H, d, *J*= 8.0 Hz, H_{ar}), 7.36 (2H, d, *J*= 8.0 Hz, H_{ar}), 7.40 (1H, s, H_{vin}). ^{13}C NMR ($CDCl_3$, 101 MHz) δ: 14.40, 17.69, 20.29, 21.52, 29.05, 31.04, 33.38, 33.93, 35.44, 39.81, 45.64, 47.31, 49.78, 50.99, 126.03, 129.60, 130.44, 132.41, 133.63, 134.21, 140.15, 160.14, 199.11, 201.66, 208.25. HRMS (ESI-TOF) *m/z*: $[M + H]^+$ Calcd for $C_{27}H_{30}O_3$ 403.2273; Found 403.2264.

4.3.3. Biological evaluation

4.3.3.1. Cell culture

Relative to the cell culture, the procedures were similar to the described at **Chapter III**, **section 3.3.3.1.**, page 118. LNCaP, PC-3 and PNT1A cells were used in passages 13th to 23rd, 34th to 40th and 10rd to 17th, respectively. Moreover, MCF-7 cell line was used in passages 18th to 23rd. Finally, NHDF cells were used in passages 9th to 12th.

4.3.3.2. Preparation of compounds solutions

The procedure applied was already described at **Chapter III**, **section 3.3.3.2.**, page 118.

4.3.3.3. MTT cell proliferation assay

The protocol implemented is the same as described at **Chapter III**, **section 3.3.3.3.**, page 118.

4.3.3.4. Fluorescence microscopy

LNCaP and PC-3 cells were trypsinized and counted by the trypan-blue exclusion assay and then cells were seeded with an initial density of 3×10^4 cells/mL in 24-well culture plates (Nunc, Apogent, Denmark) containing circular coverslips of 10 mm diameter. Following seeding (48 h), cells were treated with a 20 μM concentrations of 5-FU, as positive control, **VB 11c** (LNCaP) and **VB 10e** (PC-3) for 24, 48, and 72 h. Untreated cells were used as a negative control. Before Hoeschst-33342 staining, photomicrographs were taken using a digital camera Olympus SP-500UZ (Olympus, Tokyo, Japan) coupled to an optical microscope Olympus CKX41. Then, the medium was removed, and cells were fixed with were fixed with 4 % formalin (15 min, r.t.). After fixation, cells were washed three times with PBS and incubated in the dark for 10 min, r.t., with 30μL/coverslip of nuclear marker Hoechst-33342 (1:500, Life Technologies), prepared in PBS. Lastly, the coverslips were washed three times with PBS and mounted on a drop

of the fluoroshield mounting medium (Abcam, Plc.) on a microscope slide and left dry for 24 h. Photomicrographs were taken using an Axio Imager A1 microscope (Carl Zeiss, Göttingen, Germany) with the 40 × objective.

4.3.3.5. Analysis of cell nuclear morphology and distribution using ImageJ

The procedure implemented is similar to the described at **Chapter III**, **section 3.3.3.6.**, page 120.

4.3.3.6. Caspase-3/7 activity assay

The caspase-3/7 activity was evaluated using the Promega Caspase-Glo 3/7 assay (Promega, Madison, WI, USA). LNCaP cells were seeded in a 96 multiwells plate at a density of 4×10^4 cells/mL. After 48 h, cells were treated with the positive controls, DOX, at 5 μM and 5-FU at 20 μM, and the cells were also treated with 10 and 20 μM of **VB 11c**, during 72 h. The assay was performed at the end of treatment, following the instructions provided by the manufacturer. Data are representative of at least two experiments.

4.3.3.7. Statistical analysis

The MTT results are representative of at least two independent experiments. The data are expressed as mean±standard deviation (SD). The analysis of cell nuclear morphology and distribution experiments were performed at the border of the coverslips, where cells formed a pseudo monolayer. The experiments were performed in at least two independent cultures and the results are expressed as mean±standard error of mean (SEM). All statistical significances were determined with GraphPad Prism 6 software (GraphPad, San Diego, CA, USA) by using ANOVA followed by Dunnett's or Bonferroni's test or unpaired two tailed Student's *t*-test. Differences between groups were considered statistically significant for a *p*-value lower than 0.05 ($p< 0.05$).

4.3.4. Molecular docking

4.3.4.1. Preparation of macromolecules and ligands

The procedure applied is similar to the described at **Chapter III**, **section 3.3.4.1.**, page 121.

4.3.4.2. Grid map parameters

The protocol implemented is the same to the described at **Chapter III**, **section 3.3.4.2.**, page 121.

4.3.4.3. Method validation and molecular docking simulations

The method executed is similar to the described at **Chapter III**, **section 3.3.4.3.**, page 121.

CHAPTER V

5. Screening of 5α-reductase *in vitro* inhibitory activity of steroidal arylidene derivatives

5.1. Introduction

The 5AR overexpression increases serum DHT levels, which is implicated in some androgen-dependent disorders, including BPH, PCa and also male androgenic alopecia, tend to increase with age.[526–528] Consequently, lowering DHT levels through the inhibition of 5AR comprises an interesting and rational approach in the management of these conditions. Thus, several researchers focused their work on the discovery and development of 5ARIs. The first inhibitors were steroids that mimicked testosterone and, in many cases, were substrates themselves, not being true inhibitors.[50] Structurally, 5ARIs can be broadly grouped as steroidal and non-steroidal, with the steroidal class being larger than the non-steroidal class.[31,81]

The only two azasteroid 5ARIs that are approved for clinical use in the management of BHP are finasteride and dutasteride which have the 4-azasteroid skeleton.[31] Despite finasteride and dutasteride improve the symptom score, retarding the BPH progression, sexual adverse effects arise as the most common drug-related adverse effects which, usually, occur during the first year of treatment. The most common side effects include decreased libido, erectile dysfunction, and gynecomastia. Usually, these adverse effects seriously compromise the patients' quality of life, justifying the research for the discovery of new drugs more effective and with fewer side effects on patients' sexual life.[24,82,475] Consequently, considering the side effects of finasteride and dutasteride and the recognized importance of 5ARIs, a variety of other modified steroids, such as 20-oxime-4-azasteroidal derivatives, 16*E*-arylidene-4-aza-androstenes and oxidized steroids were obtained in an attempt to obtain new molecules with potential inhibitory activity of 5AR.[326,484,487,510,529] In this context, some motivating bioactivity results were achieved and investigations in this field are still in development.[530,531]

Currently, the most established methods available for the assessment of 5AR activity in biological samples, such as in human prostatic cells and human or rat prostatic microsomes, are principally the radio-assays, usually comprising (1) incubation of

radiolabeled testosterone with NADPH and enzyme sources of 5AR, (2) extraction of steroids with organic solvent, and (3) separation of the metabolites from testosterone by TLC or HPLC, followed by the measurement of compounds' radioactivity.[532–536] Despite the high sensitivity of radio-assays, these methods, besides being too expensive and requiring special facilities and equipment to handle radioactive compounds, are not the most appropriate for routine analysis also due to the human health hazards presented by the radiolabeled compounds.[537] Therefore, in the past decade, several methods for the assessment of 5AR inhibitory activity to prevent the use of radiolabeled compounds have emerged. The most relevant examples using biological samples as 5AR sources, are (1) the quantification of DHT by liquid chromatography coupled to tandem mass spectrometry (LC-MS/MS), (2) quantification of testosterone and DHT by gas chromatography with tandem mass spectrometry (GC-MS/MS), (3) quantification of testosterone by high performance liquid chromatography with UV detection (HPLC-UV), and (4) a simple spectrophotometric assay determining DHT and other metabolite, 5α-androstane-3α,17β-diol.[537–542] All the described approaches to measure the enzymatic activity are indirect methods, and the determination of the substrate (testosterone) and/or the metabolites is then correlated with 5AR activity through an equation obtained during the respective method validation (illustrative example in **Figure 51**).

Considering the goal of the present doctoral project of prepare novel steroidal arylidene derivatives with 5AR inhibitory capacity, the assessment of enzymatic activity is crucial to clarify the potential of these novel compounds in this ambit. Thus, this chapter describes, firstly, the partial method development for the assessment of 5AR inhibitory activity, as well as its optimization and validation. Despite the applied method is already described, its adaption and validation were still required based on followed guidelines.[543,544] The *in vitro* evaluation of 5AR inhibitory activity of the novel steroidal arylidene derivatives through an indirect method for assessment of enzymatic activity in mice liver microsomes by HPLC-DAD was performed. This HPLC method was selected considering the facilities, equipment, available reagents, and the know-how of the research group. Lastly, the *in silico* analysis of possible interactions of the most potent compounds against 5AR determined by the *in vitro* assay is reported.

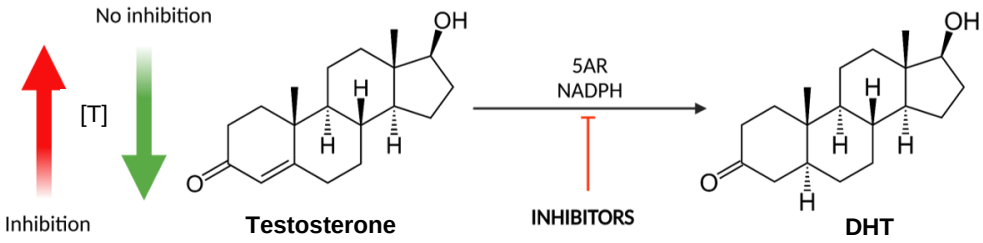

Figure 51. Indirect method to access 5α-reductase (5AR) activity by the measurement of the substrate, testosterone. When occurs enzymatic activity inhibition, concentration of remaining testosterone, [T], is higher than concentration at normal activity of 5AR. (NADPH= Nicotinamide adenine dinucleotide phosphate, DHT= 5α-Dihydrotestosterone). Created with ChemDraw and BioRender.com.

5.2. Results and discussion

5.2.1. Optimization studies and method validation

Mobile phases containing water and the organic modifier acetonitrile (ACN) in different ratios v/v (50:50; 70:30; 55:45; 60:40) were examined and the separation characteristics for testosterone were further evaluated using as a stationary phase a reversed phase column C18 LiChroCART® Purospher Star protected by a pre-column C18 LiChroCART® Purospher Star. With this optimization study, it was concluded that the mobile phase constituted of 60:40 of the mixture water/ACN, at 40 °C and flow rate of 1 mL/min, led to the best results, being 3.01 min the testosterone retention time (**Table 20**). A figure relative to the overlap of all chromatograms is provided in **Appendix 6**, **Figure Ap 13**. The wavelength selected to detect testosterone with the best resolution was 245 nm, producing a peak strait and high, as required (**Figure 52**). Under these running conditions, the peak of testosterone is clearly separated from the peak of the elution front.

Table 20. Optimization of mobile phase results. Retention time of testosterone (in min). [a]

Mobile phase (v/v)	Retention time (min)
Water/ACN 50:50	1.79
Water/ACN 70:30	9.03
Water/ACN 55:45	2.27
Water/ACN 60:40	3.01

[a] ACN= acetonitrile.

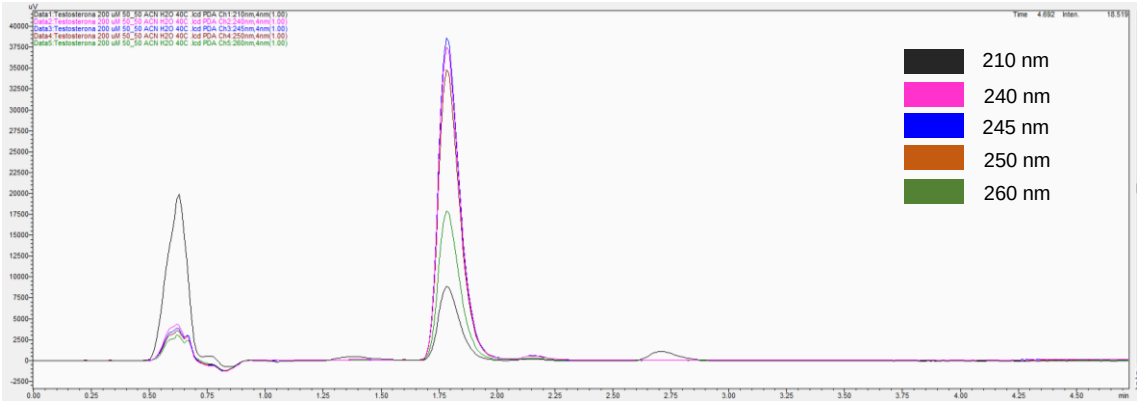

Figure 52. Chromatogram of overlapping of testosterone peaks at different wavelengths (210, 240, 245, 250, and 260 nm).

These particular conditions were a starting point to perform further optimizations, such as the selection of the internal standard (IS) and preliminary studies with the biological matrix. To select the ideal IS, several compounds available at the laboratory with structural resemblances with testosterone and with high purity level were tested. Among these compounds, perampanel (PER) seemed to be the most appropriate (**Table 21**). In addition to structural similarities with testosterone (**Figure 53**), the retention time of PER was 4.05 min, allowing an acceptable spacing between peaks as depicted in **Figure 54**. All the chromatograms acquired in the context of IS selection are presented in the **Appendix 6**, **Figure Ap 14**.

Table 21. Selection of internal standard (IS). Tested compounds and respective retention times (in min) under previously selected running conditions [water/acetonitrile (ACN) 60:40, 40 °C].

Compound	Retention time (min)	Compound	Retention time (min)
Stiripentol	6.02	Retigabine	2.41[a]
Perampanel	4.05	Paroxetine	-[b]
Tolbutamide	1.89	Clarithromycin	-[b]
Ketoconazole	1.10	Terbinafine	-[b]
Hydrocortisone	1.03	Quinidine	-[b]

[a] The split peak indicative of product degradation, possibly.
[b] Tested molecules with short retention times or that did not elute in these elution conditions.

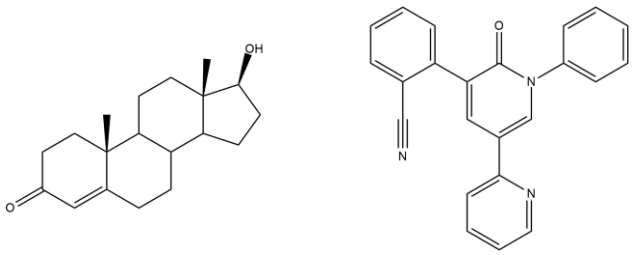

Testosterone **PER** (IS)

Figure 53. Molecular structure of testosterone and the selected internal standard (IS), perampanel (PER). Created with ChemDraw.

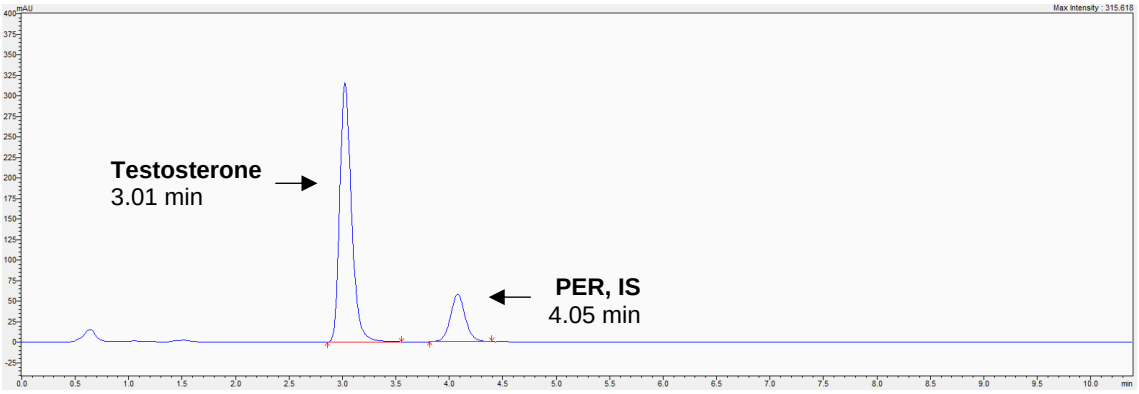

Figure 54. Representative chromatogram obtained by HPLC-DAD (λ = 245 nm) and identification of peaks (testosterone, compound to be quantified, and perampanel (PER), the internal standard, IS).

Regarding the sample processing after the *in vitro* assay, the recovery of testosterone and the IS (at 100 % and at concentration of the lower limit of quantification – LLOQ) and the study of the ideal volume of solvent for liquid-liquid extraction (LLE) were accomplished. Several volumes of DCM (1, 3, and 5 mL), the solvent used in the LLE procedure in several reported studies, were tested and the volume of 5 mL exhibited the best results in phase separation (aqueous, interphase comprising solid debris, and organic) and testosterone and IS recuperation.[540,545,546] Simultaneously, experiments with the biological matrix were performed. In this context, different blank matrices (steroid free) of mice liver microsomes were analyzed to evaluate the variability, reproducibility and the potential presence of interferents. From this study, a strong resemblance between the different acquired chromatograms from the distinct blank matrices was observed. However, the presence of some potential interferent peaks at the same or close retention times of testosterone and PER was detected. Fortunately, the calculations performed to clarify if these interferences were present in acceptable percentages considering the LLOQ proved to be within the parameters required (< 5 %).

The following step consisted on the method validation in accordance with currently method validation guidelines provided by FDA and EMA.[543,544] In this scope, considering that the biological matrix is mice liver microsomes, several validation parameters were assessed, including selectivity, carry-over effect, linearity, LLOQ, accuracy and precision, dilution integrity, recovery, stability, and incurred sample reanalysis (ISR). The selectivity was already evaluated since the possible interferents were studied in blank matrixes, and it was concluded that none of them indeed interfere at the retention times of testosterone and IS. In relation to carry-over effect, blank samples analyzed after injecting the highest calibrator of testosterone (65 μg/mL) did not display any signal > 20 % of the testosterone peak area at the LLOQ and of 5 % of the IS peak area, indicating that the method did not show any carry-over effect.

A calibration curve was prepared to cover a significant concentration range. Thus, six calibrators were prepared: 5 (LLOQ), 10, 20, 35, 50, and 65 μg/mL (upper limit of quantification – ULOQ). Linearity was obtained for testosterone within the defined calibration range ensuring a reproducible correlation between testosterone/IS peak areas ratios and the corresponding nominal concentrations. In the present study, the weighting factor considered in the linear regression model was $1/x^2$. This factor was applied to compensate the heteroscedasticity resultant from the wide calibration range.[547] The sensitivity of this method was demonstrated since the LLOQ concentration was measured with adequate precision [coefficient of variation (CV)≤ 20 %] and accuracy [deviation from nominal concentration (*bias*) ± 20 %]. Moreover, the results indicated that the present method is accurate and precise for testosterone quantification. Indeed, intra- and interday precision was demonstrated once the QC samples tested at low, medium, and high concentrations presented an intraday CV< 3.5 %, being the interday precision demonstrated by CV values < 5.1 %. Relative to accuracy assessment, intraday *bias* interval was found to be between –10.1 and 6.2 % and interday *bias* ranged from –6.0 to 5.2 %. Furthermore, the extraction recovery percentages were also studied. Applying the present method, the recovery was proved to be within suitable limits since the recovery percentages (mean±SD; n= 5) calculated using distinct QC samples (QC_1, QC_2, and QC_3) were within 98.0 ± 6.6 and 102.3 ± 3.7 %. All these described results are summarized in **Tables 22** and **23**.

Table 22. Calibration curve parameters of testosterone in mice liver microsomes (n= 3).

Linearity				
Linear range (μg/mL)	**Calibration equation (y= bx + a)**[a]		r^2	**LLOQ** (μg/mL)
	Slope[b] **(b) ± 95% CI**	**Intercept**[b] **(a) ± 95% CI**		
5 - 65	0.093973 ± 0.004998	0.009634 ± 0.015746	0.9954	5

[a] Equation of the calibration curve y= bx + a, where x is the testosterone concentration, expressed in μg/mL, and y is the testosterone to internal standard peak-area ratio, expressed in arbitrary area units.
[b] Mean values ± 95 % confidence interval (CI).
LLOQ= lower limit of quantification.

Table 23. Precision, accuracy, and recovery results. Intra- and interday precision (% CV) and accuracy (% *bias*) values obtained for testosterone in mice liver microsomes at the lower limit of quantification (QC_{LLOQ}) and at the low (QC_1), medium (QC_2), and high (QC_3) concentration levels representative of the calibration ranges. Percentage of recovery for QC_1, QC_2, and QC_3 are also shown. [a]

Precision, accuracy, and recovery									
$C_{nominal}$		**Interday** (n= 3)			**Intraday** (n= 5)			**Recovery** (%) (n= 5)	
		$C_{experimental}$ (Mean±SD)	**Precision** (% CV)	**Accuracy** (% *bias*)	**$C_{experimental}$** (Mean±SD)	**Precision** (% CV)	**Accuracy** (% *bias*)	**Mean±SD**	**CV** (%)
QC_{LLOQ}	5	4.99 ± 0.20	3.4	-0.2	4.65 ± 0.14	2.4	-7.0	ND	ND
QC_1	15	14.92 ± 0.82	5.1	-0.5	14.12 ± 0.24	1.6	-5.9	98.0 ± 6.6	6.7
QC_2	30	31.56 ± 0.40	1.2	5.2	31.86 ± 1.16	3.5	6.2	102.3 ± 3.7	3.6
QC_3	60	56.41 ± 2.34	4.1	-6.0	53.92 ± 1.43	2.6	-10.1	99.8 ± 1.6	1.6

[a] $C_{nominal}$= nominal concentration; $C_{experimental}$= experimental concentration; CV= coefficient of variation; LLOQ= lower limit of quantification; SD= standard deviation.

Lastly, stability studies were performed and the results under several working and storage conditions exhibited no significant loss of testosterone, since all mean concentrations at low and high concentration levels of QC samples were within ± 15 % of the nominal concentration. In conclusion, it is suggested that benchtop stability of testosterone can be guaranteed at least for 4 h at r.t.. Not processed samples stability during 24 and 72 h under refrigeration (4 ˚C) was also proved, as well as during at least 10 days frozen at −20 ˚C. Moreover, the stability of testosterone in processed samples was also evaluated at r.t. (autosampler stability), being showed that, for at least 24 h, the samples can be reanalyzed without a significant loss of the tested analyte. As required, all tested samples were considered stable since the stability/reference ratio was between 85 and 115 %.

5.2.2. Studies on inhibitory 5α-reductase activity of steroidal arylidene derivatives

Once completed the partial method development, optimization and respective validation, the assessment of 5AR activity was achieved. This evaluation of the effects of arylidene derivatives in the 5AR activity was accomplished using mouse liver

microsomes as the enzyme source. All new arylidene derivatives prepared in the context of master and doctoral projects, including 16*E*-arylidene-4-aza-androstenes (**VB 4a-g**), 21*E*-arylidene-4-azapregnenes (**VB 7a-g**), 16*E*-arylidene-5α,6α-epoxyepiandrosterone derivatives (**VB 9a-m**), steroidal 3β,5α,6β-triols (**VB 10a-f**), and steroidal 3,6,17-triones (**VB 11a-f**), were tested in a preliminary study at one concentration (10 μM). Then, the most promising compounds (5AR inhibition > 85 %) were subjected to an additional screening at 1 μM, before IC_{50} determination (only compounds presenting a 5AR inhibition > 80 %). In this experiment, testosterone was added to the enzymatic reaction as a substrate to be metabolized into DHT by 5AR enzyme. Moreover, the addition of the cofactor, NADPH, was crucial for the enzymatic reaction.[50] After the incubation time (30 min, at 37 °C), the samples were processed and testosterone remained from enzymatic reaction was quantified by HPLC-DAD. Incubation with finasteride was achieved as reference (positive control), being this drug used clinically in the BPH treatment since it acts as a 5ARI.[531] The results of the preliminary screening are shown in **Figure 55**.

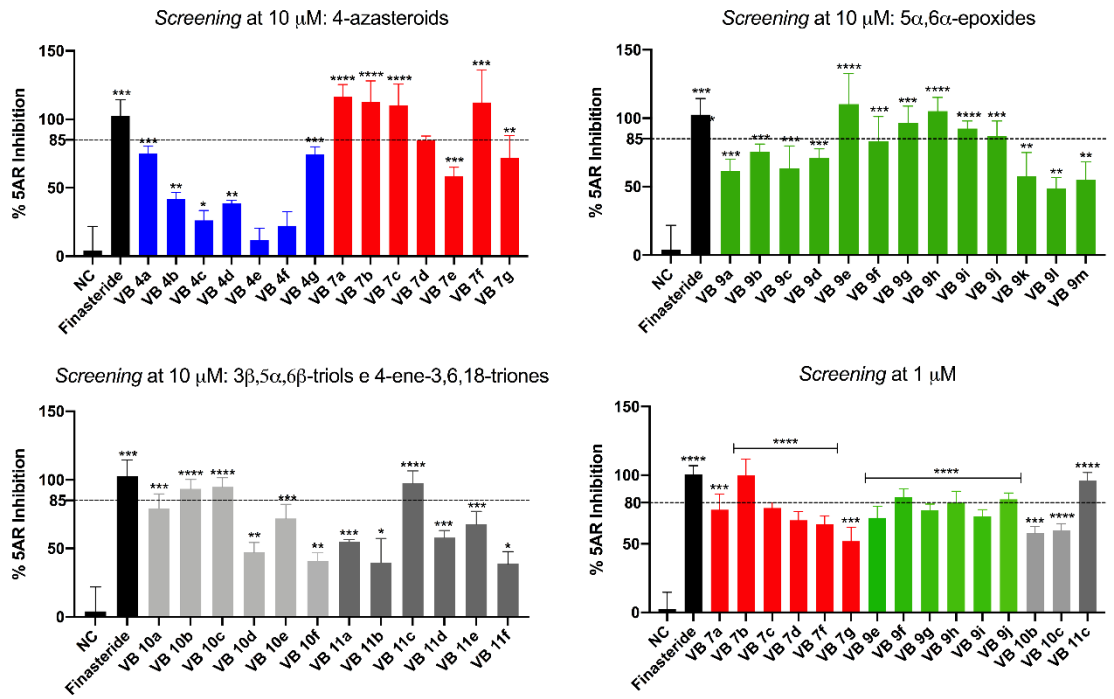

Figure 55. 5α-Reductase (5AR) inhibition screening results. Compounds that showed % inhibition > 85 % in the 10 μM screening were selected for the screening at a lower concentration (1 μM). Finasteride was used as reference (positive control). Data shown are representative of at least two independent experiments and two replicates (N≧ 2, *n*= 2). Statistical analysis was performed using Student's *t*-test, **p*< 0.05; ***p*< 0.01; ****p*< 0.001; *****p*< 0.0001. (NC= Negative control). **Blue**: 4-aza-androstenes; **red**: 4-azapregnenes; **green**: epoxyepiandrosterone derivatives; **light gray**: steroidal 3β,5α,6β-triols; **dark grey**: steroidal 3,6,17-triones.

From this preliminary assay at 10 μM, 4-azapregnenes and epoxyepiandrosterone derivatives seemed to be the most active steroids of this group against 5AR. Then, a second preliminary study at 1 μM was performed in the most promising compounds, which previously induced an 5AR inhibition clearly superior to 85 % (**VB 7a**, **VB 7b**, **VB 7c**, **VB 7d**, **VB 7f**, **VB 7g**, **VB 9e**, **VB 9f**, **VB 9g**, **VB 9h**, **VB 9i**, **VB 9j**, **VB 10b**, **VB 10c**, and **VB 11c**). Considering the results from the second experiment, steroids displaying percentages of inhibition superior to 80 % were selected to further studies to determine the IC_{50} (**VB 7b**, **VB 9f**, **VB 9h**, **VB 9j**, and **VB 11c**). In the screening with the lowest concentration (1 μM), steroids **VB 7b** and **VB 11c** showed an effect very similar to finasteride, which might be a favorable indicator of a promising 5AR inhibitory activity. The estimated IC_{50} values are shown in **Table 24**.

Table 24. Determined IC_{50} values (nM) of the most potent compounds in the preliminary assays: **VB 7b**, **VB 9f**, **VB 9h**, **VB 9j** and **VB 11c**. Finasteride was used as reference (positive control). Molecular structures created with ChemDraw.

Compound	Structure	IC_{50} (nM)	r^2
Finasteride	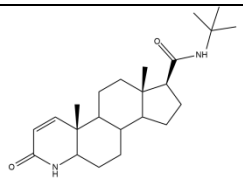	91.49	0.92
VB 7b	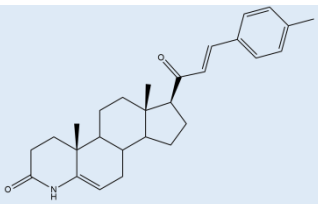	12.04	0.89
VB 9f	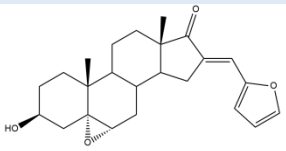	20.52	0.92
VB 9h	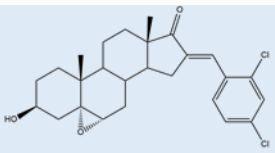	102.30	0.96
VB 9j	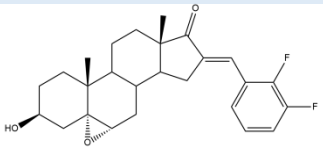	685.00	0.92
VB 11c	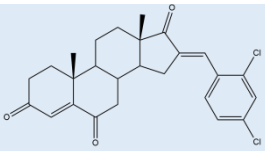	6.12	0.94

Interesting results were obtained concerning IC_{50} values for 5AR inhibitory activity of tested compounds. Among of the six tested steroids, four exhibited IC_{50} values lower than the reference [IC_{50}(finasteride)= 91.49 nM], specifically **VB 7b**, **VB 9f**, and **VB 11c**. Based on this method, the most potent compound against 5AR is **VB 11c** (IC_{50}= 6.12 nM), a steroidal 3,6,17-trione with a 2,4-dichlorobenzilidene group attached to C-16.

5.2.3. *In silico* analysis of interactions of the most potent derivatives with 5α-reductase enzyme

An additional *in silico* study of the potential interactions of the most promising compounds against 5AR was performed in the attempt of justify the inhibitory activity presented in previous assay. To achieve this aim, the output files obtained from molecular docking simulations of the most potent steroids (**VB 7b**, **VB 9f**, **VB 9h**, **VB 9j**, and **VB 11c**) against 5AR type 2 were explored and compared to finasteride as reference. Firstly, the 2D map interaction of finasteride in the active site of 5AR was analyzed in BIOVIA Discovery Studio software (**Figure 56**). However, it is important to clarify that this is a simple analysis based on the comparison of potential interactions of finasteride and tested compounds against 5AR. In addition, the study was based on output file obtained from the simulation with isolated finasteride and not using the output file obtained from the redocking simulation with NADP-DHF complex. Thus, from the 2D interaction diagram of finasteride, it was observed the establishment of some different types of interactions: van der Waals, hydrogen bonds (dipole-dipole interaction), alkyl, and π-alkyl, being the most representative the van der Walls forces. These nonionic forces are relatively weak interactions ranging from 0.5 to 1.0 kcal.mol^{-1}, occurring when adjacent atoms are close enough and the respective electron clouds barely touch. Consequently, van der Waals forces are highly distance dependent.[548]

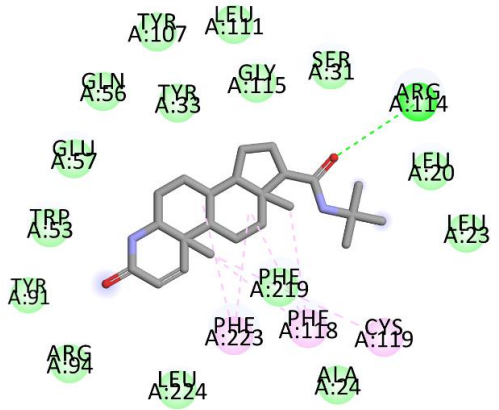

Figure 56. Predicted 5α-reductase (5AR) interactions with finasteride. **Light green=** van der Waals interactions; **Green=** conventional hydrogen bond; **Pink=** alkyl/π-alkyl interactions. Created with BIOVIA Discovery Studio.

In the other hand, π-alkyl and alkyl interactions are also weak non-covalent forces that comprise the interaction of a π-electron cloud over an aromatic group and electron group of any alkyl group (π-alkyl) or the interaction between electrons of two alkyl groups (alkyl-alkyl or only alkyl).[549,550] In this case an alkyl interaction was established with CYS119 residue and π-alkyl forces were observed with PHE118 and PHE223 residues. Moreover, a conventional hydrogen bond was observed between ARG114 and oxygen atom of ketone group C-21, which is the strongest non-covalent force (dipole-dipole).[551] Additionally, based on the study reported by Xiao et al., the residues TYR91 and GLU57 are crucial to the enzyme inhibition since dynamic experiments showed the formation of covalent bonds between these residues and finasteride.[467] Thus, in this simplistic analysis, it will be considered relevant the interaction of the tested compounds with these amino acid residues.

The 2D interaction diagrams of tested steroids are depicted in **Figure 57**. In general, these compounds displayed a higher number of interactions with the studied macromolecule, and several types of forces. In addition to those already described interactions, halogen, π-cation, π-sigma, and π-π T-shaped were also detected in some cases. Interestingly, in the majority of the simulations, arylidene groups seemed to be important in the establishment of additional interactions. In relation to the 4-azapregnenes (**VB 7b**), the presence of the ketone at C-3 which is part of the lactam seemed to be relevant to establish a hydrogen bond with SER31 amino acid residue. Moreover, a significant number of van der Waals forces were observed, including with GLU57, as well as alkyl (e.g.: with TYR91), and π-π T-shaped interactions between aromatic groups of these steroids and aromatic residues (TYR and PHE). Epoxysteroids **VB 9f**, **VB 9h**, and **VB 9j** presented similar interactions to each other. The main differences are, naturally, related to the distinct arylidene groups attached to C-16. The five membered ring attached to C-16, a furan, in steroid **VB 9f** seemed to establish a lower number and type of interactions than six membered rings (all the remaining compounds). In contrast to 4-azapregnene derivatives, none of epoxysteroids showed interaction with GLU57 and TYR91 simultaneously. Lastly, **VB 11c** seemed to establish a higher number of van der Waals interactions than all other compounds, including with GLU57 and TYR91, as well as π-alkyl forces mainly in the arylidene group area. In addition, the chlorine atoms seem to have an important role in the affinity increase to the macromolecule.

In the attempt to understand if there is a relationship between 5AR inhibitory activity observed in *in vitro* results and *in silico* data obtained from molecular docking

simulations, a table with all information summarized is shown below (**Table 25**). In this table, the estimated IC_{50} against 5AR, affinity binding energies, and common interaction between tested compounds and finasteride are presented. Despite compounds **VB 9h** and **VB 9j** exhibited the lowest binding energies, the interactions established seemed to not have importance to 5AR inhibition, since these steroids presented the highest values of IC_{50} (102.20 and 685.00 nM, respectively). Interestingly, these compounds exhibited the lowest number of common interactions with finasteride. In contrast, **VB 11c**, which presented an affinity higher than finasteride, also presented the higher number of common interactions with finasteride, including with GLU57 and TYR91, and revealed to be the most potent steroid in the *in vitro* assay (IC_{50}= 6.12 nM), being the most promising compound synthesized.

In conclusion, despite a direct correlation between affinity and 5AR inhibition cannot be recognized and established without further analysis, in general, compounds presenting interactions with the residues of interest simultaneously (GLU57 and TYR91) seemed to be more potent against 5AR.

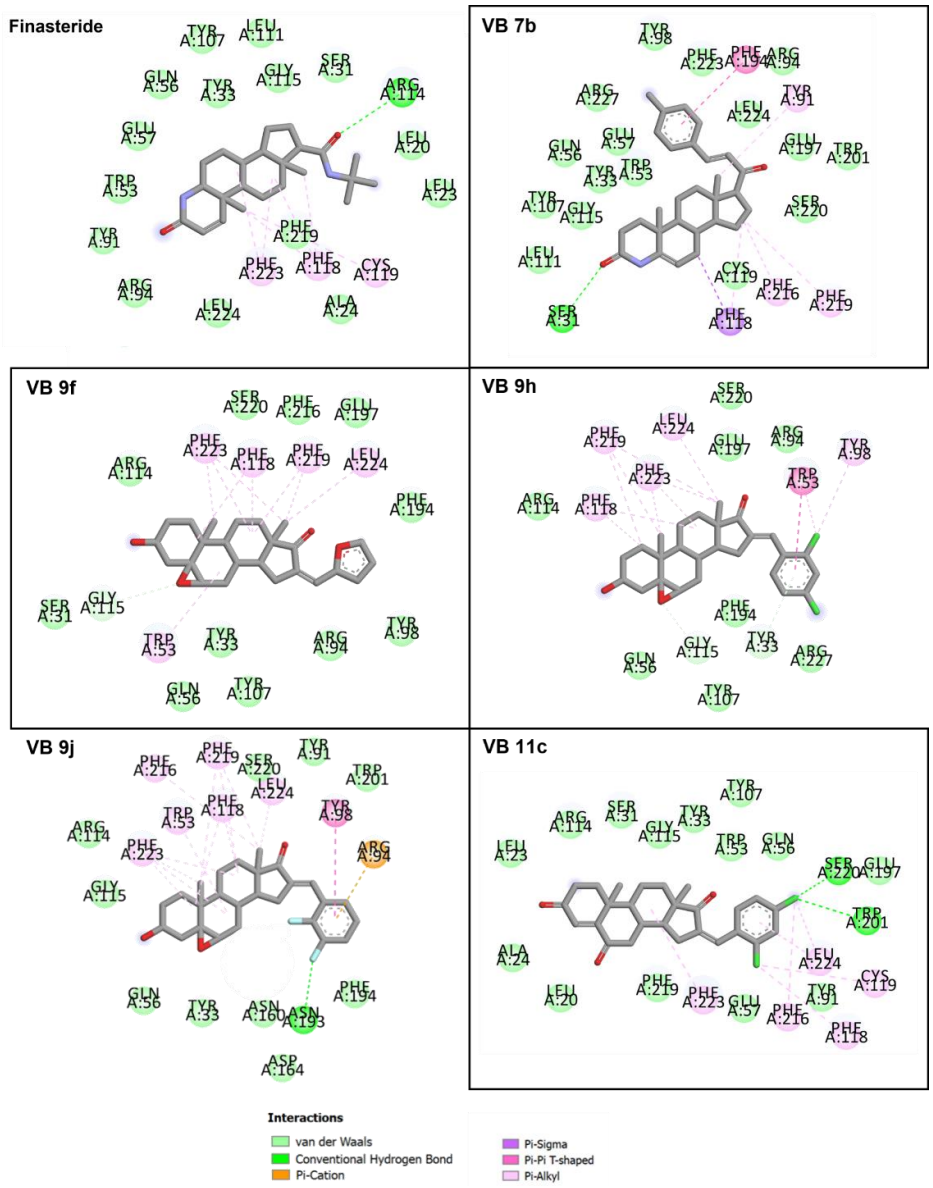

Figure 57. 2D analysis of predicted 5α-reductase (5AR) interactions with *in vitro* most potent compounds **VB 7b**, **VB 9f**, **VB 9h**, **VB 9j**, and **VB 11c** (and finasteride). Created with BIOVIA Discovery Studio.

Table 25. 5α-Reductase (5AR) inhibitory activity of the most potent compounds (IC_{50}), respective affinity binding energies obtained via vina executable, and common interactions with finasteride, used as reference, against 5AR.

Compound	IC_{50} (nM)	Binding energy (kcal.mol^{-1})	Common interactions with finasteride
Finasteride	91.49	−11.9	–
VB 7b	12.04	−12.0	**Van der Walls:** TRP53, GLU57, GLN56, TYR33, TYR107, LEU111, GLY115, LEU224, AR94, TYR91
VB 9f	20.52	−11.9	**Van der Walls:** GLN56, TYR33, TYR107, GLY115, SER31, ARG94 **Alkyl/π-alkyl:** PH 118, PHE223
VB 9h	102.30	−13.7	**Van der Walls:** GLN 56, GLY 115, TYR 107, ARG 94 **Alkyl/π-alkyl:** PHE 118, PHE 223
VB 9j	685.00	−13.0	**Van der Walls:** GLN56, TYR33, GLY115; TYR91 **Alkyl/π-alkyl:** PHE118, PHE223
VB 11c	6.12	−12.4	**Van der Walls:** GLU57, ALA24, LEU23, LEU20, SER31, GLY115, TYR107, GLN56, TRP53, TYR33, PHE219, TYR91 **Alkyl/π-alkyl:** PHE118, PHE223, CYS119

5.3. Experimental section

5.3.1. Reagents and solvents

Testosterone (> 98 % purity) and finasteride (> 98 % purity) were purchased from Sigma-Aldrich (St. Louis, MO, USA), while NADPH (> 90 % purity) was acquired from TCI (Portland, OR, USA). PER (99.9 % purity) was kindly supplied by MSN Laboratories (Hyderabad, India). ACN (HPLC grade) was acquired to Fisher Scientific (Leicestershire, UK). Moreover, DCM and MeOH (all HPLC grade) were purchased to Chem-Lab (Zedelgem, Belgium). In these assays it was used ultra-pure water (HPLC grade, > 18 MΩ.cm) prepared by a Milli-Q water apparatus from Millipore (Milford, MA, USA). Stock solutions of testosterone, finasteride, and PER were prepared by dissolving in MeOH, while NADPH stock solution was prepared by dissolving in Tris-buffer. All stock solutions were stored at −20 ˚C until use.

5.3.2. Animals

Eight-week old male ICR-CD1 mice were obtained from local certified animal facilities (Faculty of Health Sciences of the University of Beira Interior, Covilhã, Portugal). All animals were housed under controlled environmental conditions (12 h light/dark cycles, temperature at 20±2 ˚C and relative humidity of 50±5 %), receiving tap water and

standard rodent diet ad libitum. All the animal experiments were approved by the Animal Welfare and Ethics Body and were performed in conformity with the European Directive (2010/63/EU) on the protection of animals used for scientific purposes, which was transposed into the Portuguese legislation through the Decree-Law no. 113/2013.[552,553] Mice were subjected to cervical dislocation and then immediately decapitated, and the organs were collected, including the liver. The excised mice livers were washed with an aqueous solution of NaCl at 0.9 % and stored at −80 ˚C until use.

5.3.3. Preparation of mice liver microsomes

Mice microsomal suspension was prepared based on the method described by Kumar et al. with the required adaptations.[545] The excised livers were homogenized in four volumes of ice-cold 10 mM Tris-HCl buffer (pH 7.2) using an Ultra-Turrax® tissue homogenizer. After homogenization, the tissue was centrifuged at 17350 ×g for 20 min at 4 ˚C and the corresponding supernatants were collected and stored in a −20 ˚C freezer until use.

5.3.4. Measurement of *in vitro* 5α-reductase activity using HPLC-DAD

5.3.4.1. Apparatus

Chromatographic assays were performed in an HPLC system (Shimadzu LC-2010A HT Liquid Chromatography, Shimadzu Corporation, Japan) coupled with a diode-array detector (Shimadzu SPD-M20A). In the context of the present experiments, the HPLC-DADA system comprised a reverse phase column LiChroCART® Purospher Star (C18, 55 mm×4 mm; 3 μm) protected by a pre-column LiChroCART® Purospher Star (C18, 4 mm×4 mm; 5 μm). Data acquisition and instrumentation were all automatically controlled by means of LabSolutions software (Shimadzu Corp., Kyoto, Japan).

5.3.4.2. Method adaptation, optimization, and validation

5.3.4.2.1. Partial method development

In the present work, the method employed to quantify testosterone in liver microsomes was adapted from the procedure described by Matsuda et al..[546] However, some modifications were applied considering the laboratory conditions and available reagents and equipment. First of all, 20 μL of a solution of testosterone in MeOH/water (1:1 v/v) at 0.5 mg/mL was injected in HPLC-DAD to assess the optimal elution and detection conditions. Different mobile phases were studied (at 40 ˚C), including several proportions of the mixture of water/ACN (v/v): 50:50, 70:30, 55:45, and 60:40.

Simultaneously, different wavelengths to detect testosterone were evaluated (210, 240, 245, 250, and 260 nm). After this preliminary study and selection of elution conditions (60:40 ACN/water; 245 nm), a series of molecules were tested to select the appropriate IS. Thus, 20 µL of each solution of stiripentol, PER, tolbutamide, ketoconazole, hydrocortisone, retigabine, paroxetine, clarithromycin, terbinafine, and quinidine at 10 µg/mL in a mixture 1:1 v/v of MeOH/water was injected separately and analyzed (compounds available at the laboratory with structural similarities with testosterone and with high purity level). At the same time, the optimization of sample processing after *in vitro* assay was performed. At the liquid-liquid extraction (LLE) procedure with DCM, several periods and centrifugation velocities were tested until obtaining a perfect phase separation. Moreover, different blank matrices of liver microsomes (n= 6) were used to evaluate the variability and the reproducibility. Lastly, the recuperation of testosterone (at 100 % and at concentration of LLOQ) and the IS, and the analysis of possible interferents present in the matrix were achieved. The first step of recovery studies comprised the selection of optimal volume of DCM, thus, distinct volumes were tested in LLE (1, 3, and 5 mL).

5.3.4.2.2. Method validation

Once adapted and fully developed, the present method was validated according to the most recent bioanalytical method validation international guidelines (FDA and EMA).[543,544] For the biological matrix (liver microsomes), validation study included the following validation parameters: selectivity, carry-over effect, linearity, LLOQ, accuracy and precision, dilution integrity, recovery, stability, and ISR. Statistical analysis of the validation parameters was carried out using Microsoft® Excel 2016 software. Stock solutions of testosterone and PER (IS) were individually prepared in methanol at a final concentration of 5 and 1 mg/mL, respectively. Then, by appropriate dilution with methanol and Tris-buffer (1:1 v/v) of testosterone stock solution, intermediate and working solutions were prepared at corresponding concentrations. Stock solutions were stored at −20 ˚C and carefully protected from the light until further use. During method validation, the working solutions were prepared according to the guidelines.[543,544]

For selectivity assessment, six samples of drug-free blank liver microsomes obtained from six different mice were extracted and analyzed to detect possible endogenous substances that could interfere with testosterone and PER (IS) retention times. Carry-over effect was evaluated by performing five sequential injections (n= 5) of extracted blank samples after injection of the highest calibrator (65 µg/mL for testosterone) The acceptance criteria for carry-over is that the response must be less than 20 % for

testosterone at LLOQ and 5 % for the IS. Moreover, linearity was assessed by preparing six different calibrators covering different concentration ranges for testosterone. The calibration range in liver matrix was 5–65 μg/mL. The calibration curve was prepared in three different days (n= 3) using the six calibrators and was constructed by plotting the testosterone/IS peak area ratios against the corresponding nominal concentrations. The obtained data were subjected to a weighted linear regression analysis using the weighting factor $1/x^2$, being this factor selected since it generated the best fit of area ratios *versus* concentration, revealed by the lowest value of the sum of absolute percentage relative error.[554] The LLOQ of testosterone, defined as the lowest concentration of the calibration curves able to be measured with acceptable intra- and interday precision and accuracy, was determined by analyzing replicate samples on the same day (n= 5) and in different days (n= 3). The acceptance criteria for LLOQ definition were a CV not exceeding 20 % and a *bias* within ± 20 %.

Intra- and interday accuracy and precision were evaluated in a single day (n= 5) and in three consecutive days (n= 3), respectively, using quality control (QC) samples independently prepared in blank matrices. The final testosterone concentrations of the four QC samples representative of the calibration ranges (i.e., QC_{LLOQ}, QC_1, QC_2, and QC_3) in liver microsomes were 5, 15, 30 and 60 μg/mL. The considered acceptance criteria for precision were a CV value ≤ 15 % (or 20 % in LLOQ) and for accuracy a *bias* value within ± 15 % (or ± 20 % in LLOQ). Testosterone recovery was assessed at QC_1, QC_2, and QC_3 dividing the peak areas from the extracted QC samples by the corresponding peak areas of non-extracted testosterone at the same nominal concentrations (n= 5).

Additionally, stability of testosterone in liver microsomes was assessed at two concentration levels (QC_1 and QC_3, n= 5 for each concentration). Bench-top stability up to 4 h, not processed samples stability at 4 ˚C during 24 and 72 h, post-preparative stability of processed samples maintained for 24 h in the autosampler at room temperature, and long-term stability of samples maintained at −20 ˚C for 10 days were evaluated. Samples were considered stable when stability/reference ratio was between 85 and 115 %.

5.3.4.3. *In vitro* 5α-reductase activity assay

The inhibitory activity against the conversion of testosterone to DHT of all steroidal derivatives was assessed *in vitro* based on the method described by Suphrom et al., using mice livers as the enzyme source.[555] Finasteride, a 5ARI used in the treatment of BPH, was used as a positive control. The decrease of testosterone after the enzyme reaction

was determined using a HPLC-DAD method adapted from Matsuda et al. and posteriorly validated in the context of the present work, as required.[546] The test solution contained 50 µL of test compound dissolved in DMSO, 250 µL of Tris-buffer (pH 7.2), 100 µL of testosterone (0.35 mg/mL in a 1:1 v/v mixture of MeOH/Tris-buffer pH 7.2), 100 µL of PER (IS, 0.1 mg/mL in a 1:1 v/v mixture of MeOH/MiliQ water) and 350 µL of the thawed enzyme solution. The reaction was started by adding 150 µL of NADPH (5.13 mg/mL in Tris-buffer, pH 7.2). Then, the mixture was incubated at 37 ˚C for 30 min, and the reaction was stopped by adding 5 mL of DCM. The falcon tube was agitated under vortex for 1 min and centrifugated at 48 ×g (10 min, 4 ˚C), followed by another centrifugation step at 3901 ×g (25 min, 4 ˚C). The organic layer (DCM) was transferred to a test tube and evaporated to dryness. The resultant residue was dissolved in 1 mL of mobile phase (60:40 v/v mixture of water/ACN) and agitated under vortex for 1 min. Moreover, the negative control samples were prepared with all the solutions (tris-buffer, testosterone, PER, enzyme, and NADPH), including the DMSO though without the test compound. Considering the negative control, DCM was added at time 0 to assess the concentration of testosterone at the initial time ($[T]_{0\ min}$), and at the end of incubation ($[T]_{30\ min}$). A preliminary screening study at 10 µM was performed to select the most potent compounds (enzymatic inhibition > 85 %) for further studies, including a screening at 1 µM and, then the determination of the IC_{50}. The most active compounds at 1 µM (enzymatic inhibition > 80 %) were selected for IC_{50} determination studies. The IC_{50} values were determined by measuring the effects of the most potent compounds against testosterone conversion (0.005–1 µM).

5.3.4.4. Quantification of testosterone using HPLC-DAD

An aliquot of 20 µL of each sample was injected into the HPLC-DAD system comprising a reverse phase column LiChroCART® Purospher Star (C18, 55 mm×4 mm; 3 µm) protected by a pre-column LiChroCART® Purospher Star (C18, 4 mm×4 mm; 5 µm). The mobile phase was a mixture of water/ACN (60:40 v/v) with a flow rate of 1 mL/min. The separation was conducted at 40 ˚C, and the UV detector at 245 nm was used to collect data. The retention times of testosterone and of the IS, PER, were 3.01 and 4.05, respectively. It was considered 10 min for running time for each sample. The concentration of remaining testosterone, [T], in each sample is obtained using HPLC-DAD by applying the equation (**1**) previously obtained (weighted calibration curve); the "A_T" value corresponds to the area of testosterone peak, while "A_{IS}" is relative to the area of the IS peak. To convert the concentration values to the correspondent percentage of enzymatic inhibition, the equation (**2**) was applied.

$$[T] = \frac{(A_T/A_{IS}) - 0.0963}{0.0940} \qquad \textbf{(1)}$$

$$Enzymatic\ inhibition\ (\%) = \left(\frac{[T]test\ sample - [T]30min}{[T]0\ \text{min} - [T]30min}\right) \times 100 \qquad \textbf{(2)}$$

5.3.4.5. Statistical analysis

The results of enzymatic inhibition of 5AR are representative of at least two independent experiments. The data are expressed as mean±SD. All statistical significances were determined with GraphPad Prism 6 software (GraphPad, San Diego, CA, USA) by applying Student's *t*-test ($p< 0.05$; ** $p< 0.01$; ***$p< 0.001$; **** $p< 0.0001$).

5.3.4.6. Molecular docking interaction studies

The output files obtained from molecular docking simulations against 5AR type 2 (PDB ID: 7BW1) using AutoDock Vina executable, as described in the previous chapters, were used to explore the interactions of the *in vitro* most potent steroids (**VB 7b**, **VB 9f**, **VB 9h**, **VB 9j**, and **VB 11c**). The PDB output structures and 5AR were visualized simultaneously in the BIOVIA Discovery Studio software (v. 16.1, Dassault Systems, Paris, France) using the 2D interaction diagram tool to further analyze the interactions between compounds and the macromolecule.

CHAPTER VI

6. General Discussion

In this section, a more integrative discussion of the several subjects explored within the previous chapters will be provided. A critical overview of the key topics covering the overall research work carried out to accomplish the main objectives proposed at the beginning of this thesis is herein presented. In addition, to support the reading of this chapter, the **Appendix 7** provides all important molecular structures in this context.

The principal goal of the current doctoral project, as previously described, was the discovery of hit compounds for further development in the context of prostatic diseases, namely BPH and PCa. In an effort to achieve this propose, the present project comprised the preparation of novel steroidal arylidene derivatives presenting inhibitory capacity against 5AR and/or antiproliferative properties against tumoral cells.

Considering the scope of this thesis and the compounds previously synthesized during the Master's degree project (16*E*-arylidene-4-aza-androstenes and 21*E*-arylidene-4-azapregnenes), in the present thesis the biological studies of these steroids, with emphasis in the most promising arylidene-4-azasteroids was continued. The set of biological experiments performed for the referred azasteroids comprised a MTT proliferation assay on PC-3 cell line and the partial characterization of the cytotoxic effect of the most potent compound, 21*E*-[(pyridin-3-yl)methylidene]-4-azapregnene **VB 7g**, on T47-D cells through fluorescence microscopy, morphologic analysis and assessment of caspase-9 activity.

According to the results of MTT colorimetric assay, steroids **VB 7c**, the 21*E*-[(4-nitrophenyl)methylidene]-4-azapregnene derivative, and **VB 7g**, the 21*E*-[(pyridinyl)methylidene]-4-azapregnene derivative, showed to be the most potent, presenting IC_{50} values of 3.29 and 3.64 μM, respectively. Interestingly, the derivatives bearing nitrogen atoms at the arylidene group were the most potent against PC-3 cells. Despite this promising result, more specific biological experiments to characterize the effects of the most potent compound were achieved considering all the results obtained in the different cell lines (previously performed studies). Thus, as the lowest determined IC_{50} value for this group of arylidenes was 1.33 μM for steroid **VB 7g** in T47-D cells, and taking in account the resource management, more advanced studies were only performed in this cell line, despite not being prostatic cells. In fact, T47-D cells are from

a human breast carcinoma and are hormone-dependent, responding to estrogens via ERα. However, these cells also express several markers with relevance in prostatic disease context, such as the AR.[556] The results of these more advanced studies mentioned above constitute a relevant evidence of apoptotic pathway activation triggered by **VB 7g**, since this steroid triggered morphological alterations compatible with apoptotic cells and significantly increased the activity of caspase-9. Additionally, to complete the molecular docking studies already performed in the context of the Master's dissertation against important steroidal targets (AR, 5BR, ERα, CYP17A1, and aromatase), the affinity and the potential interactions of these 4-azasteroids against 5AR type 2 were assessed. The requirement to carry out this simulation emerged due to the recently discovery of three-dimensional coordinates of 5AR type 2 and the relevance of this enzyme in the context of the present work.[467] In general, the binding energies point to a strong affinity between these tested ligands and the macromolecule, being values very similar to the predicted for finasteride. Moreover, the interactions analysis, as expected, evidenced the high importance of the presence of the A-ring amine group in the establishment of significant interactions. In conclusion, the molecular docking results against 5AR type 2 demonstrate the possibility of these compounds acting as a 5ARIs.

Lastly, an attempt to clarify the relationship between the structure of arylidene-4-azasteroidal derivatives and their effect on cell proliferation on LNCaP and PC-3 cells was accomplished through a comprehensive 3D-QSAR study. Despite this approach is usually applied to enzymatic assays results, some research groups have successfully applied it using data from cell proliferation assays.[478] Thus, it was decided to apply this computational method considering the data obtained from the MTT preliminary screening assay (concentration of 30 μM, 72 h of exposition) against the referred tumoral prostatic cell lines. However, considering the input data and its heterogenicity, specific conclusions were difficult to draw. The main results obtained from this study revealed that the arylidene bulky groups seemed to be favorable to antiproliferative activity against LNCaP cells, in the case of androstane derivatives, while in PC-3 these bulky groups seemed to have the same relevance for both series (androstane and pregnane). Moreover, in both cases against both cell lines, groups with negative partial charges, namely arylidenes containing electronegative atoms, favors a decrease in cell proliferation. This study was possible due to the relevant number of 4-azasteroids evaluated in prostatic cancer cell lines and was also performed to complement the analysis of bioactivity results as well as to acquire potentially useful data for the design of analogues with higher potential.

Given the interesting results achieved with the referred 4-aza-androstanes and -pregnanes, and considering the aims of this doctoral project, it was decided to continue working in the rational design, synthesis, purification and structural characterization, as well as biological evaluation of new series of functionalized azasteroidal arylidene derivatives.[326,557] In this ambit, it was also considered the introduction of heterocyclic rings in these steroids, mainly exploring the known reactivity of the arylidene group. Therefore, several attempts to synthesize novel 3-, 6-, and 4-azasteroidal derivatives, including with heterocycles fused or attached to the D-ring were accomplished (**Appendix 3**). Based on the literature, some different approaches were applied to prepare 3- and 6-azasteroids. Therefore, despite the attempts to optimize the reactional conditions, 4-azasteroids with the desired modifications on the D-ring were not successfully prepared. Unfortunately, as none of these attempts were successfully achieved, the outline of a new strategy for the preparation of new compounds appropriate to the same purpose was mandatory and therefore naturally emerged.

Thus, in addition to the importance of the presence of an arylidene group on D-ring of steroids for the increase of antiproliferative activity, the oxidation of steroids also emerged as relevant modification to increment the bioactivity.[338,348,530] In fact, some oxidized steroidal derivatives seemed to also have important 5AR inhibitory activity.[485,532,558,559] Thus, in the context of the present work, the combination of these modifications seemed to be an interesting and rational approach to prepare new compounds potentially useful in prostatic diseases. Hence, after an extensive analysis of the literature and considering the experience and know-how of the research group in procedures of steroids oxidation the proposed and followed synthetic route is represented in **Figure 58**.[488,560–562]

Therefore, twenty-five new steroidal arylidene derivatives were successfully synthesized from DHEA, comprising three distinct series: 16*E*-arylidene-5α,6α-epoxyepiandrosterone derivatives (**VB 9a-m**), 16*E*-arylidene-3β,5α,6β-trihydroxyandrostan-17-ones (**VB 10a-g**), and 16*E*-arylidene-androst-4-ene-3,6,17-triones (**VB 11a-f**). DHEA, a steroid widely used in industry as precursor of other steroidal drugs (e.g. abiraterone), was selected as the starting material for these series of modifications since it is a steroid affordable, easy to handle and with good reactivity considering the intended chemical reactions.[563,564] Compounds **VB 8a-m** were already described in the literature and its cytotoxicity was also assessed with some promising results, thus herein these steroids were only considered synthetic intermediates.[335,338,352,388,389] The reactional routes followed were adapted from the

literature and considering the laboratory conditions to afford the desired products in acceptable yields.[348,482,512,565,566] Moreover, the reactions were relatively straightforward and, as far as possible, green chemistry principles were applied.[567] All these reactions were performed under relative smooth conditions (r.t. or 5 ˚C). Furthermore, the classic aldolic condensation and the opening of the epoxide under acidic conditions allowed the preparation of the respective products in good to excellent yields. In contrast, stereoselective epoxidation and oxidation with PCC procedures afford the respective products in lower yields.

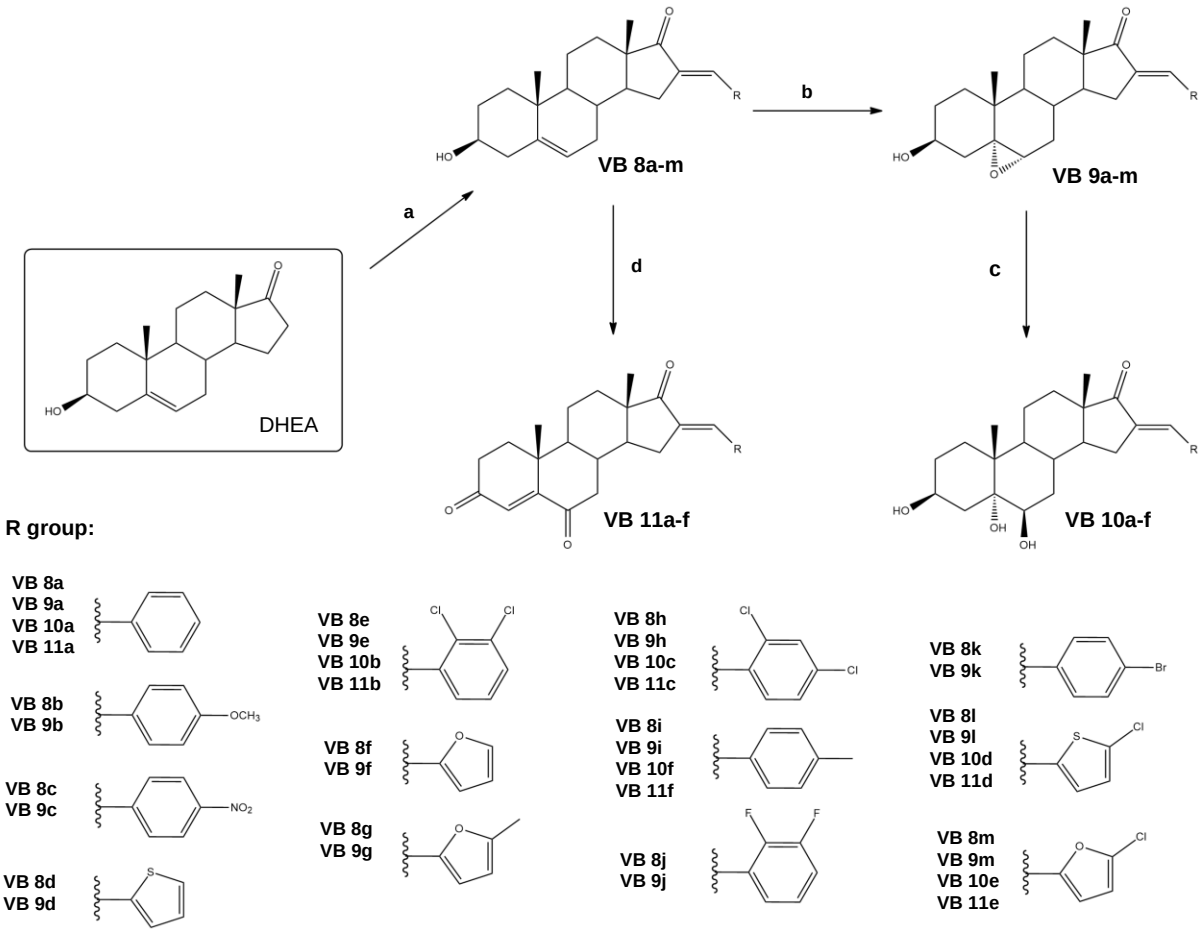

Figure 58. Overview on the synthetic pathway to obtain new series of steroidal arylidene derivatives, including 16*E*-arylidene-5α,6α-epoxyepiandrosterone derivatives, and steroidal 3β,5α,6β-triols and 4-ene-3,6,17-triones. Reactional conditions: **a)** aldehyde, aq. sol. KOH 50 %, EtOH, r.t., 2-24 h (η= 71-98 %); **b)** MMPP, DCM/water, 5 ˚C, 24-30 h (η= 33-87 %); **c)** $HClO_4$, acetone/water, r.t., 5 h (η= 82-95 %); **d)** PCC, DCM, N_2, r.t., 24 h (η= 20-70 %). (MMPP= Magnesium monoperoxyphthalate, DCM= dichloromethane, PCC= pyridinium chlorochromate). Created with ChemDraw.

As discussed in **Chapter III**, stereoselective α-epoxidation of steroids (at $\Delta^{5,6}$) is usually accomplished using *m*-CPBA. However, MMPP arise as an advantageous alternative, since it presents higher stability in solid state, lower cost, safety in handling, and work-

up procedures are relatively easy. Besides these characteristics and most important, MMPP is more selective considering the obtention of steroidal α-epoxides leading to higher yields.[482] Thus, the remotion of the residual β-epoxide is usually achieved by the recrystallization purification procedure, as it was demonstrated in the present thesis.
To prepare steroidal arylidene 3β,5α,6β-triols from the respective epoxysteroid, the acidic opening of epoxide group was performed. Perchloric acid in acetone/water was used and it comprises the typical reactional conditions for the opening of 5,6-epoxides, rendering always 5α,6β-vicinal diols.[513] Considering the oxidation of 16*E*-arylidene-3β-hydroxyandrost-5-enes, the purification step to remove PCC residues and obtain pure steroids **VB 11a-f** in one step compromised the respective yields (20-70 %). However, literature describing the same oxidation reaction also presented yields similar to the ones presented in this work.[515,517] Overall, the reaction in one step with PCC still seems to be the best option, since applying other strategies described in several researches would, namely, produce even lower global yields and would be more time-consuming.[486,565]

Steroidal arylidene 3β,5α,6β-triols (**VB 10a-g**) and 4-ene-3,6,17-triones (**VB 11a-f**) were prepared based on the data obtained from biological studies performed on steroids **VB 9a-m** (5α,6α-epoxides). Accordingly, the epoxysteroidal derivatives that displayed the best results in the *in vitro* cytotoxicity assays were posteriorly modified to prepare the respective triol and the correspondent trione. In addition, the derivative bearing the simplest arylidene group (benzylidene, **VB 9a**) was also modified to allow the comparison with the steroids comprising more complex arylidene groups (substituted aromatic rings or heterocycles). In spite of the synthetic pathway being presented as a sequential process, actually epoxysteroids were prepared and evaluated, and then, after the study of the literature to clarify the best drug design strategy, steroidal triols and triones were synthesized and also evaluated. This implied that some of epoxysteroids had to be re-synthesized since the quantity remaining was not enough to the following reactions.

Indeed, the assessment of biological activity is crucial to understand the desired activity and to potentially clarify the mechanism involved. Firstly, *in vitro* assays were performed to evaluate the effects of the novel steroidal derivatives in cell proliferation. In this scope, exciting results against tumoral cells can be indicative of the potential of tested compounds as promising antitumoral agents. Simultaneously, *in silico* methodologies were applied in an attempt of understand the potential affinity of these compounds against important steroidal targets in BPH and cancer treatment (5AR type 2, AR, ERα, CYP17A1, and aromatase).

Concerning the assessment of compounds effects on cell proliferation, the MTT colorimetric assay was selected for a first approach since it is a method simple, easy to use, relatively safe, cheap, and with relative high reproducibility.[568] Therefore, the three novel series of arylidene steroidal derivatives were tested against androgen-dependent (LNCaP) and -independent (PC-3) prostatic tumor cells, estrogen-dependent (MCF-7) breast cancer cells and in non-tumoral cells (prostatic, PNT1A, and dermal fibroblasts, NHDF, cells). Firstly, a preliminary screening at two distinct concentrations (10 and 50 μM) during 72 h was performed for all compounds in all cell lines. These two concentrations were chosen as representative since effects at concentrations > 50 μM would be indicative of low potency.[569] In relation to tumoral cells, when the treatment of cells with tested compounds led to a reduction of cell proliferation higher than 50 %, in at least at one concentration, the IC_{50} was determined (concentration range: 0.001 – 100 μM). On the contrary, IC_{50} values against non-tumoral cells were estimated for all compounds to more precisely verify the potential selectivity.

Overall, the most relevant reduction of cell proliferation was observed with compounds **VB 9e** in MCF-7 cells (IC_{50}= 3.47 μM), **VB 10e** in PC-3 cells (IC_{50}= 6.96 μM), and **VB 11c** in LNCaP cells (IC_{50}= 6.48 μM). In addition, analyzing by cell line, the three more potent compounds against each cell type and the respective estimated IC_{50} are summarized in the **Table 26**. Of these, the most active steroids against LNCaP cells were **VB 11b**, **VB 11c**, and **VB 11e**, all trione derivatives. **VB 10e**, **VB 11c**, and **VB 11e** showed significant effect on proliferation of PC-3 cells, while **VB 9e**, **VB 9h**, and **VB 10e** triggered a significant reduction of MFC-7 cells proliferation. Moreover, the estimated IC_{50} values are generally very close to the positive control (5-FU), which also supports the hypothesis of these new steroids being promising hit compounds as antitumoral agents. Interestingly, all these derivatives comprised a halogenated (hetero)arylidene group, more specifically with one or more chlorine atoms as aromatic ring substituent, suggesting their importance for antiproliferative activity. An important example of a halogenated compound clinically used as anticancer agent is 5-FU, the present positive control, which is a fluoropyrimidine that inhibits the thymidylate synthase, essential for the pyrimidine biosynthesis, leading cells to apoptosis.[336] Additionally, some recent studies have demonstrated the cytotoxicity of other halogenated compounds, however, the associated mechanisms involved remain unclear.[570–572] In relation to the epoxysteroidal derivatives studied by us, they seemed to have relative selectivity to breast cancer cells (MCF-7), and of these **VB 9e** presented the lowest IC_{50} values (3.47 μM). Thus, possibly the 5α,6α-epoxy group may contribute to this cytotoxicity in these cells. On the other hand, steroidal 4-ene-3,6,17-triones exhibited more significant effects on

prostatic cells, which constitutes a relevant fact to consider in SAR analysis and in the content of the present thesis. Lastly, in general, the contribution of 3β,5α,6β-triol group, present on compounds **VB 10a-f**, seemed not be relevant for the antiproliferation activity, with exception of **VB 10e** that exhibited relevant activity against PC-3 cells proliferation. From the analysis of the biological results provided by MTT proliferation assay, the SARs for synthesized compounds are presented in **Figure 59**.

Table 26. Arylidene steroidal derivatives most potent against each tumoral cell line (LNCaP, PC-3, and MCF-7), respective structure and IC_{50} value (μM). Determined IC_{50} values of 5-fluorouracil (5-FU), the positive control (+), are shown as reference. Molecular structures created with ChemDraw.

Cell line	Compound	Structure	IC_{50} (μM)
LNCaP	**5-FU** (+)	–	9.43
MCF-7			3.30
PC-3			6.30
MCF-7	**VB 9e**	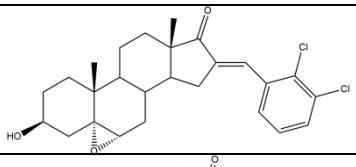	3.47
MCF-7	**VB 9h**	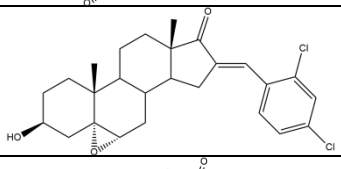	8.28
PC-3	**VB 10e**	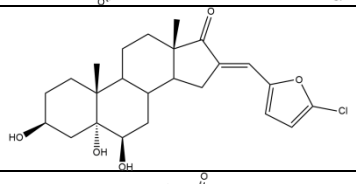	6.96
MCF-7			11.56
LNCaP	**VB 11b**	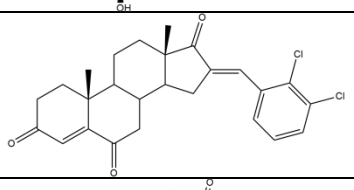	7.85
LNCaP	**VB 11c**	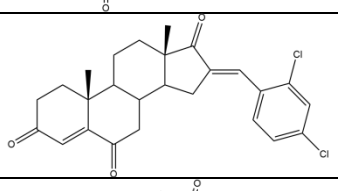	6.48
PC-3			9.79
LNCaP	**VB 11e**	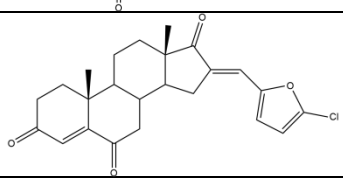	10.78
PC-3			7.21

Considering the results obtained from MTT proliferation assays, further biological studies attempting to clarify the cell death mechanism were performed with the most potent compounds in the respective cell line. The characterization of the effects on MCF-7 cells triggered by the epoxysteroid **VB 9e** was assessed through several methods:

immunocytochemistry assay, PI incorporation, and analysis of cell nuclear morphology and distribution using ImageJ software. All data obtained from this set of biological experiments constitute strong evidence that **VB 9e** displayed pro-apoptotic activity on MCF-7 cell line, since cells exhibited the main characteristics of apoptotic cells. The immunocytochemistry studies with Ki67 staining and PI incorporation evidenced a significant decrease on Ki67-positive cells and an increase on PI-positive cells after treatment with **VB 9e** at 10 μM for 48 h, which proved the existence of cell death (MCF-7).[498,500] Moreover, the analysis of cell nuclear morphology led to some evidences that are in agreement with what is described for apoptotic cells: the decrease on NA and an aleatory and more spaced cell distribution.[472]

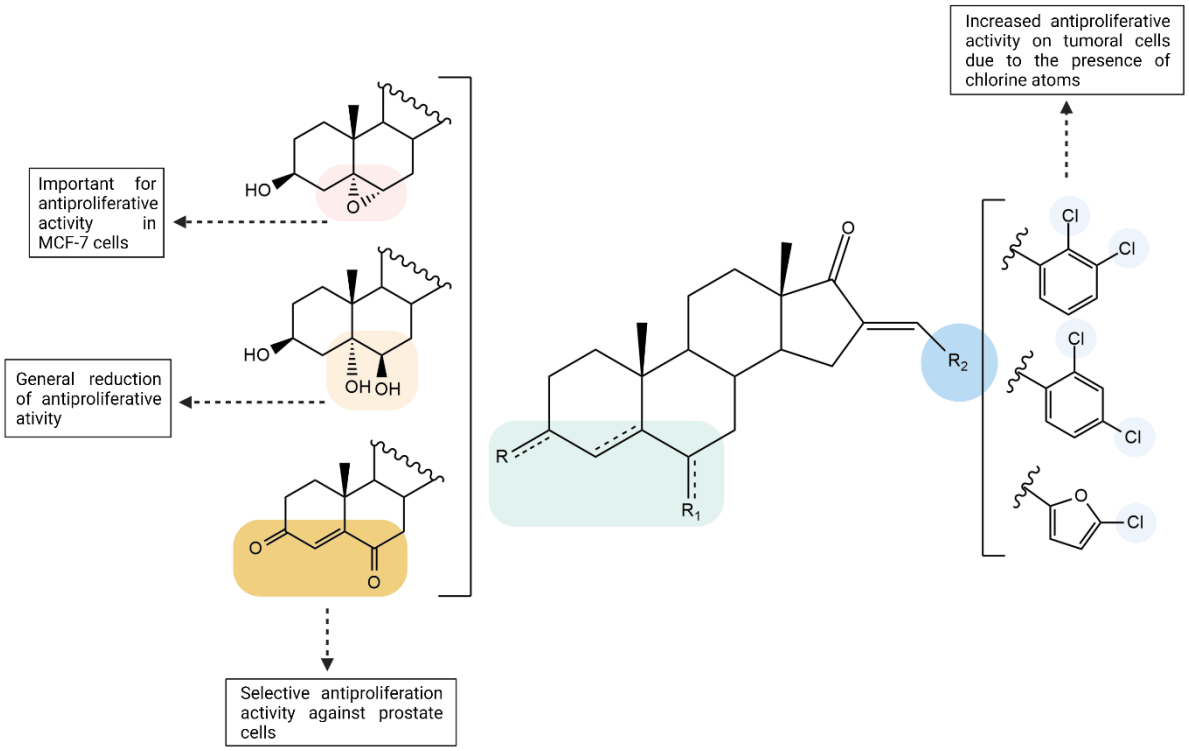

Figure 59. Structure-activity relationship (SAR) analysis of 16*E*-arylidene-dehydroepiandrosterone derivatives in relation to antiproliferative activity. Created with ChemDraw and BioRender.com.

Afterward, steroidal triols and triones, **VB 10e** and **VB 11c** effects on cell morphology were also studied, as well as the effect of **VB 11c** on caspase-3/7 activity. Considering the results from MTT assay, **VB 10e** and **VB 11c** were tested against PC-3 and LNCaP cells, respectively. Relative to experiments performed in PC-3 cells, **VB 10e** seemed not cause modifications on NA, however a significant increase on NND in relation to control were observed after 24, 48 and 72 h of incubation. Moreover, no pycnotic cells or debris were detected in microphotographs. This fact is indicative of an aleatory cell distribution and more spacing between cells, and consequently lower cell density. Thus, these data

suggest that probably **VB 10e** causes proliferation inhibition instead of activating a cell death mechanism. Interesting results were observed in LNCaP cells, constituting strong evidence that supports the triggering of apoptotic pathway by **VB 11c**. In fact, besides causing morphological changes in cells proved by NA measurement and causing a decrease on cell density (NND analysis), **VB 11c** also seemed to significantly increase the activity of caspase-3/7.

Molecular docking simulation is a typical structure-based drug design method used to assess and predict the binding energies and potential interaction between a ligand and a macromolecule, being a method relatively fast and practical.[573,574] Considering the important role of steroids in human physiology, the main targets of their action are relative to the mechanisms influencing hormonal biosynthesis. In the scope of the present work, 5AR type 2, AR, ERα, CYP17A1 and aromatase were the macromolecules selected for docking because: (1) they are known as therapeutic targets associated to hormone-dependent cancers (prostatic and breast cancers) or in BPH (5AR); (2) several steroidal derivatives were described as potent ligands of these macromolecules; (3) X-ray or NMR data with three-dimensional coordinates of these macromolecules exist complexed with endogenous molecules as DHT, estradiol, androstenedione, and semi-synthetic compounds (abiraterone and finasteride) structurally similar to the tested steroids. At this point, a simple analysis of binding energies of novel compounds against 5AR type 2, ERα, AR, CYP17A1, and aromatase was performed to understand the potential affinity, comparing the values obtained with the references for each macromolecule. The data obtained from these simulations are summarized in the heatmap depicted in **Figure 60**.

The results obtained showed clearly that the prepared steroidal derivatives do not possess significant affinity to ERα and AR, presenting high values of binding energies against these to receptors (in red, **Figure 60**). Moreover, comparing with the reference values for each macromolecule-ligand complex binding energies, the values obtained are significantly higher. This lack of affinity can possibly be explained by the presence of bulky groups (arylidene) on C-16 position, since the conformation in the active site becomes less favorable and main interactions are hampered. On the other hand, all compounds displayed energy binding values against CYP17A1 lower than the reference (abiraterone), which is indicative of a possible strong affinity. This result suggested the possibility of establishment of important interactions between tested compounds and this enzyme, which could be interesting considering the relevance of CYP17A1 in androgen signaling pathway. In fact, several CYP17 inhibitors have been prepared and

evaluated with the purpose of treat advanced PCa, being abiraterone (clinically used) and galeterone the most relevant examples.[226,507,575] Regarding 5AR type 2, tested compounds generally presented medium to high affinity in relation to the reference compound (binding energies close or inferior to the predicted for finasteride, **Figure 60**) and the best results for binding energies were verified for epoxysteroidal derivatives. Thus, these simulations seemed to favor the possibility of these new steroidal derivatives interacting with 5AR type 2, and consequently potentially acting as 5ARIs. In addition, the analysis of main interactions potentially established between 5AR and the most active compounds *in vitro* were further explored after experimental 5AR activity inhibition assays. However, these results will be discussed posteriorly. Concerning aromatase, generally, epoxysteroidal derivatives showed lower affinity (red overlaid with green, **Figure 60**) to this enzyme than steroidal 4-ene-3,6,17-triones (light green, **Figure 60**). In addition, steroidal 3β,5α,6β-triols presented values higher but close to the reference (androstenedione) against this target. Thus, possibly the modifications at A- and B-ring were crucial to these differences in affinity against aromatase.

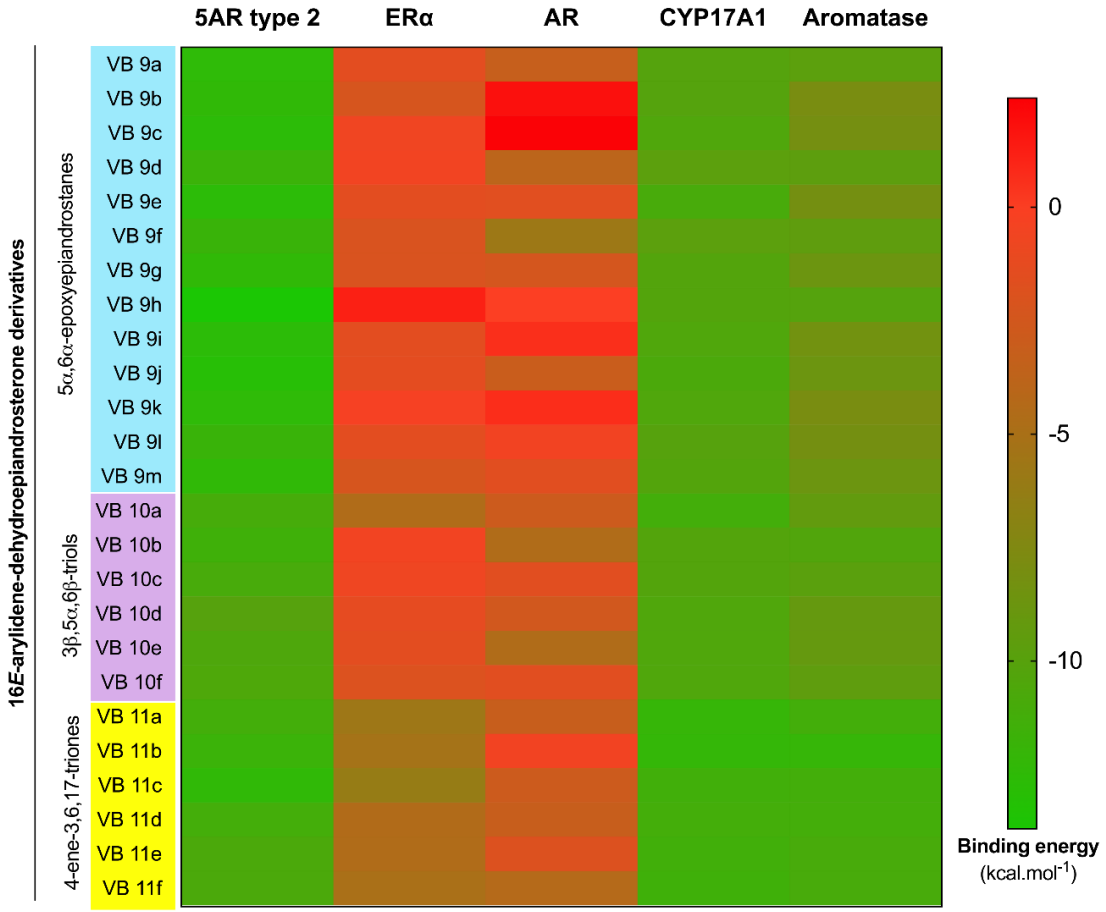

Figure 60. Heatmap of binding energies of the new series of 16*E*-arylidene-dehydroepiandrosterone derivatives against important targets of steroids. **Red** is indicative of poor affinity, while **green** is indicative of strong affinity. (5AR= 5α-Reductase, ERα= Estrogen receptor α, AR= Androgen receptor, CYP17A1= Steroid 17α-hydroxylase/17,20 lyase).

To complete the experiments planned for this doctoral project, the assessment of 5AR activity was crucial to elucidate the potential of the novel steroidal arylidene derivatives as 5ARIs, as well as the potential of the 4-azasteroids previous synthesized in the context of Master's dissertation. To achieve this goal, the *in vitro* assessment of 5AR inhibitory activity of tested compounds was performed using as enzyme source mice liver microsomes. This indirect method consisted in the measurement of remaining/free testosterone through HPLC-DAD after incubation with the steroidal arylidene derivatives. The selection of this method was based principally on the use of label/radiation-free reagents, reducing the health impact for the researcher and not contaminating the facilities. In fact, usually, the evaluation of 5AR is achieved by chromatographic techniques using radioactive testosterone and DHT.[576] Moreover, considering the available equipment, laboratory resources, team know-how, and the optimal conditions of the animal bioterium facilities, the HPLC-DAD method was considered the most suitable. Despite some authors have reported similar experiments, a previous optimization, partial development and method validation were required to proceed with this study.[538,540,545,546]

The method for testosterone quantification by HPLC-DAD was partially developed, successfully optimized and validated accordingly to the current guidelines provided by EMA and FDA.[543,544] After finishing this procedure, the assessment of 5AR activity was achieved, and all arylidene derivatives prepared were tested, initially, in a preliminary study at 10 μM. From this first screening, a high number of tested compounds (**VB 7a**, **VB 7b**, **VB 7c**, **VB 7d**, **VB 7f**, **VB 7g**, **VB 9e**, **VB 9f**, **VB 9g**, **VB 9h**, **VB 9i**, **VB 9j**, **VB 10b**, **VB 10c**, and **VB 11c**) exhibited an inhibitory activity superior to 85 %. Considering the need to manage resources and not being feasible to determine the IC_{50} for all these compounds, a second screening assay was performed at 1 μM. At this concentration, steroids **VB 7b**, **VB 9f**, **VB 9h**, **VB 9j**, and **VB 11c** displayed percentages of inhibition superior to 80 %, and, therefore, the respective IC_{50} was determined. Interestingly, 4-azasteroids and epoxysteroids showed to be, in general, more active, which is in the accordance with the affinity binding energies obtained by molecular docking simulations. Nevertheless, the most potent compound found against 5AR was **VB 11c**, a trione (IC_{50}= 6.12 nM). Moreover, only epoxysteroids **VB 9h** and **VB 9j** presented IC_{50} values (102.30 and 685.00 nM, respectively) higher than the reference, finasteride (IC_{50}= 91.49 nM). Steroids **VB 7b** and **VB 9f** also showed interesting inhibitory activity (12.04 and 20.52 nM, respectively). In general, these compounds presented promising inhibitory activity, displaying IC_{50} values close or lower than other steroidal derivatives described in the literature.[373,577,578] However, conclusion based on different applied

methods to evaluate 5AR activity can be misleading and thus errors associated with this analysis need to be also considered. In spite that Kumar and coworkers used a very similar method to assess 5AR activity in two distinct studies evaluating plant extracts, the results were expressed in terms of finasteride equivalent 5AR inhibition activity as a unit of mg finasteride equivalent per 1 g extract.[540,545] Overall, from this study, interesting and promising results were obtained when compared with the drug used as reference, being **VB 7b** (IC_{50}= 12.04 nM) and **VB 11c** (IC_{50}= 6.12 nM) strong candidates to further studies as potential 5ARIs.

Lastly, in an attempt to comprehend the inhibitory activity of the most potent compounds observed in the *in vitro* assay, a complementary *in silico* analysis of the potential interactions of steroidal derivatives against 5AR was performed. As expected, the oxygen atom of ketone at C-3 position of 16*E*-arylidene-4-azapregnenes (**VB 7b**) seemed to play an important role with respect to the formation of conventional hydrogen bonds with residues present in the active site of the enzyme. Moreover, interactions with residues considered crucial to 5AR inhibition, according to the literature, were observed, namely the interactions with GLU57 and TYR91.[467] Concerning the remaining derivatives, modifications in A- and B-rings seemed not to lead to an improvement on the number or type of interactions, being the arylidene groups responsible for the differences observed in the determined affinity. In fact, the aromatic bulky groups were capable of establish several π-alkyl interactions with enzyme residues. In addition, substituted aromatic rings (at the arylidene group) seemed to establish stronger interactions, including hydrogen bonds with halogens chlorine and fluorine atoms (acceptors).[579] In addition, the positioning and orientation of these compounds on the pocket site allowed the establishment of several interactions which can explain the high affinity to 5AR. Then, the main interactions established between each tested compounds and 5AR, compared with finasteride, the binding energy predicted from molecular docking simulations, and the estimated IC_{50} values were cross-analyzed to clarify if there is a relationship between *in vitro* and *in silico* data. Interestingly, steroid **VB 11c**, which exhibited an affinity higher than finasteride, according to docking studies, also presented the higher number of common interactions with this reference, including with GLU57 and TYR91 residues. Moreover, **VB 11c** revealed to be the most potent steroid in the *in vitro* assay (IC_{50}= 6.12 nM), being the most promising compound. In summary, despite a direct correlation between affinity/interactions and 5AR inhibitory activity cannot be recognized without further analysis, compounds displaying simultaneous interactions with the residues of interest (GLU57 and TYR91) seemed to be more potent.

Considering all the results herein present and the aim of this doctoral project, the preparation of steroidal arylidene derivatives presenting inhibitory capacity of 5AR and/or antiproliferative properties against tumoral cells were successfully accomplished. Of all compounds, steroid **VB 11c** seemed to be the most promising molecule to be considered as a hit compound. A simple and possible SAR analysis for antiproliferative and 5AR inhibitory effects of this compound are depicted in **Figure 61**. Steroid **VB 11c**, which presented selectivity to tumoral prostate cells (IC_{50} higher against other cell lines, including non-tumoral cells), also seemed to trigger the apoptotic cell death mechanism in LNCaP cell line (androgen-dependent cells). In addition to its antitumoral activity in prostate cells, this compound also revealed to be the most potent against 5AR, being a potential 5ARI.

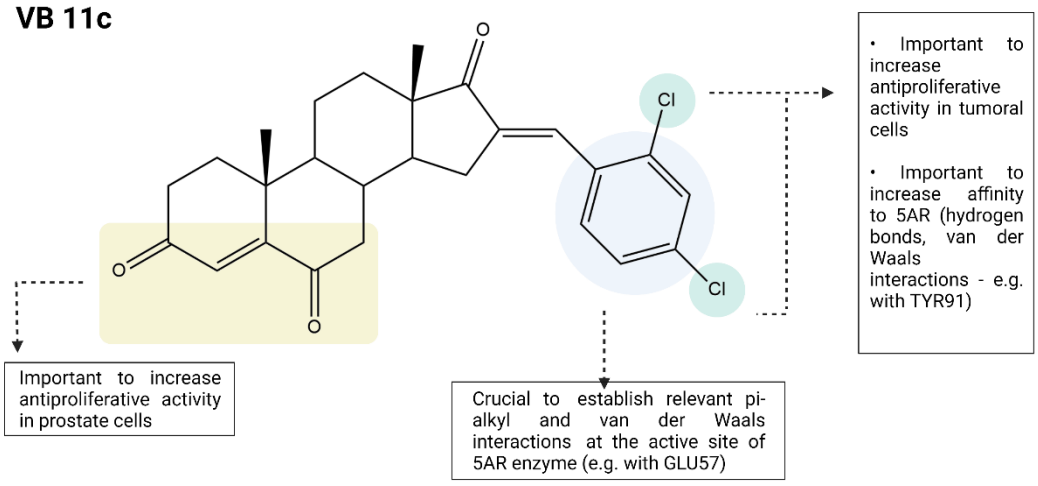

Figure 61. Structure-activity relationship (SAR) analysis of steroid **VB 11c** for antiproliferative and 5α-reductase (5AR) inhibitory activities. Created with ChemDraw and BioRender.com.

CHAPTER VII

7. Conclusions and Future Perspectives

Prostatic diseases, namely BPH and PCa, continue to be a worrying health disorder and, although several research efforts have contributed to improving diagnosis and treatment methods, it persists as a source of considerable morbidity and mortality for men worldwide. Consequently, the research for new more potent, effective, and safer drugs continues to arouse the interest of scientists. In this context, the present doctoral project was designed to found new series of steroidal arylidene derivatives potentially useful in the treatment of prostatic diseases, exhibiting inhibitory capacity against 5AR and/or antiproliferative properties against tumoral cells.

Hence, the antiproliferative and 5AR inhibitory activities of the studied steroidal arylidene derivatives found in this project were promising and justify further research following this aim. The most significant key findings drawn from all the experimental work described in the present thesis, as well as additional proposals for future work are concisely provided below:

- 3D-QSAR models were developed to clarify the activity of arylidene-4-azasteroidal derivatives prepared during the Master's project on LNCaP and PC-3 cell proliferation (prostatic cell lines). This study showed the importance of the presence of bulky groups and electronegative atoms (e.g. halogens).

- After defining a new synthetic strategy, three distinct series of oxidized arylidene steroids, comprising new twenty-five compounds, were successfully prepared in very acceptable yields: 16*E*-arylidene-5α,6α-epoxyepiandrosterone derivatives (**VB 9a-m**), 16*E*-arylidene-3β,5α,6β-trihydroxyandrostan-17-ones (**VB 10a-g**), and 16*E*-arylidende-androst-4-ene-3,6,17-triones (**VB 11a-f**). All new products were properly purified and well characterized by NMR, HRMS, and IR techniques.

- In relation to the assessment of their antiproliferative activity by the MTT assay, the most relevant reduction of cell proliferation was observed with compounds **VB 9e** in MCF-7 cells (IC_{50}= 3.47 μM), **VB 10e** in PC-3 cells (IC_{50}= 6.96 μM), and **VB 11c** in LNCaP cells (IC_{50}= 6.48 μM). A SAR analysis bearing in mind the MTT results concluded that: (1) an epoxy

group at B-ring (at **VB 9a-m**) seemed to be important for antiproliferative activity in MCF-7 cells; (2) the 5α,6β-diol (at **VB 10a-f**) seemed generally to decrease the antiproliferative effect; (3) 4-ene-3,6-dione group (at **VB 11a-f**) might be related to the selectivity against prostate cells, and (4) steroidal derivatives with arylidene groups bearing chlorine atoms seemed to display higher antiproliferative on tumoral cells.

- Complementary biological studies showed that steroidal derivatives **VB 9e** and **VB 11c** seemed to trigger apoptosis in MCF-7 and LNCaP cells, respectively. **VB 9e** caused significant alterations in Ki67 (↓) and PI (↑) staining on MFC-7 cell line, and nuclear morphology and cell distribution analysis were in accordance with the observed for apoptotic cells. On the other hand, **VB 11c**, in addition to cause the same morphological and cell distribution alterations, also increased the activity of caspase-3/7 in LNCaP cell line.

- Molecular docking studies provided interesting information about the affinity of these new compounds against several important targets of steroidal molecules (5AR type 2, ERα, AR, CYP17A1, and aromatase). In general, these new derivatives showed stronger affinity to 5AR type 2 and CYP17A1, and poor affinity to ERα and AR. In relation to aromatase, it was verified higher affinity for steroidal 4-ene-3,6,17-triones.

- The effect of the steroidal arylidene derivatives on 5AR activity was evaluated through testosterone quantification in mice liver microsomes bearing 5AR enzymes by HPLC-DAD. This method was partially developed, optimized and validated in the accordance to the current guidelines. From these experiments, compound **VB 11c** seemed to be the most potent inhibitor (IC_{50}= 6.12 nM). In addition, an *in silico* interaction study was performed and it was observed that this steroid displayed the higher number of interactions in common with finasteride, the reference, when comparing with other tested compounds. Interestingly, in this case, there is a correlation between *in silico* and experimental data.

- Of all compounds herein described, steroid **VB 11c** seemed to be the most promising molecule to be considered as a hit, presenting selectivity to tumoral prostate cells, potentially triggering the apoptotic cell death

mechanism in LNCaP cell line (androgen-dependent cells), and being the most potent against 5AR.

- The exciting results with steroid **VB 9e** in breast cancer cells (MCF-7) should not be discarded. Despite the scope of this thesis being the treatment of prostatic diseases, this discovery is also important for other future research approaches. Considering that these cells are hormone-dependent, they are usually included in the assays to verify if steroidal derivatives present some antiproliferative effect.

- Further investigations, including *in vivo* studies to assess the pharmacokinetic profile and effectiveness of the most promising compounds would be essential to clarify the potential of these compounds as 5ARIs and/or antitumoral agents in the treatment of prostatic diseases.

As final remark it can be stated that this thesis encompasses an integrated medicinal chemistry approach, comprising rational drug design, chemical synthesis, and biological evaluation using computational tools and *in vitro* experiments. In conclusion, this research work provided new information on steroidal arylidene derivatives as agents with antiproliferative and 5AR inhibitory properties. Additionally, and as projected, the results obtained showed the potentiality of developing new hit compounds for further development in the context of BPH and PCa.

CHAPTER VIII

8. References

1. Reeves, F., Everaerts, W., Murphy, D. G. & Costello, A. *The surgical anatomy of the prostate. Prostate Cancer: Science and Clinical Practice: Second Edition* (Elsevier Ltd, 2016).
2. Clark, S. & Nabity, M. *Male reproductive tract. Cowell and Tyler's Diagnostic Cytology and Hematology of the Dog and Cat* (Elsevier Inc., 2020).
3. Patel, U. *The prostate and seminal vesicles. Clinical Ultrasound* vol. 1 (Elsevier Ltd, 2011).
4. Hedayat, K. M. & Lapraz, J.-C. Disorders of the prostate: lower urinary tract obstruction and prostatitis. in *The Theory of Endobiogeny* vol. 28 135–164 (2019).
5. Coleman, W. B. *Molecular pathogenesis of prostate cancer. Molecular Pathology: The Molecular Basis of Human Disease* (INC, 2018).
6. Verze, P., Cai, T. & Lorenzetti, S. The role of the prostate in male fertility, health and disease. *Nat. Rev. Urol.* **13**, 379–386 (2016).
7. Wendell-Smith, C. Terminology of the prostate and related structures. *Clin. Anat.* **13**, 207–213 (2000).
8. McNeal, J. E. Normal histology of the prostate. *Am. J. Surg. Pathol.* **12**, (1988).
9. De Marzo, A. M. *et al.* Inflammation in prostate carcinogenesis. *Nat. Rev. Cancer* **7**, 256–269 (2007).
10. Nelson, W. G., De Marzo, A. M. & Isaacs, W. B. Prostate cancer. in *The New England journal of medicine* vol. 349 1401–1432 (2020).
11. Campbell Walsh, Patrick C.,, M. F. *Campbell's urology*. (Saunders, 1992).
12. Abdelsayed, G. A., Danial, T., Kaswick, J. A. & Finley, D. S. Tumors of the anterior prostate: implications for diagnosis and treatment. *Urology* **85**, 1224–1228 (2015).
13. Thorpe, A. & Neal, D. Benign prostatic hyperplasia. *Lancet (London, England)* **361**, 1359–1367 (2003).
14. Pagano, E., Laudato, M., Griffo, M. & Capasso, R. Phytotherapy of benign prostatic hyperplasia. A minireview. *Phytother. Res.* **28**, 949–955 (2014).
15. Lim, K. Bin. Epidemiology of clinical benign prostatic hyperplasia. *Asian J. Urol.* **4**, 148–151 (2017).
16. Guess, H. A., Arrighi, H. M., Metter, E. J. & Fozard, J. L. Cumulative prevalence of prostatism matches the autopsy prevalence of benign prostatic hyperplasia. *Prostate* **17**, 241–246 (1990).

17. Berry, S. J., Coffey, D. S., Walsh, P. C. & Ewing, L. L. The development of human benign prostatic hyperplasia with age. *J. Urol.* **132**, 474–479 (1984).
18. Taylor, B. C. *et al.* Prevalence, severity, and health correlates of lower urinary tract symptoms among older men: the MrOS study. *Urology* **68**, 804–809 (2006).
19. Kok, E. T. *et al.* Risk factors for lower urinary tract symptoms suggestive of benign prostatic hyperplasia in a community based population of healthy aging men: the Krimpen Study. *J. Urol.* **181**, 710–716 (2009).
20. Parsons, J. K. Modifiable risk factors for benign prostatic hyperplasia and lower urinary tract symptoms: new approaches to old problems. *J. Urol.* **178**, 395–401 (2007).
21. Kayode, O. T., Owolabi, A. V. & Kayode, A. A. A. Biochemical and histomorphological changes in testosterone propionate-induced benign prostatic hyperplasia in male Wistar rats treated with ketogenic diet. *Biomed. Pharmacother.* **132**, 110863 (2020).
22. Lepor, H. Pathophysiology of benign prostatic hyperplasia in the aging male population. *Rev. Urol.* **7 Suppl 4**, S3–S12 (2005).
23. Lee, C., Kozlowski, J. M. & Grayhack, J. T. Intrinsic and extrinsic factors controlling benign prostatic growth. *Prostate* **31**, 131–138 (1997).
24. Yu, Z., Yan, H., Xu, F., Chao, H. & Deng, L. Efficacy and Side Effects of Drugs Commonly Used for the Treatment of Lower Urinary Tract Symptoms Associated With Benign Prostatic Hyperplasia. *Front. Pharmacol.* **11**, 658 (2020).
25. McNeal Burroughs Wellcome Company., J. E. *The prostate gland, morphology and pathobiology*. (Published for Burroughs Wellcome Co. by Custom Pub. Services, 1983).
26. Parsons, J. K. Benign prostatic hyperplasia and male lower urinary tract symptoms: epidemiology and risk factors. *Curr. Bladder Dysfunct. Rep.* **5**, 212–218 (2010).
27. Homma, Y. *et al.* Clinical guidelines for male lower urinary tract symptoms and benign prostatic hyperplasia. *Int. J. Urol.* **24**, 716–729 (2017).
28. Langan, R. C. Benign prostatic hyperplasia. *Prim. Care - Clin. Off. Pract.* **46**, 223–232 (2019).
29. Juliao, A. A., Plata, M., Kazzazi, A., Bostanci, Y. & Djavan, B. American Urological Association and European Association of Urology guidelines in the management of benign prostatic hypertrophy: revisited. *Curr. Opin. Urol.* **22**, (2012).
30. Oesterling, J. E. Serum prostate-specific antigen in a community-based population of healthy men. *Jama* **270**, 860 (1993).
31. Salvador, J. A. R., Pinto, R. M. A. & Silvestre, S. M. Steroidal 5α-Reductase and

17α-Hydroxylase/17,20-lyase (CYP17) Inhibitors Useful in the Treatment of Prostatic Diseases. *J. Steroid Biochem. Mol. Biol.* **137**, 199–222 (2013).

32. Wen, S. *et al.* Stromal androgen receptor roles in the development of normal prostate, benign prostate hyperplasia, and prostate cancer. *Am. J. Pathol.* **185**, 293–301 (2015).
33. Hayward, S. W. *et al.* Stromal development in the ventral prostate, anterior prostate and seminal vesicle of the rat. *Acta Anat. (Basel).* **155**, 94–103 (1996).
34. Heinlein, C. A. & Chang, C. Androgen receptor in prostate cancer. *Endocr. Rev.* **25**, 276–308 (2004).
35. Biggins, J. B. & Koh, J. T. Chemical biology of steroid and nuclear hormone receptors. *Curr. Opin. Chem. Biol.* **11**, 99–110 (2007).
36. Gao, W., Bohl, C. E. & Dalton, J. T. Chemistry and structural biology of androgen receptor. *Chem. Rev.* **105**, 3353–3370 (2005).
37. Davey, R. A. & Grossmann, M. Androgen receptor structure, function and biology: from bench to bedside. *Clin. Biochem. Rev.* **37**, 3–15 (2016).
38. Schmidt, L. J. & Tindall, D. J. Steroid 5α-reductase inhibitors targeting BPH and prostate cancer. *J. Steroid Biochem. Mol. Biol.* **125**, 32–38 (2011).
39. Russell, D. W. & Wilson, J. D. Steroid 5α-Reductase: Two Genes/Two Enzymes. *Annu. Rev. Biochem.* **63**, 25–61 (1994).
40. Tan, M. E., Li, J., Xu, H. E., Melcher, K. & Yong, E.-L. Androgen receptor: structure, role in prostate cancer and drug discovery. *Acta Pharmacol. Sin.* **36**, 1–21 (2014).
41. Lee, C. Role of androgen in prostate growth and regression: stromal-epithelial interaction. *Prostate. Suppl.* **6**, 52–56 (1996).
42. Carson, C. & Rittmaster, R. The role of dihydrotestosterone in benign prostatic hyperplasia. *Urology* **61**, 2–7 (2003).
43. Svindland, A., Eri, L. M. & Tveter, K. J. Morphometry of benign prostatic hyperplasia during androgen suppressive therapy. Relationships among epithelial content, PSA density, and clinical outcome. *Scand. J. Urol. Nephrol. Suppl.* **179**, 113–117 (1996).
44. Barkin, J. Benign prostatic hyperplasia and lower urinary tract symptoms: evidence and approaches for best case management. *Can. J. Urol.* **18 Suppl**, 14–19 (2011).
45. Emberton, M., Fitzpatrick, J. M. & Rees, J. Risk stratification for benign prostatic hyperplasia (BPH) treatment. *BJU Int.* **107**, 876–880 (2011).
46. Ho, C. K. M. & Habib, F. K. Estrogen and androgen signaling in the pathogenesis of BPH. *Nat. Rev. Urol.* **8**, 29–41 (2011).

47. Fibbi, B., Penna, G., Morelli, A., Adorini, L. & Maggi, M. Chronic inflammation in the pathogenesis of benign prostatic hyperplasia. *Int. J. Androl.* **33**, 475–488 (2010).
48. Lai, K.-P. *et al.* Targeting stromal androgen receptor suppresses prolactin-driven benign prostatic hyperplasia (BPH). *Mol. Endocrinol.* **27**, 1617–1631 (2013).
49. Wilson, J. D. Sexual differentiation. *Annu. Rev. Physiol.* **40**, 279–306 (1978).
50. Azzouni, F., Godoy, A., Li, Y. & Mohler, J. The 5α-reductase isozyme family: a review of basic biology and their role in human diseases. *Adv. Urol.* **2012**, 1–18 (2012).
51. Thigpen, A. E. *et al.* Tissue Distribution and Ontogeny of Steroid 5α-Reductase Isozyme. *J. Clin. Invest.* **92**, 903–910 (1993).
52. Hsing, A. W. Hormones and prostate cancer: what's next ? *Public Health* **23**, 42–58 (2001).
53. Marchetti, P. M. & Barth, J. H. Clinical biochemistry of dihydrotestosterone. *Ann. Clin. Biochem.* **50**, 95–107 (2013).
54. Singh, A. S., Chau, C. H., Price, D. K. & Figg, W. D. Mechanisms of disease: polymorphisms of androgen regulatory genes in the development of prostate cancer. *Nat. Clin. Pract. Urol.* **2**, 101–107 (2005).
55. Djavan, B. & Barkin, J. Novel Therapeutic Strategies for Managing BPH Progression. *Eur. Urol. Suppl.* **2**, 20–26 (2003).
56. Garg, G., Singh, D., Saraf, S. & Saraf, S. Management of benign prostate hyperplasia: an overview of α-adrenergic antagonist. *Biol. Pharm. Bull.* **29**, 1554–1558 (2006).
57. Kim, E., Larson, J. & Andriole, G. Management of benign prostatic hyperplasia. *Annu. Rev. Med.* **67**, 137–151 (2016).
58. Tammela, T. Benign prostatic hyperplasia. Practical treatment guidelines. *Drugs & aging* **10**, 349–366 (1997).
59. McVary, K. T. *et al.* Update on AUA guideline on the management of benign prostatic hyperplasia. *J. Urol.* **185**, 1793–1803 (2011).
60. Foster, H. E. *et al.* Surgical management of lower urinary tract symptoms attributed to benign prostatic hyperplasia: AUA Guideline. *J. Urol.* **200**, 612–619 (2018).
61. Gravas, S. *et al.* EAU Guidelines on non-neurogenic male LUTS incl. BPO 2020. (2020).
62. McConnell, J. D., Barry, M. J. & Bruskewitz, R. C. Benign prostatic hyperplasia: diagnosis and treatment. *Clin. Pract. Guidel. Quick Ref. Guide Clin.* 1–17 (1994).
63. Sandhu, J. S. Therapeutic options in the treatment of benign prostatic

hyperplasia. *Patient Prefer. Adherence* **3**, 213–223 (2009).

64. Djavan, B. & Marberger, M. Minimally invasive procedures as an alternative to medical management for lower urinary tract symptoms of benign prostatic hyperplasia. *Curr. Opin. Urol.* **11**, 1–7 (2001).
65. Harkaway, R. C. & Issa, M. M. Medical and minimally invasive therapies for the treatment of benign prostatic hyperplasia. *Prostate Cancer Prostatic Dis.* **9**, 204–214 (2006).
66. Djavan, B., Seitz, C. & Marberger, M. Heat versus drugs in the treatment of benign prostatic hyperplasia. *BJU Int.* **91**, 131–137 (2003).
67. Andersson, K.-E. & Gratzke, C. Pharmacology of alpha1-adrenoceptor antagonists in the lower urinary tract and central nervous system. *Nat. Clin. Pract. Urol.* **4**, 368–378 (2007).
68. Kirby, R. S. Clinical pharmacology of alpha1-adrenoceptor antagonists. *Eur. Urol.* **36 Suppl 1**, 48–53; discussion 65 (1999).
69. Nickel, J. C. The use of alpha1-adrenoceptor antagonists in lower urinary tract symptoms: beyond benign prostatic hyperplasia. *Urology* **62**, 34–41 (2003).
70. Thiyagarajan, M. Adrenoceptor Antagonists in the Hyperplasia. *Pharmacology* **62**, 119–128 (2002).
71. Proudman, R. G. W., Pupo, A. S. & Baker, J. G. The affinity and selectivity of α-adrenoceptor antagonists, antidepressants, and antipsychotics for the human α1A, α1B, and α1D-adrenoceptors. *Pharmacol. Res. Perspect.* **8**, 1–16 (2020).
72. Lepor, H., Kazzazi, A. & Djavan, B. α-Blockers for benign prostatic hyperplasia: The new era. *Curr. Opin. Urol.* **22**, 7–15 (2012).
73. Azzouni, F. & Mohler, J. Role of 5α-reductase inhibitors in benign prostatic diseases. *Prostate Cancer Prostatic Dis.* **15**, 222–230 (2012).
74. Wang, K., Fan, D. D., Jin, S., Xing, N. Z. & Niu, Y. N. Differential expression of 5-alpha reductase isozymes in the prostate and its clinical implications. *Asian J. Androl.* **16**, 274–279 (2014).
75. Normington, K. & Russell, D. W. Tissue distribution and kinetic characteristics of rat steroid 5 alpha-reductase isozymes. Evidence for distinct physiological functions. *J. Biol. Chem.* **267**, 19548–19554 (1992).
76. Yamana, K., Fernand, L., Luu-The, V. & Luu-The, V. Human type 3 5α-reductase is expressed in peripheral tissues at higher levels than types 1 and 2 and its activity is potently inhibited by finasteride and dutasteride. *Horm. Mol. Biol. Clin. Investig.* **2**, 293–299 (2010).
77. Uemura, M. *et al.* Novel 5α-Steroid Reductase (SRD5A3, type-3) is Overexpressed in Hormone-refractory Prostate Cancer. *Cancer Sci.* **99**, 81–86 (2008).

78. Drobnis, E. Z. & Nangia, A. K. 5α-Reductase inhibitors (5ARIs) and male reproduction BT - impacts of medications on male fertility. in (eds. Drobnis, E. Z. & Nangia, A. K.) 59–61 (Springer International Publishing, 2017).
79. Sudduth, S. L. & Koronkowski, M. J. Finasteride: the first 5α-reductase inhibitor. *Pharmacotherapy* **13**, 309 (1993).
80. Cilotti, A., Danza, G. & Serio, M. Clinical application of 5α-reductase inhibitors. *J. Endocrinol. Invest.* **24**, 199–203 (2001).
81. Aggarwal, S., Thareja, S., Verma, A., Bhardwaj, T. R. & Kumar, M. An overview on 5α-reductase inhibitors. *Steroids* **75**, 109–153 (2010).
82. Montorsi, F. & Moncada, I. Safety and tolerability of treatment for BPH. *Eur. Urol. Suppl.* **5**, 1004–1012 (2006).
83. Diviccaro, S. *et al.* Treatment of male rats with finasteride, an inhibitor of 5alpha-reductase enzyme, induces long-lasting effects on depressive-like behavior, hippocampal neurogenesis, neuroinflammation and gut microbiota composition. *Psychoneuroendocrinology* **99**, 206–215 (2019).
84. Basaria, S. *et al.* Characteristics of men who report persistent sexual symptoms after finasteride use for hair loss. *J. Clin. Endocrinol. Metab.* **101**, 4669–4680 (2016).
85. Melcangi, R. C. *et al.* Neuroactive steroid levels and psychiatric and andrological features in post-finasteride patients. *J. Steroid Biochem. Mol. Biol.* **171**, 229–235 (2017).
86. Eglen, R. M. Muscarinic receptor subtype pharmacology and physiology. in (eds. King, F. D. & Lawton, G. B. T.-P. in M. C.) vol. 43 105–136 (Elsevier, 2005).
87. Chapple, C. R., Yamanishi, T. & Chess-Williams, R. Muscarinic receptor subtypes and management of the overactive bladder. *Urology* **60**, 82–88 (2002).
88. Sellers, D. J. & Chess-Williams, R. Muscarinic agonists and antagonists: effects on the urinary bladder BT-muscarinic receptors. in (eds. Fryer, A. D., Christopoulos, A. & Nathanson, N. M.) 375–400 (Springer Berlin Heidelberg, 2012).
89. Yamada, S., Ito, Y., Nishijima, S., Kadekawa, K. & Sugaya, K. Basic and clinical aspects of antimuscarinic agents used to treat overactive bladder. *Pharmacol. Ther.* **189**, 130–148 (2018).
90. Chapple, C. R. *et al.* The effects of antimuscarinic treatments in overactive bladder: an update of a systematic review and meta-analysis. *Eur. Urol.* **54**, 543–562 (2008).
91. Bylund, D. B. *et al.* International Union of Pharmacology nomenclature of adrenoceptors. *Pharmacol. Rev.* **46**, 121–136 (1994).
92. Ursino, M. G., Vasina, V., Raschi, E., Crema, F. & De Ponti, F. The beta3-

adrenoceptor as a therapeutic target: current perspectives. *Pharmacol. Res.* **59**, 221–234 (2009).

93. Yang, L.-K. & Tao, Y.-X. Physiology and pathophysiology of the β3-adrenergic receptor. in *G Protein Signaling Pathways in Health and Disease* (ed. Tao, Y.-X. B. T.-P. in M. B. and T. S.) vol. 161 91–112 (Academic Press, 2019).
94. Chapple, C. R., Cardozo, L., Nitti, V. W., Siddiqui, E. & Michel, M. C. Mirabegron in overactive bladder: a review of efficacy, safety, and tolerability. *Neurourol. Urodyn.* **33**, 17–30 (2014).
95. Kelleher, C. *et al.* Efficacy and tolerability of mirabegron compared with antimuscarinic monotherapy or combination therapies for overactive bladder: a systematic review and network meta-analysis. *Eur. Urol.* **74**, 324–333 (2018).
96. Ahmed, W. S., Geethakumari, A. M. & Biswas, K. H. Phosphodiesterase 5 (PDE5): structure-function regulation and therapeutic applications of inhibitors. *Biomed. Pharmacother.* **134**, 111128 (2021).
97. Fibbi, B. *et al.* Characterization of phosphodiesterase type 5 expression and functional sctivity in the human male lower urinary tract. *J. Sex. Med.* **7**, 59–69 (2010).
98. Giuliano, F. *et al.* The mechanism of action of phosphodiesterase type 5 inhibitors in the treatment of lower urinary tract symptoms related to benign prostatic hyperplasia. *Eur. Urol.* **63**, 506–516 (2013).
99. Bischoff, E. Potency, selectivity, and consequences of nonselectivity of PDE inhibition. *Int. J. Impot. Res.* **16 Suppl 1**, S11-4 (2004).
100. Kedia, G. T., Ückert, S., Jonas, U., Kuczyk, M. A. & Burchardt, M. The nitric oxide pathway in the human prostate: clinical implications in men with lower urinary tract symptoms. *World J. Urol.* **26**, 603–609 (2008).
101. Hiramatsu, I. *et al.* Tadalafil is sufficiently effective for severe chronic prostatitis/chronic pelvic pain syndrome in patients with benign prostatic hyperplasia. *Int. J. Urol.* **27**, 53–57 (2020).
102. Gacci, M. *et al.* A systematic review and meta-analysis on the use of phosphodiesterase 5 inhibitors alone or in combination with α-blockers for lower urinary tract symptoms due to benign prostatic hyperplasia. *Eur. Urol.* **61**, 994–1003 (2012).
103. Madersbacher, S., Berger, I., Ponholzer, A. & Marszalek, M. Plant extracts: sense or nonsense? *Curr. Opin. Urol.* **18**, 16–20 (2008).
104. Cornu, J.-N., Cussenot, O., Haab, F. & Lukacs, B. A widespread population study of actual medical management of lower urinary tract symptoms related to benign prostatic hyperplasia across europe and beyond official clinical guidelines. *Eur.*

Urol. **58**, 450–456 (2010).

105. Sharma, M. & Dhingra, R. C. and N. Phytotherapeutic agents for benign prostatic hyperplasia: an overview. *Mini-Reviews in Medicinal Chemistry* vol. 17 1346–1363 (2017).
106. Habib, F. K., Ross, M., Ho, C. K. H., Lyons, V. & Chapman, K. Serenoa repens (Permixon®) inhibits the 5α-reductase activity of human prostate cancer cell lines without interfering with PSA expression. *Int. J. Cancer* **114**, 190–194 (2005).
107. Kwon, Y. Use of saw palmetto (Serenoa repens) extract for benign prostatic hyperplasia. *Food Sci. Biotechnol.* **28**, 1599–1606 (2019).
108. Bent, S. *et al.* Saw palmetto for benign prostatic hyperplasia. *N. Engl. J. Med.* **354**, 557–566 (2006).
109. Vela-Navarrete, R. *et al.* Efficacy and safety of a hexanic extract of Serenoa repens (Permixon®) for the treatment of lower urinary tract symptoms associated with benign prostatic hyperplasia (LUTS/BPH): systematic review and meta-analysis of randomised controlled trials and obser. *BJU Int.* **122**, 1049–1065 (2018).
110. Morgia, G. & Privitera, S. Phytotherapy in benign prostatic hyperplasia. in *Nuts and Seeds in Health and Disiase Prevention* (eds. Morgia, G. & Russo, G. I. B. T.-L. U. T. S. and B. P. H.) 135–175 (Academic Press, 2018).
111. Leibbrand, M. *et al.* Effects of an oil-free hydroethanolic pumpkin seed extract on symptom frequency and severity in men with benign prostatic hyperplasia: a pilot study in humans. *J. Med. Food* **22**, 551–559 (2019).
112. Nishimura, M., Ohkawara, T., Sato, H., Takeda, H. & Nishihira, J. Pumpkin seed oil extracted from cucurbita maxima improves urinary disorder in human overactive bladder. *J. Tradit. Complement. Med.* **4**, 72–74 (2014).
113. Buck, A. C. Is there a scientific basis for the therapeutic effects of serenoa repens in benign prostatic hyperplasia? Mechanisms of action. *J. Urol.* **172**, 1792–1799 (2004).
114. Gandaglia, G. *et al.* The role of prostatic inflammation in the development and progression of benign and malignant diseases. *Curr. Opin. Urol.* **27**, (2017).
115. Paterniti, I. *et al.* Effects of different natural extracts in an experimental model of benign prostatic hyperplasia (BPH). *Inflamm. Res.* **67**, 617–626 (2018).
116. Ückert, S. *et al.* Emerging drugs to target lower urinary tract symptomatology (LUTS)/benign prostatic hyperplasia (BPH): focus on the prostate. *World J. Urol.* **38**, 1423–1435 (2020).
117. Chang, R. S. *et al.* In vitro studies on L-771,688 (SNAP 6383), a new potent and selective alpha1A-adrenoceptor antagonist. *Eur. J. Pharmacol.* **409**, 301–312 (2000).

118. Ford, A. P. *et al.* RS-17053 (N-[2-(2-cyclopropylmethoxyphenoxy)ethyl]-5-chloro-alpha, alpha-dimethyl-1H-indole-3-ethanamine hydrochloride), a selective alpha 1A-adrenoceptor antagonist, displays low affinity for functional alpha 1-adrenoceptors in human prostate: implicatio. *Mol. Pharmacol.* **49**, 209–215 (1996).
119. Marshall, I., Burt, R. P., Green, G. M., Hussain, M. B. & Chapple, C. R. Different subtypes of alpha 1A-adrenoceptor mediating contraction of rat epididymal vas deferens, rat hepatic portal vein and human prostate distinguished by the antagonist RS 17053. *Br. J. Pharmacol.* **119**, 407–415 (1996).
120. Kedia, G. T. *et al.* In vitro effects of cyclic AMP- and cyclic GMP-stimulating drugs on the relaxation of the prostate smooth muscle tissue contraction induced by endothelin-1. *Georgian Med. News* **131**, 7–13 (2006).
121. Kedia, G. *et al.* In vitro functional responses of isolated normal human prostatic tissue to compounds interacting with the cyclic guanosine monophosphate pathway. *Urology* **67**, 1292–1297 (2006).
122. Heuer, O. *et al.* Effects of phosphodiesterase inhibitors and nitric oxide donors on cultured human prostatic smooth muscle cells. *Eur. Urol. Suppl.* **3**, 19 (2004).
123. Ponzoni, L., Braida, D., Bondiolotti, G. & Sala, M. The non-peptide arginine-vasopressin v1a selective receptor antagonist, SR49059, Blocks the rewarding, Prosocial, and anxiolytic effects of 3,4-methylenedioxymethamphetamine and its derivatives in zebra fish. *Front. Psychiatry* **8**, (2017).
124. Palea, S., Corsi, M., Artibani, W., Ostardo, E. & Pietra, C. Pharmacological characterization of tachykinin NK2 receptors on isolated human urinary bladder, prostatic urethra and prostate. *J. Pharmacol. Exp. Ther.* **277**, 700–705 (1996).
125. Hedlund, P. Cannabinoids and the endocannabinoid system in lower urinary tract function and dysfunction. *Neurourol. Urodyn.* **33**, 46–53 (2014).
126. Hedlund, P. & Gratzke, C. The endocannabinoid system - a target for the treatment of LUTS? *Nat. Rev. Urol.* **13**, 463–470 (2016).
127. Gratzke, C. *et al.* Transient receptor potential A1 and cannabinoid receptor activity in human normal and hyperplastic prostate: relation to nerves and interstitial cells. *Eur. Urol.* **57**, 902–910 (2010).
128. Schwinn, D. A. & Roehrborn, C. G. Alpha1-adrenoceptor subtypes and lower urinary tract symptoms. *Int. J. Urol.* **15**, 193–199 (2008).
129. Pulito, V. L. *et al.* An investigation of the uroselective properties of four novel alpha(1a)-adrenergic receptor subtype-selective antagonists. *J. Pharmacol. Exp. Ther.* **294**, 224–229 (2000).
130. Marks, L. P. *et al.* Effects of a highly selective alpha-1a antagonist on urinary flow

rate in men with symptomatic BPH. in *American Urological Association Meeting (May 3, Atlanta, GA)* 2770 (2000).

131. Ehrén, I., Adolfsson, J. & Wiklund, N. P. Nitric oxide synthase activity in the human urogenital tract. *Urol. Res.* **22**, 287–290 (1994).
132. Ali, F., Guglin, M., Vaitkevicius, P. & Ghali, J. K. Therapeutic potential of vasopressin receptor antagonists. *Drugs* **67**, 847–858 (2007).
133. Gupta, J., Russell, R. J., Wayman, C. P., Hurley, D. & Jackson, V. M. Oxytocin-induced contractions within rat and rabbit ejaculatory tissues are mediated by vasopressin V 1A receptors and not oxytocin receptors. *Br. J. Pharmacol.* **155**, 118–126 (2008).
134. Bakali, E. *et al.* Distribution and function of the endocannabinoid system in the rat and human bladder. *Int. Urogynecol. J.* **24**, 855–863 (2013).
135. ClinicalTrials.gov. https://clinicaltrials.gov/.
136. Middleton, G. *et al.* Gemcitabine and capecitabine with or without telomerase peptide vaccine GV1001 in patients with locally advanced or metastatic pancreatic cancer (TeloVac): an open-label, randomised, phase 3 trial. *Lancet. Oncol.* **15**, 829–840 (2014).
137. Andersson, K. E. & Van Kerrebroeck, P. Pharmacotherapy for nocturia. *Curr. Urol. Rep.* **19**, 8 (2018).
138. Peyronnet, B., Brucker, B. M. & Michel, M. C. Lower urinary tract symptoms: what's new in medical treatment? *Eur. Urol. Focus* **4**, 17–24 (2018).
139. Sung, H. *et al.* Global Cancer Statistics 2020: GLOBOCAN estimates of incidence and mortality worldwide for 36 cancers in 185 countries. *CA. Cancer J. Clin.* **71**, 209–249 (2021).
140. Siegel, R. L., Miller, K. D. & Jemal, A. Cancer statistics, 2020. *CA. Cancer J. Clin.* **70**, 7–30 (2020).
141. Union, E. ECIS - European Cancer Information System. https://ecis.jrc.ec.europa.eu (2021).
142. Castro, E. & Eeles, R. The role of BRCA1 and BRCA2 in prostate cancer. *Asian J. Androl.* **14**, 409–414 (2012).
143. Bauer, C. M. *et al.* Hereditary prostate cancer as a feature of Lynch syndrome. *Fam. Cancer* **10**, 37–42 (2011).
144. Patel, A. R. & Klein, E. A. Risk factors for prostate cancer. *Nat. Clin. Pract. Urol.* **6**, 87–95 (2009).
145. Cremers, R. G. *et al.* The clinical phenotype of hereditary versus sporadic prostate cancer: HPC definition revisited. *Prostate* **76**, 897–904 (2016).
146. Rebbeck, T. R. *et al.* Global patterns of prostate cancer incidence, aggressiveness,

and mortality in men of african descent. *Prostate Cancer* **2013**, 560857 (2013).

147. Perdana, N. R., Mochtar, C. A., Umbas, R. & Hamid, A. R. A. The risk factors of prostate cancer and its prevention: a literature review. *Acta Med. Indones.* **48**, 228–238 (2016).
148. Ferlay, J. *et al.* Global cancer observatory: cancer tomorrow. *Lion, France: International Agency for Research on Cancer* https://gco.iarc.fr/tomorrow/en (2020).
149. Ponder, B. A. J. Cancer genetics. *Nature* **411**, 336–341 (2001).
150. Chin, S. P., Dickinson, J. L. & Holloway, A. F. Epigenetic regulation of prostate cancer. *Clin. Epigenetics* **2**, 151–169 (2011).
151. Balistreri, C. R., Candore, G., Lio, D. & Carruba, G. Prostate cancer: From the pathophysiologic implications of some genetic risk factors to translation in personalized cancer treatments. *Cancer Gene Ther.* **21**, 2–11 (2014).
152. Greten, F. R. & Grivennikov, S. I. Inflammation and cancer: triggers, mechanisms, and consequences. *Immunity* **51**, 27–41 (2019).
153. Sfanos, K. S. & De Marzo, A. M. Prostate cancer and inflammation: the evidence. *Histopathology* **60**, 199–215 (2012).
154. Knudsen, B. S. & Vasioukhin, V. *Mechanisms of prostate cancer initiation and progression. Advances in Cancer Research* vol. 109 (Elsevier Inc, 2010).
155. Ayala, A. G. & Ro, J. Y. Prostatic intraepithelial neoplasia: recent advances. *Arch. Pathol. Lab. Med.* **131**, 1257–1266 (2007).
156. Bosland, M. C. Sex steroids and prostate carcinogenesis: integrated, multifactorial working hypothesis. *Ann. N. Y. Acad. Sci.* **1089**, 168–176 (2006).
157. Troyer, D. A. *et al.* Prostate cancer detected by methylated gene markers in histopathologically cancer-negative tissues from men with subsequent positive biopsies. *Cancer Epidemiol. Biomarkers Prev.* **18**, 2717–2722 (2009).
158. Hansel, D. E. *et al.* Early prostate cancer antigen expression in predicting presence of prostate cancer in men with histologically negative biopsies. *J. Urol.* **177**, 1736–1740 (2007).
159. Gleason, D. F. Classification of prostatic carcinomas. *Cancer Chemother. reports* **50**, 125–128 (1966).
160. Epstein, J. I. *et al.* The 2014 International Society of Urological Pathology (ISUP) Consensus Conference on Gleason Grading of Prostatic Carcinoma: definition of grading patterns and proposal for a new grading system. *Am. J. Surg. Pathol.* **40**, 244–252 (2016).
161. Gleason, D. F. & Mellinger, G. T. Prediction of prognosis for prostatic adenocarcinoma by combined histological grading and clinical staging. *J. Urol.*

111, 58–64 (1974).

162. Shah, R. B. & Zhou, M. Recent advances in prostate cancer pathology: Gleason grading and beyond. *Pathol. Int.* **66**, 260–272 (2016).
163. Sharifi, N. & Auchus, R. J. Steroid biosynthesis and prostate cancer. *Steroids* **77**, 719–725 (2012).
164. Ricke, W. A., Wang, Y. & Cunha, G. R. Steroid hormones and carcinogenesis of the prostate: the role of estrogens. *Differentiation* **75**, 871–882 (2007).
165. Katsogiannou, M. *et al.* The hallmarks of castration-resistant prostate cancers. *Cancer Treat. Rev.* **41**, 588–597 (2015).
166. Vasioukhin, V. Hepsin paradox reveals unexpected complexity of metastatic process. *Cell Cycle* **3**, 1394–1397 (2004).
167. Brooks, J. D. *et al.* CG island methylation changes near the GSTP1 gene in prostatic intraepithelial neoplasia. *Cancer Epidemiol. Biomarkers Prev.* **7**, 531–536 (1998).
168. Cerveira, N. *et al.* TMPRSS2-ERG gene fusion causing ERG overexpression precedes chromosome copy number changes in prostate carcinomas and paired HGPIN lesions. *Neoplasia* **8**, 826–832 (2006).
169. Tomlins, S. A. *et al.* Recurrent fusion of TMPRSS2 and ETS transcription factor genes in prostate cancer. *Science* **310**, 644–648 (2005).
170. McMenamin, M. E. *et al.* Loss of PTEN expression in paraffin-embedded primary prostate cancer correlates with high Gleason score and advanced stage. *Cancer Res.* **59**, 4291–4296 (1999).
171. Deocampo, N. D., Huang, H. & Tindall, D. J. The role of PTEN in the progression and survival of prostate cancer. *Minerva Endocrinol.* **28**, 145–153 (2003).
172. Prins, G. S. & Putz, O. Molecular signaling pathways that regulate prostate gland development. *Differentiation.* **76**, 641–659 (2008).
173. Attard, G. *et al.* Characterization of ERG, AR and PTEN gene status in circulating tumor cells from patients with castration-resistant prostate cancer. *Cancer Res.* **69**, 2912–2918 (2009).
174. Friedlander, T. W. *et al.* Common structural and epigenetic changes in the genome of castration-resistant prostate cancer. *Cancer Res.* **72**, 616–625 (2012).
175. Andersson, S. *et al.* Molecular genetics and pathophysiology of 17 beta-hydroxysteroid dehydrogenase 3 deficiency. *J. Clin. Endocrinol. Metab.* **81**, 130–136 (1996).
176. McPhaul, M. J. Molecular defects of the androgen receptor. *J. Steroid Biochem. Mol. Biol.* **69**, 315–322 (1999).
177. Beato, M. & Klug, J. Steroid hormone receptors: an update. *Hum. Reprod. Update*

6, 225–236 (2000).

178. Miyamoto, H., Messing, E. M. & Chang, C. Androgen deprivation therapy for prostate cancer: current status and future prospects. *Prostate* **61**, 332–353 (2004).
179. He, B., Kemppainen, J. A., Voegel, J. J., Gronemeyer, H. & Wilson, E. M. Activation function 2 in the human androgen receptor ligand binding domain mediates interdomain communication with the NH(2)-terminal domain. *J. Biol. Chem.* **274**, 37219–37225 (1999).
180. Jenster, G., van der Korput, H. A., Trapman, J. & Brinkmann, A. O. Identification of two transcription activation units in the N-terminal domain of the human androgen receptor. *J. Biol. Chem.* **270**, 7341–7346 (1995).
181. Heinlein, C. A. & Chang, C. Androgen receptor (AR) coregulators: an overview. *Endocr. Rev.* **23**, 175–200 (2002).
182. Ikonen, T., Palvimo, J. J. & Jänne, O. A. Interaction between the amino- and carboxyl-terminal regions of the rat androgen receptor modulates transcriptional activity and is influenced by nuclear receptor coactivators. *J. Biol. Chem.* **272**, 29821–29828 (1997).
183. Culig, Z. & Santer, F. R. Androgen receptor signaling in prostate cancer. *Cancer Metastasis Rev.* **33**, 413–427 (2014).
184. Isaacs, J. T. Antagonistic effect of androgen on prostatic cell death. *Prostate* **5**, 545–557 (1984).
185. Turner, L. & Walters, W. A. W. Androgen or estrogen effects on human prostate. *J. Clin. Endocrinol. Metab.* **81**, 4290–4295 (1996).
186. English, H. F., Kyprianou, N. & Isaacs, J. T. Relationship between DNA fragmentation and apoptosis in the programmed cell death in the rat prostate following castration. *Prostate* **15**, 233–250 (1989).
187. Buttyan, R., Ghafar, M. A. & Shabsigh, A. The effects of androgen deprivation on the prostate gland: cell death mediated by vascular regression. *Curr. Opin. Urol.* **10**, 415–420 (2000).
188. Lane, K. E. *et al.* Suppression of testosterone and estradiol-17beta-induced dysplasia in the dorsolateral prostate of Noble rats by bromocriptine. *Carcinogenesis* **18**, 1505–1510 (1997).
189. Paterni, Iliaria. Granchi, C., Katzenellenbogen, J. & Minutolo, F. Estrogen Receptors Alpha and Beta Subtype-Selective Ligands and Clinical Potential. **18**, 1492–1501 (2011).
190. Brendler, C. B. *et al.* Spontaneous benign prostatic hyperplasia in the beagle. Age-associated changes in serum hormone levels, and the morphology and secretory

function of the canine prostate. *J. Clin. Invest.* **71**, 1114–1123 (1983).

191. Hayes, R. B. *et al.* Physical characteristics and factors related to sexual development and behaviour and the risk for prostatic cancer. *Eur. J. cancer Prev. Off. J. Eur. Cancer Prev. Organ.* **1**, 239–245 (1992).
192. Ross, R. *et al.* Serum testosterone levels in healthy young black and white men. *J. Natl. Cancer Inst.* **76**, 45–48 (1986).
193. de Jong, F. H. *et al.* Peripheral hormone levels in controls and patients with prostatic cancer or benign prostatic hyperplasia: results from the Dutch-Japanese case-control study. *Cancer Res.* **51**, 3445–3450 (1991).
194. Ricke, W. A. *et al.* Steroid hormones stimulate human prostate cancer progression and metastasis. *Int. J. cancer* **118**, 2123–2131 (2006).
195. Griffiths, K. Estrogens and prostatic disease. International Prostate Health Council Study Group. *Prostate* **45**, 87–100 (2000).
196. Feldman, H. A. *et al.* Age trends in the level of serum testosterone and other hormones in middle-aged men: longitudinal results from the Massachusetts male aging study. *J. Clin. Endocrinol. Metab.* **87**, 589–598 (2002).
197. Ellem, S. J. & Risbridger, G. P. Aromatase and prostate cancer. *Minerva Endocrinol.* **31**, 1–12 (2006).
198. Price, S., Golden, B., Wasil, E. & Denton, B. T. Operations research models and methods in the screening, detection, and treatment of prostate cancer: A categorized, annotated review. *Oper. Res. Heal. Care* **8**, 9–21 (2016).
199. American Cancer Society. Survival rates for prostate cancer. *Cancer Facts & Figures* https://www.cancer.org/cancer/prostate-cancer/detection-diagnosis-staging/survival-rates.html (2021).
200. Tosoian, J. J. *et al.* Prediction of pathological stage based on clinical stage, serum prostate-specific antigen, and biopsy Gleason score: Partin Tables in the contemporary era. *BJU Int.* **119**, 676–683 (2017).
201. Chang, A. J., Autio, K. A., Roach, M. & Scher, H. I. High-risk Prostate Cancer — Classification and Therapy. *Nat. Rev. Clin. Oncol.* **11**, 308–323 (2014).
202. Mohler, J. L. *et al.* Prostate cancer, version 3.2012: featured updates to the NCCN Guidelines. *JNCCN J. Natl. Compr. Cancer Netw.* **10**, 1081–1087 (2012).
203. Bechis, S. K., Carroll, P. R. & Cooperberg, M. R. Impact of age at diagnosis on prostate cancer treatment and survival. *J. Clin. Oncol.* **29**, 235–241 (2011).
204. Gomella, L. G., Singh, J., Lallas, C. & Trabulsi, E. J. Hormone therapy in the management of prostate cancer: Evidence-based approaches. *Ther. Adv. Urol.* **2**, 171–181 (2010).
205. Saigal, C. S., Lambrechts, S. I., Seenu Srinivasan, V. & Dahan, E. The voice of the

patient methodology: a novel mixed-methods approach to identifying treatment goals for men with prostate cancer. *Patient* **10**, 345–352 (2017).

206. Narayanan, S., Srinivas, S. & Feldman, D. Androgen-glucocorticoid interactions in the era of novel prostate cancer therapy. *Nat. Rev. Urol.* **13**, 47–60 (2016).
207. Huggins, C. & Hodges, C. V. Studies on prostatic cancer. I. The effect of castration, of estrogen and androgen injection on serum phosphatases in metastatic carcinoma of the prostate. *CA. Cancer J. Clin.* **22**, 232–240 (1972).
208. Maatman, T. J., Gupta, M. K. & Montie, J. E. Effectiveness of castration versus intravenous estrogen therapy in producing rapid endocrine control of metastatic cancer of the prostate. *J. Urol.* **133**, 620–621 (1985).
209. Bosset, P.-O. *et al.* Current role of diethylstilbestrol in the management of advanced prostate cancer. *BJU Int.* **110**, E826-9 (2012).
210. Blackard, C. E. The Veterans' Administration Cooperative Urological Research Group studies of carcinoma of the prostate: a review. *Cancer Chemother. reports* **59**, 225–227 (1975).
211. Grenader, T., Plotkin, Y., Gips, M., Cherny, N. & Gabizon, A. Diethylstilbestrol for the treatment of patients with castration-resistant prostate cancer: Retrospective analysis of a single institution experience. *Oncol. Rep.* **31**, 428–434 (2014).
212. Tolis, G. *et al.* Tumor growth inhibition in patients with prostatic carcinoma treated with luteinizing hormone-releasing hormone agonists. *Proc. Natl. Acad. Sci. U. S. A.* **79**, 1658–1662 (1982).
213. Thompson, I. M., Zeidman, E. J. & Rodriguez, F. R. Sudden death due to disease flare with luteinizing hormone-releasing hormone agonist therapy for carcinoma of the prostate. *J. Urol.* **144**, 1479–1480 (1990).
214. Labrie, F., Dupont, A., Belanger, A. & Lachance, R. Flutamide eliminates the risk of disease flare in prostatic cancer patients treated with a luteinizing hormone-releasing hormone agonist. *J. Urol.* **138**, 804–806 (1987).
215. Stricker, H. J. Luteinizing hormone-releasing hormone antagonists in prostate cancer. *Urology* **58**, 24–27 (2001).
216. Crawford, E. D. *et al.* Androgen receptor targeted treatments of prostate cancer: 35 years of progress with antiandrogens. *J. Urol.* **200**, 956–966 (2018).
217. Sharifi, N. Mechanisms of androgen receptor activation in castration-resistant prostate cancer. *Endocrinology* **154**, 4010–4017 (2013).
218. Antonarakis, E. S. *et al.* AR-V7 and resistance to enzalutamide and abiraterone in prostate cancer. *N. Engl. J. Med.* **371**, 1028–1038 (2014).
219. Lamont, K. R. & Tindall, D. J. Minireview: alternative activation pathways for the androgen receptor in prostate cancer. *Mol. Endocrinol.* **25**, 897–907 (2011).

220. Page, S. T. *et al.* Persistent intraprostatic androgen concentrations after medical castration in healthy men. *J. Clin. Endocrinol. Metab.* **91**, 3850–3856 (2006).
221. Crawford, E. D. Hormonal therapy in prostate cancer: historical approaches. *Rev. Urol.* **6 Suppl 7**, S3–S11 (2004).
222. Labrie, F. *et al.* Advantages of the combination therapy in previously untreated and treated patients with advanced prostate cancer. *J. Steroid Biochem.* **25**, 877–883 (1986).
223. Akaza, H. Combined androgen blockade for prostate cancer: Review of efficacy, safety and cost-effectiveness. *Cancer Sci.* **102**, 51–56 (2011).
224. Verhelst, J. *et al.* Endocrine profiles during administration of the new non-steroidal anti-androgen Casodex in prostate cancer. *Clin. Endocrinol. (Oxf).* **41**, 525–530 (1994).
225. Green, S. M., Mostaghel, E. A. & Nelson, P. S. Androgen action and metabolism in prostate cancer. *Mol. Cell. Endocrinol.* **360**, 3–13 (2012).
226. Gomez, L., Kovac, J. R. & Lamb, D. J. CYP17A1 inhibitors in castration-resistant prostate cancer. *Steroids* **95**, 80–87 (2015).
227. Small, E. J. *et al.* Antiandrogen withdrawal alone or in combination with ketoconazole in androgen-independent prostate cancer patients: a phase III trial (CALGB 9583). *J. Clin. Oncol.* **22**, 1025–1033 (2004).
228. Keizman, D., Huang, P., Carducci, M. A. & Eisenberger, M. A. Contemporary experience with ketoconazole in patients with metastatic castration-resistant prostate cancer: clinical factors associated with PSA response and disease progression. *Prostate* **72**, 461–467 (2012).
229. Scholz, M. *et al.* Long-term outcome for men with androgen independent prostate cancer treated with ketoconazole and hydrocortisone. *J. Urol.* **173**, 1947–1952 (2005).
230. Patel, V., Liaw, B. & Oh, W. The role of ketoconazole in current prostate cancer care. *Nat. Rev. Urol.* **15**, 643–651 (2018).
231. Hu, Q. & Hartmann, R. W. *The Renaissance of CYP17 Inhibitors for the Treatment of Prostate Cancer. Cancer Drug Design and Discovery: Second Edition* (Elsevier, 2013). doi:10.1016/B978-0-12-396521-9.00011-5.
232. Bryce, A. & Ryan, C. J. Development and Clinical Utility of Abiraterone Acetate as an Androgen Synthesis Inhibitor. *Clin. Pharmacol. Ther.* **91**, 101–108 (2009).
233. Ryan, C. J. *et al.* Abiraterone in metastatic prostate cancer without previous chemotherapy. *N. Engl. J. Med.* **368**, 138–148 (2013).
234. de Bono, J. S. *et al.* Abiraterone and increased survival in metastatic prostate cancer. *N. Engl. J. Med.* **364**, 1995–2005 (2011).

235. Ndibe, C., Wang, C. G. & Sonpavde, G. Corticosteroids in the management of prostate cancer: a critical review. *Curr. Treat. Options Oncol.* **16**, (2015).
236. Puhr, M. *et al.* The glucocorticoid receptor is a key player for prostate cancer cell survival and a target for improved antiandrogen therapy. *Clin. Cancer Res.* **24**, 927–938 (2018).
237. Montgomery, B., Cheng, H. H., Drechsler, J. & Mostaghel, E. A. Glucocorticoids and prostate cancer treatment: Friend or foe? *Asian J. Androl.* **16**, 354–358 (2014).
238. Small, E. J. *et al.* A randomized Phase II trial of sipuleucel-T with concurrent versus sequential abiraterone acetate plus prednisone in metastatic castration-resistant prostate cancer. *Clin. Cancer Res.* **21**, 3862–3869 (2015).
239. Heidenreich, A. *et al.* Safety of cabazitaxel in senior adults with metastatic castration-resistant prostate cancer: results of the European compassionate-use programme. *Eur. J. Cancer* **50**, 1090–1099 (2014).
240. Isikbay, M. *et al.* Glucocorticoid receptor activity contributes to resistance to androgen-targeted therapy in prostate cancer. *Horm. Cancer* **5**, 72–89 (2014).
241. Arora, V. K. *et al.* Glucocorticoid receptor confers resistance to antiandrogens by bypassing androgen receptor blockade. *Cell* **155**, 1309–1322 (2013).
242. Xie, N. *et al.* The expression of glucocorticoid receptor is negatively regulated by active androgen receptor signaling in prostate tumors. *Int. J. cancer* **136**, E27-38 (2015).
243. Thompson, I. M., Klein, E. A. & Lippman, S. M. Prevention of prostate cancer with finasteride: US/European perspective. *European urology* vol. 46 133–134 (2004).
244. Scardino, P. T. The prevention of prostate cancer-the dilemma continues. *The New England journal of medicine* vol. 349 297–299 (2003).
245. Thompson, I. M. *et al.* The influence of finasteride on the development of prostate cancer. *N. Engl. J. Med.* **349**, 215–224 (2003).
246. Thompson, I. M., Tangen, C. M., Goodman, P. J., Lucia, M. S. & Klein, E. A. Chemoprevention of prostate cancer. *J. Urol.* **182**, 499–507; discussion 508 (2009).
247. Kaplan, S. A. *et al.* PCPT: Evidence that finasteride reduces risk of most frequently detected intermediate- and high-grade (Gleason score 6 and 7) cancer. *Urology* **73**, 935–939 (2009).
248. Food and Drug Administration. Drugs questions and answers: 5--alpha reductase inhibitors (5ARIs) may increase the risk of a more serious form of prostate cancer. http://www.fda.gov/Drugs/DrugSafety/ucm258358.htm (2011).
249. Wang, L. *et al.* Association of finasteride with prostate cancer. *Medicine*

(Baltimore). **99**, e19486 (2020).

250. Fleshner, N. E. *et al.* Dutasteride in localised prostate cancer management: the REDEEM randomised, double-blind, placebo-controlled trial. *Lancet* **379**, 1103–1111 (2012).
251. Schröder, F. *et al.* Dutasteride treatment over 2 years delays prostate-specific antigen progression in patients with biochemical failure after radical therapy for prostate cancer: results from the randomised, placebo-controlled avodart after radical therapy for prostate canc. *Eur. Urol.* **63**, 779–787 (2013).
252. Puente, J. *et al.* Docetaxel in prostate cancer: a familiar face as the new standard in a hormone-sensitive setting. *Ther. Adv. Vaccines* **9**, 307–318 (2017).
253. Sternberg, C. N. *et al.* Efficacy and safety of cabazitaxel versus abiraterone or enzalutamide in older patients with metastatic castration-resistant prostate cancer in the CARD Study. *Eur. Urol.* **80**, 497–506 (2021).
254. Sperlich, C. & Saad, F. Optimal management of patients receiving cabazitaxel-based chemotherapy. *J. Can. Urol. Assoc.* **7**, 18–24 (2013).
255. Yamada, Y. & Beltran, H. The treatment landscape of metastatic prostate cancer. *Cancer Lett.* **519**, 20–29 (2021).
256. Drake, C. G. Prostate cancer as a model for tumour immunotherapy. *Nat. Rev. Immunol.* **10**, 580–593 (2010).
257. Kwon, E. D. *et al.* Ipilimumab versus placebo after radiotherapy in patients with metastatic castration-resistant prostate cancer that had progressed after docetaxel chemotherapy (CA184-043): a multicentre, randomised, double-blind, phase 3 trial. *Lancet Oncol.* **15**, 700–712 (2014).
258. Parker, C. *et al.* Alpha emitter radium-223 and survival in metastatic prostate cancer. *N. Engl. J. Med.* **369**, 213–223 (2013).
259. Saad, F. *et al.* Long-term efficacy of zoledronic acid for the prevention of skeletal complications in patients with metastatic hormone-refractory prostate cancer. *J. Natl. Cancer Inst.* **96**, 879–882 (2004).
260. Fizazi, K. *et al.* Denosumab versus zoledronic acid for treatment of bone metastases in men with castration-resistant prostate cancer: a randomised, double-blind study. *Lancet (London, England)* **377**, 813–822 (2011).
261. Brown, J. M. *et al.* Osteoprotegerin and rank ligand expression in prostate cancer. *Urology* **57**, 611–616 (2001).
262. Farmer, H. *et al.* Targeting the DNA repair defect in BRCA mutant cells as a therapeutic strategy. *Nature* **434**, 917–921 (2005).
263. Abida, W. *et al.* Rucaparib in men with metastatic castration-resistant prostate cancer harboring a BRCA1 or BRCA2 gene alteration. *J. Clin. Oncol.* **38**, 3763–

3772 (2020).

264. de Bono, J. *et al.* Olaparib for metastatic castration-resistant prostate cancer. *N. Engl. J. Med.* **382**, 2091–2102 (2020).
265. Chung, P. H., Gayed, B. A., Thoreson, G. R. & Raj, G. V. Emerging drugs for prostate cancer. *Expert Opin. Emerg. Drugs* **18**, 533–550 (2013).
266. Birgül, K. *et al.* Synthesis, molecular modeling, in vivo study and anticancer activity against prostate cancer of (+) (S)-naproxen derivatives. *Eur. J. Med. Chem.* **208**, (2020).
267. He, Z. X. *et al.* Design, synthesis and biological evaluation of novel thiosemicarbazone-indole derivatives targeting prostate cancer cells. *Eur. J. Med. Chem.* **210**, (2021).
268. Machulkin, A. E. *et al.* Synthesis, characterization, and preclinical evaluation of a small-molecule prostate-specific membrane antigen-targeted monomethyl auristatin E conjugate. *J. Med. Chem.* **64**, 17123–17145 (2021).
269. Kim, I.-W., Kim, J. H. & Oh, J. M. Screening of drug repositioning candidates for castration resistant prostate cancer. *Front. Oncol.* **9**, 661 (2019).
270. Liang, X. *et al.* Identification of core genes and potential Drugs for castration-resistant prostate cancer based on bioinformatics analysis. *DNA Cell Biol.* **39**, 836–847 (2020).
271. Deng, T. *et al.* Prostate cancer patients can benefit from 5-alpha-reductase inhibitor treatment: A meta-analysis. *PeerJ* **8**, 1–17 (2020).
272. Sartor, O., Gomella, L. G., Gagnier, P., Melich, K. & Dann, R. Dutasteride and bicalutamide in patients with hormone-refractory prostate cancer: the Therapy Assessed by Rising PSA (TARP) study rationale and design. *Can. J. Urol.* **16**, 4806—4812 (2009).
273. Long, B. J. *et al.* Antiandrogenic Effects of Novel Androgen Synthesis Inhibitors on Hormone-dependent Prostate Cancer. *Cancer Res.* **60**, 6630–6640 (2000).
274. Lazier, C. B., Thomas, L. N., Douglas, R. C., Vessey, J. P. & Rittmaster, R. S. Dutasteride, the Dual 5α-Reductase Inhibitor, Inhibits Androgen Action and Promotes Cell Death in the LNCaP Prostate Cancer Cell Line. *Prostate* **58**, 130–144 (2004).
275. Schmidt, L. J., Murillo, H. & Tindall, D. J. Gene expression in prostate cancer cells treated with the dual 5 alpha-reductase inhibitor dutasteride. *J. Androl.* **25**, 944–953 (2004).
276. Cayatte, C. *et al.* Protein profiling of rat ventral prostate following chronic finasteride administration: Identification and localization of a novel putative androgen-regulated protein. *Mol. Cell. Proteomics* **5**, 2031–2043 (2006).

277. Eggener, S. E. *et al.* Enhancement of intermittent androgen ablation by 'off-cycle' maintenance with finasteride in LNCaP prostate cancer xenograft model. *Prostate* **66**, 495–502 (2006).
278. Xu, Y., Dalrymple, S. L., Becker, R. E., Denmeade, S. R. & Isaacs, J. T. Pharmacologic basis for the enhanced efficacy of dutasteride against prostatic cancers. *Clin. Cancer Res.* **12**, 4072–4079 (2006).
279. Schmidt, L. J. *et al.* Effects of the 5 alpha-reductase inhibitor dutasteride on gene expression in prostate cancer xenografts. *Prostate* **69**, 1730–1743 (2009).
280. Borah, P. & Banik, B. K. *Diverse synthesis of medicinally active steroids*. *Green Approaches in Medicinal Chemistry for Sustainable Drug Design* (Elsevier Inc., 2020). doi:10.1016/b978-0-12-817592-7.00012-5.
281. Lednicer, D. *Steroid chemistry at a glance*. (Wiley, 2011).
282. Brueggemeier, R. W. & Li, P. Fundamentals of Steroid Chemistry and Biochemistry. *Burger's Med. Chem. Drug Discov.* 1–37 (2021) doi:10.1002/0471266949.bmc053.pub3.
283. Burger, A., Abraham, D. J. & Rotella, D. P. *Burger's medicinal chemistry, drug discovery and development. Vol. 7, Vol. 7,*. (Wiley, 2010).
284. Tantawy, M. A., Nafie, M. S., Elmegeed, G. A. & Ali, I. A. I. Auspicious role of the steroidal heterocyclic derivatives as a platform for anti-cancer drugs. *Bioorg. Chem.* **73**, 128–146 (2017).
285. Vil, V. A., Terent, A. O., Savidov, N. & Gloriozova, T. A. Hydroperoxy steroids and triterpenoids derived from plant and fungi: origin, structures and biological activities. *J. Steroid Biochem. Mol. Biol.* **190**, 76–87 (2019).
286. Dembitsky, V. M. Progress in lipid research antitumor and hepatoprotective activity of natural and synthetic neo steroids. *Prog. Lipid Res.* **79**, 101048 (2020).
287. Xiao, J., Gao, M., Fei, B., Huang, G. & Diao, Q. Nature-derived anticancer steroids outside cardica glycosides. *Fitoterapia* **147**, 104757 (2020).
288. Latham, K. A. *et al.* Estradiol treatment redirects the isotype of the autoantibody response and prevents the development of autoimmune arthritis. *J. Immunol.* **171**, 5820–5827 (2003).
289. Dubey, R., Oparil, S., Imthurn, B. & Jackson, E. Sex hormones and hypertension. *Cardiovasc. Res.* **53**, 688–708 (2002).
290. Sheridan, P. J., Blum, K. & Trachtenberg, M. C. Steroid Receptors and Disease: Cancer, Autoimmune, Bone, and Circulatory Disorders. *Trends Pharmacol. Sci.* **10**, 122 (1988).
291. Holst, J. P. *et al.* Use of steroid profiles in determining the cause of adrenal insufficiency. *Steroids* **72**, 71–84 (2006).

292. Jursic, B. S., Kumar, S., Creech, C. C. & Neumann, D. M. Novel and efficient synthesis and antifungal evaluation of 2,3-functionalized cholestane and androstane derivatives. *Bioorg. Med. Chem. Lett.* **20**, 7372–7375 (2020).
293. Banday, A. H., Zargar, M. I. & Ganaie, B. A. Synthesis and antimicrobial studies of chalconyl pregnenolones. *Steroids* **76**, 1358–1362 (2011).
294. Na, M. S., Tantawy, M. A. & Elmgeed, G. A. Screening of different drug design tools to predict the mode of action of steroidal derivatives as anti-cancer agents. *Steroids* **152**, (2019).
295. Lemke, T. L., Williams, D. A., Roche, V. F. & Zito, S. W. *Foye's principles of medicinal chemistry: Seventh edition*. (2012).
296. Huang, X. *et al.* Design and synthesis of novel dehydroepiandrosterone analogues as potent antiproliferative agents. *Molecules* **23**, 1–14 (2018).
297. Acharya, P. C., Bansal, R., Kharkar, P. S., Res, D. & Bansal, R. Hybrids of steroid and nitrogen mustard as antiproliferative agents: synthesis, in vitro evaluation and in silico inverse screening authors. *Drug Res. (Stuttg).* **68**, 100–103 (2018).
298. Fan, N. *et al.* Synthesis and cytotoxic activity of some novel steroidal C-17 pyrazolinyl derivatives. *Eur. J. Med. Chem.* **69**, 182–190 (2013).
299. Gogoi, J. *et al.* Synthesis of a novel class of steroidal tetrazolo[1,5-a]pyridines via intramolecular 1,3-dipolar cycloadditions. *Tetrahedron Lett.* **53**, 1497–1500 (2012).
300. Delong, W., Yongling, W., Lanying, W., Juntao, F. & Xing, Z. Design, synthesis and evaluation of 3-erylidene azetidin-2-ones as potential antifungal agents against alternaria solani sorauer. *Bioorg. Med. Chem.* **25**, 6661–6673 (2017).
301. Szymanska, E. & Kiec-Kononowicz, K. Antimycobacterial activity of 5-arylidene aromatic derivatives of hydantoin. *Farm.* **57**, 355–362 (2002).
302. Ottanà, R. *et al.* Identification of 5-arylidene-4-thiazolidinone derivatives endowed with dual activity as aldose reductase inhibitors and antioxidant agents for the treatment of diabetic complications. *Eur. J. Med. Chem.* **46**, 2797–2806 (2011).
303. Stadnicka, K., Broda, A., Filipek, B. & Kiec, K. Synthesis, structure–activity relationship of some new anti-arrhythmic 5-arylidene imidazolidine-2,4-dione derivatives. *Eur. J. Med. Chem.* **40**, 259–269 (2005).
304. Li, N. *et al.* Antitumor agents with biological evaluation in vitro and in vivo. *Eur. J. Med. Chem.* **147**, 21–33 (2018).
305. Amr, A. E. & Abdulla, M. M. Anti-inflammatory profile of some synthesized heterocyclic pyridone and pyridine derivatives fused with steroidal structure. *Bioorg. Med. Chem.* **14**, 4341–4352 (2006).

306. Jain, S., Kumar, A. & Saini, D. Experimental parasitology novel arylidene derivatives of quinoline based thiazolidinones: synthesis, in vitro, in vivo and in silico study as antimalarials. *Exp. Parasitol.* **185**, 107–114 (2018).
307. Valla, A. *et al.* New syntheses and potential antimalarial activities of new 'retinoid-like chalcones'. *Eur. J. Med. Chem.* **41**, 142–146 (2006).
308. Maccari, R. *et al.* Structure-activity relationships and molecular modelling of new 5-arylidene-4-thiazolidinone derivatives as aldose reductase inhibitors and potential anti-inflammatory agents. *Eur. J. Med. Chem.* **81**, 1–14 (2014).
309. Hee, S. *et al.* Heme oxygenase 1 mediates anti-inflammatory effects of 2',4',6'-tris(methoxymethoxy) chalcone. *Eur. J. Pharmacol.* **532**, 178–186 (2006).
310. Banday, A. H., Mir, B. P., Lone, I. H., Suri, K. A. & Kumar, H. M. S. Studies on novel D-ring substituted steroidal pyrazolines as potential anticancer agents. *Steroids* **75**, 805–809 (2010).
311. Taylor, P., Schultz, T. W. & Yarbrough, J. W. Trends in structure-toxicity relationships for carbonyl-containing α,β-unsaturated compounds. *SAR QSAR Environ. Res.* **2**, 37–41 (2007).
312. Eder, E., Scheckenbach, S., Deininger, C. & Hoffman, C. The possible role of α,β-unsaturated carbonyl compounds in mutagenesis and carcinogenesis. *Toxicol. Lett.* **67**, 87–103 (1993).
313. Aguilera, E. *et al.* A nature-inspired design yields a new class of steroids against trypanosomatids. *Molecules* **8**, 1–22 (2019).
314. Al-masoudi, N. A. *et al.* Synthesis and CYP17 a hydroxylase inhibition activity of new 3α- and 3β-ester derivatives of pregnenolone and related ether analogues. *Med. Chem. Res.* **25**, 310–321 (2016).
315. Poirier, D., Chang, H., Azzi, A., Boivin, R. P. & Lin, S. Estrone and estradiol C-16 derivatives as inhibitors of type 1 17b-hydroxysteroid dehydrogenase. *Mol. Cell. Endocrinol.* **248**, 236–238 (2006).
316. Bansal, R., Guleria, S., Young, L. C. & Harvey, A. L. Synthesis of Quaternary Ammonium Salts of 16E-[4-(2-Alkylaminoethoxy)-3-methoxybenzylidene]androstene Derivatives as Skeletal Muscle Relaxants. *Steroids* **76**, 254–260 (2011).
317. Guo, H. *et al.* Synthesis, characterization and biological evaluation of some 16E-arylidene androstane derivatives as potential anticancer agents. *Steroids* **76**, 709–723 (2011).
318. Fan, N., Han, Y., Li, Y., Gao, J. & Tang, J. Synthesis of novel 4′-acylamino modified 21E-benzylidene steroidal derivatives and their cytotoxic activities. *Steroids* **123**, 20–26 (2017).

319. Dubey, S., Kaur, P., Jindal, D. P., Satyanarayan, Y. D. & Piplani, P. Synthesis, evaluation and QSAR studies of 16-(4 & 3,4-substituted) benzylidene androstene derivatives as anticancer agents. *Med. Chem. (Los. Angeles).* **4**, 229–236 (2008).
320. Jiang, C. *et al.* Synthesis and Biological Evaluation of 21-arylidenepregnenolone Derivatives as Neuroprotective Agents. *Bioorg. Med. Chem. Lett.* **22**, 2226–2229 (2012).
321. Huang, L. H. *et al.* Synthesis of novel D-ring fused 7'-aryl-androstano[17,16-d][1,2,4]triazolo[1,5-a]pyrimidines. *Steroids* **77**, 367–374 (2012).
322. Huang, L.-H. *et al.* Synthesis and Biological Evaluation of Novel Steroidal[17,16-d][1,2,4]triazolo[1,5-a]pyrimidines. *Steroids* **77**, 710–715 (2012).
323. Brito, V., Alves, G., Almeida, P. & Silvestre, S. Highlights on steroidal arylidene derivatives as a source of pharmacologically active compounds: A review. *Molecules* **26**, 1–21 (2021).
324. Furniss, B. S., Hannaford, A. J., Smith, P. W. G. & Tatchell, A. R. *Vogel's Textboom of Practical Organic Chemistry*. (Pearson, 1989).
325. Karatas, S., Çapan, İ. & Servi, S. Synthesis of indole and benzimidazole substituted novel 16-arylidene steroid derivatives. *Lett. Org. Chem.* **16**, 884–890 (2019).
326. Brito, V., Santos, A. O., Almeida, P. & Silvestre, S. Novel 4-Azaandrostenes as Prostate Cancer Cell Growth Inhibitors: Synthesis, Antiproliferative Effects and Molecular Docking Studies. *Comptes Rendus Chim.* **22**, 73–83 (2018).
327. Ke, S., Shi, L., Zhang, Z. & Yang, Z. Steroidal[17,16-d]pyrimidines derived from dehydroepiandrosterone: A convenient synthesis, antiproliferation activity, structure-activity relationships, and role of heterocyclic moiety. *Nat. Publ. Gr.* **7**, 1–7 (2017).
328. Dubey, S., Kaur, P. & Paul, D. Synthesis and QSAR studies of 16-(3-methoxy-4-substitued benzylidene) androstene derivatives as anticancer agents. *Indian J. Chem.* **49B**, 948–955 (2010).
329. Dubey, S., Piplani, P. & Jindal, D. P. Synthesis and in vitro Antineoplastic Evaluation of Certain 16-(4-Substituted Benzylidene) Derivatives of Androst-5-ene. *Chem. Biodivers.* **1**, 1529–1536 (2004).
330. Kakati, D., Sarma, R. K., Saikia, R., Barua, N. C. & Sarma, J. C. Rapid Microwave Assisted Synthesis and Antimicrobial Bioevaluation of Novel Steroidal Chalcones. *Steroids* **78**, 321–326 (2013).
331. Mótyána, G., Molnár, B., Wölfling, J. & Frank, É. Microwave-assisted stereoselective heterocyclization to novel ring D-fused arylpyrazolines in the estrone series. *Molecules* **24**, 1–15 (2019).
332. Riebe, S. *et al.* Synthesis of 16-E-([aryl]idene)-3-methoxy-estrones by a palladium

catalysed Mizoroki-Heck reaction. *Tetrahedron Lett.* **58**, 2801–2803 (2017).

333. Peña-López, M., Ayán-Varela, M., Sarandeses, L. A. & Pérez Sestelo, J. Palladium-catalyzed cross-coupling reactions of organogold(I) reagents with organic electrophiles. *Chemistry* **16**, 9905–9909 (2010).
334. Yu, B., Shi, X., Qi, P., Yu, D. & Liu, H. Design, synthesis and biological evaluation of novel steroidal spiro-oxindoles as potent antiproliferative agents. *J. Steroid Biochem. Mol. Biol.* **141**, 121–134 (2014).
335. Chattopadhaya, R., Jindal, D. P., Minu, M. & Gupta, R. Synthesis and cytotoxic studies of hydroximino derivatives of some 16E-arylidenosteroids. *Arzneim. Forshung - Drug Res.* **556**, 551–556 (2004).
336. Longley, D. B., Harkin, D. P. & Johnston, P. G. 5-Fluorouracil: mechanisms of action and clinical strategies. *Nat. Rev. Cancer Cancer* **3**, 330–338 (2003).
337. Narváez-Pita, X., Rheingold, A. L. & Meléndez, E. Ferrocene-steroid conjugates: synthesis, structure and biological activity. *J. Organomet. Chem.* **846**, 113–120 (2017).
338. Vosooghi, M. *et al.* Synthesis and in vitro Cytotoxic Activity Evaluation of (E)-16-(substituted benzylidene) Derivatives of Dehydroepiandrosterone. *Daru* **21**, 34 (2013).
339. Bansal, R. & Acharya, P. C. Synthesis and antileukemic activity of 16E-[4-(2-carboxy)ethoxybenzylidene]-androstene amides. *Steroids* **77**, 552–7 (2012).
340. Bansal, R. & Guleria, S. Synthesis of 16E-[3-methoxy-4-(2-aminoethoxy)benzylidene]androstene derivatives as potent cytotoxic agents. *Steroids* **73**, 1391–1399 (2008).
341. Chumsri, S., Howes, T., Bao, T., Sabnis, G. & Brodie, A. Aromatase, Aromatase Inhibitors, and Breast Cancer. *J. Steroid Biochem. Mol. Biol.* **125**, 13–22 (2012).
342. Lonning, P. E. & Eikesdal, H. P. Aromatase inhibition 2013: clinical state of the art and questions that remain to be solved. *Endocr. Relat. Cancer* **20**, 183–201 (2013).
343. Coates, A. S. *et al.* Five years of letrozole compared with tamoxifen as initial adjuvant therapy for postmenopausal women with endocrine-responsive early breast cancer: update of study BIG 1-98. *J. Clin. Oncol.* **25**, 486–492 (2007).
344. Amir, E., Seruga, B., Niraula, S., Carlsson, L. & Ocaña, A. Toxicity of adjuvant endocrine therapy in postmenopausal breast cancer patients: a systematic review and meta-analysis. *J. Natl. Cancer Inst.* **103**, 1299–1309 (2011).
345. Sobral, A. F., Amaral, C., Correia-da-silva, G. & Teixeira, N. Unravelling exemestane: from biology to clinical prospects. *J. Steroid Biochem. Mol. Biol.* **163**, 1–11 (2016).

346. Gasi, K. M. P. *et al.* New D-modified androstane derivatives as aromatase inhibitors. *Steroids* **66**, 645–653 (2001).
347. Banday, A. H., Akram, S. M. M. & Shameem, S. A. Benzylidine Pregnenolones and their Oximes as Potential Anticancer Agents: Synthesis and Biological Evaluation. *Steroids* **84**, 64–69 (2014).
348. Bansal, R. *et al.* Synthesis and aromatase inhibitory activity of some new 16E-arylidenosteroids. *Bioorg. Chem.* **45**, 36–40 (2012).
349. Bansal, R., Guleria, S., Thota, S., Hartmann, R. W. & Zimmer, C. Synthesis of imidazole-derived steroidal hybrids as potent aromatase inhibitors. *Med. Chem. Res.* **22**, 692–698 (2013).
350. Singh, R. & Panda, G. An overview of synthetic approaches for heterocyclic steroids. *Tetrahedron* **69**, 2853–2884 (2013).
351. Zhu, L. *et al.* Synthesis and anti-inflammatory activity evaluation of 2-dehydroepiandrosterone benzene methyl derivatives. *Chinese J. Org. Chem.* **39**, 2625–2631 (2019).
352. Singh, R. & Bansal, R. Investigations on 16-arylideno steroids as a new class of neuroprotective agents for the treatment of Alzheimer's and Parkinson's diseases. *ACS Chem. Neurosci.* **8**, 186–200 (2017).
353. Semenenko, A. N. *et al.* New ylidene and spirocyclopropyl derivatives of cholestanone and dehydroepiandrosterone series and their ability to induce cholesteric mesophase in nematic solvent. *Synth. Commun.* **48**, 1008–1015 (2018).
354. Boyd, M. R. The NCI Human Tumor Cell Line (60-Cell) Screen. in *Cancer Drug Discovery and Development: Anticancer Drugs Development Guide: Preclinical Screening, Clinical Trials, and Approval - Part I* (eds. Teicher, B. A. & Andrews, P. A.) 41–61 (Humana Press Inc., 2004).
355. Fan, N.-J. *et al.* Synthesis and Cytotoxicity of Some Novel 21E-Benzylidene Steroidal Derivatives. *Steroids* **78**, 874–9 (2013).
356. Abood, N. K. & Ibraheem, H. H. Synthesis , characterize and antimicrobial study of new chalcones and pyrazole derivatives from progesterone. *Int. J. Sci. Res.* **5**, 2319–7064 (2016).
357. Shan, L. *et al.* Synthesis of 3b, 7a, 11a-trihydroxy-pregn-21-benzylidene-5-en-20-one derivatives and their cytotoxic activities. *Bioorg. Med. Chem. Lett.* **19**, 6637–6639 (2009).
358. Bernstein, L. & Ross, R. K. Endogenous Hormones and Breast Cancer Risk. *Epidemiol. Rev.* **15**, 48–65 (1993).
359. Smuc, T. *et al.* Disturbed estrogen and progesterone action in ovarian

endometriosis. *Mol. Cell. Endocrinol.* **301**, 59–64 (2009).

360. Sawetawan, C., Milewich, L., Word, R. A., Carr, B. R. & Rainey, W. E. Compartmentalization of Type I 17β-Hydroxysteroid Oxidoreductase in the Human Ovary. *Mol. Cell. Endocrinol.* **99**, 161–168 (1994).
361. Fournet-Dulguerov, N. *et al.* Immunohistochemical Localization of Aromatase Cytochrome P-450 and Estradiol Dehydrogenase in the Syncytiotrophoblast of the Human Placenta*. *J. Clin. Endocrinol. Metab.* **65**, 757–764 (1987).
362. Vihko, P. & Herrala, A. Control of cell proliferation by steroids: the role of 17HSDs. **248**, 141–148 (2006).
363. Kruchten, P., Werth, R., Marchais-oberwinkler, S., Frotscher, M. & Hartmann, R. W. Molecular and Cellular Endocrinology Development of a biological screening system for the evaluation of highly active and selective 17 □ -HSD1-inhibitors as potential therapeutic agents. **301**, 154–157 (2009).
364. Allan, G. M. *et al.* Modification of Estrone at the 6, 16, and 17 Positions: Novel Potent Inhibitors of 17-Hydroxysteroid Dehydrogenase Type 1. *J. Med. Chem.* **49**, 1325–1345 (2006).
365. Mueck, A. O. & Seeger, H. 2-Methoxyestradiol - Biology and Mechanism of Action. *Steroids* **75**, 625–631 (2010).
366. Wang, C. *et al.* Discovery of chalcone-modified estradiol analogs as antitumour agents that inhibit tumour angiogenesis and epithelial to mesenchymal transition. *Eur. J. Med. Chem.* **176**, 135–148 (2019).
367. Minu, M. & Jindal, D. P. Synthesis and Biological Activity of 16-Arylidene Derivatives of Estrone and Estrone Methyl Ether. *Indian J. Chem.* **42**, 166–172 (2003).
368. Canário, C. *et al.* Δ9,11-Estrone Derivatives as Potential Antiproliferative Agents: Synthesis, in vitro Biological Evaluation and Docking Studies. *Comptes Rendus Chim.* **23**, 201–217 (2020).
369. Kolo, A. M., İpek, E., Çapan, İ. & Servi, S. Synthesis of Heterocyclic-Substituted Novel Hydroxysteroids with Regioselective and Stereoselective Reactions. *J. Heterocycl. Chem.* **55**, 492–497 (2018).
370. Thamotharan, S., Parthasarathi, V. & Gupta, R. Two Androst-5-ene Derivatives: 16-[4-(3-chloropropoxy)-3-methoxybenzylidene]-17-oxoandrost-5-en-3β-ol and 16-[3-methoxy-4-(2-pyrrolidin-1-ylethoxy)benzylidene]-3β-pyrrolidinoandrost-5-en-17β-ol monohydrate. *Acta Crystallogr. Sect. C Cryst. Struct. Commun.* **60**, 75–78 (2004).
371. Choudhary, M. I. *et al.* Pregnenolone derivatives as potential anticancer agents. *Steroids* **76**, 1554–1559 (2011).

372. Bastos, D. A. & Antonarakis, E. S. Galeterone for the treatment of advanced prostate cancer: the evidence to date. *Drug Des. Devel. Ther.* **10**, 2289–2297 (2016).
373. Banday, A. H., Shameem, S. A., Banday, J. A. & Ganaie, B. A. Synthesis, 17α-hydroxylase-C 17,20-lyase inhibitory and 5α-reductase activity of novel pregnenolone derivatives. *Anticancer. Agents Med. Chem.* **18**, 1919–1926 (2018).
374. El-Naggar, M., Amr, A. E. E., Fayed, A. A. & Elsayed, E. A. Potent anti-ovarian cancer with inhibitor activities on both topoisomerase II and V600E BRAF of synthesized substituted estrone candidates. *Molecules* **24**, 2054 (2019).
375. Amr, A. E., Mohamed, A. M., Mohamed, S. F., Abdel-hafez, N. A. & Hammam, A. E. G. Anticancer activities of some newly synthesized pyridine, pyrane and pyrimidine derivatives. *Bioorg. Med. Chem.* **14**, 5481–5488 (2006).
376. Shi, Y., Wang, B., Shi, X. & Zhao, Y. Synthesis and biological evaluation of new steroidal pyridines as potential anti-prostate cancer agents. *Eur. J. Med. Chem.* **145**, 11–22 (2018).
377. Amr, A. E. E. *et al.* Design, Synthesis, Anticancer Evaluation and Molecular Modeling of Novel Estrogen Derivatives. *Molecules* **24**, 416 (2019).
378. Babu, A. R. S. & Raghunathan, R. An easy access to novel steroidal dispiropyrrolidines through 1,3-dipolar cycloaddition of azomethine ylides. *Tetrahedron Lett.* **49**, 4618–4620 (2008).
379. Gavaskar, D., Babu, A. R. S., Raghunathan, R., Dharani, M. & Balasubramanian, S. An expedient sequential one-pot four component synthesis of novel steroidal spiro-pyrrolidine heterocycles in ionic liquid. *Steroids* **109**, 1–6 (2016).
380. Mótyána, G. *et al.* Anti-cancer activity of novel dihydrotestosterone-derived ring A-condensed pyrazoles on androgen non-responsive prostate cancer cell lines. *Int. J. Mol. Sci.* **20**, 2170 (2019).
381. Iványi, Z. *et al.* Novel Series of 17β-Pyrazolylandrosta-5,16-diene Derivatives and their Inhibitory Effect on 17α-Hydroxylase/C17,20-lyase. *Steroids* **77**, 1152–1159 (2012).
382. Banday, A. H., Shameem, S. a. & Jeelani, S. Steroidal pyrazolines and pyrazoles as potential 5α-reductase inhibitors: synthesis and biological evaluation. *Steroids* **92**, 13–19 (2014).
383. Singh, J. *et al.* Targeting progesterone metabolism in breast cancer with L-proline derived new 14-azasteroids. *Bioorganic Med. Chem.* **25**, 4452–4463 (2017).
384. Singh, R., Thota, S. & Bansal, R. Studies on 16,17-pyrazoline substituted heterosteroids as anti-Alzheimer and anti-Parkinsonian agents using LPS induced neuroinflammation models of mice and rats. *ACS Chem. Neurosci.* **9**, 272–283

(2018).

385. Amr, A. E. E., Abdel-latif, N. A. & Abdalla, M. M. Synthesis and antiandrogenic activity of some new 3-substituted androstano [17,16-c]-5'-aryl-pyrazoline and their derivatives. *Bioorg. Med. Chem.* **14**, 373–384 (2006).
386. Lall, S. I. *et al.* Polycations. Part X. LIPs, a new category of room temperature ionic liquid based on polyammonium salts. *R. Soc. Chem.* 2413–2414 (2000).
387. Mitchell, H. J. *et al.* Design, Synthesis, and Biological Evaluation of 16-Substituted 4-Azasteroids as Tissue-Selective Androgen Receptor Modulators (SARMs). *J. Med. Chem.* **52**, 4578–4581 (2009).
388. Dubey, S., Jindal, D. P. & Piplani, P. Synthesis and antineoplastic activity of some 16-benzylidene substituted steroidal oximes. *Indian J. Chem.* **44**, 2126–2137 (2005).
389. Dubey, S., Piplani, P. & Jindal, D. P. Synthesis and evaluation of some 16-benzylidene substituted 3,17-dioximino androstene derivatives as anticancer agents. *Lett. Drug Des. Discov.* **2**, 537–545 (2005).
390. Mitchell, H. J. *et al.* Design, Synthesis, and Biological Evaluation of 16-Substituted 4-Azasteroids as Tissue-selective Androgen Receptor Modulators (SARMs). *J. Med. Chem.* **52**, 4578–4581 (2009).
391. Patrick, G. L. *An Introduction to Medicinal Chemistry*. (Oxford University Press, 2013).
392. Sinha, S. & Vohora, D. Drug discovery and development: an overview. in *Pharmaceutical Medicine and Translational Clinical Research* 15–28 (Elsevier Inc., 2018). doi:10.1016/B978-0-12-802103-3.00002-X.
393. Gallego, V., Naveiro, R., Roca, C., Ríos Insua, D. & Campillo, N. E. AI in drug development: a multidisciplinary perspective. *Mol. Divers.* **25**, 1461–1479 (2021).
394. Merk. Target identification & validation for early drug discovery. *Pharmacology & Drug Discovery Process* https://www.sigmaaldrich.com/PT/en/technical-documents/technical-article/research-and-disease-areas/pharmacology-and-drug-discovery-research/target-identification-and-validation-for-early-drug-discovery (2016).
395. Hughes, J. P., Rees, S. S., Kalindjian, S. B. & Philpott, K. L. Principles of early drug discovery. *Br. J. Pharmacol.* **162**, 1239–1249 (2011).
396. Imming, P., Sinning, C. & Meyer, A. Drugs, their targets and the nature and number of drug targets. *Nat. Rev. Drug Discov.* **5**, 821–834 (2006).
397. Lindsay, M. A. Target discovery. *Nat. Rev. Drug Discov.* **2**, 831–838 (2003).
398. Lee, J. & Bogyo, M. Target deconvolution techniques in modern phenotypic profiling. *Curr. Opin. Chem. Biol.* **17**, 118–126 (2013).

399. Cao, C. & Moult, J. GWAS and drug targets. *BMC Genomics* **15**, S5 (2014).
400. Sioud, M. Main approaches to target discovery and validation. *Methods Mol. Biol.* **360**, 1–12 (2007).
401. Plenge, R. M., Scolnick, E. M. & Altshuler, D. Validating therapeutic targets through human genetics. *Nat. Rev. Drug Discov.* **12**, 581–594 (2013).
402. Rudmann, D. G. On-target and off-target-based toxicologic effects. *Toxicol. Pathol.* **41**, 310–314 (2013).
403. LePage, D. F. & Conlon, R. A. Animal models for disease: knockout, knock-in, and conditional mutant mice. *Methods Mol. Med.* **129**, 41–67 (2006).
404. Smith, C. Drug target validation: hitting the target. *Nature* **422**, 342–345 (2003).
405. Fox, S. *et al.* High-throughput screening: update on practices and success. *J. Biomol. Screen.* **11**, 864–869 (2006).
406. Law, R. *et al.* The multiple roles of computational chemistry in fragment-based drug design. *J. Comput. Aided. Mol. Des.* **23**, 459–473 (2009).
407. Neves, B. J. *et al.* QSAR-based virtual screening: advances and applications in drug discovery. *Front. Pharmacol.* **9**, 1–7 (2018).
408. McInnes, C. Virtual screening strategies in drug discovery. *Curr. Opin. Chem. Biol.* **11**, 494–502 (2007).
409. Cherkasov, A. *et al.* QSAR modeling: where have you been? Where are you going to? *J. Med. Chem.* **57**, 4977–5010 (2014).
410. Leeson, P. Chemical beauty contest. *Nature* **481**, 455–456 (2012).
411. Murray, C. W. & Rees, D. C. The rise of fragment-based drug discovery. *Nat. Chem.* **1**, 187–192 (2009).
412. Williams, M. Qualitative pharmacology in a quantitative world: diminishing value in the drug discovery process. *Curr. Opin. Pharmacol.* **11 5**, 496–500 (2011).
413. Hefti, F. F. Requirements for a lead compound to become a clinical candidate. *BMC Neurosci.* **9**, 1–7 (2008).
414. Honek, J. Preclinical research in drug development. *Med. Writ.* **26**, 5–8 (2017).
415. Andrade, E. L. *et al.* Non-clinical studies required for new drug development – Part I: early in silico and in vitro studies,new target discovery and validation,proof of principles and robustness of animal studies. *Brazilian J. Med. Biol. Res.* **49**, 1–9 (2016).
416. de Jong, L. A. A., Uges, D. R. A., Franke, J. P. & Bischoff, R. Receptor–ligand binding assays: technologies and applications. *J. Chromatogr. B* **829**, 1–25 (2005).
417. Elliott, N. T. & Yuan, F. A review of three-dimensional in vitro tissue models for drug discovery and transport studies. *J. Pharm. Sci.* **100**, 59–74 (2011).

418. Bowes, J. *et al.* Reducing safety-related drug attrition: the use of in vitro pharmacological profiling. *Nat. Rev. Drug Discov.* **11**, 909–922 (2012).
419. Everitt, J. I. The future of preclinical animal models in pharmaceutical discovery and development: a need to bring in cerebro to the in vivo discussions. *Toxicol. Pathol.* **43**, 70–77 (2015).
420. Faqi, A. S. *A comprehensive guide to toxicology in preclinical drug development*. (Academic Press, 2013).
421. Herter-Sprie, G. S., Kung, A. L. & Wong, K.-K. New cast for a new era: preclinical cancer drug development revisited. *J. Clin. Invest.* **123**, 3639–3645 (2013).
422. Grever, M. R. Accelerating safe drug development: an ideal approach to approval. *Hematology Am. Soc. Hematol. Educ. Program* **2013**, 24–29 (2013).
423. Glass, H. E., DiFrancesco, J. J., Glass, L. M. & Tran, P. Are Phase 3 clinical trials really becoming more complex? *Ther. Innov. Regul. Sci.* **49**, 852–860 (2015).
424. Ciociola, A. A., Cohen, L. B. & Kulkarni, P. How drugs are developed and approved by the FDA: current process and future directions. *Am. J. Gastroenterol.* **109**, 620–623 (2014).
425. Purandare, A. V. Understanding drug development: a primer on the Food and Drug Administration. *J. Pediatric Infect. Dis. Soc.* **10**, 977–981 (2021).
426. Williams, C. T. Food and Drug Administration drug approval process. A history and overview. *Nurs. Clin. North Am.* **51**, 1–11 (2016).
427. Suvarna, V. Phase IV of drug development. *Perspect. Clin. Res.* **1**, 57–60 (2010).
428. Kiriiri, G. K., Njogu, P. M. & Mwangi, A. N. Exploring different approaches to improve the success of drug discovery and development projects: a review. *Futur. J. Pharm. Sci.* **6**, 27 (2020).
429. Zhang, H.-Y. One-compound-multiple-targets strategy to combat Alzheimer's disease. *FEBS Lett.* **579**, 5260–5264 (2005).
430. Pinzi, L. & Rastelli, G. Molecular docking: Shifting paradigms in drug discovery. *Int. J. Mol. Sci.* **20**, 18 (2019).
431. Li, H. *et al.* TarFisDock: a web server for identifying drug targets with docking approach. *Nucleic Acids Res.* **34**, W219–W224 (2006).
432. Xie, T. *et al.* ACTP: A webserver for predicting potential targets and relevant pathways of autophagy-modulating compounds. *Oncotarget* **7**, 10015–10022 (2016).
433. Wang, J.-C., Chu, P.-Y., Chen, C.-M. & Lin, J.-H. idTarget: a web server for identifying protein targets of small chemical molecules with robust scoring functions and a divide-and-conquer docking approach. *Nucleic Acids Res.* **40**, W393–W399 (2012).

434. Labbé, C. M. *et al.* MTiOpenScreen: a web server for structure-based virtual screening. *Nucleic Acids Res.* **43**, W448-54 (2015).
435. Irwin, J. J. *et al.* Automated Docking Screens: A Feasibility Study. *J. Med. Chem.* **52**, 5712–5720 (2009).
436. Hopkins, A. L. Network pharmacology: the next paradigm in drug discovery. *Nat. Chem. Biol.* **4**, 682–690 (2008).
437. Chandran, U., Mehendale, N., Saniya, P., Rathnam, C. & Bhushan, P. Network pharmacology. in *Innovative Approaches in Drug Discovery* 127–164 (2017).
438. Kibble, M. *et al.* Network pharmacology applications to map the unexplored target space and therapeutic potential of natural products. *Nat. Prod. Rep.* **32**, 1249–1266 (2015).
439. Paolini, G. V., Shapland, R. H. B., Van Hoorn, W. P., Mason, J. S. & Hopkins, A. L. Global mapping of pharmacological space. *Nat. Biotechnol.* **24**, 805–815 (2006).
440. Azvolinsky, A. Repurposing existing drugs for new indications. *The Scientist* **1**, 31 (2017).
441. Sahragardjoonegani, B., Beall, R. F., Kesselheim, A. S. & Hollis, A. Repurposing existing drugs for new uses: a cohort study of the frequency of FDA-granted new indication exclusivities since 1997. *J. Pharm. Policy Pract.* **14**, 1–8 (2021).
442. Wang, M. *et al.* Remdesivir and chloroquine effectively inhibit the recently emerged novel coronavirus (2019-nCoV) in vitro. *Cell Res.* **30**, 269–271 (2020).
443. Zhou, Y. *et al.* Network-based drug repurposing for novel coronavirus 2019-nCoV/SARS-CoV-2. *Cell Discov.* **6**, 14 (2020).
444. EMA. Veklury. *European Medicines Agency* https://www.ema.europa.eu/en/medicines/human/EPAR/veklury (2020).
445. Eastman, R. T. *et al.* Remdesivir: a review of its discovery and development leading to emergency use authorization for treatment of COVID-19. *ACS Cent. Sci.* **6**, 672–683 (2020).
446. Grover, A. K. Use of allosteric targets in the discovery of safer drugs. *Med. Princ. Pract.* **22**, 418–426 (2013).
447. Bade, R., Chan, H.-F. & Reynisson, J. Characteristics of known drug space. Natural products, their derivatives and synthetic drugs. *Eur. J. Med. Chem.* **45**, 5646–5652 (2010).
448. Robles, O. & Romo, D. Chemo- and Site-Selective Derivatizations of Natural Products Enabling Biological Studies. *Nat. Prod. Rep.* **31**, 318–334 (2014).
449. Horman, S. R. Complex High-Content Phenotypic Screening. in *Special Topics in Drug Discovery* (eds. Chen, T. & Chai, S. C.) (IntechOpen, 2016).

doi:10.5772/65387.

450. Lage, O. M. *et al.* Current screening methodologies in drug discovery for selected human diseases. *Mar. Drugs* **16**, 1–31 (2018).
451. Morrow, T. & Felcone, L. H. Defining the difference: what makes biologics unique. *Biotechnol. Healthc.* **1**, 24–9 (2004).
452. Lappin, G., Noveck, R. & Burt, T. Microdosing and drug development: past, present and future. *Expert Opin. Drug Metab. Toxicol.* **9**, 817–834 (2013).
453. Lessl, M., Bryans, J. S., Richards, D. & Asadullah, K. Crowd sourcing in drug discovery. *Nat. Rev. Drug Discov.* **10**, 241–242 (2011).
454. Paul, S. M. *et al.* How to improve R&D productivity: the pharmaceutical industry's grand challenge. *Nat. Rev. Drug Discov.* **9**, 203–214 (2010).
455. Vander Schee, B. Crowdsourcing: why the power of the crowd is driving the future of business. *J. Consum. Mark.* **26**, 305–306 (2009).
456. Flier, J. S. Academia and industry: allocating credit for discovery and development of new therapies. *J. Clin. Invest.* **129**, 2172–2174 (2019).
457. Yadav, M. R., Sabale, P., Giridhar, R., Zimmer, C. & Hartmann, R. Steroidal carbonitriles as potential aromatase inhibitors. *Steroids* **77**, 850–857 (2012).
458. Li, X. *et al.* Synthesis and in Vitro Evaluation of 4-Substituted N-(1,1-Dimethylethyl)-3-oxo-4-androstene-17.beta.-carboxamides as 5.alpha.-Reductase Inhibitors and Antiandrogens. *J. Med. Chem.* **38**, 1456–1461 (1995).
459. Roy, J., DeRoy, P. & Poirier, D. 2β-(N-Substituted Piperazino)-5α-Androstane-3α,17β-Diols: Parallel Solid-Phase Synthesis and Antiproliferative Activity on Human Leukemia HL-60 Cells. *J. Comb. Chem.* **9**, 347–358 (2007).
460. Ajdukovi, J. J. *et al.* 17(E)-Picolinylidene androstane derivatives as potential inhibitors of prostate cancer cell growth: Antiproliferative activity and molecular docking studies. *Bioorg. Med. Chem.* **21**, 7257–7266 (2013).
461. Trost, L., Saitz, T. R. & Hellstrom, W. J. G. Side effects of 5α-reductase inhibitors: a comprehensive review. *Sex. Med. Rev.* **1**, 24–41 (2013).
462. Huang, L.-H., Xu, H.-D., Yang, Z.-Y., Zheng, Y.-F. & Liu, H.-M. Synthesis and Anticancer Activity of Novel C6-Piperazine Substituted Purine Steroid-nucleosides Analogues. *Steroids* **82**, 1–6 (2014).
463. Huang, L.-H., Xu, H.-D., Yao, Z.-Y., Wang, Y.-G. & Liu, H.-M. Synthesis and biological evaluation of novel C6-amino substituted 4-azasteroidal purine nucleoside analogues. *Bioorg. Med. Chem. Lett.* **24**, 973–5 (2014).
464. Huang, L. H., Li, Y., Xu, H. De, Zheng, Y. F. & Liu, H. M. Synthesis and Biological Evaluation of Novel C6-cyclo Secondary Amine Substituted Purine Steroid-nucleosides Analogues. *Steroids* **85**, 13–17 (2014).

465. Cortés-Benítez, F., Cabeza, M., Teresa, M., Apan, R. & Bratoeff, E. Synthesis of 17b-N-arylcarbamoylandrost-4-en-3-one derivatives and their antiproliferative effect on human androgen-sensitive LNCaP cell line. *Eur. J. Med. Chem.* **4**, 737–746 (2016).
466. Brito, V. Development of novel 4-azasteroid derivatives as potential 5α-reductase inhibitors: synthesis, biological and computational evaluation. *Master's Dissertation* (University of Beira Interior, 2016).
467. Xiao, Q., Wang, L., Fan, H. & Wei, Z. Structure of human steroid 5α-reductase 2 with the anti-androgen drug finasteride. *Nat. Commun.* **11**, 5430 (2020).
468. Figueiredo, J. *et al.* Trisubstituted barbiturates and thiobarbiturates: Synthesis and biological evaluation as xanthine oxidase inhibitors, antioxidants, antibacterial and anti-proliferative agents. *Eur. J. Med. Chem.* **143**, 829–842 (2018).
469. Baji, Á. *et al.* Multicomponent access to androstano-arylpyrimidines under microwave conditions and evaluation of their anti-cancer activity in vitro. *J. Steroid Biochem. Mol. Biol.* **172**, 79–88 (2017).
470. de la Guardia, C. *et al.* Antiviral Activity of Novel Quinoline Derivatives against Dengue Virus Serotype 2. *Molecules* **23**, (2018).
471. Yu, S., Kim, T., Yoo, K. H. & Kang, K. The T47D cell line is an ideal experimental model to elucidate the progesterone-specific effects of a luminal A subtype of breast cancer. *Biochem. Biophys. Res. Commun.* (2017) doi:10.1016/j.bbrc.2017.03.114.
472. Eidet, J. R., Pasovic, L., Maria, R., Jackson, C. J. & Utheim, T. P. Objective assessment of changes in nuclear morphology and cell distribution following induction of apoptosis. *Diagn. Pathol.* **9**, 1–9 (2014).
473. Li, P., Zhou, L., Zhao, T., Liu, X. & Zhang, P. Caspase-9: structure, mechanisms and clinical application. *Oncotarget* **8**, 23996–24008 (2017).
474. Tosco, P. & Balle, T. Open3DQSAR: a new open-source software aimed at high-throughput chemometric analysis of molecular interaction fields. *J. Mol. Model.* **17**, 201—208 (2011).
475. Verma, J., Khedkar, V. M. & Coutinho, E. C. 3D-QSAR in drug design - a review. *Curr. Top. Med. Chem.* **10**, 95–115 (2010).
476. Gueto, C., Torres, J. & Vivas-Reyes, R. CoMFA, LeapFrog and blind docking studies on sulfonanilide derivatives acting as selective aromatase expression regulators. *Eur. J. Med. Chem.* **44**, 3445–3451 (2009).
477. Längle, D. *et al.* Design, synthesis and 3D-QSAR studies of novel 1,4-dihydropyridines as TGFβ/Smad inhibitors. *Eur. J. Med. Chem.* **95**, 249–266

(2015).

478. Catarro, M. *et al.* Novel 4-acetamide-2-alkylthio-N-acetanilides resembling nimesulide: synthesis, cell viability evaluation and in silico studies. *Bioorg. Med. Chem.* **25**, 4304–4313 (2017).
479. Emmerich, J., Hu, Q., Hanke, N. & Hartmann, R. W. Cushing's Syndrome: Development of Highly Potent and Selective CYP11B1 Inhibitors of the (Pyridylmethyl)pyridine Type. *J. Med. Chem.* **56**, 6022–6032 (2013).
480. Trapani, G. *et al.* A rapid method for obtaining finasteride, a 5α-reductase inhibitor, from commercial tablets. *Brain Res. Protoc.* **9**, 130–134 (2002).
481. Morris, G. M. *et al.* Automated docking using a Lamarckian genetic algorithm and an empirical binding free energy function. *J. Comput. Chem.* **19**, 1639–1662 (1998).
482. Carvalho, F. S., Silva, M. M. C. & Sa, M. L. Highly efficient epoxidation of unsaturated steroids using magnesium bis(monoperoxyphthalate) hexahydrate. *Tetrahedron* **65**, 2773–2781 (2009).
483. Chávez-riveros, A. *et al.* Synthesis and cytotoxic effect of pregnenolone derivatives with one or two α,β-unsaturated carbonyls and an ester moiety at C-21 or C-3. *Steroids* **131**, 37–45 (2018).
484. Kim, S., Kim, Y. & Ma, E. Synthesis and 5α-Reductase Inhibitory Activity of C21 Steroids Having 1,4-diene or 4,6-diene 20-ones and 4-Azasteroid 20-Oximes. *Molecules* **17**, 355–368 (2012).
485. Bratoeff, E. *et al.* Molecular interactions of progesterone derivatives with 5α-reductase types 1 and 2 and androgen receptors. *Steroids* **75**, 499–505 (2010).
486. Chávez-Riveros, A. *et al.* Synthesis and Identification of Pregnenolone Derivatives as Inhibitors of Isozymes of 5α-Reductase. *Arch. Pharm. (Weinheim).* **348**, 808–816 (2015).
487. Pérez-Ornelas, V. *et al.* New 5α-reductase Inhibitors: in vitro and in vivo Effects. *Steroids* **70**, 217–24 (2005).
488. Salvador, J. A. R., Silvestre, S. M. & Moreira, V. M. Catalytic oxidative processes in steroid chemistry: allylic oxidation, β-selective epoxidation, alcohol oxidation and remote functionalization reactions. *Curr. Org. Chem.* **10**, 2227–2257 (2006).
489. Brougham, P., Cooper, M., Cummerson, D., Heaney, H. & Thompson, N. Oxidation Reactions Using Magnesium Monoperphthalate: A Comparison with m -Chloroperoxybenzoic Acid. *Synthesis-stuttgart* **1987**, 1015–1017 (1987).
490. Meninno, S., Villano, R. & Lattanzi, A. Magnesium Monoperphthalate (MMPP): a Convenient Oxidant for the Direct Rubottom Oxidation of Malonates, β-Keto Esters, and Amides. *European J. Org. Chem.* **2021**, 1758–1762 (2021).

491. ten Brink, G. J., Arends, I. W. C. E. & Sheldon, R. A. The Baeyer-Villiger reaction: New developments toward greener procedures. *Chem. Rev.* **104**, 4105–4123 (2004).
492. Dzhemilev, U. M. & Vostrikov, N. S. Oxidation with p-(methoxycarbonyl) perbenzqic acid 1. Stereochemistry of epoxidation of Δ5-steroids. *Bull. Acad. Sci. USSR Div. Chem. Sci.* 23–26 (1978) doi:10.1007/BF00923883.
493. Li, T., Chen, Y. & Li, C. Androsterone-based gels enable diastereospecific reductions and diastereoselective epoxidations of gelators. *Org. Biomol. Chem.* **16**, 6791–6800 (2018).
494. Gerdes, J. *et al.* Immunobiochemical and molecular biologic characterization of the cell proliferation-associated nuclear antigen that is defined by monoclonal antibody Ki-67. *Am. J. Pathol.* **138**, 867–873 (1991).
495. Scholzen, T. & Gerdes, J. The Ki-67 protein: from the known and the unknown. *J. Cell. Physiol.* **182**, 311–322 (2000).
496. Fitzgibbons, P. L. *et al.* Prognostic factors in breast cancer. College of American Pathologists Consensus Statement 1999. *Arch. Pathol. Lab. Med.* **124**, 966–978 (2000).
497. Gerdes, J. *et al.* Cell cycle analysis of a cell proliferation-associated human nuclear antigen defined by the monoclonal antibody Ki-67. *J. Immunol.* **133**, 1710–1715 (1984).
498. Tan, P. H. *et al.* Immunohistochemical detection of Ki67 in breast cancer correlates with transcriptional regulation of genes related to apoptosis and cell death. *Mod. Pathol.* **18**, 374–381 (2005).
499. Syed, A. *et al.* Ki67 in Breast Cancer Patients and Its Correlation with Clinico Pathology Factors. *Eur. J. Cancer* **48**, S121 (2012).
500. Chang-Jing, G. Y., Bae-Li, H. & Faulk, W. P. Propidium iodide as a nuclear marker in immunofluorescence. ii. use with cellular identification and viability studies. *J. Immunol. Methods* **43**, 269–275 (1981).
501. Brana, C., Benham, C. & Sundstrom, L. A method for characterising cell death in vitro by combining propidium iodide staining with immunohistochemistry. *Brain Res. Protoc.* **10**, 109–114 (2002).
502. Monette, R., Small, D. L., Mealing, G. & Morley, P. A fluorescence confocal assay to assess neuronal viability in brain slices. *Brain Res. Protoc.* **2**, 99–108 (1998).
503. Santos, T. *et al.* Blue light potentiates neurogenesis induced by retinoic acid-loaded responsive nanoparticles. *Acta Biomater.* **59**, 293–302 (2017).
504. Ziegler, U. & Groscurth, P. Morphological features of cell death. *News Physiol. Sci. an Int. J. Physiol. Prod. jointly by Int. Union Physiol. Sci. Am. Physiol. Soc.* **19**,

124–128 (2004).

505. Stuppia, L. *et al.* Morphometric and functional study of apoptotic cell chromatin. *Cell Death Differ.* **3**, 397–405 (1996).
506. Falcieri, E. *et al.* The behaviour of nuclear domains in the course of apoptosis. *Histochemistry* **102**, 221–231 (1994).
507. Claessens, F. & Moris, L. The influence of steroid metabolism on CYP17A1 inhibitor activity. *Nat. Rev. Urol.* **14**, 590–592 (2017).
508. Dai, C., Heemers, H. & Sharifi, N. Androgen signaling in prostate cancer. *Cold Spring Harb. Perspect. Med.* **7**, (2017).
509. Morris, G. M. *et al.* AutoDock4 and AutoDockTools4: Automated docking with selective receptor flexibility. *J. Comput. Chem.* **30**, 2785–2791 (2009).
510. Bratoeff, E. *et al.* Aromatic esters of progesterone as 5α-reductase and prostate growth inhibitors. *J. Enzyme Inhib. Med. Chem.* **24**, 655–662 (2009).
511. Garrido, M. *et al.* New steroidal lactones as 5a-reductase inhibitors and antagonists for the androgen receptor. *J. Steroid Biochem. Mol. Biol.* **127**, 367–373 (2011).
512. Bernardo-Otero, Y. *et al.* Synthesis and biological activity of epoxy analogues of 3-dehydroteasterone. *J. Chem. Res.* 268–271 (2007) doi:10.3184/030823407x210884.
513. Carvalho, J. F. S., Silva, M. M. C. & Sá e Melo, M. L. Efficient trans-diaxial hydroxylation of Δ5-steroids. *Tetrahedron* **66**, 2455–2462 (2010).
514. Salvador, J. A. R., Silvestre, S. M. & Pinto, R. M. A. Bismuth(III) reagents in steroid and terpene chemistry. *Molecules* **16**, 2884–2913 (2011).
515. Denancé, M., Guyot, M. & Samadi, M. Short synthesis of 16β-hydroxy-5α-cholestane-3,6-dione a novel cytotoxic marine oxysterol. *Steroids* **71**, 599–602 (2006).
516. Piancatelli, G. & Luzzio, F. A. Pyridinium Chlorochromate. *Encyclopedia of Reagents for Organic Synthesis* (2007) doi:https://doi.org/10.1002/9780470842898.rp288.pub2.
517. Li, S. H. & Li, T. S. Steroidal 5-en-3-ones, intermediates of the transformation of steroidal 5-en-3β-ols to steroidal 4-en-3,6-diones oxidized by pyridinium dichromate and pyridinium chlorochromate. *Steroids* **63**, 76–79 (1998).
518. Cepa, M. M. D. S., Tavares Da Silva, E. J., Correia-Da-Silva, G., Roleira, F. M. F. & Teixeira, N. A. A. Structure-activity relationships of new A,D-ring modified steroids as aromatase inhibitors: Design, synthesis, and biological activity evaluation. *J. Med. Chem.* **48**, 6379–6385 (2005).
519. Galluzzi, L. *et al.* Molecular mechanisms of cell death: Recommendations of the

Nomenclature Committee on Cell Death 2018. *Cell Death Differ.* **25**, 486–541 (2018).

520. ATCC. LNCaP clone FGC CRL-1740™. *www.atcc.org* https://www.atcc.org/products/crl-1740 (2022).
521. ATCC. PC-3 CRL-1435™. *www.atcc.org* https://www.atcc.org/products/crl-1435#product-references (2022).
522. Lakhani, S. A. *et al.* Caspases 3 and 7: Key mediators of mitochondrial events of apoptosis. *Science (80-.).* **311**, 847–851 (2006).
523. Brentnall, M., Rodriguez-Menocal, L., Guevara, R. L., Cepero, E. & Boise, L. H. Caspase-9, caspase-3 and caspase-7 have distinct roles during intrinsic apoptosis. *BMC Cell Biol.* **14**, 1–9 (2013).
524. Mcilwain, D. R., Berger, T. & Mak, T. W. Caspase Functions in Cell Death and Disease. *Cold Spring Harb. Perspect. Biol.* **5**, a008656 (2013).
525. Numazawa, M., Tsuji, M. & Mutsumi, A. Studies on aromatase inhibition with 4-androstene-3,6,17-trione: Its 3β-reduction and time-dependent irreversible binding to aromatase with human placental microsomes. *J. Steroid Biochem.* **28**, 337–344 (1987).
526. Swerdloff, R., Dudley, R., Page, S., Wang, C. & Salameh, W. Dihydrotestosterone: biochemistry, physiology, and clinical implications of elevated blood levels. *Endocr. Rev.* **38**, 220–254 (2017).
527. Egan, K. B. The epidemiology of benign prostatic hyperplasia associated with lower urinary tract symptoms: prevalence and incident rates. *Urol. Clin. North Am.* **43**, 289–297 (2016).
528. Hamilton, J. Patterned loss of hair in man: types and incidence. *Ann. N. Y. Acad. Sci.* **53**, 708–728 (1951).
529. Kim, S. & Ma, E. Synthesis of Pregnane Derivatives, Their Cytotoxicity on LNCap and PC-3 Cells, and Screening on 5α-Reductase Inhibitory Activity. *Molecules* **14**, 4655–4668 (2009).
530. Brito, V., Alves, G., Almeida, P. & Silvestre, S. M. Oxidized steroids as 5α-reductase inhibitors with potential interest in prostatic diseases: a review. in *Advances in Health and Diseases* (ed. Duncan, L. T.) 1–35 (Nova Science Publishers, 2022).
531. Sun, J., Xiang, H., Yang, L. & Chen, J. A review on steroidal 5α-reductase inhibitors for treatment of benign prostatic hyperplasia. *Curr. Med. Chem.* **18**, 3576–3589 (2011).
532. Bratoeff, E., Cabeza, M., Pérez-Ornelas, V., Recillas, S. & Heuze, I. In vivo and in vitro effect of novel 4,16-pregnadiene-6,20-dione derivatives, as 5α-reductase inhibitors. *J. Steroid Biochem. Mol. Biol.* **111**, 275–281 (2008).

533. Arellano, Y. *et al.* New ester derivatives of dehydroepiandrosterone as 5α-reductase inhibitors. *Steroids* **76**, 1241–6 (2011).
534. Seo, E. K. *et al.* Inhibitors of 5alpha -reductase type I in LNCaP cells from the roots of Angelica koreana. *Planta Med.* **68 2**, 162–163 (2002).
535. Kim, S., Kim, Y. U. & Ma, E. Synthesis and 5α-reductase inhibitory activity of C 21 steroids having 1,4-diene or 4,6-diene 20-ones and 4-Azasteroid 20-oximes. *Molecules* **17**, 355–368 (2012).
536. Pratis, K., O'Donnell, L., Ooi, G. T., McLachlan, R. I. & Robertson, D. M. Enzyme assay for 5alpha-reductase type 2 activity in the presence of 5alpha-reductase type 1 activity in rat testis. *J. Steroid Biochem. Mol. Biol.* **75**, 75–82 (2000).
537. Amaral, C. *et al.* Development of a new gas chromatography–mass spectrometry (GC–MS) methodology for the evaluation of 5α-reductase activity. *Talanta* **107**, 154–161 (2013).
538. Srivilai, J. *et al.* A new label-free screen for steroid 5α-reductase inhibitors using LC-MS. *Steroids* **116**, 67–75 (2016).
539. Kim, D. *et al.* Development of a Liquid Chromatography/Mass Spectrometry-Based Inhibition Assay for the Screening of Steroid 5-α Reductase in Human and Fish Cell Lines. *Molecules* **26**, 893 (2021).
540. Kumar, N., Rungseevijitprapa, W., Narkkhong, N. & Suttajit, M. 5α-Reductase Inhibition and Hair Growth Promotion of Some Thai Plants Traditionally Used for Hair Treatment. *J. Ethnopharmacol.* **139**, 765–771 (2012).
541. Koseki, J. *et al.* Inhibition of Rat 5α-Reductase Activity and Testosterone-Induced Sebum Synthesis in Hamster Sebocytes by an Extract of Quercus acutissima Cortex. *Evidence-Based Complement. Altern. Med.* **2015**, 1–9 (2015).
542. Iwai, A. *et al.* Spectrophotometric method for the assay of steroid 5α-reductase activity of rat liver and prostate microsomes. *Anal. Sci. Int. J. Japan Soc. Anal. Chem.* **29**, 455–459 (2013).
543. European Medicines Agency. Guideline on bioanalytical method validation. EMEA/CHMP/EWP/192217/2009 Rev. 1. https://www.ema.europa.eu/en/documents/scientificguideline/guideline-bioanalytical-method-validation_en.pdf (2009).
544. Administration, U. F. and D. Guidance for Industry: Bioanalytical method validation. https://www.fda.gov/files/drugs/published/BioanalyticalMethod-Validation-Guidance-for-Industry.pdf (2018).
545. Kumar, T., Chaiyasut, C., Rungseevijitprapa, W. & Suttajit, M. Screening of steroid 5a-reductase inhibitory activity and total phenolic content of Thai plants. *J. Med. Plants* **5**, 1265–1271 (2011).

546. Matsuda, H., Sato, N., Yamazaki, M., Naruto, S. & Kubo, M. Testosterone 5a-Reductase Inhibitory Active Constituents from Anemarrhenae Rhizoma. *Biol. Pharm. Bull.* **24**, 586–587 (2001).
547. Almeida, A. M., Castel-Branco, M. M. & Falcao, A. C. Linear regression for calibration lines revisited: weighting schemes for bioanalytical methods. *J. Chromatogr. B* **774**, 215–222 (2002).
548. Pollard, T. D., Earnshaw, W. C., Lippincott-Schwartz, J. & Johnson, G. Biophysical Principles. in *Cell Biology* 53–62 (Elsevier, 2017). doi:https://doi.org/10.1016/B978-0-323-34126-4.00004-9.
549. Giese, M. & Albrecht, M. Alkyl-Alkyl Interactions in the Periphery of Supramolecular Entities: From the Evaluation of Weak Forces to Applications. *Chempluschem* **85**, 715–724 (2020).
550. Ribas, J., Cubero, E., Luque, F. J. & Orozco, M. Theoretical study of alkyl-pi and aryl-pi interactions. Reconciling theory and experiment. *J. Org. Chem.* **67**, 7057–7065 (2002).
551. Szalewicz, K. Hydrogen Bond. in *Encyclopedia of Physical Science and Technology* (ed. Meyers, R. A. B. T.-E. of P. S. and T. (Third E.) 505–538 (Academic Press, 2003). doi:https://doi.org/10.1016/B0-12-227410-5/00322-7.
552. Ministério da Agricultura, do M. do A. e do O. do T. Decreto-Lei n.º 113/2013 de 7 de agosto. *Diário da República* 4709–4739 (2013).
553. Sellick, J. Enhancing the protection of animals used for scientific purposes. *Environ. Law Manag.* **23**, 75–82 (2011).
554. Sonawane, S. S., Chhajed, S. S., Attar, S. S. & Kshirsagar, S. J. An approach to select linear regression model in bioanalytical method validation. *J. Anal. Sci. Technol.* **10**, 1 (2019).
555. Suphrom, N. *et al.* Anti-androgenic effect of sesquiterpenes isolated from the rhizomes of Curcuma aeruginosa Roxb. *Fitoterapia* **83**, 864–871 (2012).
556. ATCC. T-47D HTB-133™. *www.atcc.org* https://www.atcc.org/products/htb-133 (2022).
557. Brito, V., Santos, A. O., Alves, G., Almeida, P. & Silvestre, S. M. Novel 4-Azapregnene Derivatives as Potential Anticancer Agents: Synthesis, Antiproliferative Activity and Molecular Docking Studies. *Molecules* **27**, 1–18 (2022).
558. Cabeza, M. *et al.* New progesterone derivatives as inhibitors of 5α-reductase enzyme and prostate cancer cell growth. *J. Enzyme Inhib. Med. Chem.* **21**, 371–378 (2006).
559. Cabeza, M. *et al.* Novel C-6 substituted and unsubstituted pregnane derivatives as

5α-reductase inhibitors and their effect on hamster flank organs diameter size. *Steroids* **74**, 793–802 (2009).

560. Silvestre, S. M. & Salvador, J. A. R. Capítulo IV - Oxidação de alcenos a enonas utilizando clorito de sódio, na ausência de catalisadores metálicos. *PhD Thesis* (Universidade de Coimbra, 2007).
561. Silvestre, S. M., Salvador, J. A. R. & Clark, J. H. β-Selective epoxidation of Δ5-steroids by O2 using surface functionalised silica supported cobalt catalysts. *J. Mol. Catal. A Chem.* **219**, 143–147 (2004).
562. Silvestre, S. M. & Salvador, J. A. R. Allylic and benzylic oxidation reactions with sodium chlorite. *Tetrahedron* **63**, 2439–2445 (2007).
563. Potter, G. A., Hardcastle, I. R. & Jarman, M. A Convenient, Large-scale Synthesis of Abiraterone Acetate [3β-acetoxy-17-(3- pyridyl)androsta-5,16-diene], a Potential New Drug for the Treatment of Prostate Cancer. *Org. Prep. Proced. Int.* **29**, 123–128 (1997).
564. Zhang, J. *et al.* Synthesis of dehydroepiandrosterone by co-immobilization of keto reductase and glucose dehydrogenase. *J. Chem. Technol. Biotechnol.* **95**, 2530–2536 (2020).
565. Korde, S. S., Udasi, R. A. & Trivedi, G. K. Oxidation of steroidal 5-en-3β-ol with pyridinium chlorochromate: Isolation of key intermediate, steroidal 6β-hydroxy-4-en-3-one. *Synth. Commun.* **27**, 3419–3430 (1997).
566. Silvestre, S. M., Silva, M. M. C. & Salvador, J. A. R. Recent Highlights in Green Oxidative Chemical Processes Applied to Steroid Chemistry. *Green Nanotechnol. - Overv. Furth. Prospect.* (2016) doi:10.5772/62381.
567. Anastas, P. T. & Warner, J. C. *Green chemistry: theory and practice*. (Oxford University Press, 1998).
568. Aslantürk, Ö. S. In Vitro Cytotoxicity and Cell Viability Assays: Principles, Advantages, and Disadvantages. in *Genotoxicity - A Predictable Risk to Our Actual World* (IntechOpen, 2018).
569. Shargel, L. & Yu, A. B. C. *Applied Biopharmaceutics & Pharmacokinetics*. (McGraw-Hill, 2016).
570. De Inés, C. *et al.* Cytotoxic activity of halogenated monoterpenes from Plocamium cartilagineum. *Zeitschrift fur Naturforsch. - Sect. C J. Biosci.* **59**, 339–344 (2004).
571. Halim, P. A. *et al.* Synthesis and biological evaluation of halogenated phenoxychalcones and their corresponding pyrazolines as cytotoxic agents in human breast cancer. *J. Enzyme Inhib. Med. Chem.* **37**, 189–201 (2022).
572. Huwaimel, B. I. *et al.* Discovery of Halogenated Benzothiadiazine Derivatives with

Anticancer Activity. *ChemMedChem* **16**, 1143–1162 (2021).

573. Ballante, F. Protein-Ligand Docking in Drug Design: Performance Assessment and Binding-Pose Selection. in *Rational Drug Design. Methods in Molecular Biology* (eds. Mavromoustakos, T. & Kellici, T. F.) 67–88 (Springer New York, 2018). doi:10.1007/978-1-4939-8630-9_5.
574. Ferreira, L., dos Santos, R., Oliva, G. & Andricopulo, A. *Molecular Docking and Structure-Based Drug Design Strategies*. *Molecules* vol. 20 (2015).
575. Attard, G. *et al.* Selective inhibition of CYP17 with abiraterone acetate is highly active in the treatment of castration-resistant prostate cancer. *J. Clin. Oncol.* **27**, 3742–3748 (2013).
576. Bratoeff, E. *et al.* Synthesis and biological activity of progesterone derivatives as 5α-reductase inhibitors, and their effect on hamster prostate weight. *J. Enzyme Inhib. Med. Chem.* **25**, 306–311 (2010).
577. Bratoeff, E. *et al.* Effect of dehydroepiandrosterone derivatives on the activity of 5α-reductase isoenzymes and on cancer cell line PC-3. *Bioorg. Med. Chem.* **22**, 6233–6241 (2014).
578. Sánchez-Márquez, A. *et al.* Synthesis and biological evaluation of esters of 16-formyl-17-methoxy-dehydroepiandrosterone derivatives as inhibitors of 5α-reductase type 2. *J. Enzyme Inhib. Med. Chem.* **31**, 1170–1176 (2016).
579. Kovács, A. & Varga, Z. Halogen acceptors in hydrogen bonding. *Coord. Chem. Rev.* **250**, 710–727 (2006).
580. Thareja, S. Steroidal 5α-reductase inhibitors: a comparative 3D-QSAR study review. *Chem. Rev.* **115**, 2883–2894 (2015).
581. Ibrahim-ouali, M., Dumur, F., Ibrahim-ouali, M. & Dumur, F. Recent syntheses of steroidal derivatives containing heterocycles. *Arkivoc* **2019**, 304–339 (2020).
582. Salvador, J. A. R., Sá, M. L. & Salvador, J. A. R. Anticancer steroids: linking natural and semi-synthetic compounds. *Nat. Prod. Rep.* **30**, 324–374 (2013).
583. Zavarzin, I. V, Chertkova, V. V, Levina, I. S. & Chernoburova, E. I. Steroids fused to heterocycles at positions 16, 17 of the D-ring. *Russ. Chem. Rev.* **80**, 661–682 (2011).
584. Hirshburg, J. M., Kelsey, P. A., Therrien, C. A., Gavino, A. C. & Reichenberg, J. S. Adverse effects and safety of 5-alpha reductase inhibitors (finasteride, dutasteride): a systematic review. *J. Clin. Aesthet. Dermatol.* **9**, 56–62 (2016).
585. Kaur, M., Dhingra, R., Bhardwaj, T. R. & Dhingra, N. Synthesis and antiproliferative activity of 3-aza steroids as 5α-reductase inhibitors. *Lett. Drug Des. Discov.* **14**, 1335–1346 (2017).
586. Haffner, C. D. *et al.* 6-Azasteroids: structure-activity relationships for inhibition

of type 1 and 2 human 5α-reductase and human adrenal 3β-hydroxy-Δ5-steroid isomerase. *J. Med. Chem.* **37**, 2352–2360 (1994).

587. Thareja, S., Rajpoot, T. & Verma, S. K. Generation of comparative pharmacophoric model for steroidal 5a-reductase I and II inhibitors: A 3D-QSAR study on 6-azasteroids. *Steroids* **95**, 96–103 (2015).
588. Frye, S. V *et al.* Structure-activity relationships for inhibition of type 1 and 2 human 5α-reductase and human adrenal 3β-hydroxy-Δ5-steroid dehydrogenase/3-keto-Δ5-steroid isomerase by 6-azaandrost-4-en-3-ones: optimization of the C17 Substituent. *J. Med. Chem.* **38**, 2621–2627 (1995).
589. Cui, J. *et al.* Synthesis and cytotoxic activity of some 4,6-diaza-A,B-dihomo-steroid bilactams. *Steroids* **79**, 14–18 (2014).
590. Wang, C. *et al.* Chlorotrimethylsilane-promoted one-pot synthesis of steroidal[17,16-d]pyrimidines. *Steroids* **75**, 1033–8 (2010).
591. Devore, N. M. & Scott, E. E. Cancer drugs abiraterone and Tok-001. *Nature* **482**, 116–119 (2012).
592. Khaireldin, N. Y., El-hashash, M. A., Abdelhalim, M. M., Rayan, D. A. & Mohamed, N. R. Progesterone utility in the synthesis of steroidal heterocyclic compounds with antitumor activity. *Chem. Process Eng. Res.* **9**, 23–38 (2013).
593. DeVore, N. M. & Scott, E. E. Structures of cytochrome P450 17A1 with prostate cancer drugs abiraterone and TOK-001. *Nature* **482**, 116–119 (2012).
594. Frye, S. V *et al.* 6-Azasteroids: potent dual inhibitors of human type 1 and 2 steroid 5α-reductase. *J. Med. Chem.* **36**, 4313–4315 (1993).
595. Haffner, C., Moore, F. & Carolina, N. Synthesis o f 6-azacholesten-3-ones: potent inhibitors of 5α-reductase. *Tetrahedron Lett.* **36**, 4039–4042 (1995).
596. Ibrahim-Ouali, M. & Rocheblave, L. Recent advances in azasteroids chemistry. *Steroids* **73**, 375–407 (2008).
597. Cui, J. *et al.* Synthesis and antiproliferative evaluation of some novel B-nor-D-homosteroids. *Steroids* **98**, 138–142 (2015).
598. Pérez-Gómez, C. O. *et al.* Synthesis and structural characterization of an oxaziridine derived from 6-azadiosgenin. *J. Mol. Struct.* **1255**, 132386 (2022).
599. Chen, S. R., Shen, F. J., Feng, G. L. & Yuan, R. X. Synthesis and anticancer activity of 4-azasteroidal-20-oxime derivatives. *J. Chem. Res.* **39**, 527–530 (2015).
600. Dhaniram, D., Collins, A., Singh, K. & Voulvoulis, N. Industrial Chemicals. *Pollut. Hum. Heal. Environ. A Risk Based Approach* **77**, 147–179 (2012).
601. Amr, A. G. E. & Abdulla, M. M. Synthesis and anti-inflammatory activities of new cyanopyrane derivatives fused with steroidal nuclei. *Arch. Pharm. (Weinheim).* **339**, 88–95 (2006).

602. Zhang, B. *et al.* Design and synthesis of novel D-ring fused steroidal heterocycles. *Steroids* **78**, 1200–1208 (2013).
603. Iványi, Z. *et al.* Synthesis of D-ring-substituted (5'R)- and (5'S)-17β-pyrazolinylandrostene epimers and comparison of their potential anticancer activities. *Steroids* **77**, 566–574 (2012).

APPENDICES

All the supplementary data relevant in the context of the present thesis will be presented in this section, supporting validity of the used experimental methods.

Appendix 1

In this appendix, data relative to the new MTT screening assay results of 4-azasteroids prepared during the Master's project (**VB 4a-g** and **VB 7a-g**), synthetic precursors, synthetic intermediates (**VB 1-3**, **VB 5**, and **VB 6**), and compounds used as references at 30 μM, after 72 h of exposure, against PC-3 cells are shown (**Table Ap 1**). In **Chapter II** data are shown in graphical format, thus the precise average % of negative control±SD is presented in the following table. Furthermore, all data relative to the determination of IC_{50} values of the most active 4-azasteroids prepared during the Master's project (**VB 4a-g** and **VB 7a-g**), after 72 h of exposure, against the complete panel of cell lines (NHDF, LNCaP, PC-3, and T47-D) are shown (**Table Ap 2**).

Table Ap 1. *In vitro* antiproliferative activities of the tested compounds: testosterone, progesterone, 5α-dihydrotestosterone (DHT), **VB 1-3**, **VB 4a-g**, **VB 5**, **VB 6**, **VB 7a-g**, finasteride, and 5-fluorouracil (5-FU) against PC-3 cell line, after 72 h of exposure. MTT screening results at 30 μM (data presented as average % of negative control±SD and are representative of at least two independent experiments).

Compound	**Cell proliferation** (%±SD)	**Compound**	**Cell proliferation** (%±SD)
Testosterone	89.5±9.0	**VB 4g**	79.9±6.4
Progesterone	42.9±5.4	**VB 5**	102.1±5.2
DHT	93.1±4.9	**VB 6**	96.7±9.3
VB 1	123.1±10.3	**VB 7a**	1.4±1.0
VB 2	91.4±15.6	**VB 7b**	25.9±3.8
VB 3	114.6±15.7	**VB 7c**	0.7±0.5
VB 4a	31.5±11.6	**VB 7d**	58.2±6.0
VB 4b	73.5±11.4	**VB 7e**	82.7±6.5
VB 4c	74.8±6.3	**VB 7f**	108.1±7.8
VB 4d	119.4±2.8	**VB 7g**	0.1±0.1
VB 4e	110.2±5.4	**Finasteride**	78.8±8.7
VB 4f	68.0±5.0	**5-FU**	10.8±3.1

Table Ap 2. Estimated IC_{50} values for most active 4-azaandrostene (**VB 4a-g**) and 4-azapregnene (**VB 7a-g**) derivatives against NHDF, LNCaP, PC-3, and T47-D cells. [a]

Compound	NHDF		LNCaP		PC-3		T47-D	
	IC_{50}	r^2	IC_{50}	r^2	IC_{50}	r^2	IC_{50}	r^2
VB 4a	–	–	24.30	0.82	22.63	–	>100	–
VB 4b	–	–	28.28	0.82	–	–	–	–
VB 4c	>100	–	37.20	0.84	–	–	–	–
VB 4d	–	–	–	–	–	–	–	–
VB 4e	–	–	–	–	–	–	–	–
VB 4f	–	–	–	–	–	–	–	–
VB 4g	–	–	–	–	–	–		
VB 7a	63.99	0.91	27.47	0.93	12.60	0.96	16.94	0.97
VB 7b	–	–	–	–	25.94	0.98	44.99	0.98
VB 7c	6.94	0.93	16.26	0.97	3.29	0.99	6.56	0.98
VB 7d	–	–	–	–	–	–	–	–
VB 7e	–	–	–	–	–	–	–	–
VB 7f	–	–	–	–	–	–	–	–
VB 7g	3.09	0.90	10.20	0.90	3.64	0.98	1.33	0.98
Finasteride	>100	–	70.95	0.95	>100	–	>100	–
5-FU	29.44	0.97	1.50	0.98	2.30	0.96	0.70	0.99

[a] The cells were treated at various concentrations (0.01, 0.1, 1, 10, 50, and 100 μM) for 72 h. and the IC_{50} values were calculated by sigmoidal fitting. The data shown are representative of at least two independent experiments. The coefficient of determination (r^2) is indicative of how closely the sigmoidal curve generated can be fitted with nonlinear regression statistics for the cell lines and incubation periods tested. 5-FU= 5-Flurouracil.

Furthermore, in the **Table Ap 3** are show all the results relative to the predicted affinity binding energies against all targets tested during the Master's dissertation project, and not only against 5AR type 2, obtained from molecular docking simulations. Considering the absence of three-dimensional coordinates of 5AR during the Master's project execution, a homologous enzyme, 5β-reductase (5BR), was selected to predict the potential interaction between these novel compounds and 5AR. In **Chapter II**, the data presented are only relative to the work developed in the doctoral project context, both with regard to the estimation of IC_{50} as well as *in silico* studies.

Table Ap 3. Predicted binding energies of previously prepared 4-azasteroids (**VB 4a-g** and **VB 7a-g**) calculated from molecular docking against important targets of steroidal molecules. Binding energies of ligands (in yellow) present in the X-ray crystal structures were calculated by re-docking. [a]

Compound	5BR	5AR type 2	AR	ERα	CYP17A1
				Autodock binding energy (kcal.mol^{-1})	
VB 4a	−9.5	−12.9	−9.6	−8.9	−11.3
VB 4b	−10.0	−13.2	−6.8	−7.5	−11.4
VB 4c	−10.1	−12.7	−2.6	−7.9	−11.1
VB 4d	−9.8	−12.2	−11.8	−9.2	−10.9
VB 4e	−10.0	−12.3	−10.4	−8.1	−11.2
VB 4f	−10.0	−12.7	−10.2	−8.0	−11.4
VB 4g	−9.9	−12.1	−10.8	−9.1	−10.2
VB 7a	−10.9	−11.8	−9.4	−10.9	−11.2
VB 7b	−11.5	−12.0	−8.9	−11.4	−9.3
VB 7c	−9.0	−11.7	−5.1	−10.4	−12.0
VB 7d	−10.6	−11.6	−7.3	−11.0	−11.0
VB 7e	−10.1	−11.1	−9.7	−10.8	−10.9
VB 7f	−10.1	−11.2	−9.9	−11.4	−10.9
VB 7g	−9.9	−11.7	−10.4	−10.7	−10.9
Finasteride	**−9.9**	**−11.9**	–	–	–
DHT	–	–	**−11.2**	–	–
17β-Estradiol	–	–	–	**−9.3**	–
Abiraterone	–	–	–	–	**−11.8**

[a] 5BR= 5β-Reductase, 5AR= 5α-Reductase, AR= Androgen receptor, ERα= Estrogen receptor α, CYP17A1= Steroid 17α-hydroxylase/17,20 lyase, DHT= 5α-Dihydrotestosterone.

Appendix 2

To validate the molecular docking method, simulations were carried out between crystallized ligands/drugs with the respective proteins and all control re-docking simulations were able to reproduce the ligand-protein interaction geometries presented in the respective crystal structures retrieved from PDB with a RMSD ≤ 2.0 Å. The results of re-docking are shown in **Table Ap 4** and it can be observed that all simulations exhibit an RMSD lower than 2.0 Å. These data are valid for all simulations performed in the context of the present thesis (**Chapters II**, **III**, and **IV**).

Table Ap 4. Re-docking results using vina executable of protein-ligand complexes, protein data bank (PDB) accession codes, and resolution.

Macromolecule	**PDB ID**	**Resolution** (Å)	**Co-crystalized ligand**	**Energy** (kcal.mol^{-1}) **and RMSD** (Å)		
				Lowest energy	**RMSD for lowest energy conformation**	**Average RMSD**
5α-Reductase (5AR) **type 2**	7BW1	2.8	Adduct of finasteride/NADPH	−11.9	0.78	1.80
Estrogen receptor α (ERα)	1A52	2.8	Estradiol	−10.4	0.51	0.53
Androgen receptor (AR)	2AMA	1.9	5α-Dihydrotestosterone (DHT)	−11.2	0.79	0.79
Steroid 17α-hydroxylase/17,20 lyase (CYP17A1)	3RUK	2.6	Abiraterone	−10.2	0.23	0.29
Aromatase	3EQM	2.9	Androstenedione	−10.1	0.43	0.89

Appendix 3

A.3. Attempts to synthesize new 3-, 4- and 6-azasteroids

A.3.1. Introduction

The substitution of one or more carbon atoms of the steroid molecule by a heteroatom affects its chemical properties, which may result in a relevant change in its biological activity, with heterosteroids is an important opportunity in medicinal chemistry research.[350,580,581] In this context, steroids containing a nitrogen atom in their skeleton, azasteroids, constitute a relevant example, and they can interfere in several biological processes, having a crucial role in the treatment of several diseases, as referred.[31] Within this broad group, 4-azasteroids stand out for their inhibitory activity of 5AR enzymes, responsible for the irreversible conversion of testosterone into DHT.[31,582] However, the excessive activity of this enzyme, and consequently, the augmented levels of DHT seems to have an important role in the development and progression of PCa and BPH, diseases extremely common in elderly men. Given the high prevalence of these pathologies and their high social and economic impact, some strategies have been established for their treatment, with emphasis on the inhibition of 5AR enzymes in the case of BPH.[461,582,583] Thus, several steroidal and non-steroidal 5ARIs have been prepared, such as finasteride, a semi-synthetic 4-azasteroid and the first type 2 5AR inhibitor approved for BPH treatment of. In addition, dutasteride showed to act as an inhibitor of 5AR type 1 and 2, and turosteride acts as a selective inhibitor of 5AR type 2.[31,582] However, these compounds exhibit marked side effects and low relative potency, thus there is a clear need to synthesize more potent and safer compounds.[24,461,584] Therefore, to overlap these gaps, among other chemical modifications, the exploration of several other positions of the heteroatom on the steroidal skeleton has also been the focus of numerous studies. Consequently and as example, several new 6- and 10-azasteroids have been prepared and evaluated.[585–589]

Additionally, modifications on steroidal D-ring, as previously described, such as the introduction of heterocycles (e.g. arylpyrazolines, arylpyrimidines, and pyridines), have been associated to several interesting bioactivities.[321,590] In fact, some of these compounds displayed anti-inflammatory and antibacterial properties, inhibitory activity against kinases and 5AR enzymes, and anticancer effects.[321,462,583,590–592] For instance, more recently, abiraterone acetate (**Chapter I**, page 31) was introduced into clinical practice for the treatment of PCa. This compound and their analog galeterone have an aromatic nitrogen heterocycle attached to the D-ring and act principally by inhibiting

androgen biosynthesis.[31,591,593] Additionally, azasteroids with D-ring heterocycles attached or fused to the D-ring have been described as *in vitro* inhibitors of proliferation of several cell lines and, in some cases, with more significant results in prostatic cells.[322,462,591,592] Thus, the conjugation of the azasteroid nucleus with heterocycles in the D-ring could constitute a relevant strategy in the development of new potentially useful compounds for more effective and safer treatment of cancer and BPH.

Considering all these, mainly the potential of the conjugation of azasteroid skeleton with heterocycles fused or attached to the D-ring, the initial goal of this doctoral project was to synthesize new 3-, 4-, and 6-azasteroids with a modified D-ring. Posteriorly to chemical synthesis, the novel compounds would be biologically evaluated (antiproliferative activity, cytotoxicity, 5AR inhibition) through *in vitro* studies. However, the preparation of these compounds proved to be more challenging and problematic than expected. In this section, the different approaches and attempts to synthesize the new azasteroids with modifications on the D-ring will be resumed and the principal problems will be presented and discussed.

A.3.2. Results and discussion

A.3.2.1. Approaches to synthesize 3- and 6-azasteroids

Over the years, several azasteroids have been synthesized and evaluated as competitive or non-competitive 5ARIs. Among azasteroidal compounds, 3-azasteroids have not been explored as 5ARIs. Recently, Kaur and colleagues reported the synthesis and the antiproliferative activity of 3-azasteroids as potential 5ARIs, with interesting cytotoxicity in PC-3 cells, when compared with the reference drug, dutasteride, being observed. However, these authors have not evaluated the 5AR inhibitory effect of the prepared compounds.[585] Considering these results, the importance of the lactam for the bioactivity and the poor exploration of 3-azasteroids in this context, it was considered by us the preparation of new 3-azasteroids. In the attempt of synthesize these compounds, the reactional conditions reported by Kaur et. al with some required adaptations were applied (**Figure Ap 1**).

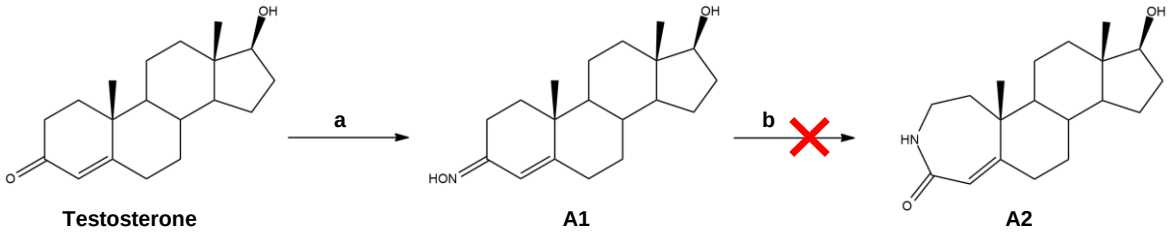

Figure Ap 1. Attempt to prepare 3-azasteroids from testosterone. Reactional conditions: **a)** $NH_2OH.HCl$, pyridine, 6 h, reflux; **b)** $SOCl_2$/dioxane, toluene, 15 °C. Created with ChemDraw.

Firstly, the synthesis of an oxime attached to C-3 of testosterone was successfully achieved, considering the TLC and the information provided in the literature, and the product **A1** was supposedly obtained . Then, the attempt for the formation of the lactam at the A-ring was accomplished, using thionyl chloride ($SOCl_2$) as catalyst, again as described by Kaur and coworkers. However, several issues emerged, and the product was not obtained. Initially, after the reported time for the completion of the reaction (17 min), no evolution was observed in the TLC analysis. Then, the reaction was poured in an inert atmosphere (N_2) and let react for more 1 h. Despite the modifications applied, after 1 h the TLC showed the same result, and then, an equal portion of reagents was added, and the reaction was let for more 2 h. However, the result remained the same, and the work up to recover the substrate was accomplished.

Considering the lack of success on the preparation of 3-azasteroids, and trying not to spend substantial time, attempts to synthesize new 6-azasteroidal derivatives were then tried. 6-Azasteroids, which have been more explored than 3-azasteroids, have also shown interesting results as 5AR inhibitors.[586,594,595] To synthetize these compounds, two different approaches were applied (**Figure Ap 2**). The first one comprised the same basic steps applied for the preparation of 4-azasteroids already described by us, namely, the oxidative cleavage of an α,β-unsaturated ketone on B-ring, and, if it successfully occurs, the azacyclization to obtain the lactam.[326,557] Thus, considering DHEA acetate as starting material, an additional step of allylic oxidation at C-7 position was required to obtain the corresponding 7-oxoderivative (an α,β-unsaturated ketone). This additional step occurred as expected, without registered complications, using sodium chlorite ($NaClO_2$) as oxidative agent combined with *N*-hydroxyphthalimide (NHPI).[488,562] From this reaction, **A3** was obtained in good yield (75 %). Then, the oxidative cleavage procedure with sodium carbonate (Na_2CO_3), sodium periodate ($NaIO_4$)/potassium permanganate ($KMnO_4$) in isopropanol (*i*-PrOH) utilizing **A3** as substrate was performed to obtain steroid **A4**. When these conditions are applied to the A-ring, the reactional time is about 4 h.[326,557] Consequently, in this case, the first monitorization using TLC was performed at this time, and it was observed that the reaction barely progressed. The reaction was let under reflux for more 16 h, being controlled periodically. Despite the appearance of a new spot with a retention factor which should correspond to the desired product, after the work up, the sample analyzed through NMR showed that the product was not obtained, and that probably occurred the degradation of the substrate. A similar tentative was performed using pregnenolone acetate in alternative to DHEA acetate, but without success.

Considering the failure of the first strategy, a more employed method, according to the literature, was tried using pregnenolone acetate as starting material.[594,596–598] This new approach, based on the reported by Cui et al., involved two different steps: B-ring opening (in two phases) and azacyclization with formation of a B-ring with 7 members (**Figure Ap 2**).[594,597,598] Therefore, to obtain **A5**, firstly, the $\Delta^{5,6}$ epoxidation using *m*-CPBA (6 h, r.t.) and then, the B-ring oxidation with opening using the Jones reagent (acetone/DCM, 3 h, 50 °C), were performed. Despite the excellent yield of epoxidation reaction (96 %), the global yield of this two-step was low (25 %), which means that the second step (oxidation and ring opening) is the most critical phase. Consequently, the poor amount of product **A5** obtained (51 mg) will compromise the next step, the azacyclization. Then, the steroid **A5** synthesized was used in the azacyclization procedure, being mixed with ammonium acetate (CH_3COONH_4) in glacial acid acetic (GAA). The reactional mixture was refluxed for 1 day, more time than the reported in several studies, however, no evidence of **A6** formation was observed in TLC analysis.[326,535,557,599] In addition to the longer reaction time, another half portion of reagents was added, although no progress was noticed. After acquisition of NMR proton spectrum, as expected, it was confirmed the absence of peaks corresponding to the desired product.

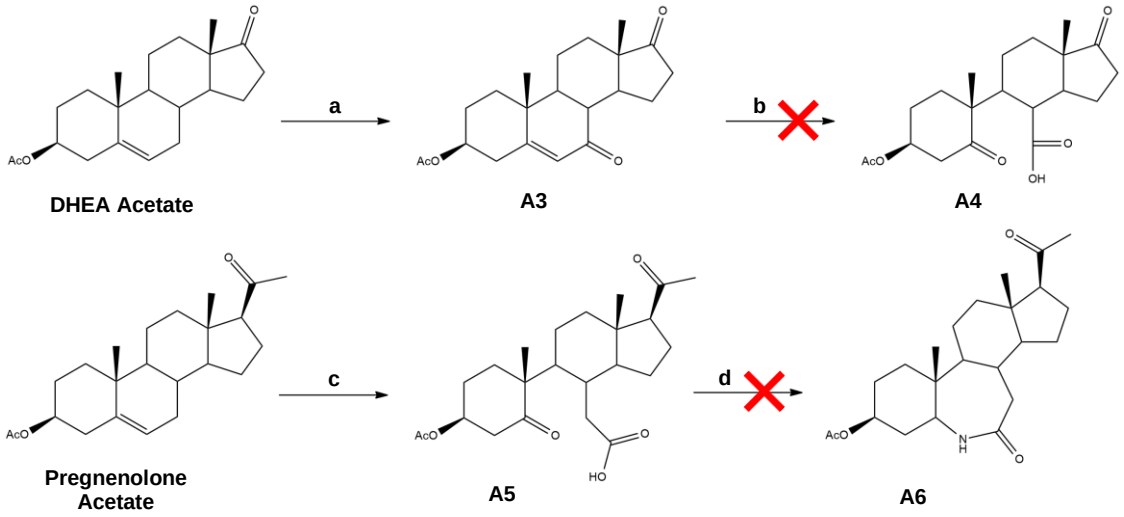

Figure Ap 2. Attempts to synthesize 6-azasteroids from pregnenolone acetate using two different approaches. Reactional conditions: **a)** ACN/H_2O, NHPI/$NaClO_2$, 6 h, 50 °C; **b)** Na_2CO_3, $NaIO_4$/$KMnO_4$, *i*-PrOH, reflux; **c) 1**. *m*-CPBA, 6 h, r.t., **2.** Jones reagent/acetone/DCM, 3 h, 50 °C; **d)** CH_3COONH_4, GAA, reflux. (DHEA= Dehydroepiandrosterone, ACN= Acetonitrile, DMSO= Dimethyl sulfoxide, GAA= Glacial acetic acid). Created with ChemDraw.

Considering the failure of these several attempts to synthesize 3- and 6-azasteroids and the associated time consumption, it was decided to proceed with further experiments in an attempt to synthesize new 4-azasteroids with a heterocycle fused or attached to the D-ring. The experiments performed are described in the next section.

A.3.2.2. Approaches to prepare new 4-azasteroids

Considering the unquestionable importance of heterocycles in terms of bioactivity, a remarkable effort to synthesize 4-azasteroids with a heterocycle fused/attached to the D-ring, from the derivatives already obtained was made. In this context, several attempts to prepare new steroidal arylpyrimidines, arylpyrazolines, and arylpyridones were accomplished. However, these attempts were not successful. Moreover, considering the vast information about the synthetic procedures reported by several research groups to prepare these heterocycles, initially some reactions were performed using as starting material the aryl-4-azasteroids already prepared instead of more simple substrates.[310,327,331] However, unfortunately, applying the same reactional conditions of some described studies in other steroids, in general, the reactivity observed in our azasteroids showed to be very low. Consequently, the same reactions were later repeated but using more simple substrates to understand the reasons of the failure (e.g. need of optimization of reactional conditions, lack of reactivity of the 4-azasteroidal derivatives or both). In addition, it is important to clarify that some of the following reactions were performed simultaneously.

Figure Ap 3 shows the attempt to synthesize a new steroidal arylpyrimidine (**A7**) from 16*E*-benzylidene-4-aza-androstene (**VB 4a**), by using a procedure adapted from Ke et al..[327] During the reaction, the progress was assessed through TLC, and it was observed that the substrate was consumed. However, several spots were observed in the TLC, namely due to degradation of the substrate and/or other not desired reactions. Then, the reaction was stopped, and the work up was performed. To confirm the non-formation of the desired product, a sample was analyzed by NMR, and unfortunately, it was verified that the formation of **A7** did not occur.

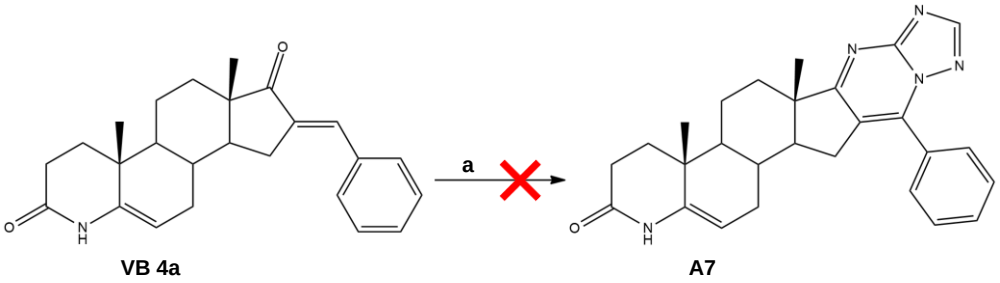

Figure Ap 3. Attempt to synthesize the arylpyrimidine **A7** from a 4-azasteroid derivative (**VB 4a**) previously prepared. Reactional conditions: **a)** 3-AT, *t*-BuOK, *t*-BuOH, reflux. (3-AT= 3-Amino-1,3,4-triazole). Created with ChemDraw.

At the same time, several attempts using different strategies to obtain steroidal arylpyrazolines were accomplished (**Figures Ap 4-7**). In the first of these studies, it was used another 4-azasteroid already prepared, 21*E*-(4'-methylbenzilydene)-4-azapregnene (**VB 7b**), as starting material (**Figure Ap 4**), and was considered the consistent information reported in the literature about the reactional conditions required for the synthesis of steroidal arylpyrazolines. In general, to synthesize this type of heterocycles several authors described a simple method: a mixture of substrate (an α,β-unsaturated ketone) and hydrazine monohydrate ($NH_2NH_2.H_2O$) in GAA under reflux for 2 h.[310,382,385] However, similar to the previous reaction, the desired product was not obtained. After 2 h of reaction, no evolution was observed, and the reaction mixture was refluxed for more 1 h, but the TLC analyses showed the same pattern: no consumption of the substrate. Consequently, the reaction was stopped, and the substrate was partially recovered to be used in a further chemical reaction.

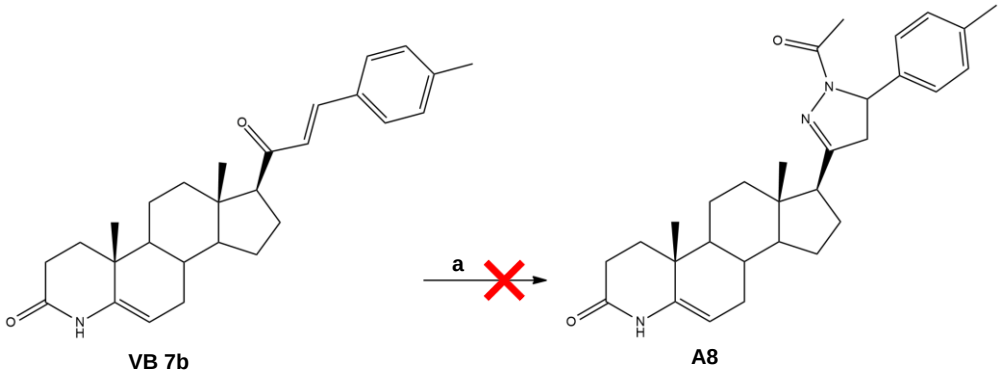

Figure Ap 4. Attempt of obtain a new arylpyrazoline from a 21*E*-arylidene-4-azasteroidal derivative (**A8**) already synthesized (**VB 7b**). Reactional conditions: **a)** $NH_2NH_2.H_2O$, GAA, reflux. (GAA= Glacial acetic acid). Created with ChemDraw.

Then it was decided to apply the same synthetic strategy, though using a simpler substrate, pregnenolone, to verify the feasibility of this type of reaction (**Figure Ap 5**). For this, prior to the synthesis of the steroidal arylpyrazoline, the substrate was prepared through an aldol condensation reaction with benzaldehyde in basic medium, in very smooth reactional conditions. As expected, compound **A9** was obtained without difficulty in an excellent yield (96 %). Then, steroid **A9** was used as substrate to synthesize **A10**, following the same protocol of the attempt above described in Figure 40. Interestingly, through the monitorization by TLC, in addition to the formation of the non-acetylated product (at C-3), the acetylated pyrazoline derivative was also formed. Consequently, an additional step of esterification of the remaining non-acetylated product was achieved using the classical reactional conditions (acetic anhydride/pyridine, r.t.) to prepare pure **A10**. This reaction was preferred over hydrolysis since it is simple and effective (producing high yields). After this procedure, the NMR spectrum of the solid obtained was analyzed and, indeed, the desired product was successfully synthesized. This was proved by the presence of the characteristic signals in the spectrum, namely the singlet of the methoxy group at 3' position at 2.00 ppm, and the singlet of proton at 4' position at 5.36 ppm, and by the absence of the signal corresponding to the vinylic proton.[310] In addition, the carbon 13 spectrum also presented signals that corroborate the formation of **A10**, such as the disappearing of the peak corresponding to the ketone at C-20, which usually presents a deviation around 200 ppm. Therefore, the synthesis of an arylpyrazoline attached to the D-ring of pregnenolone was achieved and it was possible to conclude that the substrate can be important in the observed reactivity.

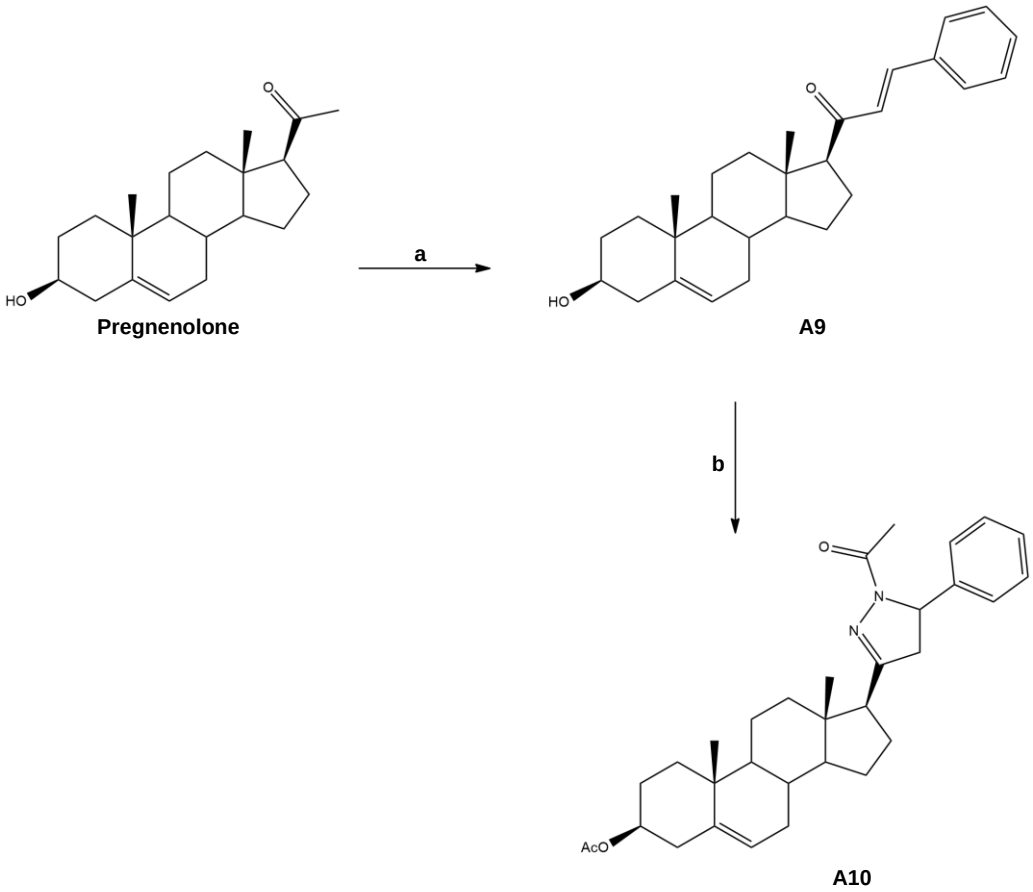

Figure Ap 5. Preparation of a steroidal arylpyrazoline from pregnenolone. Reactional conditions: **a)** benzaldehyde, aq. sol. KOH 50 %, EtOH, 24 h, r.t.; **b) 1.** $NH_2NH_2.H_2O$, GAA, 5 h, reflux; **2.** acetic anhydride, pyridine, 8 h, r.t.. (GGA= Glacial acetic acid). Created with ChemDraw.

At the same time, to explore the conditions and the feasibility of the synthetic pathway to prepare steroidal D-ring fused arylpyrazolines, a sequence of reactions from a simpler substrate, DHEA, was also performed (**Figure Ap 6**). Firstly, the 16*E*-arylidene derivative (**A11**) was successfully obtained from DHEA, as expected (η= 88 %). As previously, the next step comprised the heterocycle formation at the D-ring in similar reactional conditions ($NH_2NH_2.H_2O$, GAA, 3 h, reflux), and it was also observed, through the analysis of TLC, the formation of a mixture of non-acetylated and acetylated product at C-3 position. However, the esterification procedure was performed separately, which involved two distinct work-ups (not one-pot synthesis), to obtain **A12.2**. Acetic anhydride and DMAP in THF (5 h, r.t.) were the reactional conditions applied, which are smoother conditions contemplating the risks associated to the use of pyridine.[600] The final product, the steroidal arylpyrazoline, was obtained in a reasonable yield (57 % from **A11**) and the confirmation of its formation was also proved by NMR analysis.[384] In the proton spectrum, it is possible to verify the inexistence of the signal correspondent to the vinylic proton, and the presence of the main characteristic signals, such as the signal of 3'-CH at 5.33 ppm.

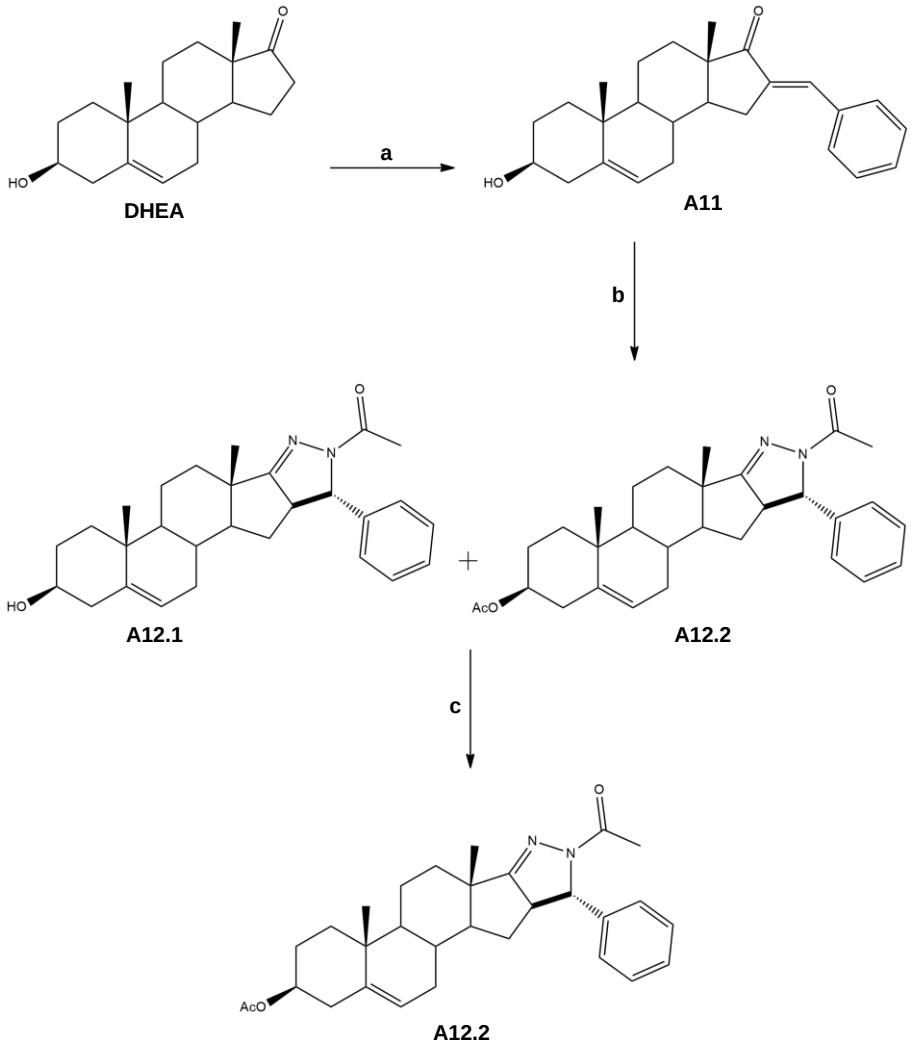

Figure Ap 6. Pathway to prepare steroidal arylpyrazolines from DHEA. Reactional conditions: **a)** benzaldehyde, aq. sol. KOH 50 %, EtOH, 24 h, r.t.; **b)** $NH_2NH_2.H_2O$, GAA, 3 h, reflux; **c)** acetic anhydride, DMAP, THF, 5 h, r.t.. (DHEA= Dehydroepiandrosterone, GAA= glacial acetic acid, DMAP= 4-Dimethylaminopyridine, THF= Tetrahydrofuran) Created with ChemDraw.

After these preliminary studies and their success, an attempt to obtain the arylpyrazoline fused to the D-ring (**A13**) of 16*E*-(4-methylbenzylidene)-4-aza-androstene (**VB 4b**) was tried (**Figure Ap 7**). The reactional conditions employed were similar to those described for the previous reactions ($NH_2NH_2{\cdot}H_2O$, GAA, reflux). The reaction was controlled through TLC, and after apparent product formation, the reaction was stopped. After the work up, the amount of product obtained was minimal (12 mg), and, consequently, the sample was analyzed through NMR even before any additional purification step to prove the formation of **A13**. Nevertheless, the analysis of the proton spectrum was hampered by the excessive number of interference peaks, indicating impurities. Therefore, a recrystallization was performed with MeOH, but as expected the quantity obtained was very low for further NMR analysis. Therefore, it was considered that this synthetic

procedure is of low practical interest particularly due to the several synthetic steps until obtaining compound **VB 4b** or other aryl-4-azasteroidal derivative. This procedure comprises a relatively long pathway with several steps, which involves a high quantity of starting material and some steps with low yields. Consequently, the product loss during the procedure is significative, becoming unproductive and with a high associated time expense to obtain a reasonable quantity of product.

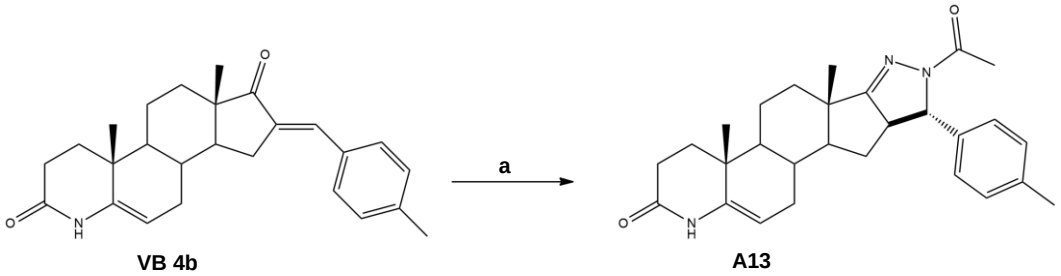

Figure Ap 7. Synthesis of D-ring fused arylpyrazoline-4-aza-androstene derivative from a 16*E*-aryl-4-azasteroid (**VB 4b**) already synthesized. Reactional conditions: **a)** $NH_2NH_2 \cdot H_2O$, GAA, 3 h, reflux. (GAA= Glacial acetic acid). Created with ChemDraw.

Meantime, another attempt to synthesize steroidal arylpyrimidines attached to the D-ring was accomplished (**Figure Ap 8**). **A9,** previously prepared by an aldol-condensation already described, was used as starting material. After 2 days under reflux and without evident evolution according to TLC analysis, the reaction was stopped. The solid obtained after work up was analyzed by NMR, and it was detected the presence of a mixture of different steroids, being observed the duplication of the signals of the methylene groups (18- and 19-CH_3), and the majority of signals corresponded to the substrate. Additionally, the other signals detected in the spectrum did not allow to understand if the minor compound was the desired product. Even considering the possibility of the minor product being **A14**, a further step of purification to isolate **A14**, namely a chromatographic column, was not practicable due to the low quantity of product obtained.

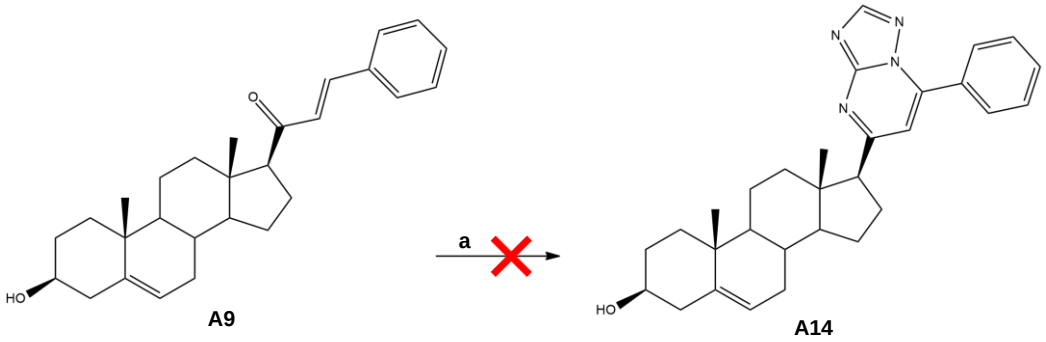

Figure Ap 8. Attempt of synthesis of steroidal arylpyrimidines attached to the D-ring from a 21*E*-arylideneandrostene derivative (**A9**). Reactional conditions: **a)** 3-AT, *t*-BuOK, *t*-BuOH, reflux. (3-AT= 3-Amino-1,3,4-triazole). Created with ChemDraw.

After all the attempts to prepare steroidal arylpyrimidines and arylpyrazolines, a new approach to obtain 4-azasteroids with heterocycles fused/attached to the D-ring was tried. The aim of this approach was to synthesize new steroidal arylpyridones and involved a preliminary test in a simpler substrate (androstenedione) (**Figure Ap 9**) and, posteriorly, reactions using arylidene-4-azasteroidal derivatives as starting material (**Figure Ap 10**).

Relative to the preliminary test, firstly, androstenedione was prepared from testosterone by an oxidation with PCC to form a ketone at C-17, able to react in the next synthetic step. Then, an aldol-condensation reaction was successfully performed to synthesize 16*E*-benzylidene-androstenedione (**A15**) in an excellent yield (98 %). In order to synthesize the steroidal fused D-ring arylpyridone (**A16**), based on the procedure described by Amr et al., a solution of **A15**, ammonium acetate and cyanoacetate in EtOH were refluxed for 12 h.[305,601] After control through TLC, it was observed that, apparently, the substrate was totally consumed and new spot appeared, as desired. After the work up, a semi-solid impure crude was obtained, and consequently, a recrystallization procedure with MeOH/AE was achieved to isolate the product. Nevertheless, the amount of product resultant was insufficient to analyze through NMR.

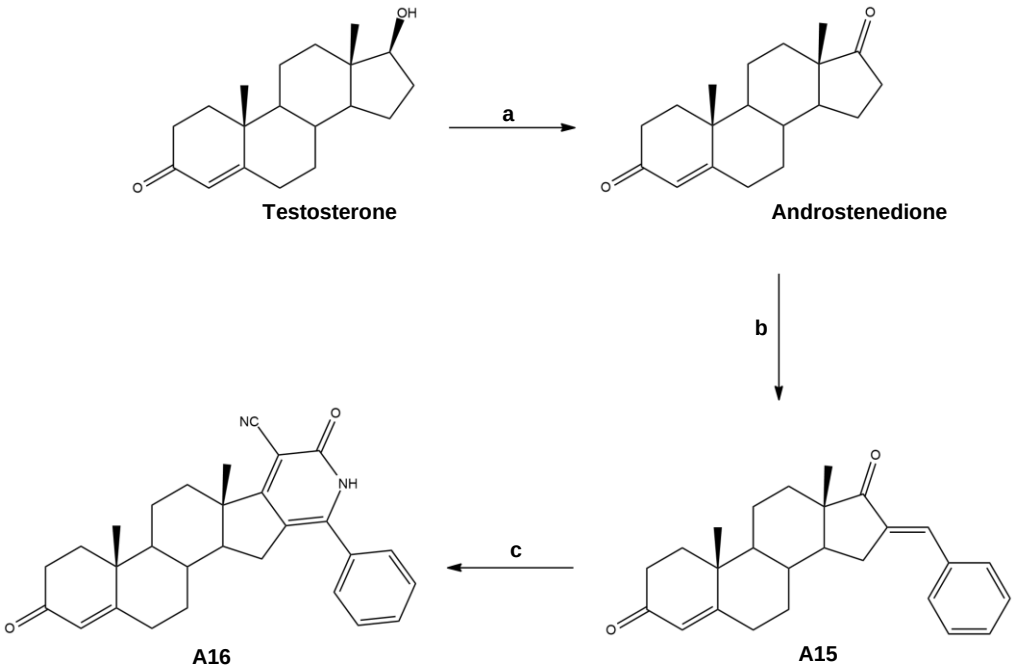

Figure Ap 9. Synthetic pathway to prepare steroidal arylpyridones from testosterone. Reactional conditions: **a)** PCC, DCM, 3 h, r.t.; **b**) benzaldehyde, aq. sol. KOH 50 %, EtOH, 2 days, r.t.; **c)** ethyl cyanoacetate, ammonium acetate, EtOH, 24 h, reflux. (PCC= Pyridinium chlorochromate, DCM= Dichloromethane). Created with ChemDraw.

Despite uncertainty regarding the success of the preparation of **A16**, an effort to synthesize several new arylpyridones (**A17-A19**) from 4-azasteroids was made (**Figure Ap 10**). Three distinct attempts using as starting material **VB 4a**, **VB 4b**, and **VB 7a** were accomplished, however without favorable results. In general, the monitoring of these reactions by TLC revealed to be inconclusive, remaining unclear the formation of the desired products. The reactional mixtures were refluxed for 1 to 6 days, which presents a higher period than it was expected, hoping to observe some visible progress in the TLC monitoring. However, no evolution was noticed, and the reactions were stopped. Thus, the work up was performed to isolate the steroids to analyze through NMR to confirm the absence of the desired products. Even after several optimizations and modifications to the original protocol, such as the increment of the quantity of reagents, the lack of reactivity of these 4-azasteroids is evident.

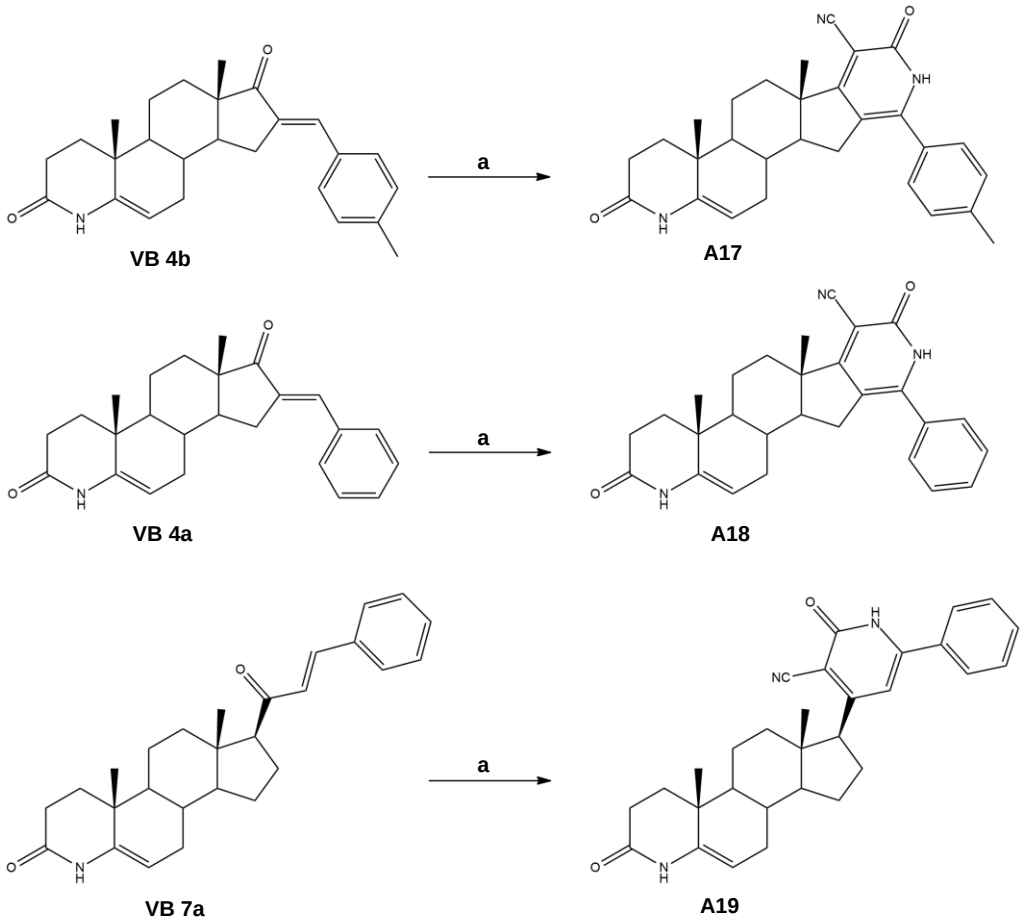

Figure Ap 10. Attempts of preparation of new steroidal fused/attached D-ring arylpyridones from different 4-azasteroids previously synthesized. Reactional conditions: **a)** ethyl cyanoacetate, ammonium acetate, EtOH, 1-6 days, reflux. Created with ChemDraw.

In a last effort to obtain heterocycles fused to the steroidal D-ring and this time without the use of arylidenesteroids, an approach comprising a C-16 bromination followed by the formation of D-ring fused with 2-amino-tiazole was applied. This synthetic pathway was based on the method described by Zhang et al., and the attempts performed at the present study are shown in **Figure Ap 11**.[602] Initially, this strategy was applied using DHEA as starting material to understand its feasibility, and then it was applied to 4-aza-androstene **VB 3**. Indeed, the attempt using DHEA occurred as reported by the authors, without relevant difficulties, affording **A20**, the brominated intermediary product, in an excellent yield (92 %), and posteriorly **A21** in an acceptable yield (55 %). Then, using as substrate **VB 3**, a 4-azasteroid previously synthesized, the bromination procedure was employed, and the reaction occurred successfully, affording **A22** in an excellent yield (97 %). Next, expecting to obtain good results and synthesize **A23**, a solution of **A22**, thiourea and triethylamine (NEt_3) in EtOH was refluxed, and after 2 days without

evidence of significative progression (TLC control), the reaction was interrupted. As expected, after work-up, the proton spectrum proved that the substrate did not react.

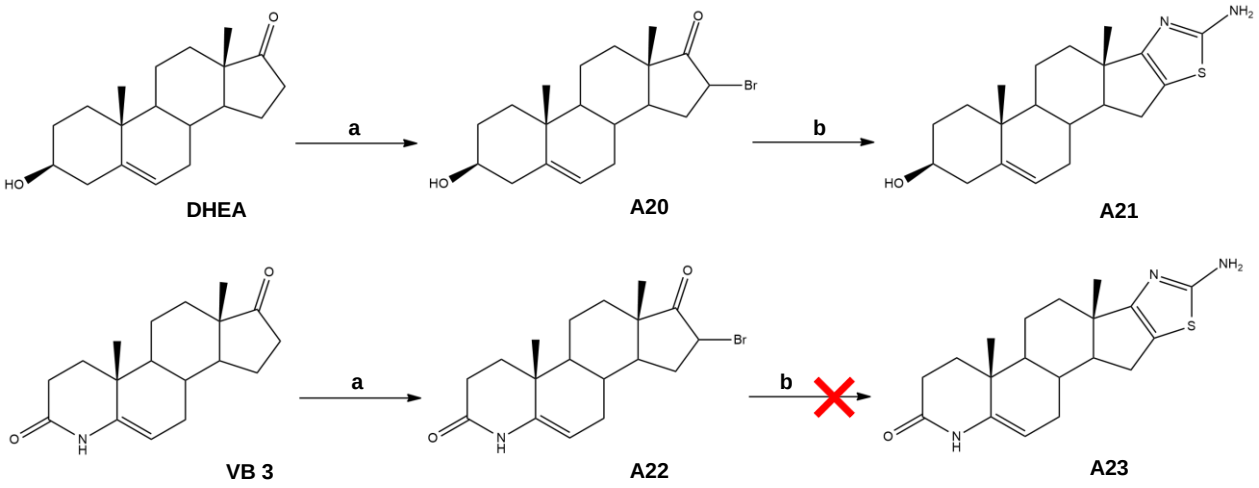

Figure Ap 11. Attempt to prepare steroidal derivatives with a heterocycle fused to the D-ring from dehydroepiandrosterone (DHEA) and from the 4-aza-androstene **VB 3**. Reactional conditions: **a)** $CuBr_2$ (II), MeOH, 20 h, reflux; **b)** thiourea, NEt_3, EtOH, 2 days, reflux. Created with ChemDraw.

In summary, the preparation of new series of azasteroids, principally with heterocycles fused or attached to the D-ring revealed to be unfeasible in the present conditions. Despite the numerous reactions reporting the synthesis of steroidal arylpyrazolines, arylpyrimidines, arylpyridones and D-ring fused 2-amino-thiazoles, and the effort to successfully apply the same protocols with the required adaptations to the present project, the 4-azasteroids prepared seemed to be unreactive under the same or similar conditions. This was proved by applying the same reactional conditions with more simple substrates. In these cases, reactions occurred successfully, although some adaptations were made in relation to the original protocols. Additionally, the use of small quantities of substrate for test the conditions may also influenced the reactions progression. However, considering the relatively extensive synthetic pathway to prepare aryl-4-azasteroids, it was considered not viable the use of higher quantities. Considering this results, new approaches to synthesize novel molecules in the context of this project were studied.

A.3.3. Experimental section

A.3.3.1. General remarks

This information was already provided at **Chapter III**, in **section 3.3.1.**, page 111.

A.3.3.2. Chemical synthesis: procedures of the attempts

Procedures of attempts to prepare 3-aza-androstenes

*Synthesis of **A1***

A solution of testosterone (250 mg, 0.8 mmol), hydroxylamine hydrochloride ($NH_2OH.HCl$) (250 mg), and pyridine (5 mL) was refluxed for 6 h.

The reaction mixture was poured into the ice-cold water (50 mL) along with stirring. The precipitated material was filtered under vacuum, washed with cold water repeatedly to remove pyridine and dried to yield **A1**, without further purification as a beige solid (216 mg, 89 %). Considering the assurance of the obtention of the desired product, it was decided to proceed immediately to the next reaction without performing an NMR analysis.

*Attempt of synthesis of **A2***

A solution of thionyl chloride ($SOCl_2$) (75 µL) in dioxane (175 µL) was added dropwise to a stirred solution of **A1** (91 mg, 3 mmol) in toluene (6.0 mL) and cooled to 15 °C. Then, the reaction mixture was cooled down and kept at 20 °C for 17 min. After this period, the TLC showed no evolution, and the reactional mixture was kept at 20 °C for more 1 h under inert atmosphere (N_2). After 1 h TLC showed the same result, and then, in a last effort, an equal portion of reagents was added to the mixture.

However, 2 h later the result remained the same, and then it was added 5.0 mL of ice-cold water to the solution, and it was alkalized with ammonia and extracted with chloroform (3×20.0 mL). The organic layer was washed with water, dried with anhydrous sodium sulfate (Na_2SO_4), and the solvent was removed under reduced pressure to obtain a crude residue.

Procedures of attempts to prepare 6-azasteroids

*Synthesis of **A3***

To a solution of DHEA acetate (661 mg, 2 mmol) in ACN (16 mL), $NaClO_2$ (271 mg) and NHPI (33 mg) were added. Then, water (8 mL) was added dropwise, and the solution was heated to 50 °C for 6 h.

Once completed (monitored by TLC), the reactional mixture was stirred with sodium sulfite (Na_2SO_3) during 3 h (r.t.). Then, the product was extracted with ethyl acetate (AE) (2×100 mL), and the organic layer was washed with hydrochloric acid (HCl) 10 % (50 mL), with a saturated solution of $NaHCO_3$ (50 mL) and 25 mL of water. The organic phase was dried with anhydrous Na_2SO_4 and the AE was removed under reduced pressure to yield **A3**. White solid (520 mg, 75 %), ^1H NMR ($CDCl_3$, 400 MHz) δ: 0.83

(3H, s, 18-CH_3), 1.17 (3H, s, 19-CH_3), 1.99 (3H, s, 3-COOCH3), 4.66 (1H, m, 3-CH), 5.69 (1H, s, 6-CH).[562]

*Attempt of synthesis of **A4***

To a solution of **A3** (172 mg, 0.5 mmol) in *i*-PrOH (8 mL) was added a heated solution of Na_2CO_3 (85 mg) in water (1.5 mL). The mixture was brought to reflux and a solution of $NaIO_4$ (895 mg) and $KMnO_4$ (12 mg) in warm water (3 mL) was added dropwise over a period of 1 h and reflux was maintained for more 20 h. The reaction was controlled periodically by TLC, until the completion or a state without alterations.

Then, the reaction was cooled to 30 °C and the solids were removed by filtration using celite and washed with water. The filtrate was concentrated under reduced pressure to remove the organic solvent. The aqueous residue was cooled and acidified with concentrated hydrochloric acid until precipitate formation. Then, the product was extracted with ethyl acetate (3×50 mL), washed with brine, and dried with anhydrous Na_2SO_4. After removal of the solvent under reduced pressure. The solid obtained was analyzed through NMR and the spectrum revealed that **A4** was not successfully synthesized.

*Synthesis of **A5***

Step 1) To a solution of pregnenolone acetate (179 mg, 0.5 mmol) in DCM (8 mL), *m*-CPBA (135 mg) was added, and the reactional mixture was stirred for 6 h at r.t (controlled by TLC).

After the reaction is complete, DCM (40 mL) was added, and the organic layer was washed with a saturated solution of Na_2CO_3 (30 mL), water (30 mL), and 30 mL of brine. Then, the organic phase was dried with anhydrous Na_2SO_4, and DCM was removed under reduced pressure to yield the intermediate product (180 mg, 96 %).

Step 2) The product obtained previously (180 mg, 0.48 mmol) was dissolved in acetone/DCM (6 mL/4 mL), and the Jones reagent (114 mg chromium trioxide, 0.5 mL water, 96 µL sulfuric acid) was added. The reactional mixture was heated to 50 °C during 3 h.

After TLC analysis showed the completion of the reaction, the mixture was cooled down and *i*-PrOH was added until mixture turned blue (≈ 15 mL). The resultant residues were eliminated by filtration, and the *i*-PrOH was removed under reduce pressure. Then, the solid was dissolved in ethyl ether (40 mL) and washed with oxalic acid (15 mL) and brine (15 mL). The organic phase was dried with Na_2SO_4, and ethyl ether was removed under reduced pressure. To purify the product obtained, a chromatographic column with 1:1 PE/AE was performed to afford **A5**. Pallid yellow solid (51 mg, 26 %), ^{1}H NMR ($CDCl_3$,

400 MHz) δ: 0.61 (3H, s, 18-CH_3), 1.09 (3H, s, 19-CH_3), 1.99 (3H, s, 21-CH_3), 2.04 (3H, s, 3-$COOCH_3$), 4.89 (1H, m, 3-CH).[594]

*Attempt of synthesis of **A6***

The substrate **A5** (51 mg, 0.125 mmol) and CH_3COONH_4 (60 mg) were dissolved in GAA (5 mL) 24 h, and mixture was heated to the reflux temperature. The reaction was controlled through TLC and after 24 h the reaction was stopped, given the poor extension of product formation.

After cooling down, water was added to the solution and the steroid was extracted with DCM (3×50 mL). Then, the organic layer was washed with brine (3×20 mL), dried with anhydrous Na_2SO_4, and the solvent was removed under reduced pressure. After NMR analysis, as expected, the desired product was not successfully prepared.

Procedures of attempts to prepare new 4-azasteroids with heterocycles fused or attached to the D-ring

*Attempt of synthesis of **A7***

A mixture of the 4-azasteroid **VB 4a** previously prepared (49 mg, 0.125 mmol), 3-AT (25 mg), and potassium *t*-butoxide (*t*-BuOK) (28 mg) was dissolved in *tert*-butyl alcohol (*t*-BuOH) (20 mL). The reactional mixture was refluxed for 2 days, without signals of the product formation (monitored by TLC).

After cooling down, ice-cold water was poured into the solution to precipitate the steroid. The steroid was collected and washed with water through filtration under reduced precure. To confirm the failure of the reaction, the solid was analyzed by NMR.

*Attempt of synthesis of **A8***

A mixture of **VB 7b** (60 mg, 0.145 mm), $NH_2NH_2{\cdot}H_2O$ (20 µL) and GAA (3 mL) was brough to reflux during 3 h. The reaction was controlled by TLC, and it was not observed any progress after all the reactional period.

After cooling down, ice-cold water (75 mL) was added to precipitate the steroid, followed by the filtration of the solid under reduced pressure, and the solid was let dry to partially recover the substrate.

*Synthesis of **A9***

To a solution of pregnenolone (1.08 g, 3 mmol) in ethanol (EtOH) (45 mL), benzaldehyde (370 µL) and an aq. solution of potassium hydroxide 50 % (KOH) (1.5 mL) were added. The reactional mixture was stirred during 24 h at r.t. and its progress was monitored by TLC.

Ice-cold water was added after the end of the reaction, and the solid was filtered and washed with cold water. Then, the collected solid was air dried to afford **A9**. Yellow solid (1.04 g, 96 %), ^{1}H NMR ($CDCl_3$, 400 MHz) δ: 0.62 (3H, s, 18-CH_3), 0.97 (3H, s, 19-CH_3), 3.51 (1H, m, 3-CH), 5.33 (1H, s, 6-CH); 6.76 (1H, d, *J*= 15.71 Hz, H_{vin}), 7.36 (3H, m, H_{ar}), 7.52 (3H, m, H_{ar}).[603]

*Synthesis of **A10***

A9 (202 mg, 0.5 mmol) and $NH_2NH_2{\cdot}H_2O$ (243 µL) were dissolved in GAA (10 mL), and the mixture was refluxing for 5 h.

After reaction mixture has cooled, ice-cold water (≈ 100 mL) was added and the precipitated solid was filtrated, washed, and collected. After dried, to this solid was added pyridine (2.5 mL) and acetic anhydride (2.5 mL). This solution was stirred at r.t. for 8 h. Then, water was added, the product was washed and filtrated, and dried to yield **A10**. Pallid yellow solid (203 mg, 81 %), ^{1}H NMR ($CDCl_3$, 400 MHz) δ (ppm): 0.64 (3H, s, 18-CH_3), 0.98 (s, 3H, 19-CH_3), 2.00 (s, 3H, 3'-$NCOCH_3$), 2.30 (s, 3H, 3-$COOCH_3$), 3.31 (1H, m, 3-CH), 4.57 (1H, m, 6-CH), 5.36 (1H, s, 4'-CH), 7.12 (2H, d, *J*= 7.03 Hz, H_{ar}), 7.20 (1H, t, *J*= 7.03 Hz, H_{ar}), 7.28 (2H, d, *J*= 7.03 Hz, H_{ar}). ^{13}C ($CDCl_3$, 101 MHz) δ (ppm): 13.35, 19.26, 20.85, 21.37, 21.81, 24.31, 24.51, 27.66, 31.66, 31.92, 36.55, 36.94, 38.01, 38.36, 43.82, 46.19, 49.91, 51.65, 56.22, 59.05, 73.78, 122.25, 125.26, 127.32, 128.78, 139.63, 142.23, 159.20, 168.61, 170.51.[603]

*Synthesis of **A11***

To DHEA (864 mg, 3 mmol) dissolved in EtOH (65 mL) and aq. solution of KOH 50% (1.5 mL), benzaldehyde (400 µL) was added and the mixture stirred for 24 h r.t..

After the completion of the reaction (monitored by TLC), the reactional mixture was poured into ice-cold water. The precipitate thus obtained was filtered, washed with water, and air dried to afford **A11**. Beige solid (989 mg, 88 %), ^{1}H NMR ($CDCl_3$, 400 MHz) δ: 0.91 (3H, s, 18-CH_3), 1.06 (3H, s, 19-CH_3), 3.46 (1H, m, 3-CH), 5.33 (1H, s, 6-CH); 7.33 (4H, m, H_{ar}+H_{vin}), 7.47 (2H, d, *J*= 7.61 Hz, H_{ar}).[305]

*Synthesis of **A12.2***

A solution of **A11** (188 mg, 0.5 mmol) and $NH_2NH_2{\cdot}H_2O$ (250 µL) in GAA (10 mL) was refluxed for 3 h and supervised by TLC.

The reaction mixture was poured into the ice-cold water (100 mL). Then, the precipitated material was filtrated under vacuum, washed and air dried to yield a mixture of **A12.1**+**A12.2** (non-acetylated product + acetylated product) (214 mg). To the mixture obtained, **A12.1+A12.2** (214 mg), dissolved in tetrahydrofuran (THF) (5 mL), acetic

anhydride (85 μL) and 4-(dimethylamino)-pyridine (DMAP) (30 mg) were added. The reactional mixture was stirred at r.t. during 5 h (the progress was controlled by TLC analysis). Then, the product was extracted with DCM (50 mL) and washed with HCl 10% (10 mL), with a sat. solution of $NaHCO_3$ (10 mL) and water (15 mL). The organic layer was dried with anhydrous Na_2SO_4, filtered and the solvent was removed under reduced pressure to only afford **A12.2**. Yellow solid (135 mg, 57 %), ^{1}H NMR ($CDCl_3$, 400 MHz) δ: 0.56 (3H, s, 18-CH_3), 0.99 (3H, s, 19-CH_3), 2.00 (3H, s, 2'-$NCOCH_3$), 2.36 (3H, s, 3-COOCH3), 3.94 (1H, m, 3-CH), 4.47 (1H, dd, *J*= 11.8 Hz, 6-CH), 4.57 (1H, m, 3-CH), 5.33 (1H, m, 3'-CH); 7.37 (3H, m, H_{ar}), 7.71 (2H, m, H_{ar}). ^{13}C ($CDCl_3$, 101 MHz) δ: 12.31, 19.30, 20.89, 21.44, 21.64, 27.64, 31.07, 31.62, 32.21, 36.62, 36.94, 38.07, 38.78, 45.73, 47.72, 49.44, 49.62, 54.73, 72.14, 73.81, 121.83, 126.92, 128.67, 129.92, 131.12, 139.75, 140.03, 157.47, 169.38, 170.54.[385]

*Synthesis of **A13***

VB 4b (80 mg, 0.2 mmol) and $NH_2NH_2{\cdot}H_2O$ (156 μL) in GAA (4 mL) were refluxed during 3 h and the reaction was monitored through TLC.

After terminated, the mixture was let cooling down and ice-cold water (50 mL) was added. Then, the solid was collected by filtration, washed, and dried. Since the quantity of product obtained was very low and it was analyzed through NMR, before any additional purification step, in the attempt to verify the formation of **A13**. However, it was not possible considering the high number of interference peaks in the NMR spectrum. Consequently, a recrystallization procedure was performed with MeOH, but as expected the quantity obtained was very low for further analysis.

*Attempt of synthesis of **A14***

A solution of **A9** (202 mg, 0.5 mmol), 3-AT (124 mg) and *t*-BuOK (167 mg) in *t*-BuOH (5 mL) was refluxed for 2 days (monitored by TLC).

After no significative evolution of the reaction, the solvent was removed under reduced pressure. Then, DCM was added to dissolve the product and solids remaining in suspension were eliminated through a filtration under vacuum. The DCM was also removed under reduced pressure and the resultant solid was dried. After NMR spectrum analysis it was observed that the desired product was not successfully obtained in a pretended extension.

Synthesis of androst-5-ene-3,17-dione (Androstenedione)

Testosterone (1.44 g, 5 mmol) and pyridinium chlorochromate (PCC) (1.80 g) were dissolved in DCM (225 mL), and the reactional mixture was stirred for 3 h (r.t.).

After the consumption of substrate (controlled by TLC), the solution was filtered with celite under vacuum to remove the solid residues. Then, the DCM was removed under reduced pressure and the product was purified through chromatographic column with 3:1 AE/EP to afford androstenedione. White solid (1.38 g, 97 %), ^{1}H NMR ($CDCl_3$, 400 MHz) δ: 0.85 (3H, s, 18-CH_3), 1.15 (3H, s, 19-CH_3), 5.68 (1H, s, 4-CH).[326]

*Synthesis of **A15***

To androstenedione (215 mg, 0.75 mmol) dissolved in EtOH (11.25 mL) and aq. solution of KOH 50% (375 µL), benzaldehyde (188 µL) was added and the mixture stirred for 2 days r.t..

After the completion of the reaction (monitored by TLC), the reactional mixture was poured into ice-cold water. The precipitate thus obtained was filtered, washed with water, and airdried to afford **A15**. Beige solid (275 mg, 98 %), ^{1}H NMR ($CDCl_3$, 400 MHz) δ: 0.98 (3H, s, 18-CH_3), 1.21 (3H, s, 19-CH_3), 5.73 (1H, s, 4-CH), 7.39 (3H, m, H_{ar}+H_{vin}); 7.51 (2H, d, *J*= 7.31 Hz, H_{ar}).[335]

*Synthesis of **A16***

A solution of **A15** (112 mg, 0.3 mmol), ammonium acetate (195 mg), ethyl cyanoacetate (35 µL) in EtOH (8 mL) was refluxed for 12 h and controlled through TLC analysis.

After the completion of the reaction, the EtOH was removed under reduced pressure and water was added (20 mL). The product was extracted with AE (3×35 mL) and the organic layer was washed with HCl 10 % (30 mL) and brine (30 mL). The organic phase was dried with anhydrous Na_2SO_4, filtered and the AE was evaporated through reduced pressure. The crude obtained were recrystallized with MeOH/AE to afford **A16**. However, the quantity obtained was insufficient to acquire an NMR spectrum.

*General procedure of the attempts to synthesize fused/attached D-ring arylpyridones from different arylidene-4-azasteroids (**A17-A19**)*

A mixture of 0.25 mmol of a 4-azasteroid (**VB 4a**, **VB 4b**, and **VB 7a**), ethyl cyanoacetate (30 µL), ammonium acetate (163 mg) in EtOH (6 mL) was reflux for 1-6 days.

The reactions were monitored by TLC, and after completion EtOH was removed under reduced pressure. Then it was added water, and the product was extracted multiple times with AE (3×30 mL), washed with HCl 10 % (25 mL) and brine (25 mL), and dried with anhydrous with Na_2SO_4. Lastly, the solvent was removed under reduced pressure, and after dried, without further purification step, the solids obtained were analyzed through NMR, and it was concluded that the desired products were not obtained.

*Synthesis of **A20***

A solution of DHEA (144 mg, 0.5 mmol) and $CuBr_2$ (223 mg) in MeOH (5 mL) was refluxed for 20 h, and the reaction was controlled by TLC.

After the consumption of the substrate, MeOH was removed under reduced pressure, and the solid was stirred in a mixture of DCM (50 mL)/water (25 mL) for 20 min. Then, DCM (50 mL) was added, and the product was extracted, washed with brine (75 mL), and dried with anhydrous with Na_2SO_4. The solvent was removed under reduced pressure to afford **A20** (169 mg, 92 %). Considering the assurance of the obtention of the desired product, the NMR analysis was not performed, and it was decided to proceed to the next reactional step.

*Synthesis of **A21***

A mixture of **A20** (92 mg, 0.25 mmol), thiourea (91 mg), NEt_3 (125 µL) in EtOH (5 mL) was refluxed for 2 days (controlled through TLC).

After precipitation of a yellow solid, the reactional mixture was let cooling down and was placed in a refrigerator to force the precipitation. Then, the solid was filtered under vacuum and washed with ice-cold water to afford **A21**. Yellow solid (47 mg, 55 %), ^{1}H NMR (DMSO-d_6, 400 MHz): 0.99 (3H, s, 18-CH_3), 1.05 (3H, s, 19-CH_3), 3.44 (1H, m, 3-CH), 5.29 (1H, s, 6-CH). ^{13}C (DMSO-d_6, 101 MHz): 17.09, 19.03, 19.55, 20.60, 27.75, 30.49, 31.19, 31.90, 34.68, 36.90, 42.33, 50.80, 56.49, 59.49, 70.46, 117.07, 120.07, 142.13, 165.67, 171.98.[602]

*Synthesis of **A22***

A solution of **VB 3** (432 mg, 1.5 mmol) and $CuBr_2$ (677 mg) in MeOH (18 mL) was refluxed for 18 h (monitored by TLC).

After the completion of the reaction, MeOH was removed under reduced pressure, and the solid was stirred in a mixture of DCM (150 mL)/water (100 mL) for 20 min. Then, DCM 1(50 mL) was added, and the product was extracted, washed with brine (90 mL), and dried with anhydrous with Na_2SO_4. The solvent was removed under reduced pressure to yield **A22** (580 mg, 97 %). ^{1}H NMR (DMSO-d_6, 400 MHz): 0.88 (3H, s, 18-CH_3), 1.13 (3H, s, 19-CH_3), 5.09 (1H, m, 16-CH), 5.30 (1H, s, 6-CH); 7.50 (1H, s, 4-NH). ^{13}C (DMSO-d_6, 101 MHz): 13.56, 18.78, 20.21, 21.63, 28.31, 30.93, 31.44, 33.31, 35.62, 37.50, 38.84, 47.49, 47.65, 51.02, 99.59, 136.86, 168.96, 219.63.

*Attempt to synthesize **A23***

A mixture of **A22** (92 mg, 0.25 mmol), thiourea (91 mg), NEt_3 (125 µL) in EtOH (5 mL) was refluxed for 2 days and the reaction was controlled through TLC.

After precipitation of a yellow solid, the reactional mixture was let cooling down and was placed in a refrigerator to force the precipitation. However, the quantity of precipitate was insufficient to apply the filtration method. Then, the steroid was extracted with DCM (3×25 mL) and washed with water (30 mL). The organic layer was dried with anhydrous Na_2SO_4, and the solvent was removed under reduced pressure. Despite the effort, **A23** was not successfully obtained.

Appendix 4

This appendix presents the data relative to the MTT screening assay results of compounds described at **Chapters III** and **IV** at 10 and 50 µM, after 72 h of exposure, against non-tumoral – PNT1A and NHDF (**Table Ap 5**), and tumoral cells – LNCaP, PC-3, and MCF-7 (**Table Ap 6**). In these chapters data are shown in graphical format, thus the precise average % of negative control±SD is presented in the following tables.

Table Ap 5. *In vitro* antiproliferative activities of the tested compounds: **VB 9a-m**, **VB 10a-f**, **VB 11a-f**, and 5-fluorouracil (5-FU) against non-tumoral cell lines (PNT1A and NHDF), after 72 h of exposure. MTT screening results at 10 and 50 µM (data presented as average % of negative control±SD and are representative of at least two independent experiments).

Compound	PNT1A		NHDF	
	10 µM	**50 µM**	**10 µM**	**50 µM**
VB 9a	86.3±7.3	38.9±14.6	85.8±9.6	22.7±3.0
VB 9b	87.8±10.9	74.8±7.9	83.7±9.3	45.3±7.1
VB 9c	76.7±11.6	71.9±6.5	64.1±4.8	32.7±5.1
VB 9d	74.2±15.0	29.3±8.1	69.8±5.3	24.5±5.7
VB 9e	68.2±9.4	1.2±1.2	71.2±8.3	5.8±2.0
VB 9f	83.3±4.9	64.0±4.1	79.8±5.7	46.6±6.9
VB 9g	83.9±4.0	37.5±4.7	84.0±5.7	22.7±3.4
VB 9h	67.7±9.2	0.2±1.3	96.3±6.6	8.9±3.7
VB 9i	73.5±6.6	10.6±9.9	79.5±4.4	29.0±3.1
VB 9j	83.5±9.1	33.4±3.8	84.4±8.3	36.7±4.0
VB 9k	69.5±7.5	4.9±2.3	66.8±10.4	3.5±2.4
VB 9l	87.6±6.0	20.0±6.8	66.5±5.5	19.0±2.3
VB 9m	89.7±6.0	35.8±3.4	67.1±5.0	29.4±4.1
VB 10a	76.3±2.7	67.0±8.1	101.9±9.9	97.9±6.7
VB 10b	87.6±4.8	6.5±3.7	106.0±6.8	4.6±4.3
VB 10c	69.8±11.8	9.9±3.3	96.2±3.3	76.7±11.6
VB 10d	74.2±15.0	74.2±15.0	100.5±6.9	96.9±13.3
VB 10e	61.7±3.8	59.8±6.0	97.3±7.5	82.9±1.7
VB 10f	76.6±9.7	56.2±5.1	93.4±5.6	75.2±7.5
VB 11a	66.0±10.6	50.6±5.5	68.0±7.3	6.5±3.2
VB 11b	80.7±6.8	11.6±9.3	91.5±6.4	11.6±4.2
VB 11c	74.3±2.2	50.6±5.5	90.9±6.6	10.9±6.9
VB 11d	76.1±3.5	46.7±1.9	77.5±13.6	42.5±2.3
VB 11e	66.6±9.0	50.6±5.5	70.2±3.5	2.1±2.0
VB 11f	75.3±7.7	16.0±1.8	109.2±7.2	7.1±5.6
5-FU	51.2±10.5	42.8±3.3	46.1±0.5	32.4±2.8

Table Ap 6. *In vitro* antiproliferative activities of the tested compounds: **VB 9a-m**, **VB 10a-f**, **VB 11a-f**, and 5-fluorouracil (5-FU) against tumoral cell lines (LNCaP, PC-3, and MCF-7), after 72 h of exposure. MTT screening results at 10 and 50 μM (data presented as average % of negative control±SD and are representative of at least two independent experiments).

Compound	LNCaP		PC-3		MCF-7	
	10 μM	**50 μM**	**10 μM**	**50 μM**	**10 μM**	**50 μM**
VB 9a	104.5±11.3	57.7±13.7	104.2±2.9	12.0±3.1	88.2±7.3	22.7±5.8
VB 9b	105.0±10.9	69.3±9.5	112.0±3.8	26.2±17.4	84.8±6.6	56.4±2.5
VB 9c	106.0±8.6	61.2±12.6	110.9±6.1	101.4±11.9	78.8±11.2	37.2±9.8
VB 9d	99.1±6.4	55.5±10.8	101.1±10.2	21.1±5.0	92.1±8.4	59.9±9.5
VB 9e	89.2±5.1	3.6±3.8	74.5±9.7	8.2±2.4	30.2±2.0	0.1±0.3
VB 9f	103.6±12.0	63.7±11.8	99.8±5.3	87.5±4.5	71.5±10.7	67.2±11.8
VB 9g	91.1±11.9	52.7±13.0	96.0±5.5	72.1±8.9	86.1±8.6	51.7±6.7
VB 9h	98.2±11.6	6.3±6.3	91.6±8.0	9.4±2.3	80.8±11.7	0.2±0.3
VB 9i	103.8±8.7	13.6±9.6	98.0±7.6	7.6±2.0	87.1±14.0	3.4±0.6
VB 9j	103.0±17.9	70.5±11.2	95.3±8.8	34.6±6.4	87.9±7.4	63.9±8.5
VB 9k	103.3±10.5	19.4±13.4	80.0±4.9	6.9±2.2	82.2±6.5	7.0±3.4
VB 9l	90.4±3.9	4.6±4.8	92.8±3.0	6.5±2.4	66.3±6.3	29.9±8.4
VB 9m	99.8±20.8	26.4±9.8	97.6±5.5	35.2±4.2	65.3±1.3	23.6±10.6
VB 10a	73.8±14.4	39.5±3.7	94.4±9.8	34.9±12.3	82.3±5.0	60.0±8.5
VB 10b	78.8±6.4	1.6±2.8	72.7±7.5	4.9±2.9	73.5±13.0	0.9±1.3
VB 10c	75.9±10.4	1.7±3.1	34.7±1.4	5.0±4.4	66.5±6.3	1.7±1.7
VB 10d	85.6±8.3	57.2±5.2	82.9±5.5	50.8±10.1	74.0±6.2	51.0±1.5
VB 10e	91.5±10.9	23.6±4.3	62.3±9.1	10.0±3.5	68.6±7.3	21.7±8.3
VB 10f	93.6±13.1	32.7±5.9	74.6±4.2	11.1±0.9	71.9±16.1	57.6±8.6
VB 11a	66.4±4.2	28.4±4.8	99.0±15.4	38.4±6.2	74.5±10.0	64.8±6.0
VB 11b	42.1±6.3	1.6±5.2	73.3±6.4	34.9±5.2	69.5±12.3	18.3±3.1
VB 11c	37.4±8.3	1.1±4.2	44.3±5.7	21.6±9.7	53.0±13.4	23.9±12.5
VB 11d	74.1±7.4	30.8±4.5	85.6±11.6	66.1±4.0	92.6±9.2	72.2±7.8
VB 11e	61.7±4.4	0.5±3.7	77.0±11.0	9.5±3.3	72.4±12.5	26.5±5.7
VB 11f	93.0±2.4	12.5±2.6	93.2±5.6	13.8±3.3	64.0±11.2	15.9±9.1
5-FU	65.2±6.0	27.2±5.5	72.4±4.0	37.9±4.5	51.5±12.8	39.2±10.8

Appendix 5

The most representative acquired photograph shots in the context of the immunocytochemistry assay described at **Section 3.3.3.4**., **Chapter III** are shown in the **Figure Ap 12**.

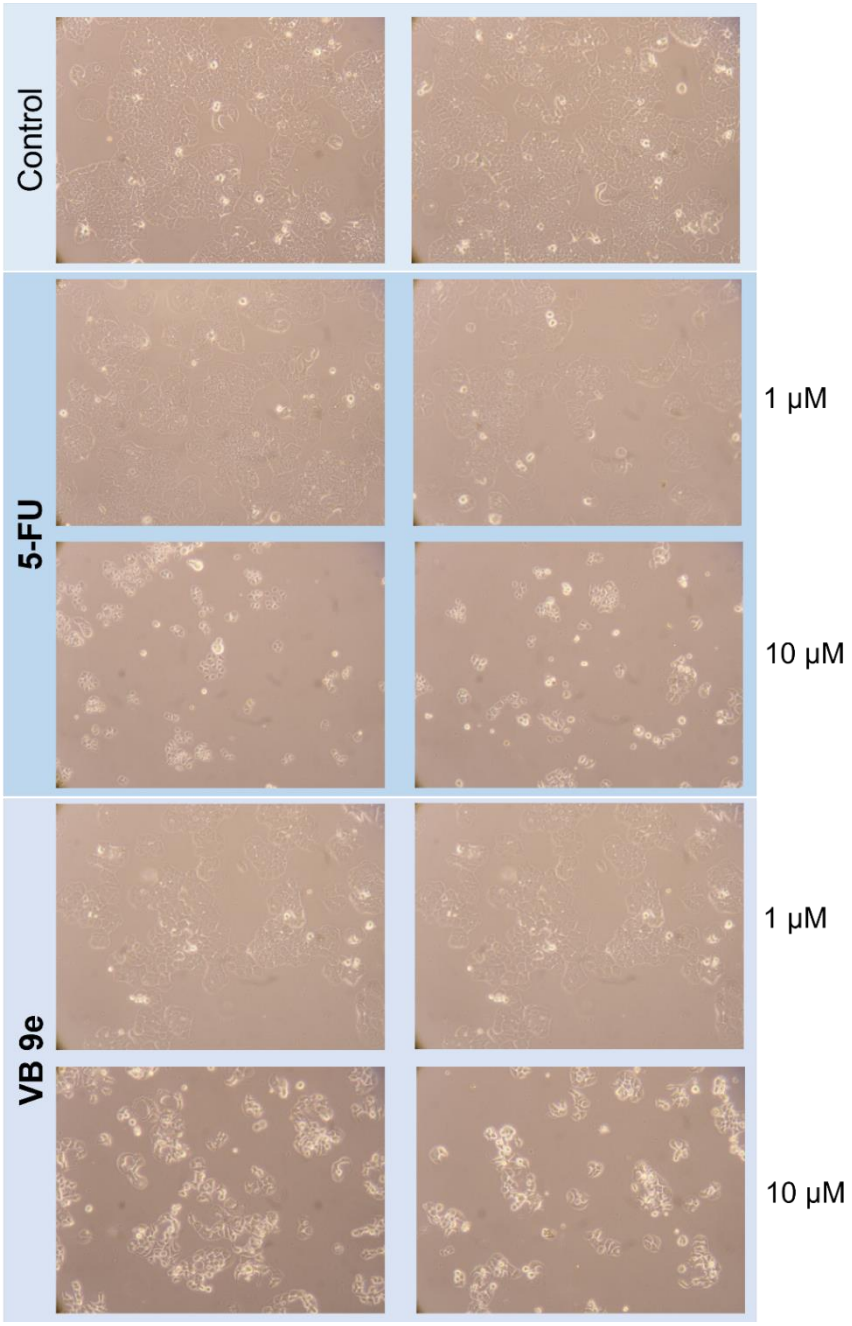

Figure Ap 12. Representative photograph shots of MCF-7 cells after 48 h of treatment with 5-fluorouracil (5-FU) and steroid **VB 9e** at 1 and 10 µM, and respective negative control (optical microscope coupled with a digital camera, zoom: 100 ×).

Appendix 6

Herein, several representative chromatograms with respect to the HPLC-DAD partial method development described in **Chapter V** are provided.

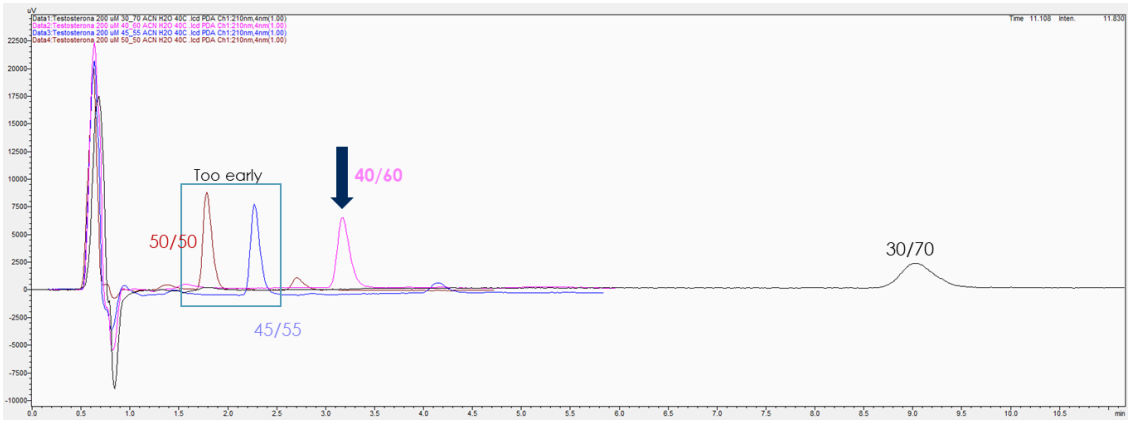

Figure Ap 13. Overlap of chromatograms of all tested mobile phase constitutions [water/acetonitrile (ACN): 50/50, 45/55, 40/60, and 30/70].

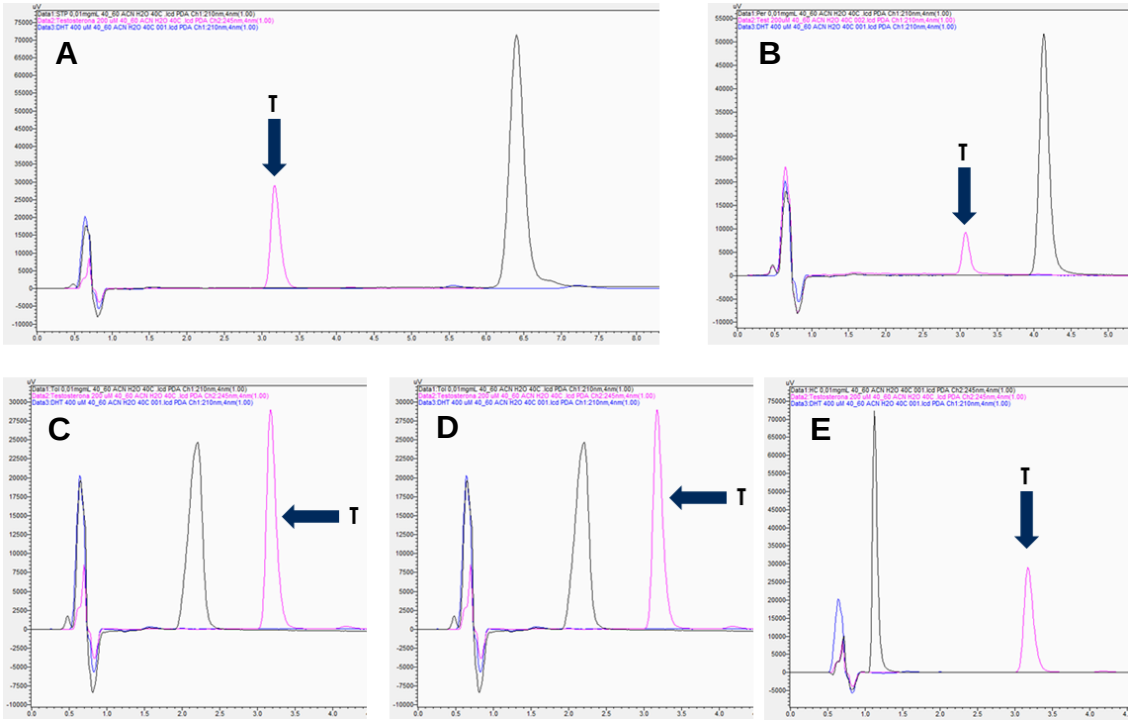

Figure Ap 14. Internal standard (IS) selection – overlap of chromatograms of potential IS (in **black**) and testosterone (in **pink**). (**A**) Stiripentol, (**B**) perampanel, (**C**) tolbutamide, (**D**) ketoconazole, and (**E**) hydrocortisone.

Appendix 7

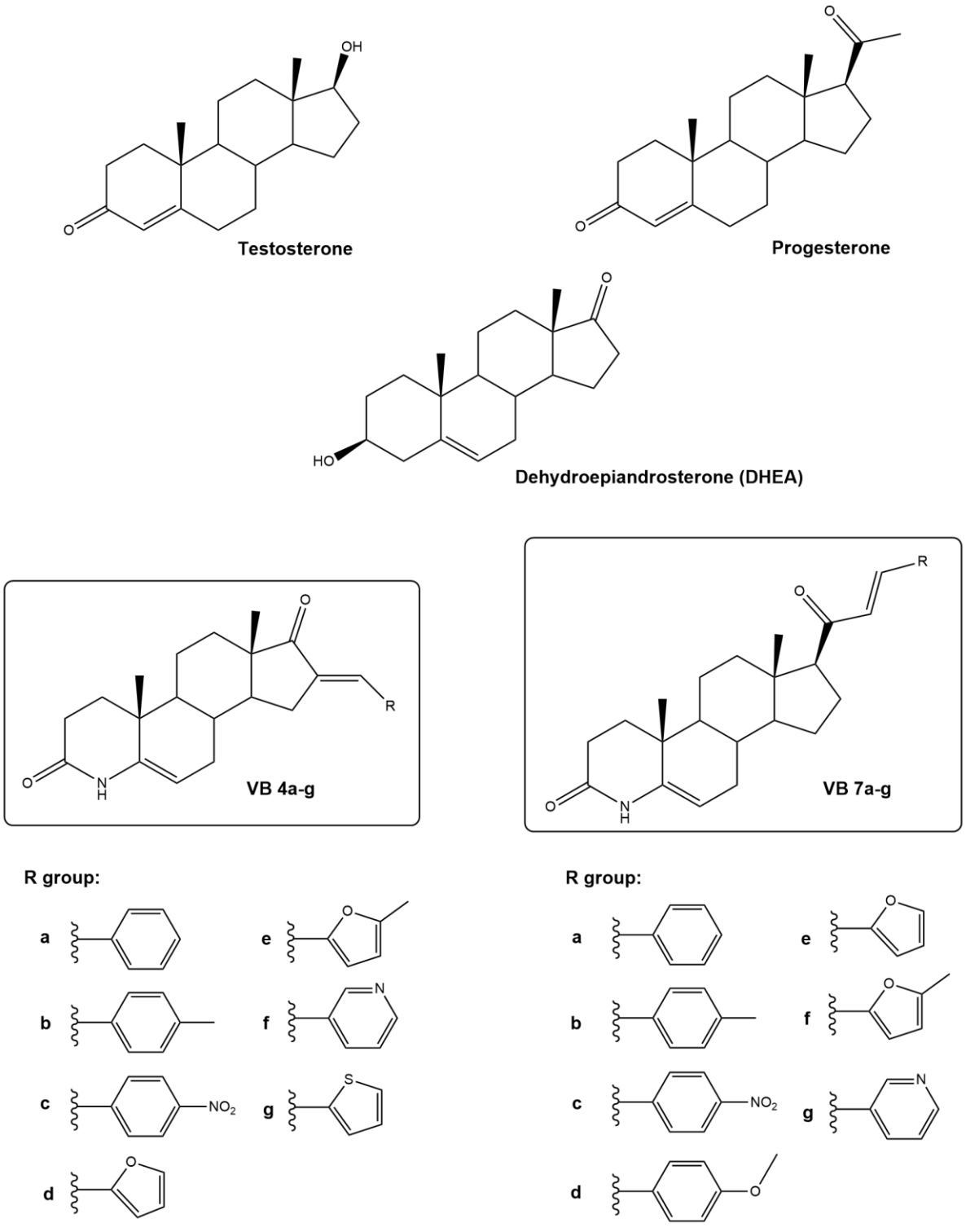

Figure Ap 15. Auxiliar figure of molecular structures of starting materials and synthesized steroids **VB 4a-g** and **VB 7a-g**. Created with ChemDraw.

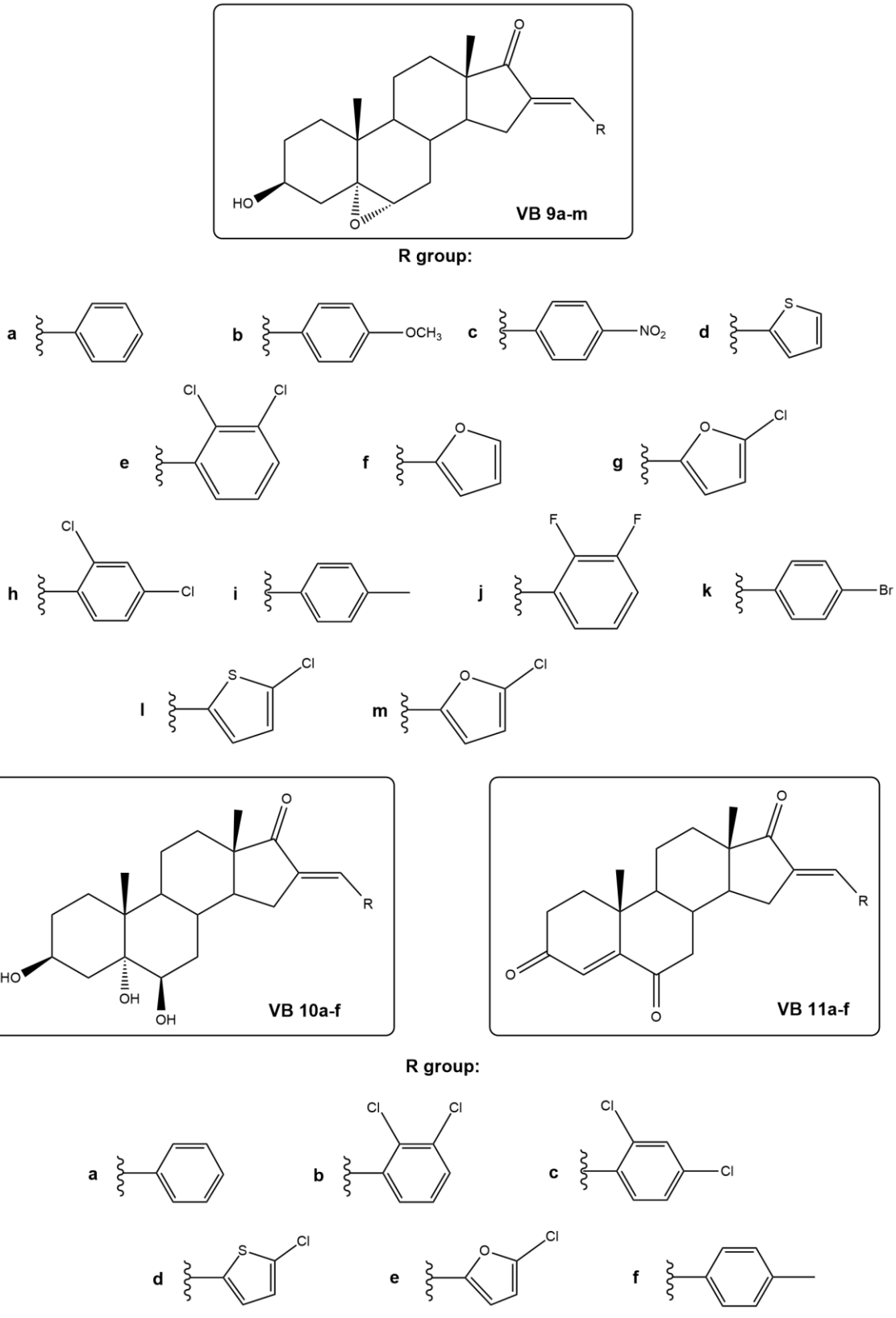

Figure Ap 16. Auxiliar figure of molecular structures of steroidal epoxides **VB 9a-m**, triols **VB 10a-f**, and triones **VB 11a-f.** Created with ChemDraw.

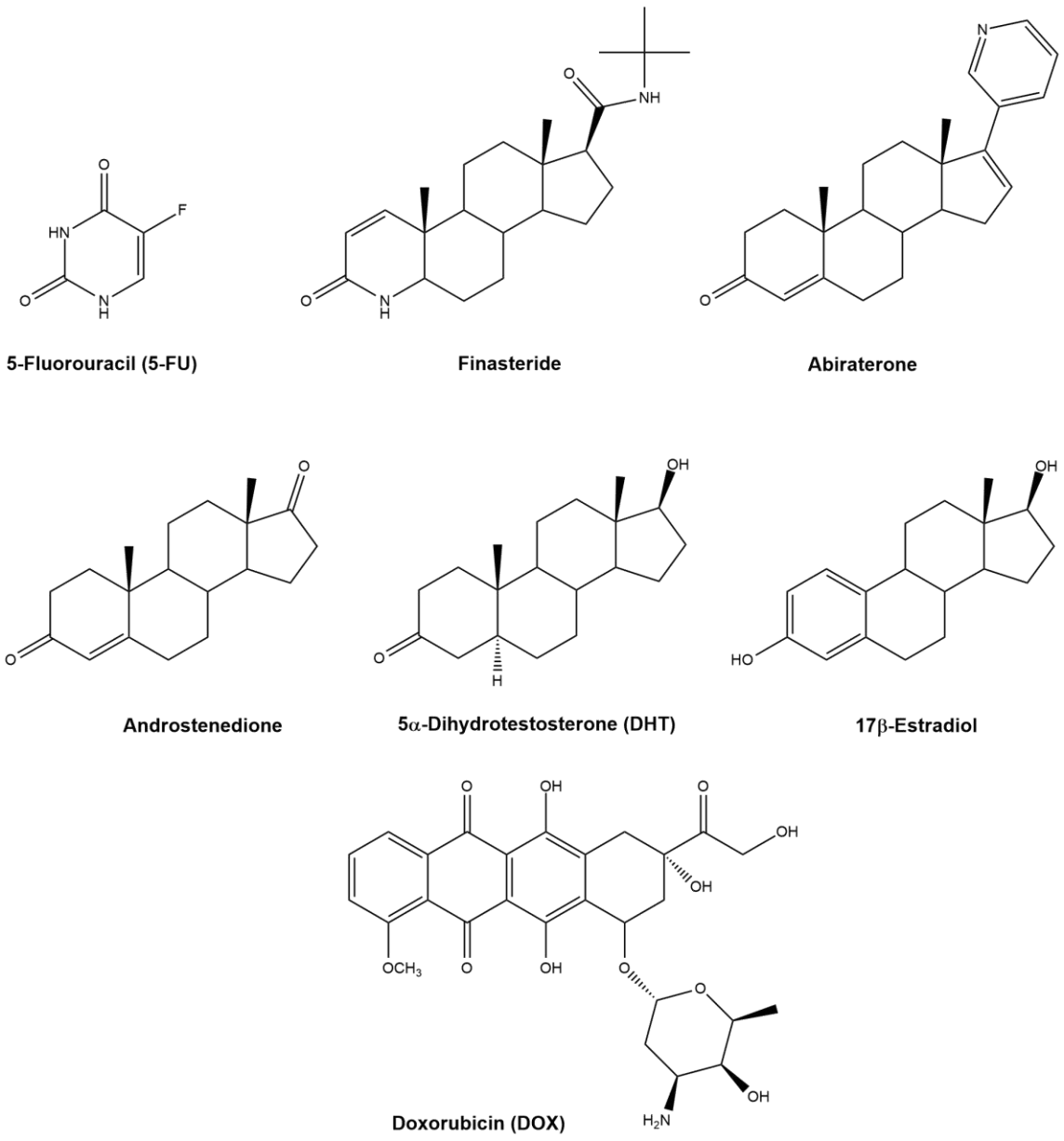

Figure Ap 17. Auxiliar figure of molecular structures of important reference compounds in the context of the present thesis. Created with ChemDraw.